NATIONAL CENTER FOR EARTHQUAKE
ENGINEERING RESEARCH
State University of New York at Buffalo

PB94-181740

NCEER-Taisei Corporation Research Program on Sliding Seismic Isolation Systems for Bridges:

Experimental and Analytical Study of Systems Consisting of Sliding Bearings, Rubber Restoring Force Devices and Fluid Dampers

Volume I

by

P. Tsopelas, S. Okamoto, M.C. Constantinou, D. Ozaki and S. Fujii
State University of New York at Buffalo
Department of Civil Engineering
Buffalo, New York 14260
and
Taisei Corporation
Sanken Building
25-1, Hyakunin-cho 3-chome
Shinjuku-Ku 169
Tokyo, Japan

Technical Report NCEER-94-0002

February 4, 1994

This research was conducted at the State University of New York at Buffalo and Taisei Corporation and was partially supported by the National Science Foundation under Grant No. BCS 90-25010 and the New York State Science and Technology Foundation under Grant No. NEC-91029.

NOTICE

This report was prepared by the State University of New York at Buffalo and Taisei Corporation as a result of research sponsored by the National Center for Earthquake Engineering Research (NCEER) through grants from the National Science Foundation, the New York State Science and Technology Foundation, and other sponsors. Neither NCEER, associates of NCEER, its sponsors, the State University of New York at Buffalo, Taisei Corporation, nor any person acting on their behalf:

a. makes any warranty, express or implied, with respect to the use of any information, apparatus, method, or process disclosed in this report or that such use may not infringe upon privately owned rights; or

b. assumes any liabilities of whatsoever kind with respect to the use of, or the damage resulting from the use of, any information, apparatus, method or process disclosed in this report.

Any opinions, findings, and conclusions or recommendations expressed in this publication are those of the author(s) and do not necessarily reflect the views of NCEER, the National Science Foundation, the New York State Science and Technology Foundation, or other sponsors.

NCEER-Taisei Corporation Research Program on Sliding Seismic Isolation Systems for Bridges:

Experimental and Analytical Study of Systems Consisting of Sliding Bearings, Rubber Restoring Force Devices and Fluid Dampers

Volume I

by

P. Tsopelas[1], S. Okamoto[2], M.C. Constantinou[3], D. Ozaki[2] and S. Fujii[4]

February 4, 1994

Technical Report NCEER-94-0002

NCEER Project Numbers 90-2101 and 91-5411B
and
Taisei Corporation Grant 150-6889A

NSF Master Contract Number BCS 90-25010
and
NYSSTF Grant Number NEC-91029

1 Research Assistant, Department of Civil Engineering, State University of New York at Buffalo
2 Research Engineer, Technology Research Center, Taisei Corporation, Yokohama, Japan
3 Associate Professor, Department of Civil Engineering, State University of New York at Buffalo
4 Manager, Technology Development Department, Taisei Corporation, Tokyo, Japan

NATIONAL CENTER FOR EARTHQUAKE ENGINEERING RESEARCH
State University of New York at Buffalo
Red Jacket Quadrangle, Buffalo, NY 14261

PREFACE

The National Center for Earthquake Engineering Research (NCEER) was established to expand and disseminate knowledge about earthquakes, improve earthquake-resistant design, and implement seismic hazard mitigation procedures to minimize loss of lives and property. The emphasis is on structures in the eastern and central United States and lifelines throughout the country that are found in zones of low, moderate, and high seismicity.

NCEER's research and implementation plan in years six through ten (1991-1996) comprises four interlocked elements, as shown in the figure below. Element I, Basic Research, is carried out to support projects in the Applied Research area. Element II, Applied Research, is the major focus of work for years six through ten. Element III, Demonstration Projects, have been planned to support Applied Research projects, and will be either case studies or regional studies. Element IV, Implementation, will result from activity in the four Applied Research projects, and from Demonstration Projects.

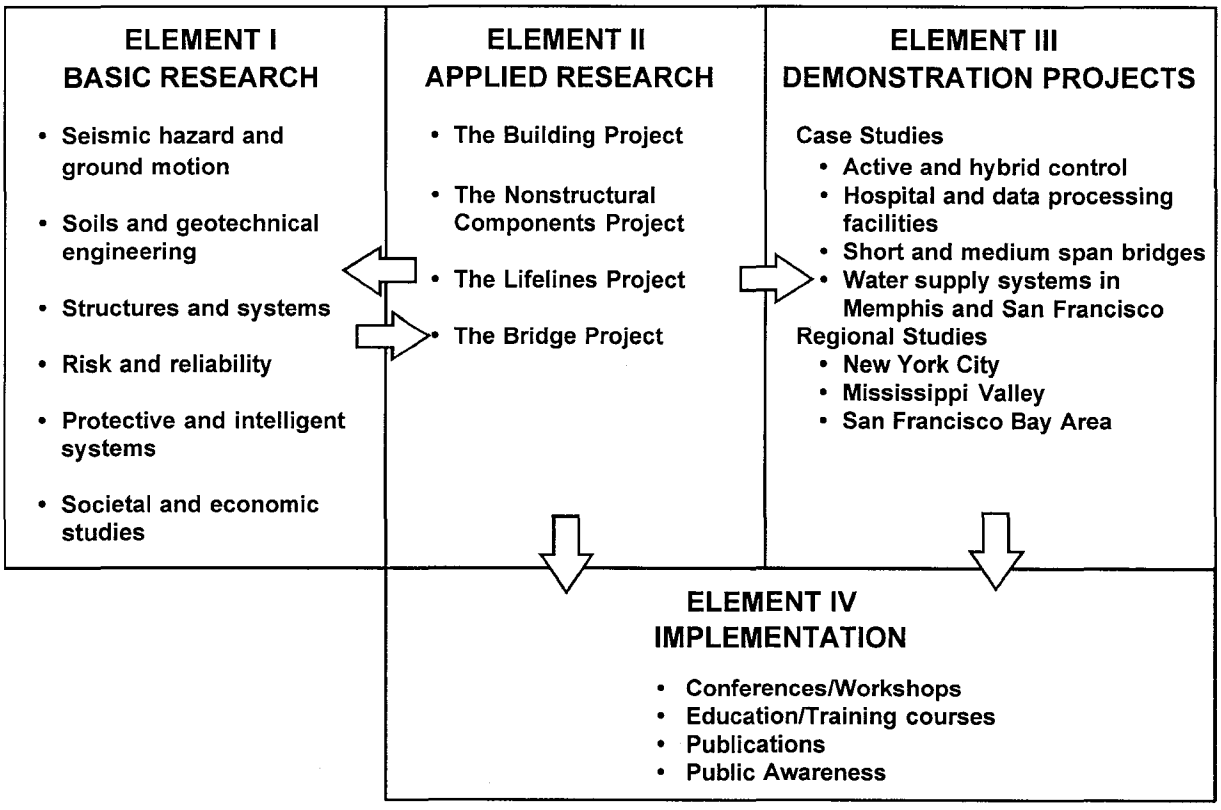

Research tasks in the **Bridge Project** expand current work in the retrofit of existing bridges and develop basic seismic design criteria for eastern bridges in low-to-moderate risk zones. This research parallels an extensive multi-year research program on the evaluation of gravity-load design concrete buildings. Specifically, tasks are being performed to:

ACKNOWLEDGMENTS

Financial support for this project has been provided by Taisei Corporation, Japan and the National Center for Earthquake Engineering Research, Projects No. 902101 and 915411B.

The sliding bearing used in the study were manufactured by Watson Bowman Acme Corporation, Amherst, NY. The sliding interface of these bearings consisted of unfilled and glass filled PTFE, which were manufactured in the United States and Japan. Furthermore, PTFE-based composites, which were manufactured in the United States, were used.

The rubber restoring force devices were designed and manufactured in Japan by Taisei Corporation.

The fluid dampers were manufactured by Taylor Devices, Inc., North Tonawanda, NY.

TABLE OF CONTENTS

TABLE OF CONTENTS (cont'd)

LIST OF ILLUSTRATIONS

LIST OF ILLUSTRATIONS (cont'd)

LIST OF ILLUSTRATIONS (cont'd)

LIST OF ILLUSTRATIONS (cont'd)

LIST OF ILLUSTRATIONS (cont'd)

LIST OF ILLUSTRATIONS (cont'd)

LIST OF TABLES

SECTION 1

INTRODUCTION

Seismic isolation systems are typified by the use of either elastomeric or sliding bearings. Elastomeric isolation systems have been used in the seismic isolation of buildings in Japan and the United States (Buckle 1990, Soong 1992, Kelly 1993). Several other countries, such as New Zealand and Italy among others, have a number of applications of elastomeric isolation systems in buildings (Buckle 1990, Martelli 1993).

Sliding isolation systems in buildings have been widely used in the former Soviet Union, where over 200 buildings are now seismically isolated (Constantinou 1991a, Eisenberg 1992). In Japan, Taisei Corporation constructed three buildings on the TASS sliding isolation system (Kawamura 1988, Constantinou 1991a). In the United States, sliding isolation systems have recently been selected for the retrofit of three buildings (Soong 1992, Kelly 1993). In particular, spherical sliding or FPS bearings (Zayas 1987, Mokha 1990b and 1991) have been selected for the retrofit of the U.S. Court of Appeals building in San Francisco. This historic structure with a floor area of 31500m^2, will be, when completed, the largest base-isolated structure in the U.S. and one of the largest in the world (Soong 1992).

For the first time in the U.S., the isolation system selection for U.S. Court of Appeals was based on technical rating and competitive bidding of elastomeric and sliding isolation systems. Interestingly, the FPS isolation system received the highest technical rating and had the least cost (Palfalvi 1993). This represents a turning point for the implementation of seismic isolation in the U.S. Sliding isolation systems are now regarded as technically equivalent and potentially less expensive than elastomeric isolation systems.

Seismic isolation of bridge structures has been widely implemented in New Zealand and Italy (Buckle 1990, Medeot 1991, Martelli 1993). While in New Zealand the application is exclusively with elastomeric systems, in Italy the application is primarily with sliding systems. Over 150 km of isolated bridge deck in Italy is supported by sliding bearings

together with various forms of restoring force and energy dissipation devices (Medeot 1991, Constantinou 1991a).

Japan has over 100 concrete railway bridges of the Shinkansen supported by sliding bearings together with viscous fluid devices, called the KP-stoppers, for restricting displacements within acceptable limits (Buckle 1990, Constantinou 1991a). This system is regarded as an early form of sliding isolation system.

More recently, Japan moved towards a cautious implementation of modern seismic isolation systems in bridges. So far, the application is restricted to only longitudinal isolation using elastomeric systems (Kawashima 1991).

The application of seismic isolation to bridges in the U.S. followed an interesting development. Until 1989, only six bridges were isolated, of which five were retrofit projects in California and one was a new construction in Illinois (Buckle 1990). While the 1989 Loma Prieta earthquake resulted in an accelerated implementation of seismic isolation systems to buildings, this has not been the case in bridges. Rather, we observe a renewed interest and new applications of bridge seismic isolation following the development of specifications for seismic isolation design (ICBO 1991, AASHTO 1991) and the adoption of seismic design guidelines for bridges in the entire U.S. The lack of specifications for the design of seismic isolated structures was regarded as an impediment to the application of the technology (Mayes 1990). Today (October 1993), 57 isolated bridges of total deck length exceeding 11 km are opened to traffic or they are in either the construction or in the design process in the U.S. The isolation system of these bridges consists of either lead-rubber bearings, sliding bearings with restoring force devices or sliding bearings with mild steel dampers. Interestingly, the majority of these bridges are located in the Eastern United States.

While seismic isolation systems found application to over 200 bridges, large scale testing of bridge isolation systems has been so far limited to three studies which concentrated on elastomeric systems (Kelly 1986, Kawashima 1991) and one specific sliding system (Constantinou 1991a). All three studies were restricted to models with rigid piers or

abutments and rigid decks. The effects of pier flexibility, pier strength, deck flexibility and distribution of isolation elements could not be studied in these experimental programs. Rather, these effects were studied by analytical techniques and found to be significant (Constantinou 1991a, Kartoum 1992).

The study reported herein concentrates on a new class of sliding isolation systems. It was carried out as part of the NCEER-Taisei Corporation research project on bridge seismic isolation systems. This program included the development of advanced sliding isolation systems for bridges and a comprehensive testing program utilizing a flexible pier model. This study concentrates on systems consisting of flat sliding bearings, rubber restoring force devices and fluid dampers.

SECTION 2

NCEER-TAISEI CORPORATION RESEARCH PROJECT ON BRIDGE SLIDING SEISMIC ISOLATION SYSTEMS

In 1991, the National Center for Earthquake Engineering Research and Taisei Corporation began a collaborative research project on the development and verification of advanced sliding seismic isolation systems for bridges (Constantinou 1992b). The project included also the study of established sliding isolation systems such as the Friction Pendulum (or FPS) system (Zayas 1987, Mokha 1990b and 1991, Constantinou 1993) and the lubricated sliding bearing/hysteretic steel damper system used in a large number of bridges in Italy (Medeot 1991, Marioni 1991).

The project had two portions: one concentrated on active systems and was carried out at Taisei Corporation and Princeton University, and the other concentrated on passive systems and was carried out at the University at Buffalo and Taisei Corporation. The Buffalo/Taisei portion of the project had the objective of producing a class of advanced passive sliding seismic isolation systems by modifying and/or adapting existing technology. Particular emphasis has been given to the adaptation and use of aerospace and military hardware in either the form of restoring force and damping devices or in the form of high performance composite materials in the construction of sliding bearings. The following systems were experimentally studied:

(1) Flat sliding bearings consisting of PTFE or PTFE-based composites in contact with polished stainless steel (coefficient of sliding friction at high velocity of sliding in the range of 0.07 to 0.15) and in combination with

   (a) Rubber restoring force devices,

   (b) Rubber restoring force devices and fluid viscous dampers,

   (c) Wire rope restoring force devices, and

(d) Fluid restoring force/damping devices.

(2) Spherically shaped FPS sliding bearings.

(3) Flat lubricated PTFE-stainless steel sliding bearings in combination with yielding E-shaped mild steel devices.

This report contains the results of the experimental study, interpretation of the results and analytical modeling of systems consisting of flat sliding bearings, rubber restoring force devices and fluid dampers.

SECTION 3

ISOLATION SYSTEMS

3.1 Design Requirements

The studied isolation systems consisted of three components :

(1) Flat sliding bearings to support the weight of the deck and provide a mechanism for energy dissipation.

(2) Rubber devices for providing restoring force, that is, recentering capability.

(3) Fluid viscous dampers for enhancing the energy dissipation capability of the system.

The three components of the isolation system provided load carrying capacity, restoring force capability (stiffness) and hysteretic and viscous damping which were not interrelated. This facilitated optimum performance for specific design requirements.

The specific design requirements of the isolation systems were to minimize the transmission of force to the substructure, that is piers and foundation, while bearing displacements in the scale of the model (length scale factor equal to 4) did not exceed 50 mm. These requirements were to be met for seismic motions representative of bridge design spectra in California (CalTrans) (Gates 1979) and in Japan (Level 2) (CERC 1992) for all ground conditions. Furthermore, the performance of the isolated bridge should be better, in terms of transmission of force to the substructure, than a comparable non-isolated bridge under weak seismic excitation, such as the Japanese Level 1 motions (CERC 1992).

The severe requirement on the maximum bearing displacement (50 mm in the scaled model or 200 mm in prototype scale) under strong seismic excitation reflects some design and economic considerations in bridge seismic isolation. A maximum bearing displacement of 200 mm allows the use of short multidirectional expansion joints and eliminates the need

for knock-off elements. Short expansion joints are less expensive, require less maintenance and produce less noise on automobile crossing than long ones.

3.2 Sliding Bearings

Four multidirectional sliding bearings of the disc type were used. Illustrated in Figures 3-1 and 3-2, this bearing consisted of a bottom plate which was supported by a high hardness Adiprene disc and a shear restriction mechanism. The disc provided rotational capability to the bottom plate so that the sliding interface was always in full contact.

The sliding interface consisted of austenitic stainless steel, conforming to ASTM A-240, type 304 requirements and polished to mirror finish. The roughness of the polished stainless steel surface was measured with a Surtronic 3P instrument (stylus radius=2.5 μm, cutoff length=0.8 mm, traverse length=4.5 mm) and found to be 0.04 μm R_a (Arithmetic Average, AA, or Center Line Average, CLA).

The bottom plate of the sliding bearing was delivered with a circular recess, which could accept plates faced with PTFE of other materials. This facilitated replacement of the sliding interface in order to achieve a friction coefficient at large velocity of sliding in the range of 0.07 to 0.15. Table 3-I lists these materials, the bearing pressure and the parameters in the model of friction. The coefficient of sliding friction, μ, followed the relation (Constantinou 1990a)

$$\mu = f_{\max} - (f_{\max} - f_{\min})\exp(-a|\dot{u}|) \qquad (3\text{-}1)$$

where f_{max} is the coefficient of friction at high velocity of sliding, f_{min} is the coefficient of friction at essentially zero velocity of sliding, a is a parameter controlling the variation of the coefficient of friction with velocity of sliding and $\dot{u}$ is the velocity of sliding. Figure 3-3 presents a comparison of experimental results on the coefficient of friction of the three bearings to predictions of the calibrated model of Equation (3-1).

The PTFE-based composite material used in the bearing C1 was identical to the material No. 1 used in the tests of the FPS bridge isolation system (Constantinou 1993) and also used in the bearings of the U.S. Court of Appeals building in San Francisco (Soong 1992).

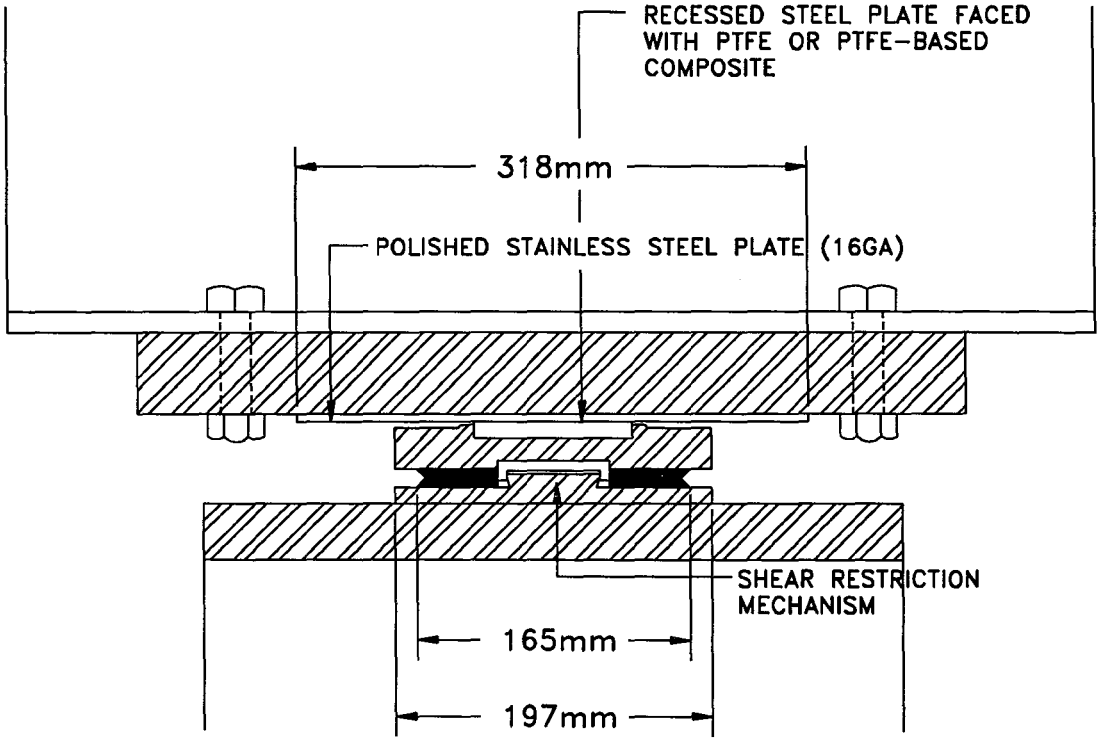

Figure 3-1 Sliding Disc Bearing Design.

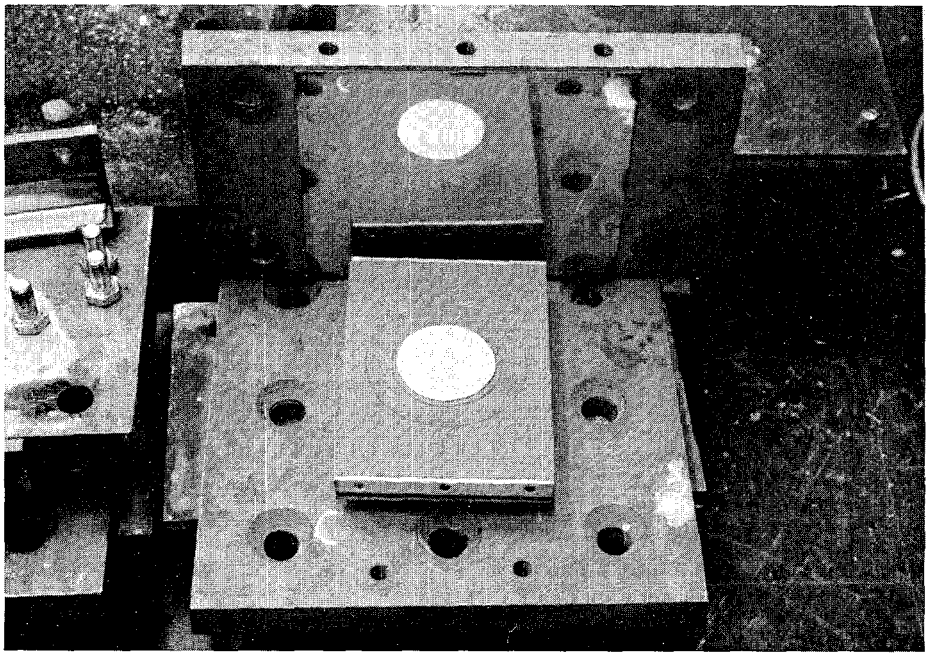

Figure 3-2 View of Sliding Disc Bearing.

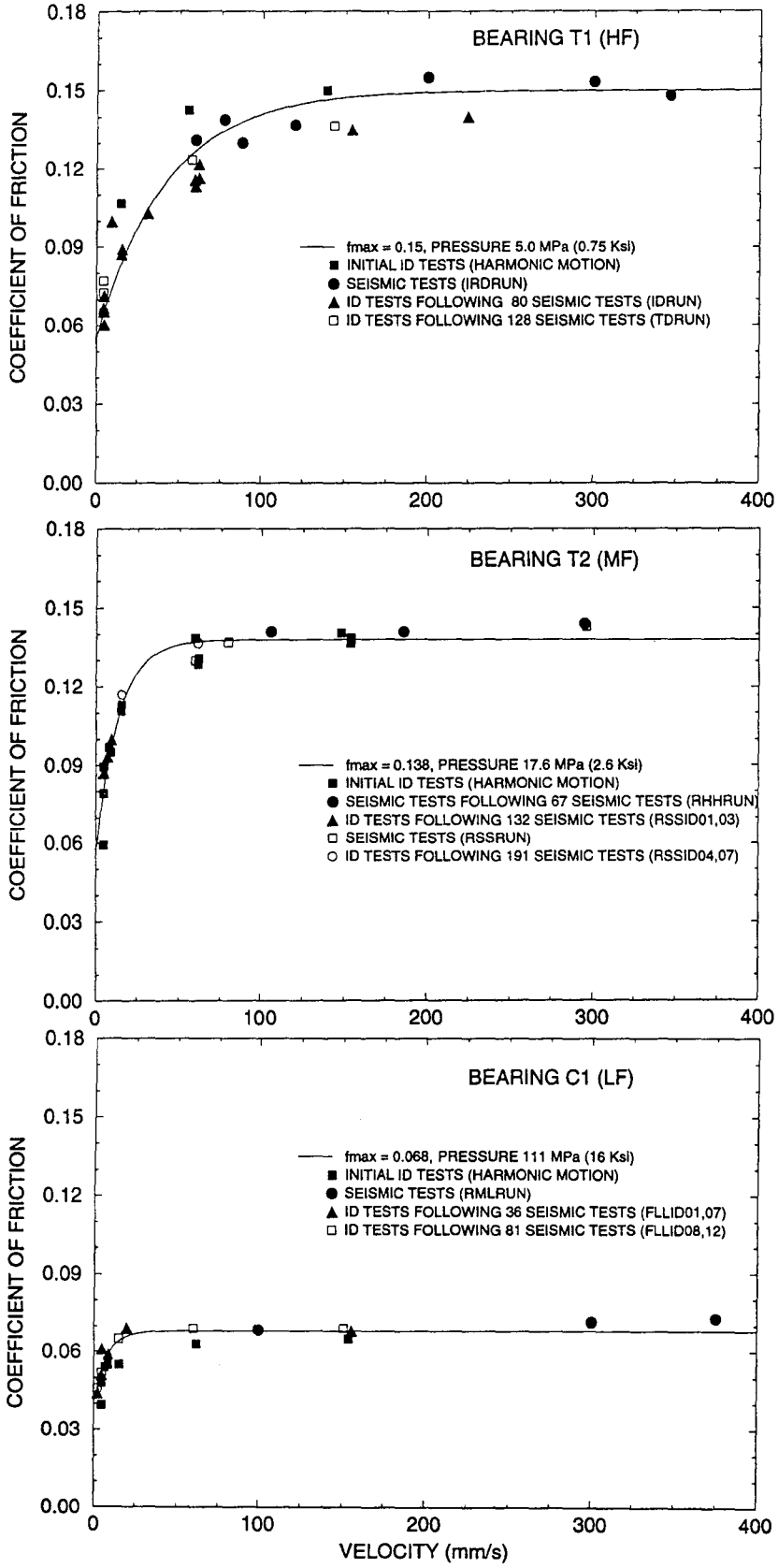

Figure 3-3 Coefficient of Sliding Friction as Function of Sliding Velocity of Sliding Disc Bearings.

Table 3-I Properties of Sliding Disc Bearings

Bearing	Characterization of Friction	Material	Contact Area (mm^2)	Bearing Pressure (MPa)	f_{max}	f_{min}	a (s/m)
T1	High Friction (HF)	Unfilled PTFE	7090	5.0	0.150	0.055	23.7
T2	Medium Friction (MF)	Glass-Filled PTFE (Taisei Type)	2040	17.6	0.138	0.055	75.0
C1	Low Friction (LF)	PTFE-Based Composite	320	111.0	0.068	0.040	130.0

Of interest is to note in Figure 3-3 that some of the test data were obtained after a significant number of previous tests. The glass-filled PTFE and the PTFE-based composite exhibited remarkably stable properties over this large number of tests. However, the unfilled PTFE exhibited some scatter in the recorded values of the coefficient of friction, which had the tendency to reduce with increasing number of cycles. This is consistent with observations made by Mokha, 1988.

3.3 Rubber Restoring Force Devices

The rubber restoring force devices acted as horizontal springs with displacement restraint. Figure 3-4 shows the construction of the rubber restoring force device. It provided stiffness by deforming in the manner shown in Figure 3-5, that is, by imposing tension to the elements of the device. The rubber elements on the compression side were ineffective until they were compressed against the outer steel cylinder. At that stage, the device exhibited increased stiffness and acted as a displacement restrainer. It allowed a maximum displacement of about 50 mm.

Devices with three values of stiffness were used in the testing. The different values of stiffness were achieved by using natural rubber of different hardness as shown in Table 3-II. Figure 3-6 shows representative force displacement loops of the three devices. The devices exhibited nearly linear behavior to displacements of about 35 mm. Beyond this limit they displayed increasing stiffness to the limit of about 50 mm. After that the devices exhibited nearly rigid behavior as illustrated in Figure 3-7.

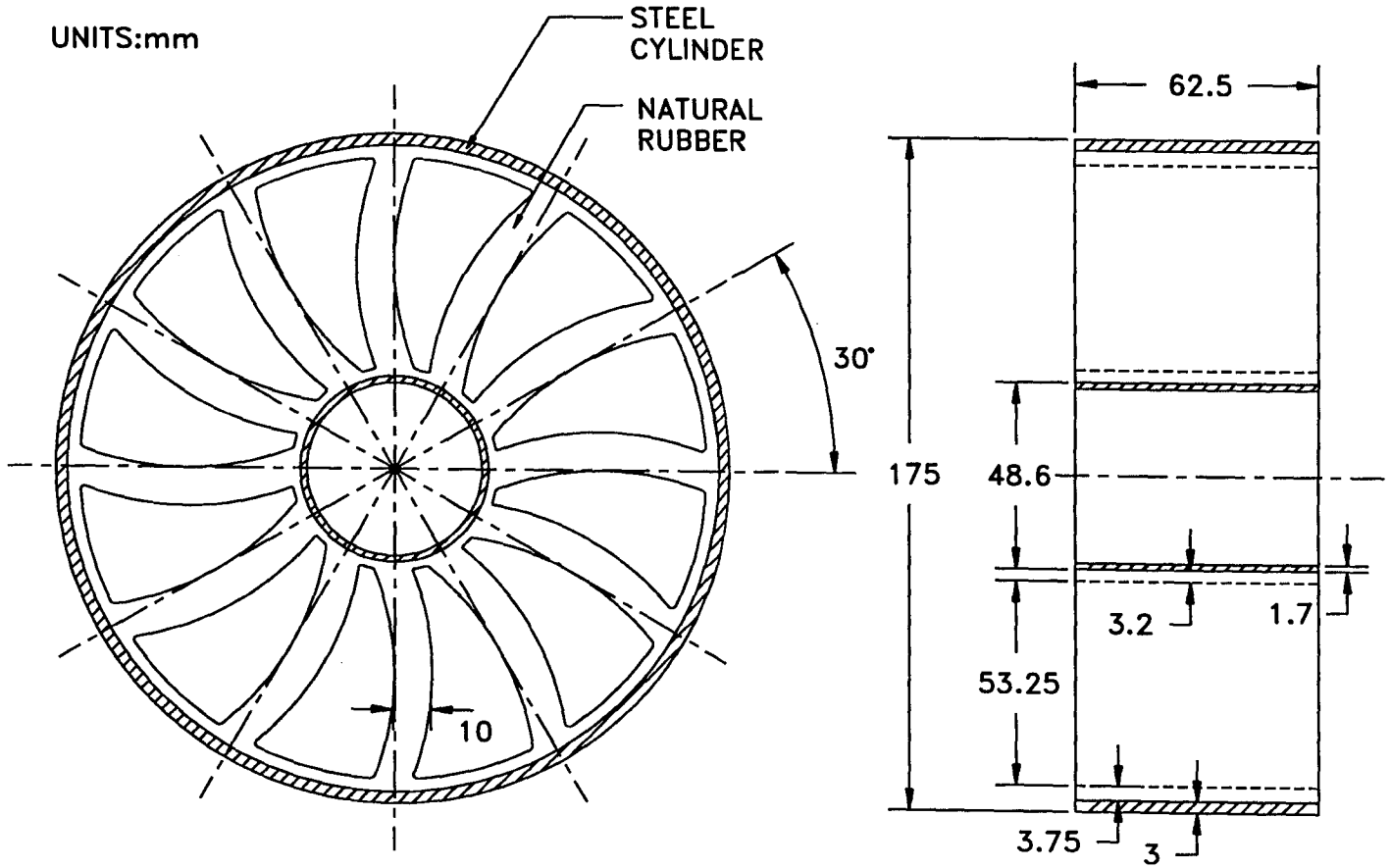

Figure 3-4 Construction of Rubber Restoring Force Device (Units: mm).

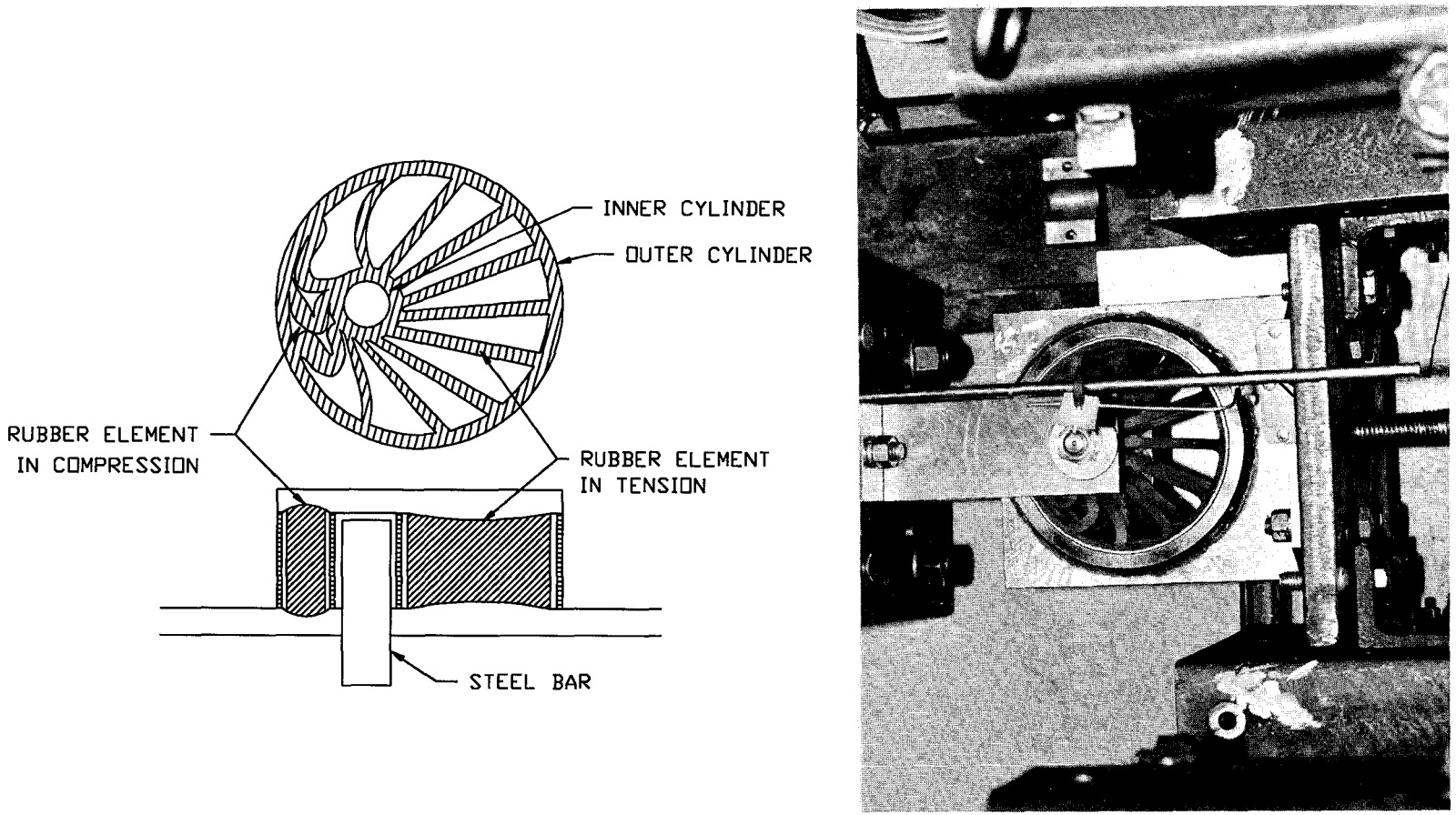

Figure 3-5 Operation of Rubber Restoring Force Device.

Rubber devices were installed one at each pier location. For this configuration the period of vibration of the isolated model deck is given in Table 3-II. This value of period was calculated from the secant stiffness of two devices at 35 mm displacement and the weight of deck (143 kN). The period should be regarded as a measure of the stiffness of the restoring force devices in relation to the weight of the deck.

Table 3-II Properties of Rubber Restoring Force Devices

No.	Rubber Hardness (shore A)	Characterization of Stiffness	Stiffness[1] (kN/m)	Period of Isolated Bridge[2] (sec)
1	45	Low	46.9	2.47
2	67	Medium	112.3	1.60
3	80	High	162.2	1.33

[1] Each device. Stiffness is secant at displacement of 35 mm.

[2] In model scale for two devices.

The mechanical properties of the rubber devices were only marginally affected by the frequency of motion. Evidence for this behavior is provided in Figure 3-8 for the No. 3 device (the one with highest stiffness and area enclosed by the hysteresis loop).

The effective stiffness and effective damping ratio of the devices were dependent on the amplitude of motion, as it is evident in the results of Figures 3-6 to 3-8. To obtain a measure of the energy dissipation capability of the rubber devices, the effective damping ratio (defined in accordance with the 1991 AASHTO) was obtained in tests at amplitude of 35 mm, thus prior to initiation of stiffening of the devices. It was found to be in the range of 2.4 to 3.8% for the low stiffness device, 4.0 to 5.8% for the medium stiffness device and 6.5 to 7.8% for the high stiffness device. This range of values was obtained in cyclic tests with frequency varying from 0.01 Hz (static) to 2 Hz.

3.4 Fluid Viscous Dampers

The fluid dampers used in the tests were identical to those used by Constantinou, 1992c in the testing of a building model. These fluid dampers evolved from shock isolation systems of military hardware. The typical construction of these devices is shown in Figure 3-9.

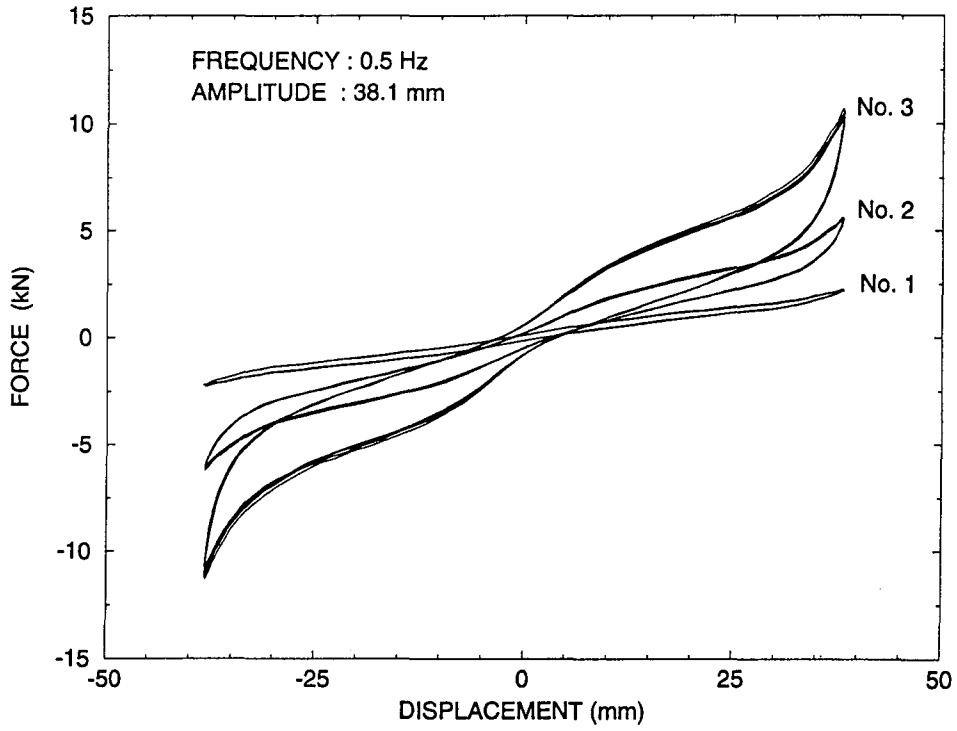

Figure 3-6 Force Displacement Loops of Rubber Restoring Force Devices.

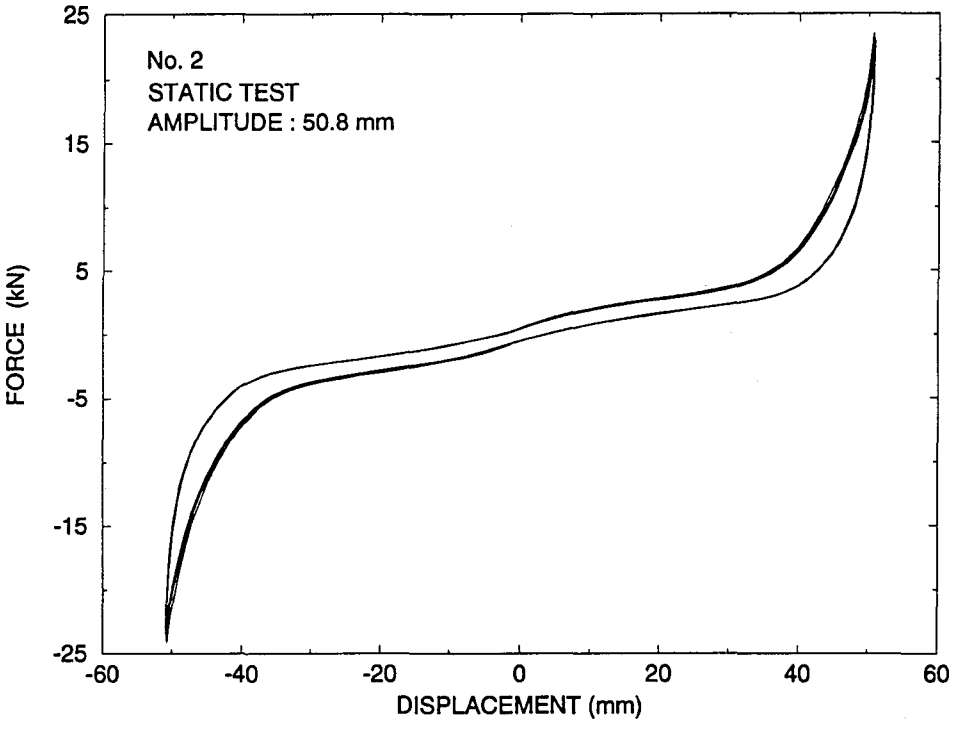

Figure 3-7 Force Displacement Relation of No. 2 Rubber Restoring Force Device for Displacement Beyond the Limit of 50 mm.

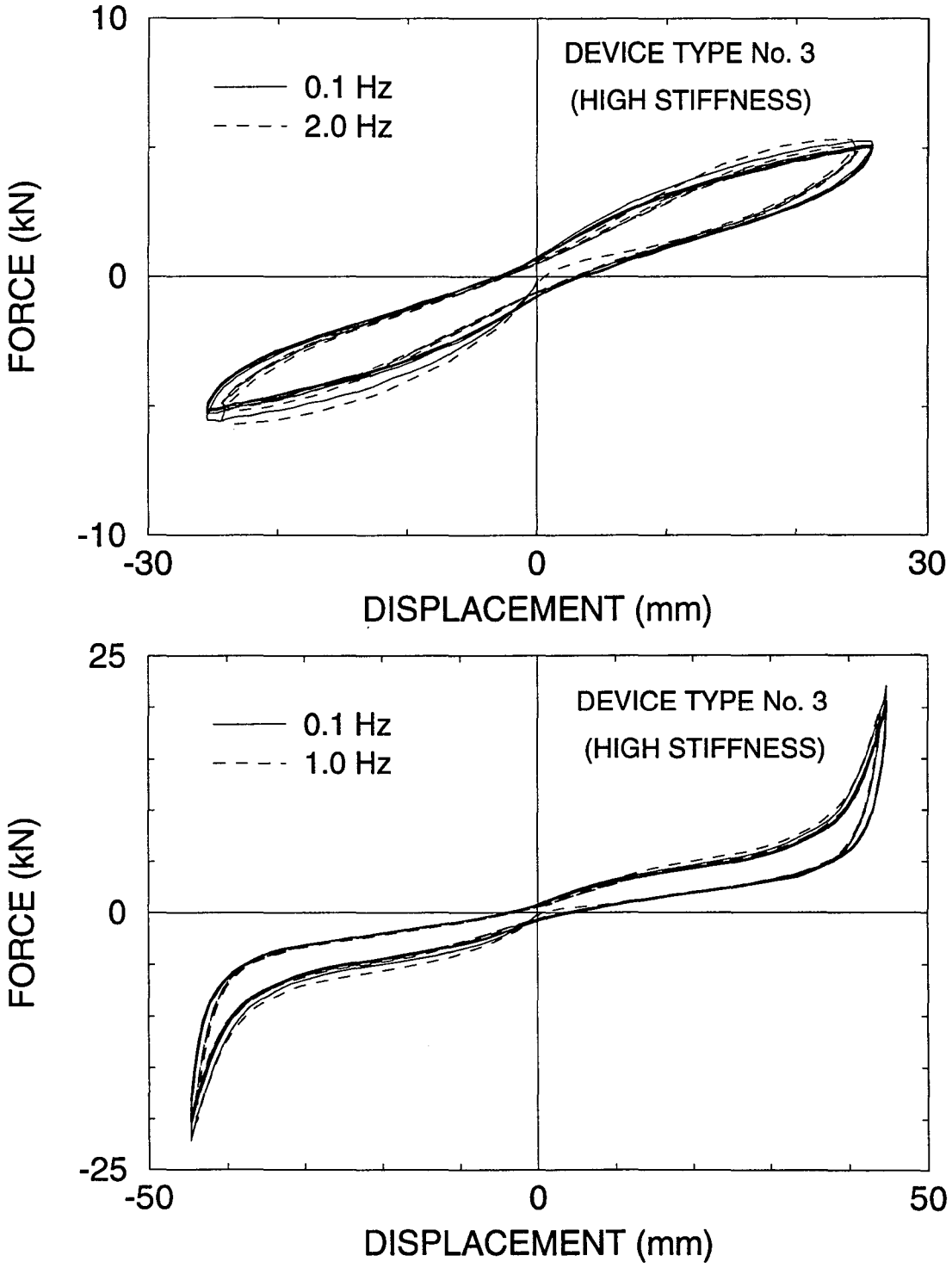

Figure 3-8 **Recorded Force-Displacement Loops of No. 3 Rubber Device at Low and High Frequency Motion. Properties are Unaffected by Frequency.**

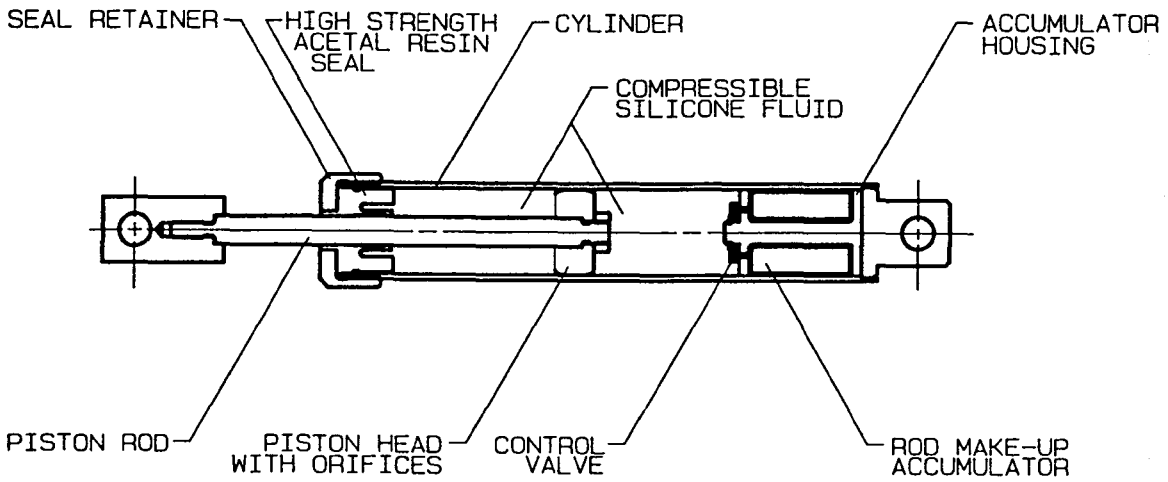

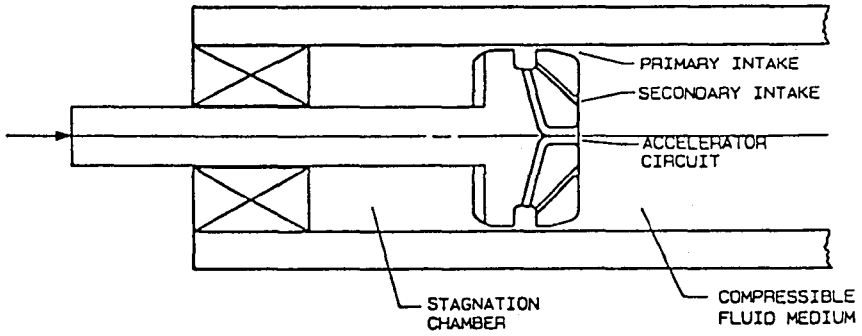

Fluidic Control Orifice

Figure 3-9 Construction of Fluid Viscous Damper.

The device operates on the principle of fluid flow through orifices. The device consists of a stainless steel piston, with bronze orifice head and an accumulator. It is filled with silicone oil. The orifice flow is compensated by passive bi-metallic thermostat that allows operation of the device over a temperature range of -40 °C to 70 °C. The orifice configuration, mechanical construction, fluid and thermostat used in this device originated within a device used in a classified application on the U.S. Air Force B-2 Stealth Bomber. Thus, the device includes performance characteristics considered as state-of-the-art in hydraulic technology. Furthermore information on applications of fluidic devices in earthquake engineering may be found in Shinozuka, 1992.

Unlike typical fluid dampers which utilize cylindrical orifices, this device utilizes a series of specially shaped passages to alter flow characteristics with fluid speed. A schematic of this orifice is shown in Figure 3-9. It is known as Fluidic Control Orifice. It provides forces which are proportional to $|\dot{u}|^{\alpha}$, where α is a predetermined coefficient in the range of 0.5 to 2.0. A design with coefficient α equal to 0.5 is useful in applications involving extremely high velocity shocks. They are typically used in the shock isolation of military hardware. A design with $\alpha = 1$ results in essentially linear viscous behavior. The devices utilized in this testing program were designed to have this behavior.

Force-displacements loops of the fluid dampers used in the tests are shown in Figure 3-10. Obtained in cyclic testing at frequencies of 1, 2 and 4 Hz and temperature in the range of 1 to 47 °C, these loops demonstrate linear viscous behavior and marked insensitivity to temperature. Four of these devices were used in a selected number of tests with the configuration of high friction bearings (T1) and medium stiffness rubber devices (period = 1.60 s) to provide viscous damping of over 50% of critical.

The dampers behaved as linear viscous devices with output force proportional to the velocity of the piston rod with respect to the housing:

$$P = C_o \dot{u} \tag{3-2}$$

The single parameter describing the behavior of the damper was derived from the graphs of Figure 3-11, which present the peak recorded force versus the peak velocity in cyclic

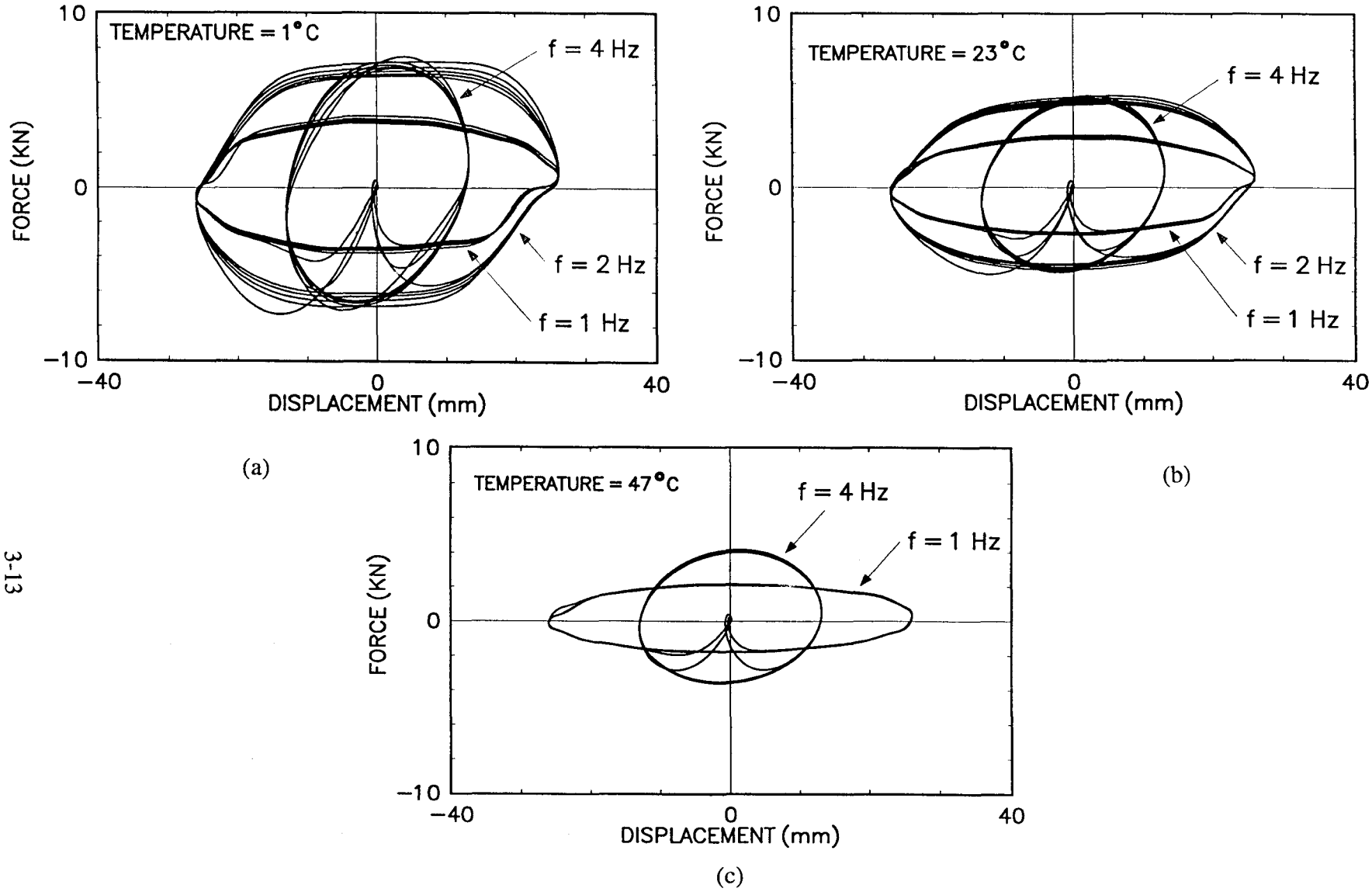

Figure 3-10 Recorded Force Displacement Loops of Fluid Damper at (a) Low Temperature, (b) Normal Temperature, and (c) High Temperature.

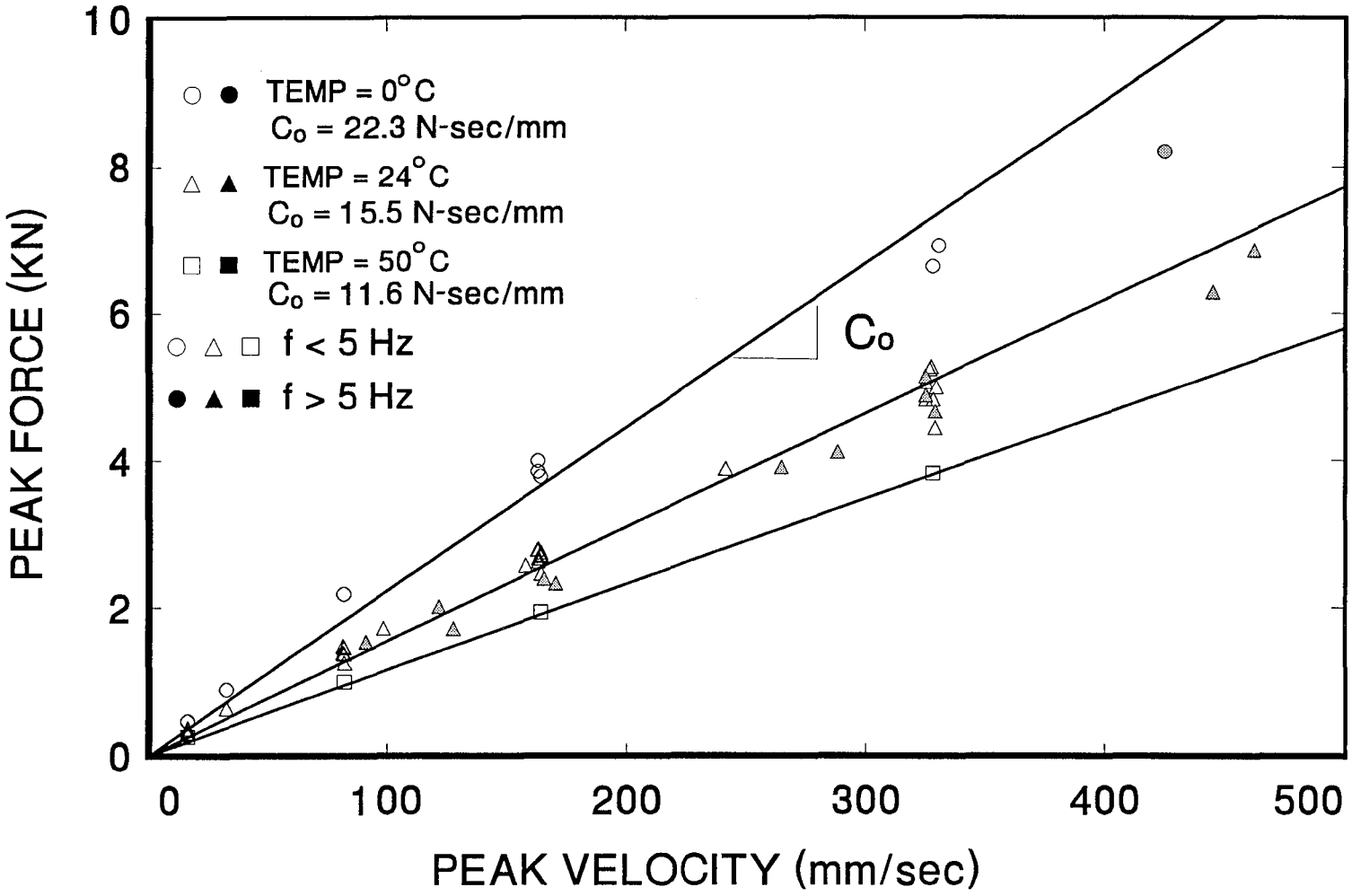

Figure 3-11 Recorded Values of Peak Force vs Velocity for Low , Normal and High Temperature Tests.

sinusoidal tests. The experimental results may be fitted with straight lines with slope equal to C_o, the damping coefficient of the device. For normal temperature (24 °C) and above, the behavior is indeed linear viscous to velocities of about 500 mm/sec and beyond. As temperature drops, the experimental results deviate from linearity at a lower velocity.

The values of coefficient C_o in Figure 3-11 demonstrate that the damper exhibits a stable behavior over a wide range of temperatures. This is particularly important in bridge applications where ambient temperatures vary over a significant range.

The results of Figures 3-10 and 3-11 demonstrate reductions of the damping coefficient with increasing ambient temperature, although the rate of reduction reduces with increasing temperature. The reduction of the damping coefficient is a result of the reduction of the density and viscosity of the fluid at higher temperatures. This phenomenon is partially compensated by the bi-metallic thermostat of the device which adjusts the flow area. At high temperatures, the effect of reduction of the density and viscosity of the fluid may be completely reversed by the increase of fluid volume. This is the reason for reduced sensitivity on temperature of the properties of the damper at high temperatures.

Since the properties of the damper exhibit some dependency on temperature, it is worthy of investigating the effect of the heat generated by the work done by the damper.

The problem is one of non-isothermal flow and the equations that form the starting point are those of heat transfer and fluid flow (Bird 1987). Herein we attempt to derive an approximate simple expression for the temperature rise due to conversion of mechanical to thermal energy. Thus, we neglect flow and consider only the heat equation

$$c\frac{\partial T}{\partial t} = K\nabla^2 T + q \tag{3-3}$$

where T = temperature, c = heat capacity per unit volume, K = thermal conductivity and q = heat generated per unit volume. We assume uniform rise of the temperature and uniform heat generation over the entire volume of fluid, so that Equation (3-3) simplifies to

$$c\frac{dT}{dt} = \frac{P\dot{u}}{V_F} \tag{3-4}$$

where P = damper force, $\dot{u}$ = damper piston velocity and V_F = fluid volume. Of course, Equation (3-4) is valid for perfectly insulated boundaries. This is not true since there is heat transfer to the steel housing of the device. Thus, Equation (3-4) will give an upper bound to the temperature rise.

Use of Equation (3-2) and integration of Equation (3-4) over a cycle of harmonic motion at frequency ω and amplitude u_o gives

$$\Delta T < \frac{\pi C_o u_o^2 \omega}{c V_F} \tag{3-5}$$

where ΔT = temperature rise in a complete cycle. The heat capacity per unit volume of silicon oil in the damper is c = 0.834 N-mm/mm^3- °F (121 in-lb/in^3- °F) and the oil volume is V_F = 98320 mm^3 (6 in^3). Thus, for the tests of Figure 3-10b with five cycles at amplitude of 25 mm and frequency of 1 Hz, we estimate a temperature rise of less, probably substantially less, than 12 °F or about 6 °C. This rise in temperature is too small to alter the force output of the damper.

Therefore, for the tested dampers the heat generated in a typical earthquake is totally insignificant. The reader is referred to Section 3.5 for further discussion in the case of sustained motion for over 100 cycles.

3.5 Behavior of Isolation Systems

Seven different configurations of isolation systems were tested. These configurations and the resulting properties of the tested isolation system are listed in Table 3-III. A number of identification tests were conducted in order to determine the force-displacement characteristics of these isolation systems. For this purpose the piers of the bridge model were braced for increasing their stiffness and the deck was connected to a nearby erected frame, while on the shake table. Load cells monitored the force transmitted by the connection of the deck to the reaction frame, while the shake table below was driven at specified harmonic motion. Thus, the load cells measured the total force transmitted

Table 3-III Tested Configurations and Properties of Isolation Systems.

SLIDING BEARINGS (Type)		RUBBER RESTORING FORCE DEVICES (Stiffness)		FLUID VISCOUS DAMPERS (Number)		FRICTION COEFF. (f_{max})		RUBBER DEVICE STIFFNESS (kN/m)		FLUID DAMPER COEFF. Co (kN-s/m)		PERIOD OF VIBRATION[2] (sec)	VISCOUS DAMPING RATIO[3]
SOUTH PIER	NORTH PIER	SOUTH PIER	NORTH PIER	SOUTH PIER	NORTH PIER	SOUTH PIER	NORTH PIER	SOUTH PIER	NORTH PIER	SOUTH PIER	NORTH PIER		
T1	T1	Medium	Medium	0	0	0.150	0.150	112.3	112.3	0	0	1.60	0.050
T1	T1	Medium	Medium	2	2	0.150	0.150	112.3	112.3	30.80	30.80	1.60	0.588
T2	T2	Medium	Medium	0	0	0.138	0.138	112.3	112.3	0	0	1.60	0.050
T2	T2	High	High	0	0	0.138	0.138	162.2	162.2	0	0	1.33	0.073
T2	T2	Low	Low	0	0	0.138	0.138	46.9	46.9	0	0	2.47	0.035
T2	C1	High	Medium	0	0	0.138	0.068	162.2	112.3	0	0	1.45	0.060
C1	C1	High	High	0	0	0.068	0.068	162.2	162.2	0	0	1.33	0.073

[1] Secant Stiffness at 35 mm Displacement.

[2] Based on Secant Stiffness of Rubber Devices and Deck Weight of 143 kN (in Model Scale).

[3] Based on Damping of Fluid Devices plus Equivalent Damping Ratio of Rubber Devices.

through the isolation system. Furthermore, load cells, which supported the sliding bearings, monitored the friction force.

The load cells provided reliable measurements of the friction force in all identification tests. The results of these measurements have been included in the graphs of Figure 3-3. However, the reaction frame had some flexibility which resulted in motion of the deck in tests with high frequency motion. This disturbed the measurement of the total force transmitted through the isolation system. Thus, reliable measurements of the total force were made only in identification tests at frequencies equal to 0.03 Hz.

Figures 3-12 to 3-17 show recorded loops of friction force in each of the sliding bearing and of total force in tests of the six systems without fluid dampers. All tests were conducted at frequency of 0.03 Hz, amplitude of 50 mm and for either two or five cycles. The force in Figures 3-12 to 3-17 is normalized either by the axial load on each sliding bearing (35.75 kN), in order to directly give the friction coefficient, or by the deck weight (143 kN) in the case of the isolation system force, in order to give the base shear coefficient.

A different test was conducted to obtain loops of force versus displacement in the system with fluid dampers. The deck was disconnected from the reaction frame and the now isolated deck was excited by the motion of the shake table, which was driven with sinusoidal motion of 1 Hz frequency. The input motion was adjusted until stable response at bearing displacement amplitude of 25 mm was achieved. Over 40 cycles of motion at this amplitude were recorded (total number exceeded 100). Figure 3-18 shows loops of the recorded deck acceleration, bearing friction force and combined force from rubber devices and fluid dampers versus displacement.

The deck acceleration, when multiplied by the mass of the deck, gives the isolation system shear force provided that the deck is infinitely rigid. Actually the deck had some flexibility, which resulted in the wavy form of the loops in Figure 3-18 (see extended discussion in Section 5.2). The combined force in the rubber devices and fluid dampers was obtained by subtracting the recorded friction force (measured by load cells) from the

total isolation system force. Thus, it also has the same wavy form in its loop as the acceleration of the deck from where it was extracted.

What is of interest to note in Figure 3-18 is the marked stability of both the frictional properties of the sliding bearings and of the characteristics of the fluid dampers. The behavior of the fluid dampers is particularly interesting since estimates of the rise in fluid temperature, as a result of the work done by the damper, are at about 45 °C (see Section 3.4 for details). At this temperature the fluid density and viscosity reduce while its volume increases. The effects of these two phenomena, together with the action of the bi-metalic thermostat, appear to counteract each other, so that the damper output force is practically unaffected.

From the recorded combined loops of the two rubber devices and four fluid dampers in Figure 3-18, we calculate the storage stiffness as approximately K_1= 230 N/mm and the damping coefficient C = 69 N-s/mm. For the deck weight of 143 kN, the resulting values of period and damping ratio are 1.58 secs and 0.596, respectively. These values are in very good agreement with the postulated values from the component test results (see Table 3-III).

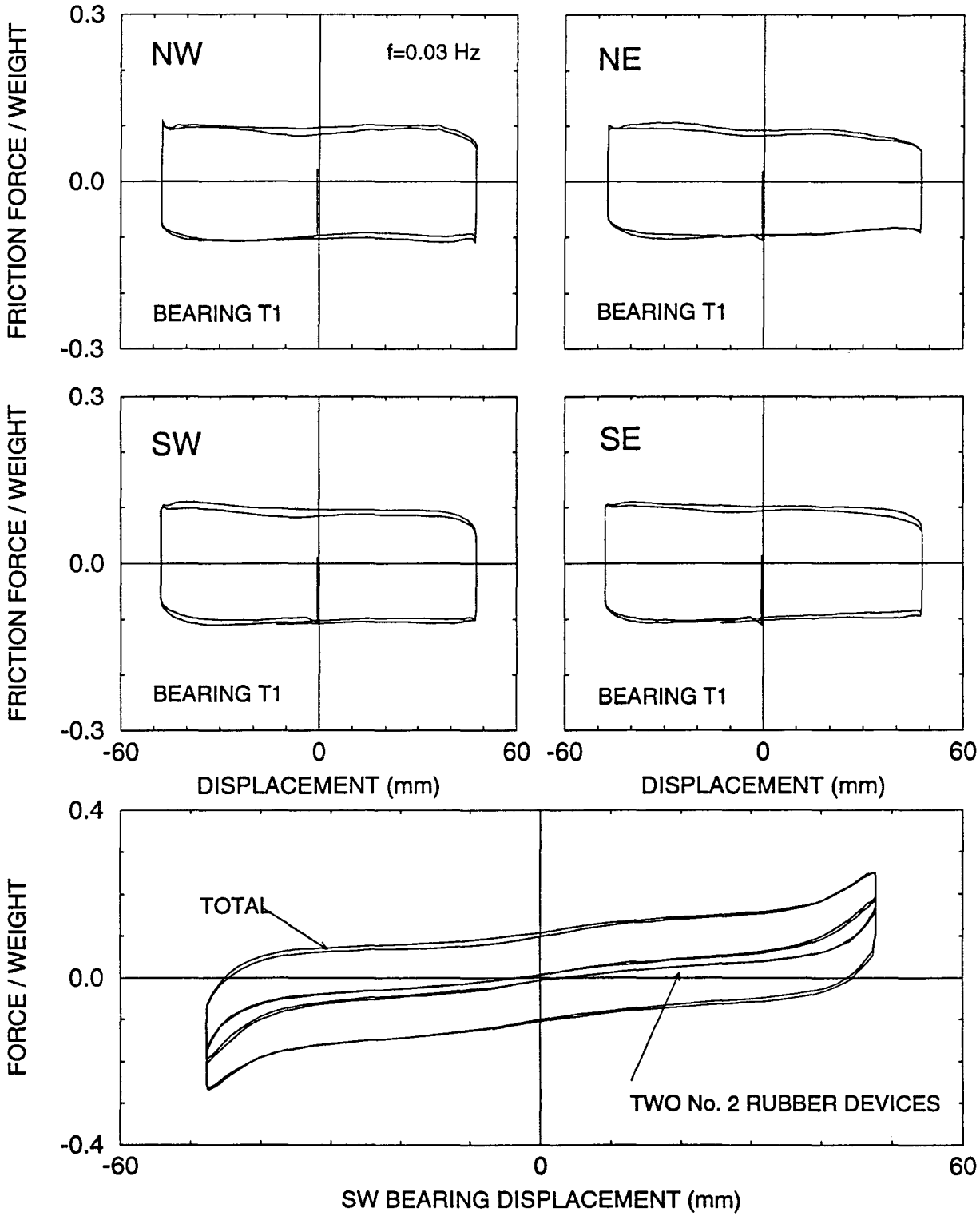

Figure 3-12 Friction Force and Total Force Versus Displacement Loops of System with Four High Friction (T1) Bearings and Two Medium Stiffness (No. 2) Rubber Devices.

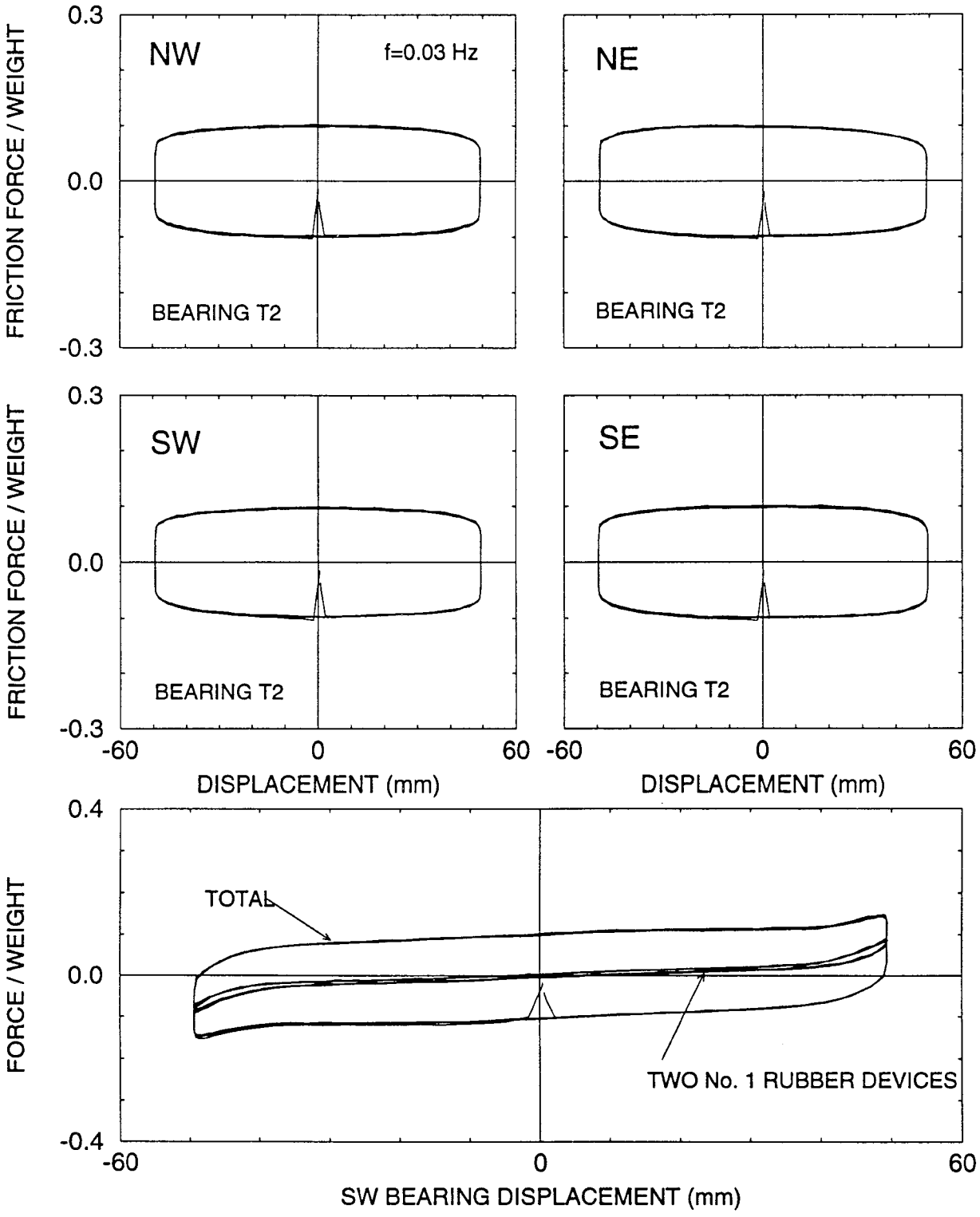

Figure 3-13 Friction Force and Total Force Versus Displacement Loops of System with Four Medium Friction (T2) Bearings and Two Low Stiffness (No. 1) Rubber Devices.

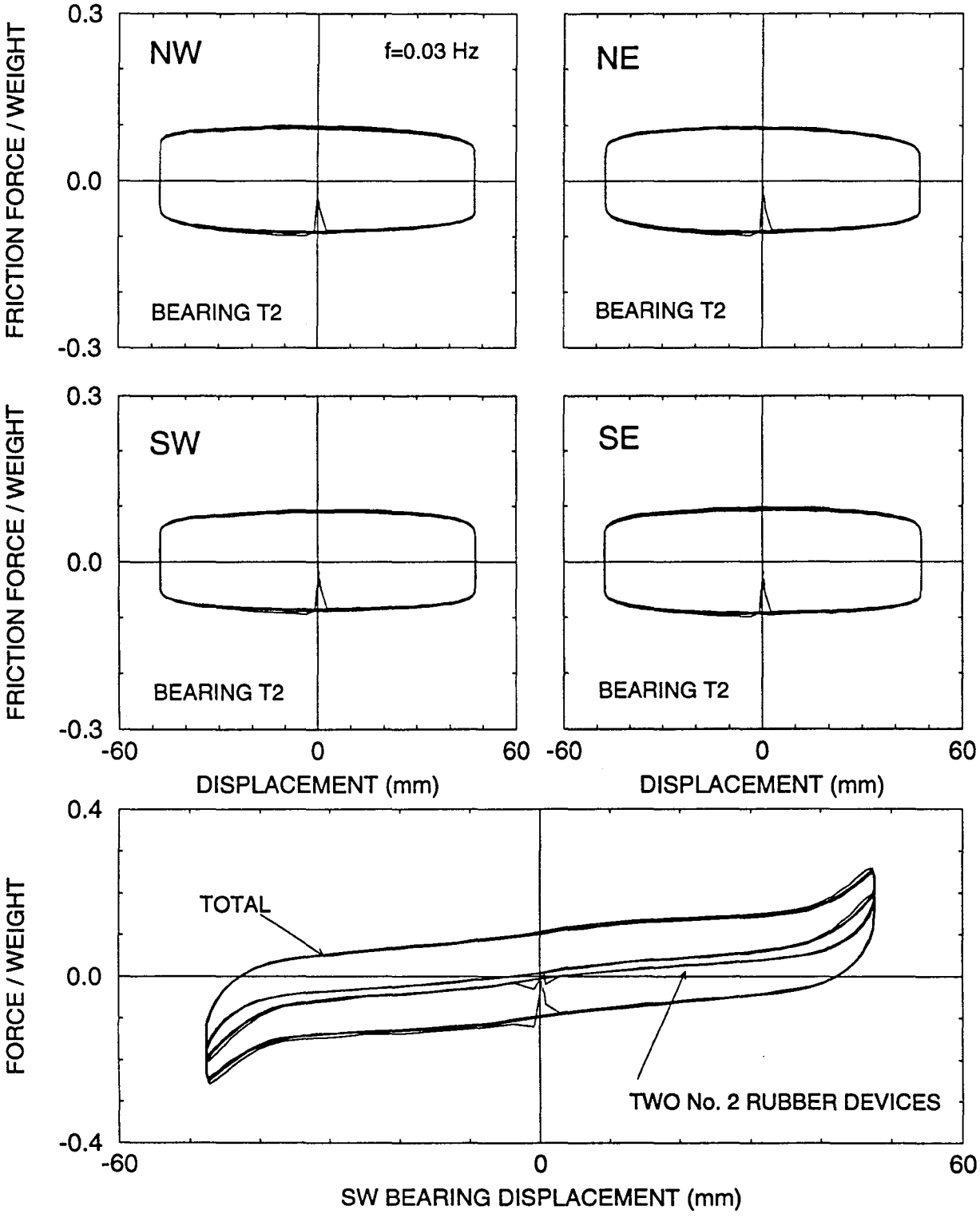

Figure 3-14 Friction Force and Total Force Versus Displacement Loops of System with Four Medium Friction (T2) Bearings and Two Medium Stiffness (No. 2) Rubber Devices.

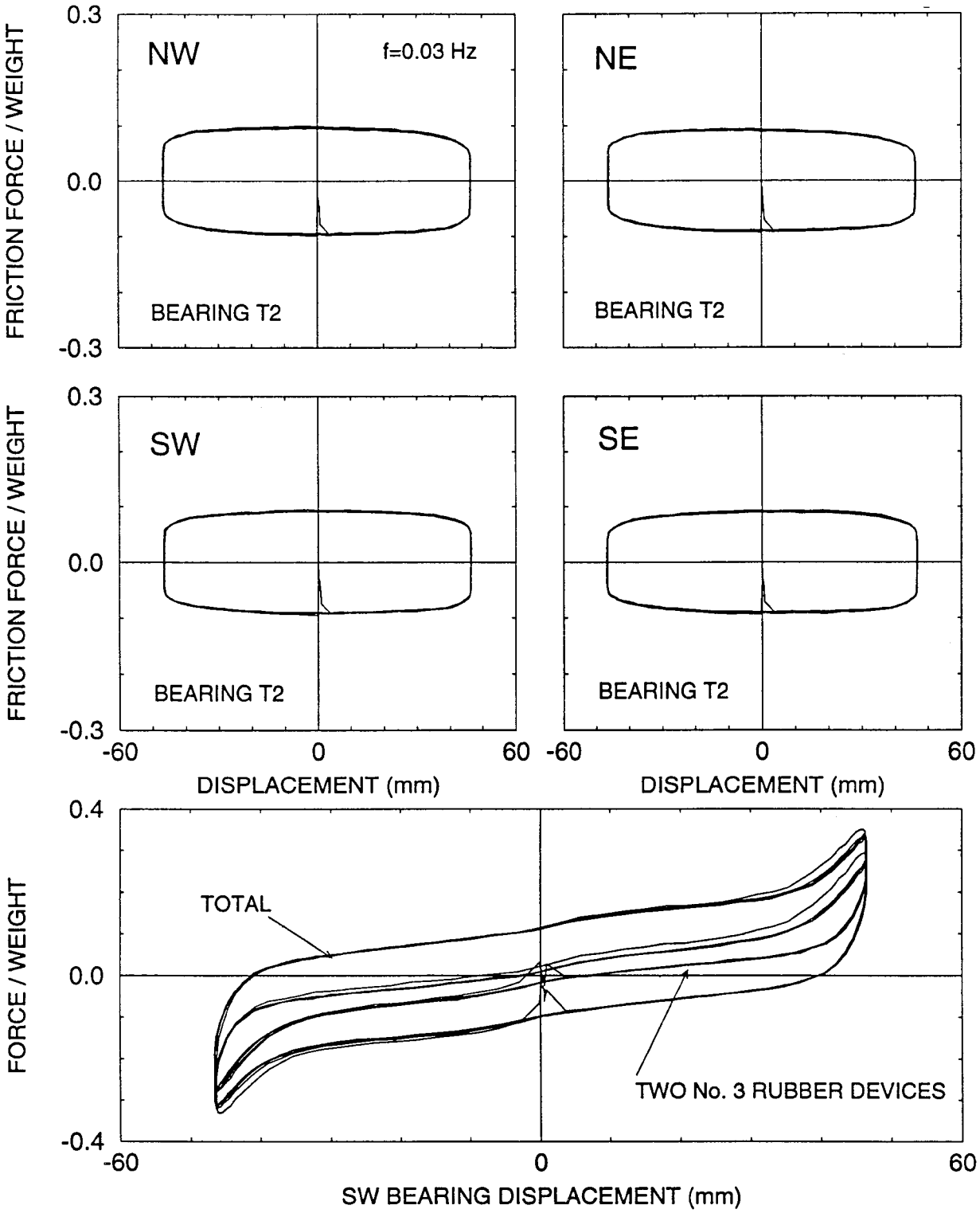

Figure 3-15 **Friction Force and Total Force Versus Displacement Loops of System with Four Medium Friction (T2) Bearings and Two High Stiffness (No. 3) Rubber Devices.**

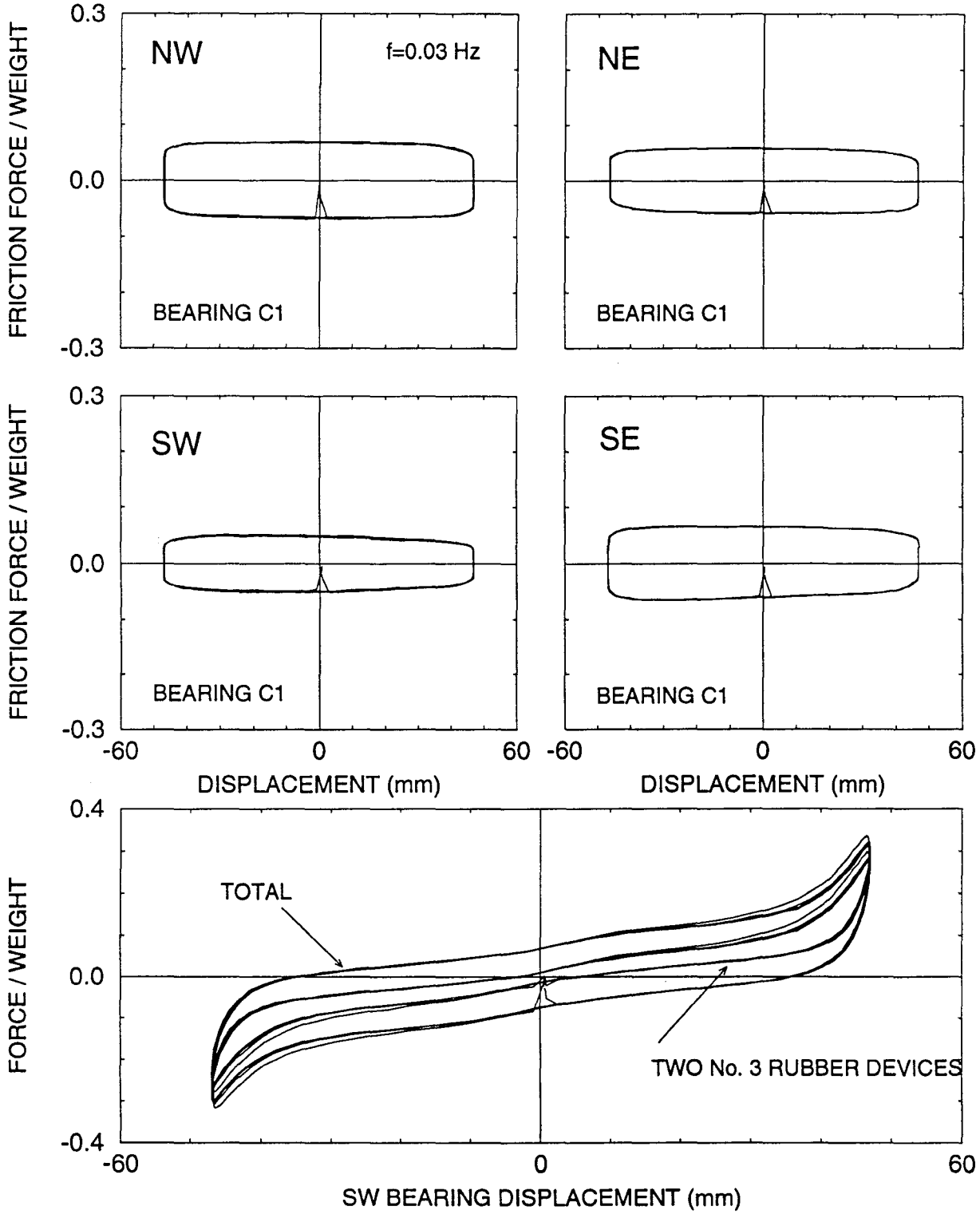

Figure 3-16 Friction Force and Total Force Versus Displacement Loops of System with Four Low Friction (C1) Bearings and Two High Stiffness (No. 3) Rubber Devices.

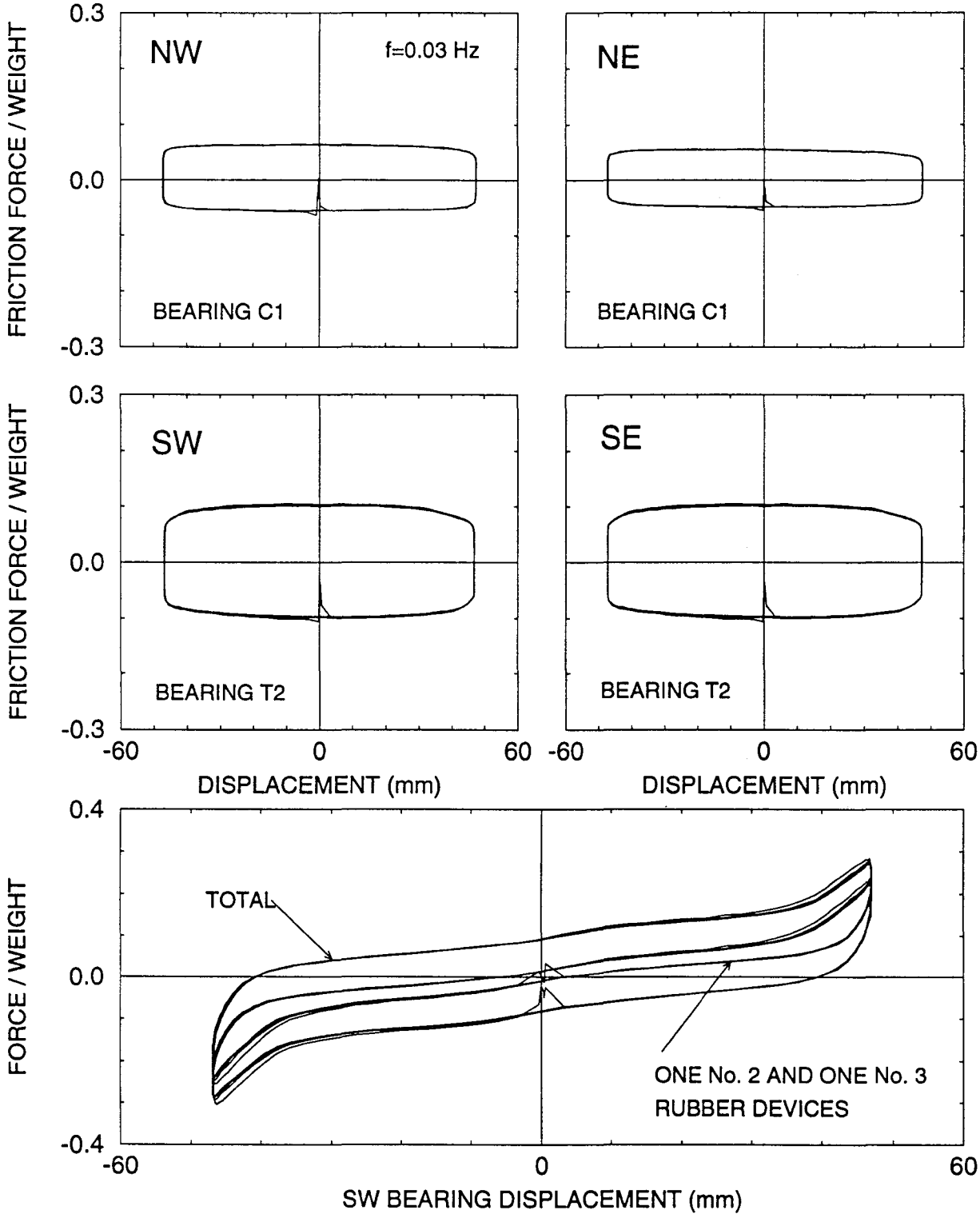

Figure 3-17 Friction Force and Total Force Versus Displacement Loops of System with Two Low Friction (C1) Bearings and One Medium Stiffness (No. 2) Rubber Device at the North Pier and Two Medium Friction (T2) Bearings and One High Stiffness (No. 3) Rubber Device at the South Pier.

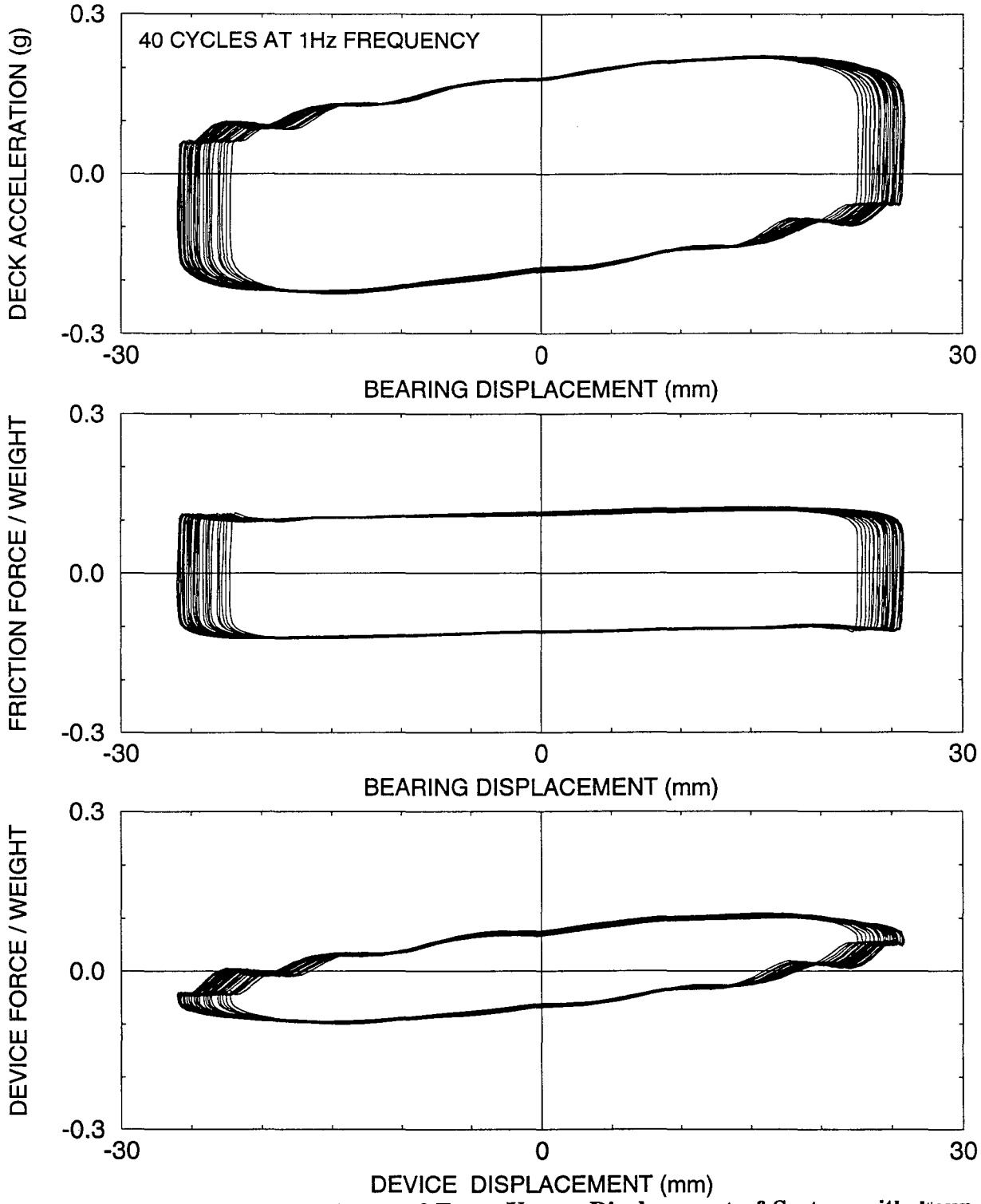

Figure 3-18 Recorded Loops of Force Versus Displacement of System with Four High Friction (T1) Bearings, Two Medium Stiffness (No. 2) Rubber Devices and Four Fluid Dampers in Test with Harmonic Motion at 1Hz (Device Force = Combined Force in Rubber Devices and Fluid Dampers).

SECTION 4

MODEL FOR EARTHQUAKE SIMULATOR TESTING

4.1 Bridge Model

The bridge model was designed to have flexible piers so that under non-isolated conditions the fundamental period of the model in the longitudinal direction is 0.25s (or 0.5s in prototype scale).

The bridge model is shown in Figure 4-1. At quarter length scale, it had a clear span of 4.8m (15.7 feet), height of 2.53m (8.3 feet) and total weight of 157.8 kN (35.5 kips). The deck consisted of two AISC W14x90 sections which were transversely connected by beams. Additional steel and lead weights were added to reach the model deck weight of 143 kN (32.1 kips), as determined by the similitude requirements. Each pier consisted of two AISC TS 6 x 6 x 5/16 columns with a top made of a channel section which was detailed to have sufficient torsional rigidity. The tube columns were connected to beams which were bolted to a concrete extension of the shake table. In this configuration, the column loads were transferred at a point located 0.57 m (1.87 ft) beyond the edge of the shake table. While the overhangs of the concrete shake table extension could safely carry the column load of over 80 kN (18 kips), they had some limited vertical flexibility which during seismic testing resulted in vertical motion of the piers and the supported deck.

The piers were designed to have in their free standing cantilever position a period of 0.1 s (0.2 s in prototype scale) when fully loaded (load cells and bottom part of bearings). Furthermore, the piers were detailed to yield under the combined effects of gravity load (40 kN each column) and 50 percent of the gravity load applied as horizontal load at each bearing location. The stiffness of each pier was verified by pulling the piers against each other on the shake table. During the test the piers were also proof-loaded to their rated capacity and the results were used to calibrate the strain gage load cell of each column.

Identification of the model was conducted by exciting the shake table with a 0-20 Hz banded white noise of 0.03g peak acceleration. Acceleration transfer functions of each

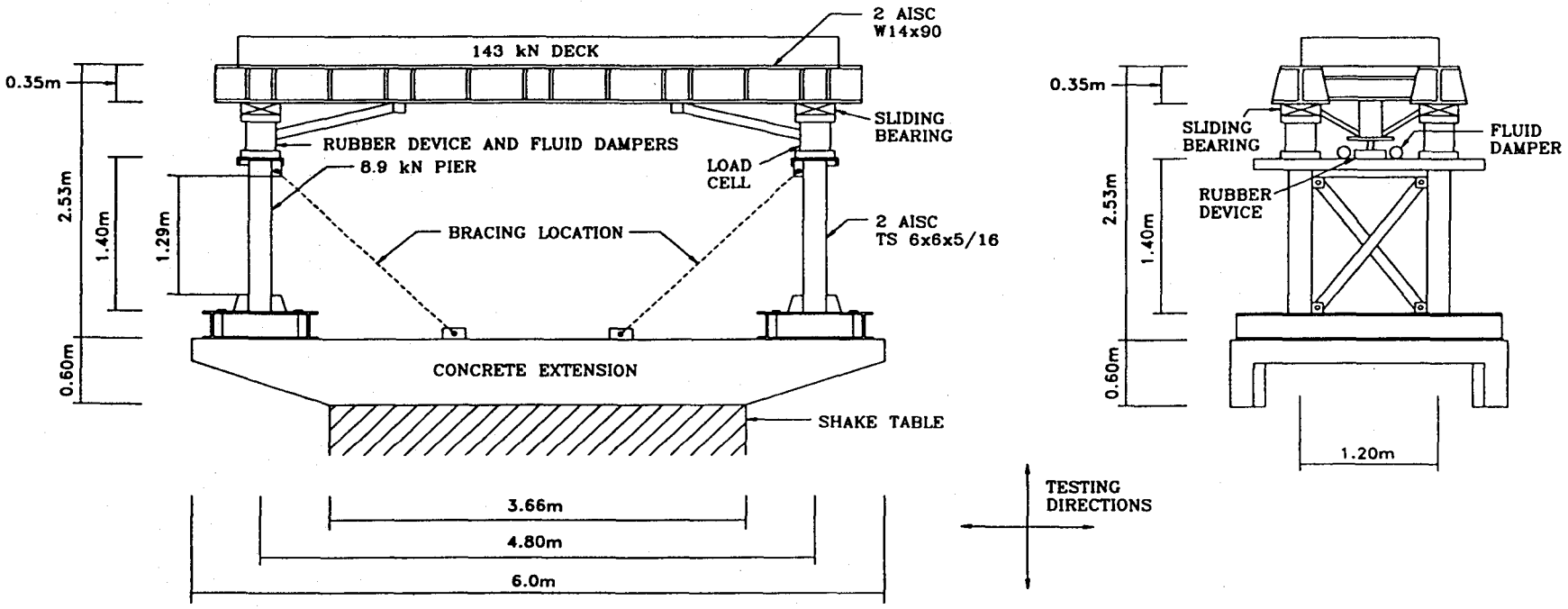

Figure 4-1 Schematic of Quarter Scale Bridge Model.

free standing pier and of the assembled bridge model with all bearings fixed against translational movement (but not rotation) revealed the following properties: fundamental period of free standing pier equal to 0.096s and fundamental period of non-isolated bridge in the longitudinal direction equal to 0.26s. These values are in excellent agreement with the design values of 0.1s and 0.25s, respectively.

Damping in the model was estimated to be 0.015 of critical for the free standing piers and 0.02 of critical for the entire model in its non-isolated condition. Identification tests of the model were also conducted with white noise input of 0.1g peak table acceleration to obtain a fundamental period of 0.25s and corresponding damping ratio of 0.04 of critical. The increased damping was the result of hysteretic action, not in the columns of the model but in the overhangs of the concrete extension of the shake table. During shake table testing of the non-isolated model, the recorded loops of shear force versus displacement of the piers displayed hysteretic action (see Section 5). Estimates of damping ratio from these loops were in the range of 0.04 to 0.08 of critical. Thus while the columns of the piers remained elastic, the pier system displayed realistic hysteretic action with equivalent damping ratio of at least 5 percent of critical.

The design of the model bridge was based in the similitude laws for artificial mass simulation (Sabnis 1983). A summary of the scale factors in the model is presented in Table 4-I.

4.2 Instrumentation

The instrumentation consisted of load cells, accelerometers and displacement transducers. Figure 4-2 shows the overall instrumentation diagram, whereas Figures 4-3 and 4-4 show the instrumentation diagrams for accelerometers and displacement transducers, respectively. A list of monitored channels and their corresponding descriptions are given in Table 4-II. A total of 53 channels were monitored.

Table 4-I : Summary of Scale Factors in Bridge Model

QUANTITY	DIMENSION	SCALE FACTOR[1]
Linear Dimension	L	4
Displacement	L	4
Velocity	LT^{-1}	2
Acceleration	LT^{-2}	1
Time	T	2
Frequency	T^{-1}	0.5
Force	F	16
Pressure	FL^{-2}	1
Strain	---	1

[1] PROTOTYPE/MODEL

4.3 Test Configurations

Testing of the bridge model was performed in five different bridge configurations and seven different isolation system configurations. Figure 4-5 shows the five bridge configurations. They were :

(1) The sliding bearings were locked by side plates to represent a non-isolated bridge, as shown in Figure 4-6. In this configuration, the structure was identified in tests with banded white noise table motion. Furthermore, a selected number of seismic tests was conducted.

(2) Braces were installed to stiffen the piers (see Figure 4-7) and the deck was connected by stiff rods to a nearby reaction wall. In this configuration, the shake table was driven in displacement-controlled mode with specified frequency and amplitude of harmonic motion. This motion was nearly the motion experienced by the sliding bearings. Loops of bearing horizontal force versus bearing dispacement were recorded and used to extract the frictional properties of the sliding bearings.

(3) Both piers were stiffened by braces so that they represented stiff abutments. In this configuration, the model resembled a single span isolated bridge (see Figure 4-7).

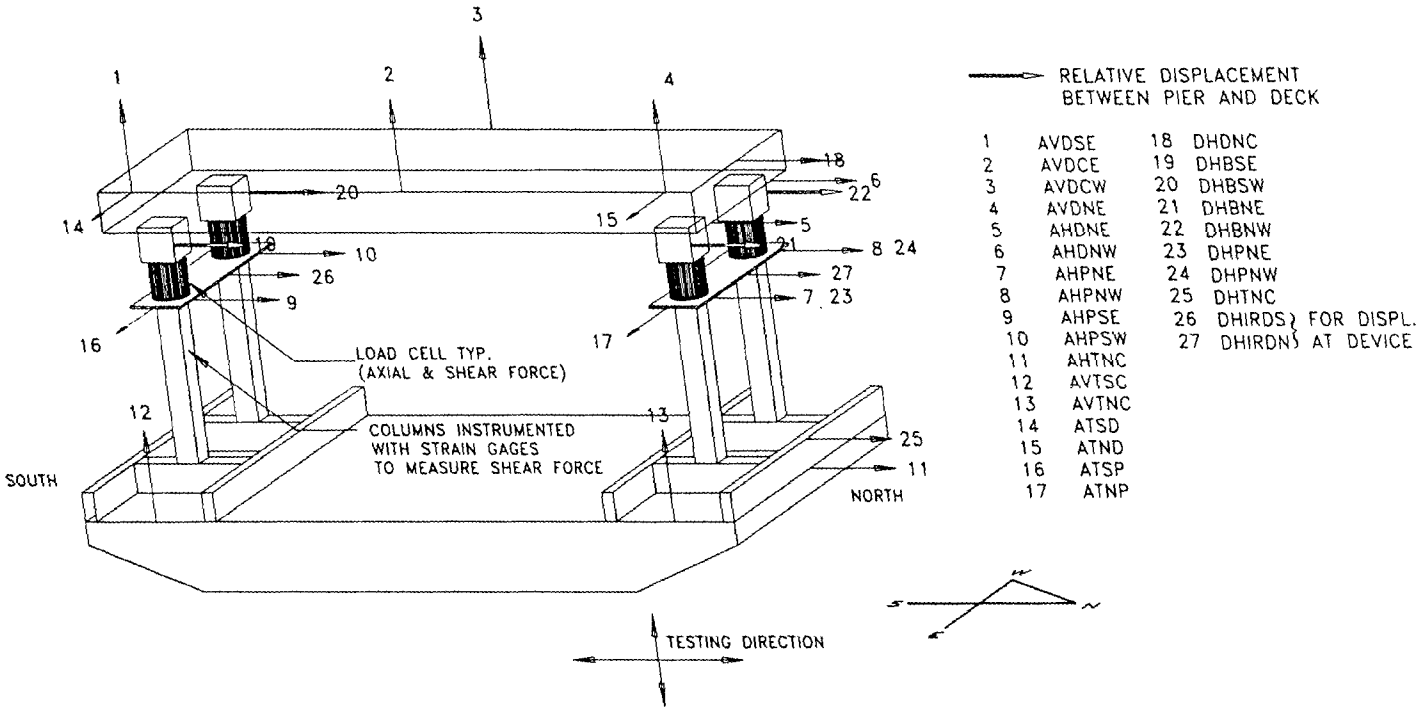

Figure 4-2 Overall Instrumentation Diagram.

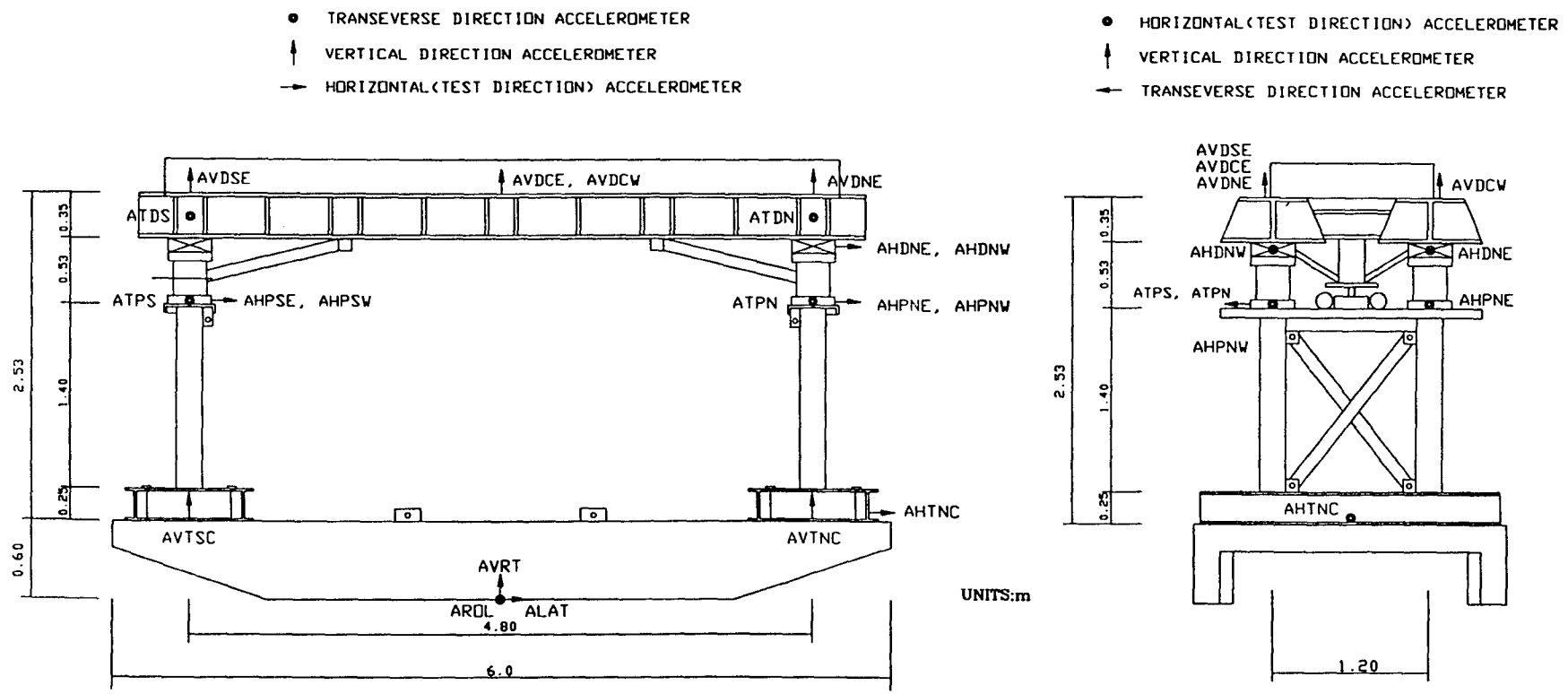

Figure 4-3 Location of Accelerometers (Units:m)

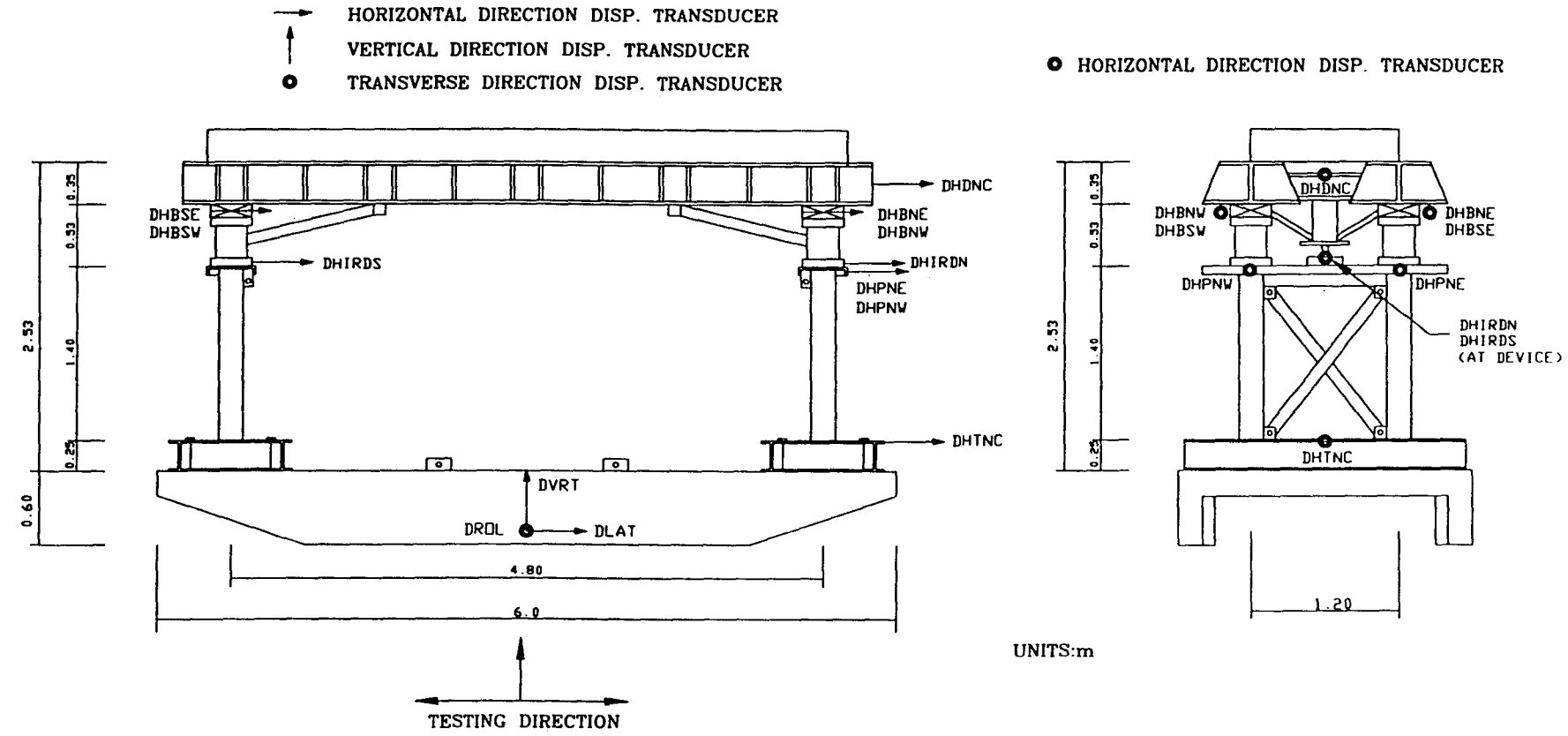

Figure 4-4 Location of Displacement Transducers (Units:m)

Table 4-II List of Channels (with reference to Figures 4-2 to 4-4)

CHANNEL	NOTATION	INSTRUMENT	RESPONSE MEASURED
1	AVDSE	ACCL	Deck Vertical Accel.-South East Corner
2	AVDCE	ACCL	Deck Vertical Accel.-East Side at Center
3	AVDCW	ACCL	Deck Vertical Accel.-West Side at Center
4	AVDNE	ACCL	Deck Vertical Accel.-North East Corner
5	AHDNE	ACCL	Deck Horizontal Accel.-North East Corner
6	AHDNW	ACCL	Deck Horizontal Accel.-North West Corner
7	AHPNE	ACCL	Pier Horizontal Accel.-North East
8	AHPNW	ACCL	Pier Horizontal Accel.-North West
9	AHPSE	ACCL	Pier Horizontal Accel.-South East
10	AHPSW	ACCL	Pier Horizontal Accel.-South West
11	AHTNC	ACCL	Table Horizontal Accel.-North Side at Center
12	AVTSC	ACCL	Table Vertical Accel.-South Side at Center
13	AVTNC	ACCL	Table Vertical Accel.-North Side at Center
14	ATSD	ACCL	Deck Transverse Accel.-South Side
15	ATND	ACCL	Deck Transverse Accel.-North Side
16	ATSP	ACCL	Pier Transverse Accel.-South
17	ATNP	ACCL	Pier Transverse Accel.-North
18	DHDNC	DT	Deck Total Horizontal Displ.-North Side Center
19	DHBSE	DT	Bearing Horizontal Displ.-South East
20	DHBSW	DT	Bearing Horizontal Displ.-South West
21	DHBNE	DT	Bearing Horizontal Displ.-North East
22	DHBNW	DT	Bearing Horizontal Displ.-North West
23	DHPNE	DT	Pier Total Horizontal Displ.-North East
24	DHPNW	DT	Pier Total Horizontal Displ.-North West
25	DHTNC	DT	Table Horizontal Displ.-North Side at Center
26	DHIRDS	DT	Displacement of South Pier Rubber Device
27	DHIRDN	DT	Displacement of North Pier Rubber Device
28	DHBAV	DT	Bearing Horizontal Average Displ.
29	DLAT	DT	Table Horizontal Displ.
30	ALAT	ACCL	Table Horizontal Accel.
31	DVRT	DT	Table Vertical Displ.
32	AVRT	ACCL	Table Vertical Accel.
33	DROL	DT	Table Rolling Displ.
34	AROL	ACCL	Table Rolling Accel.

ACCEL=Accelerometer, DT=Displacement Transducer

Table 4-II (Cont'd)

CHANNEL	NOTATION	INSTRUMENT	RESPONSE MEASURED
35	SX1	LOAD CELL	Shear Bearing Force-South West
36	SX2	LOAD CELL	Shear Bearing Force-South East
37	SX3	LOAD CELL	Shear Bearing Force-North West
38	SX4	LOAD CELL	Shear Bearing Force-North East
39	SCNE	LOAD CELL	Column Shear Force-North East
40	SCSE	LOAD CELL	Column Shear Force-South East
41	SCNW	LOAD CELL	Column Shear Force-North West
42	SCSW	LOAD CELL	Column Shear Force-South West
43	N1SW	LOAD CELL	Axial Bearing Force-South West
44	N2SE	LOAD CELL	Axial Bearing Force-South East
45	N3NW	LOAD CELL	Axial Bearing Force-North West
46	N4NE	LOAD CELL	Axial Bearing Force-North East
47	SCN	LOAD CELL	Average Column Shear Force-North
48	SCS	LOAD CELL	Average Column Shear Force-South
49	DHDSW	DT	Deck Total Horizontal Displ.-South West Corner
50	DHDSE	DT	Deck Total Horizontal Displ.-South East Corner
51	LCNE	LOAD CELL	East Friction Force-North East Corner(ID-test)
52	LCNW	LOAD CELL	West Friction Force-North West Corner(ID-Test)
53	LCTOT	LOAD CELL	Average Friction Force(ID-Test)

ACCEL=Accelerometer, DT=Displacement Transducer

(4) The south location pier was stiffened by braces so that it represented a stiff abutment. In this configuration, the model resembled a two-span bridge with two stiff abutments and a centrally located flexible pier. A view of this configuration on the shake table is shown in Figure 4-8.

(5) A configuration with two flexible piers which resembled portion of a multiple span bridge between expansion joints. A view of this configuration on the shake table is shown in Figure 4-9.

The seven isolation system configurations were identified in Section 3.5. Views of the isolation system with details of installation of the various components are shown in Figures 4-10 and 4-11. A total of 351 seismic tests were conducted with a variety of

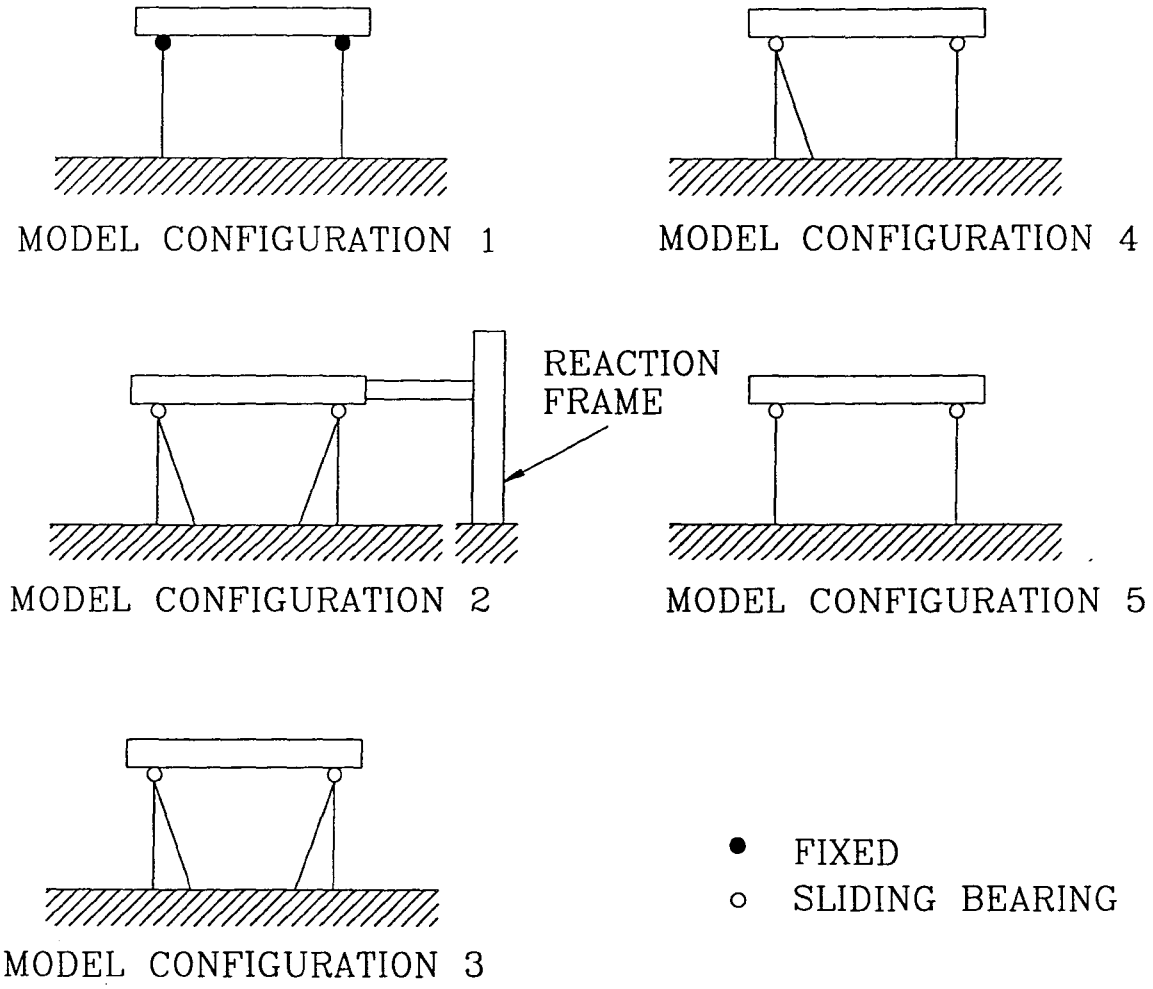

Figure 4-5 **Model Configurations in Testing (1:Non-isolated Bridge, 2:Identification of Frictional Properties, 3:Single Span Model, 4:Two-Span Model, 5:Multiple Span Model).**

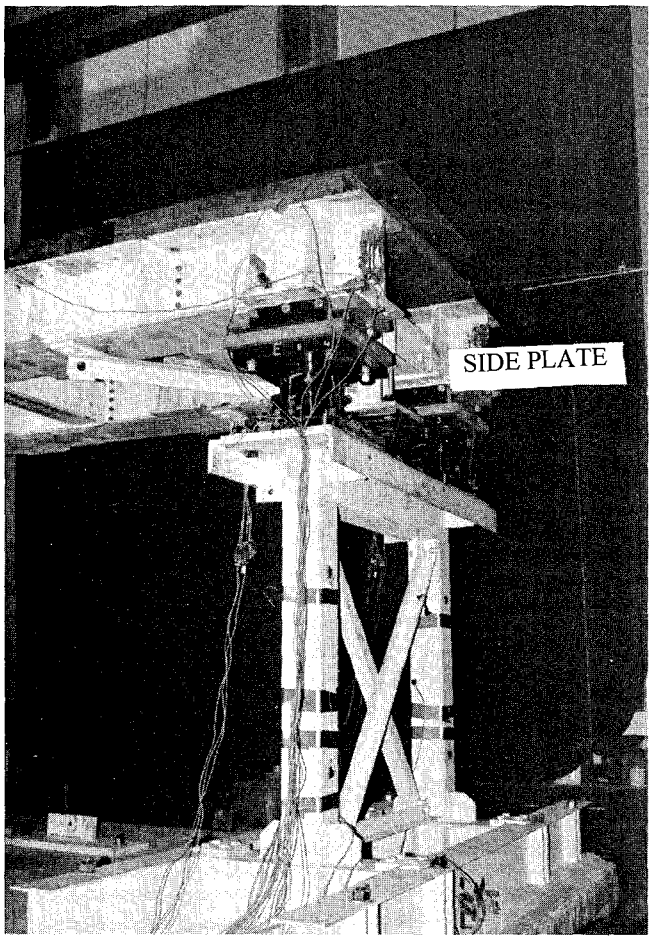

Figure 4-6 View of Bridge Model with Sliding Bearings Locked by Side Plates (Configuration No. 1).

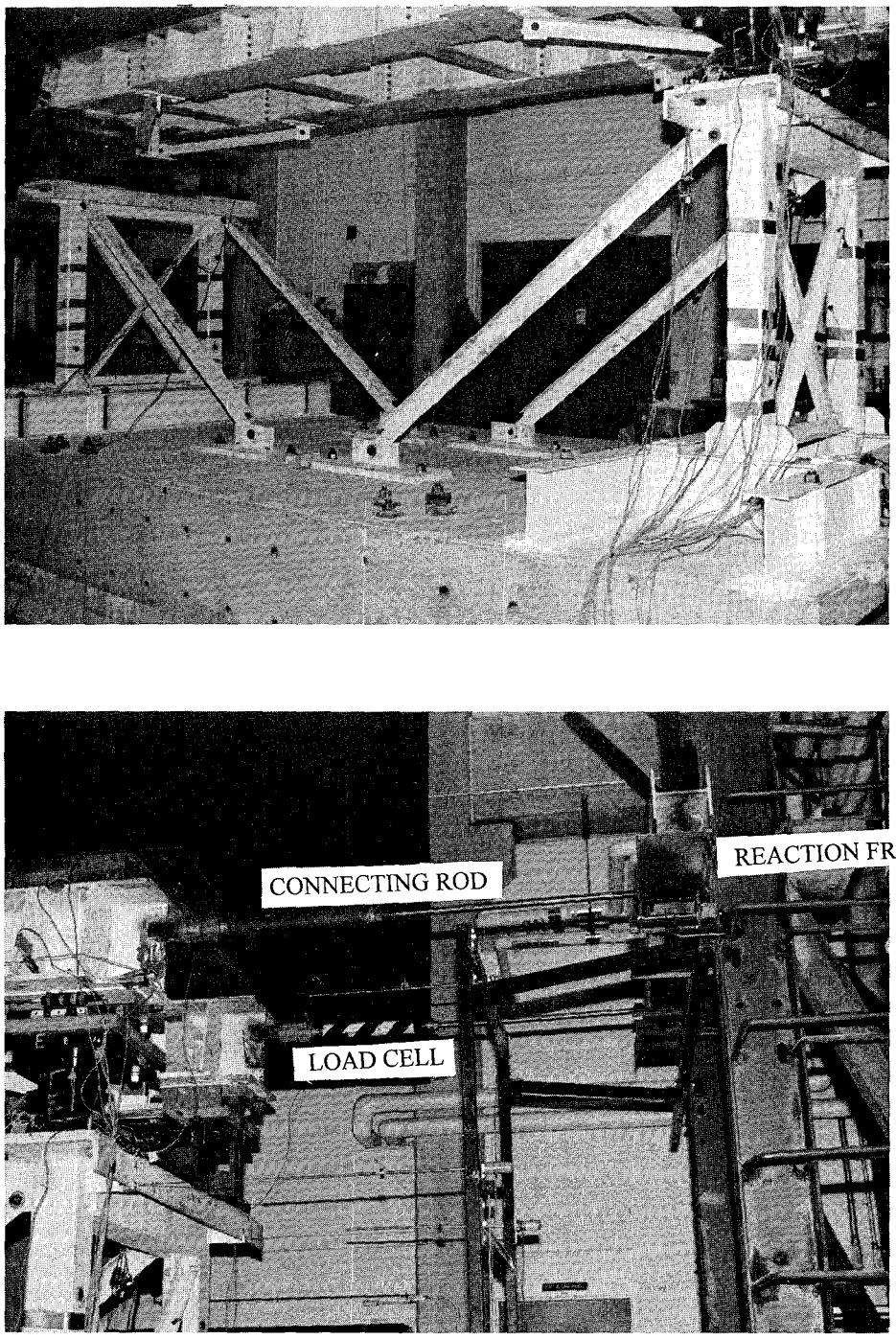

Figure 4-7 Views of Bridge Model in Configuration No. 2 (Identification of Frictional Properties of Sliding Bearings).

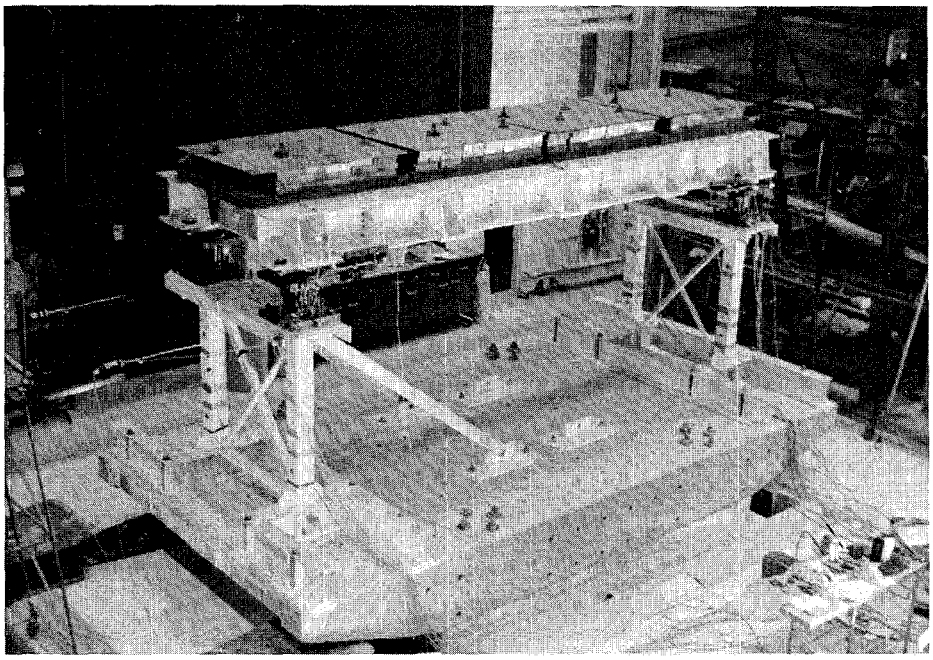

Figure 4-8 View of Bridge Model with One Flexible Pier and One Stiff Pier.

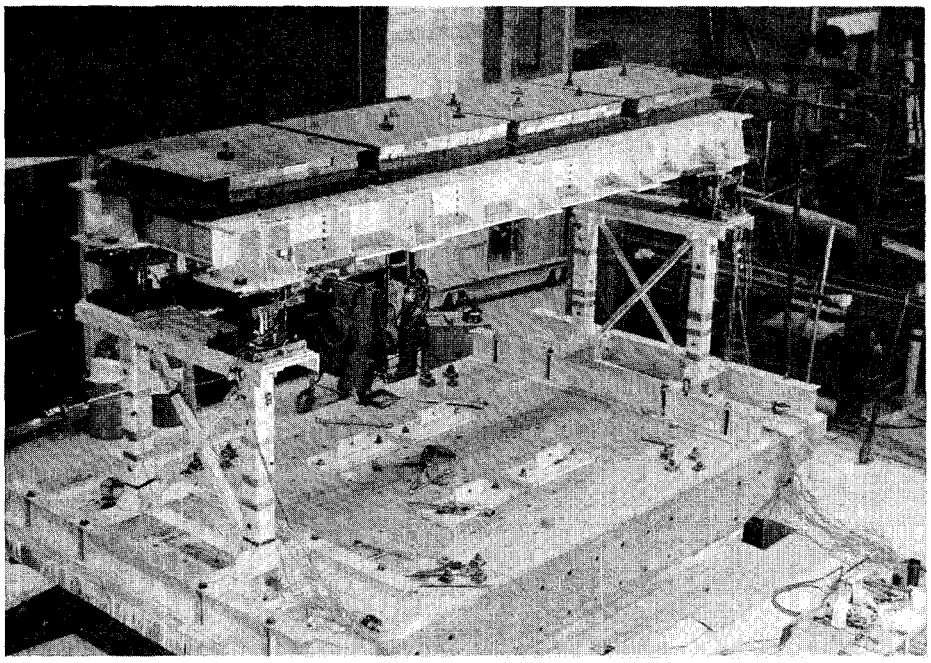

Figure 4-9 View of Bridge Model in Configuration with Two Flexible Piers.

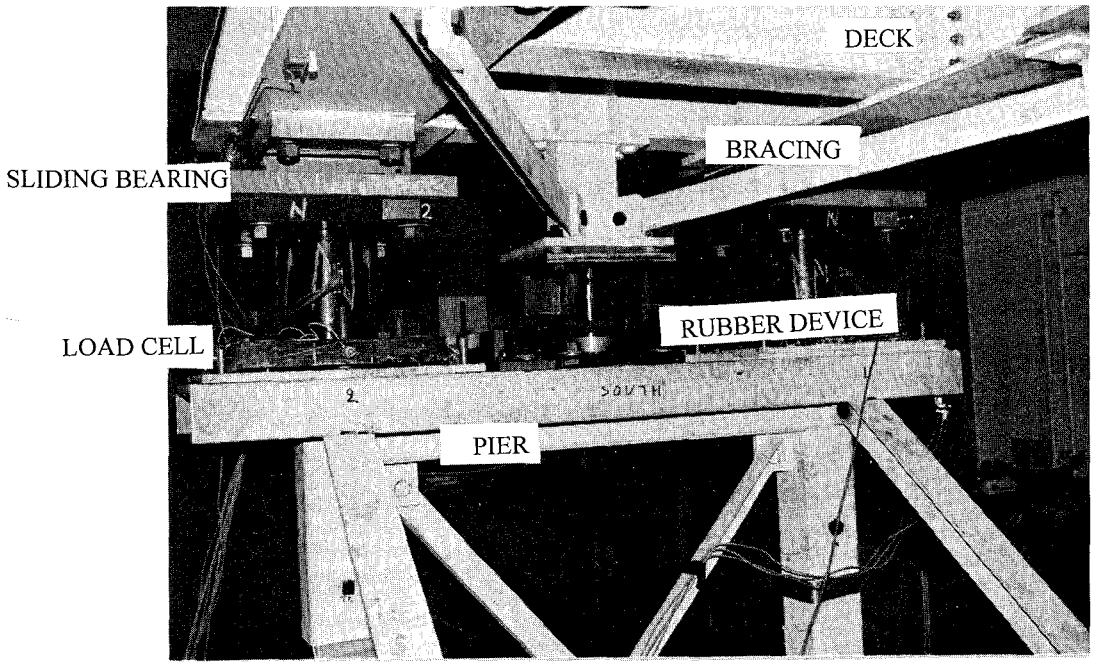

Figure 4-10 View of Isolation System Consisting of Sliding Bearings and Rubber Devices.

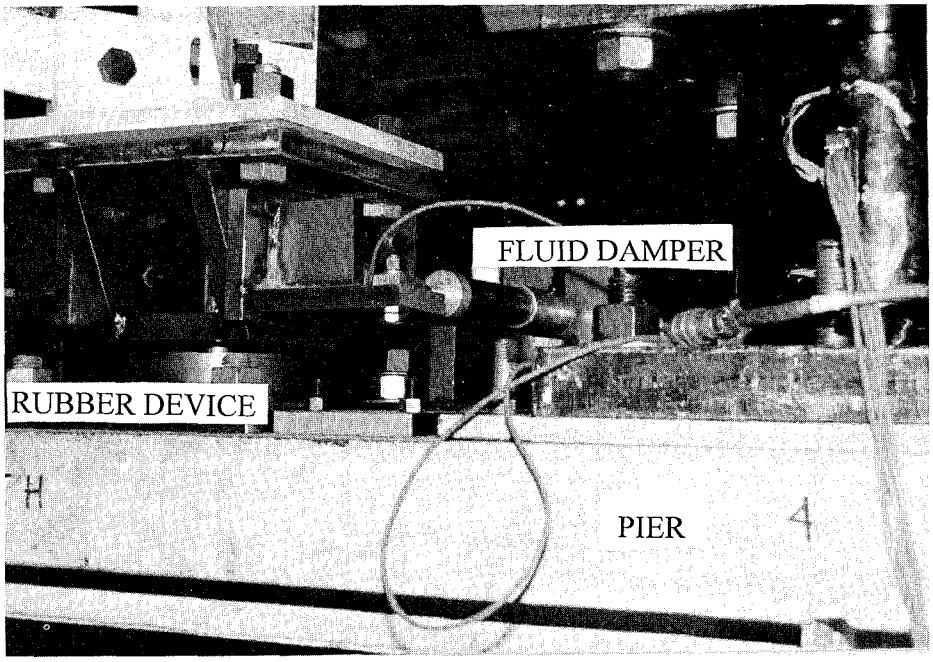

Figure 4-11 View of Isolation System with Details of the Installation of Fluid Dampers.

combinations of isolation system properties and bridge configurations. These combinations are listed in Table 4-III.

4.4 Test Program

A total of 351 earthquake simulation tests were performed on the model bridge. Tests were conducted with only horizontal input and with combined horizontal and vertical input. The earthquake signals and their characteristics are listed in Table 4-IV. The earthquake signals consisted of historic earthquakes and artificial motions compatible with:

(a) The Japanese bridge design spectra for Level 1 and Level 2 and ground conditions 1 (rock), 2 (alluvium) and 3 (deep alluvium) (CERC 1992). In Japan, it is required that bridges are designed for two levels of seismic loading. In Level 1 seismic loading, it is required that the bridge remains undamaged and fully elastic. In Level 2 seismic loading, inelastic behavior is permitted. Tables 4-V and 4-VI describe the shapes of the 5%-damped acceleration spectra of the Japanese Level 1 and 2 motions.

(b) The California Department of Transportation (CalTrans) bridge spectra (Gates 1979). These motions were identical to those used in the testing of another bridge model by Constantinou, 1991a.

(c) Site specific spectra for a location in Boston, Massachusetts.

Each record was compressed in time by a factor of two to satisfy the similitude requirements. Figure 4-12 to 4-31 show recorded time histories of the table motion in tests with input being the earthquake signals of Table 4-IV. The acceleration and displacement records were directly measured, whereas the velocity record was obtained by numerical differentiation of the displacement record. It may be observed that the peak ground motion was reproduced well, but not exactly, by the table generated motion.

Table 4-III Bridge and Isolation System Configurations

TEST No.	NUMBER OF TESTS	PIER CONDITION		SLIDING BEARINGS (Type)		RUBBER RESTORING FORCE DEVICES (stiffness)		FLUID VISCOUS DAMPERS (Number)	
		SOUTH	NORTH	SOUTH PIER	NORTH PIER	SOUTH PIER	NORTH PIER	SOUTH PIER	NORTH PIER
IRDRUN01-26	26	STIFF	STIFF	T1	T1	Medium	Medium	0	0
IRDRUN27-65	39	FLEXIBLE	FLEXIBLE	T1	T1	Medium	Medium	0	0
DRDRUN01-14	14	FLEXIBLE	FLEXIBLE	T1	T1	Medium	Medium	2	2
RD2RUN01-34	34	STIFF	STIFF	T2	T2	Medium	Medium	0	0
RD2RUN35-67	33	FLEXIBLE	FLEXIBLE	T2	T2	Medium	Medium	0	0
RHHRUN01-27	27	STIFF	STIFF	T2	T2	High	High	0	0
RHHRUN28-65	38	FLEXIBLE	FLEXIBLE	T2	T2	High	High	0	0
RSSRUN01-27	27	STIFF	STIFF	T2	T2	Low	Low	0	0
RSSRUN28-59	32	FLEXIBLE	FLEXIBLE	T2	T2	Low	Low	0	0
RMLRUN01-18	18	STIFF	FLEXIBLE	T2	C1	High	Medium	0	0
RMLRUN19-36	18	FLEXIBLE	FLEXIBLE	T2	C1	High	Medium	0	0
RLLRUN01-23	23	STIFF	STIFF	C1	C1	High	High	0	0
RLLRUN24-45	22	FLEXIBLE	FLEXIBLE	C1	C1	High	High	0	0

Table 4-IV Earthquake Motions Used in Test Program and Characteristics in Prototype Scale

NOTATION	RECORD	PEAK ACC. (g)	PEAK VEL. (mm/sec)	PEAK DIS. (mm)
EL CENTRO S00E	Imperial Valley, May 18 1940, Component S00E	0.34	334.50	108.70
TAFT N21E	Kern County, July 21,1952, Component N21E	0.16	157.20	67.10
MEXICO S90W	Mexico City, September 19, 1985 SCT building, Component N90W	0.17	605.00	212.00
PACOIMA S16E	San Fernando, February 9, 1971, Component S16E	1.17	1132.30	365.30
PACOIMA S74W	San Fernando, February 9, 1971, Component S74E	1.08	568.20	108.20
HACHINOHE N-S	Tokachi, Japan, May 16, 1968 Hachinohe, Component N-S	0.23	357.10	118.90
MIYAGIKEN OKI	Miyaki, Japan, June 12, 1978 Ofunato-Bochi, Component E-W	0.16	141.00	50.80
AKITA N-S	Nihonkai Chuubu, Japan, May 23, 1983 Component N-S	0.19	292.00	146.00
JP. L1G1	Artificial Compatible with Japanese Level 1 Ground Condition 1	0.10	215.00	90.00
JP. L1G2	Artificial Compatible with Japanese Level 1 Ground Condition 2	0.12	251.00	69.00
JP. L1G3	Artificial Compatible with Japanese Level 1 Ground Condition 3	0.14	274.00	132.00
JP. L2G1	Artificial Compatible with Japanese Level 2 Ground Condition 1	0.37	864.00	526.00
JP. L2G2	Artificial Compatible with Japanese Level 2 Ground Condition 2	0.43	998.00	527.00
JP. L2G3	Artificial Compatible with Japanese Level 2 Ground Condition 3	0.45	1121.00	700.00
CALTRANS 0.6g A2	Artificial Compatible with CalTrans 0.6g 80'-150'Alluvium Spectrum, No.2	0.60	836.40	282.90
CALTRANS 0.6g S2	Artificial Compatible with CalTrans 0.6g 10'-80'Alluvium Spectrum, No.2	0.60	765.00	248.90
CALTRANS 0.6g S3	Artificial Compatible with CalTrans 0.6g 10'-80'Alluvium Spectrum, No.3	0.60	778.00	438.90
CALTRANS 0.6g R1	Artificial Compatible with CalTrans 0.6g Rock Spectrum, No.1	0.60	530.90	443.80
CALTRANS 0.6g R2	Artificial Compatible with CalTrans 0.6g Rock Spectrum, No.2	0.60	510.00	274.30
CALTRANS 0.6g R3	Artificial Compatible with CalTrans 0.6g Rock Spectrum, No.3	0.60	571.00	342.40
BOSTON 1	Artificial Compatible with a Site in Boston, No. 1	0.15	123.50	26.30
BOSTON 2	Artificial Compatible with a Site in Boston, No. 2	0.15	110.10	25.10
BOSTON 3	Artificial Compatible with a Site in Boston, No. 3	0.15	99.70	21.70

Table 4-V Spectral Acceleration of Japanese Bridge Design Spectra, Level 1

G.C.	Spectral Acceleration (S_{10}) in units of cm/sec^2 as Function of Period T_i in units of seconds		
1	$T_i < 0.1$ $S_{10} = 431T_i^{1/3}$ $S_{10} \geq 160$	$0.1 \leq T_i \leq 1.1$ $S_{10}=200$	$1.1 < T_i$ $S_{10}=220/T_i$
2	$T_i < 0.2$ $S_{10} = 427T_i^{1/3}$ $S_{10} \geq 200$	$0.2 \leq T_i \leq 1.3$ $S_{10}=250$	$1.3 < T_i$ $S_{10}=325/T_i$
3	$T_i < 0.34$ $S_{10} = 430T_i^{1/3}$ $S_{10} \geq 240$	$0.34 \leq T_i \leq 1.5$ $S_{10}=300$	$1.5 < T_i$ $S_{10}=450/T_i$

Table 4-VI Spectral Acceleration of Japanese Bridge Design Spectra, Level 2

G.C.	Spectral Acceleration (S_{20}) in units of cm/sec^2 as Function of Period T_i in units of seconds		
1	$T_i \leq 1.4$ $S_{20}=700$		$1.4<T_i$ $S_{20}=980/T_i$
2	$T_i < 0.18$ $S_{20} = 1506T_i^{1/3}$ $S_{20} \geq 700$	$0.18 \leq T_i \leq 1.6$ $S_{20}=850$	$1.6 < T_i$ $S_{20}=1360/T_i$
3	$T_i < 0.29$ $S_{20} = 1511T_i^{1/3}$ $S_{20} \geq 700$	$0.29 \leq T_i \leq 2.0$ $S_{20}=1000$	$2.0 < T_i$ $S_{20}=2000/T_i$

Figures 4-12 to 4-31 also show the response spectra of acceleration of the table motions. The 5% damped acceleration spectrum is compared to the spectrum of the target record to demonstrate the good reproduction of the motion by the table.

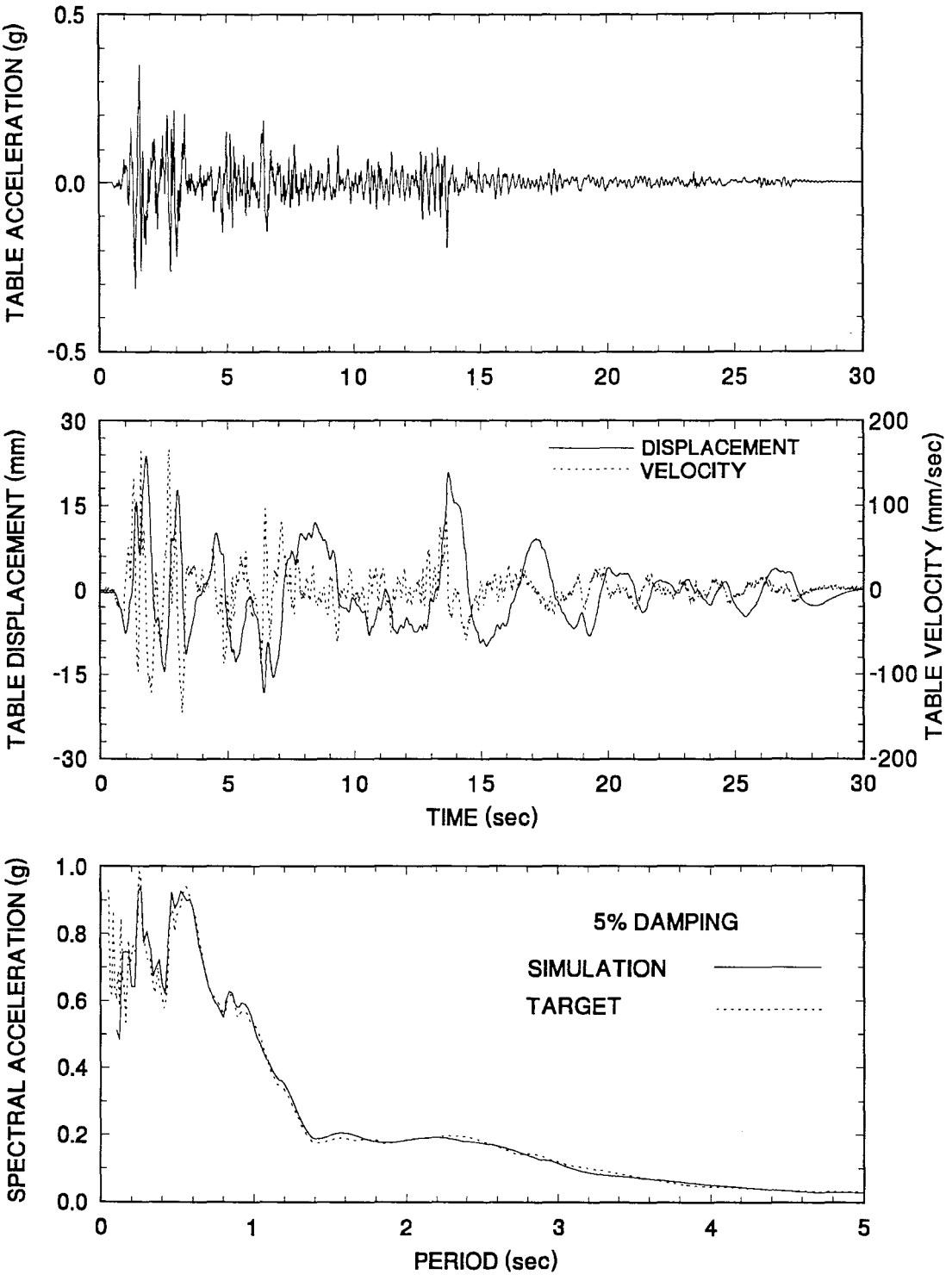

Figure 4-12 Time Histories of Displacement, Velocity and Acceleration and Acceleration Response Spectrum of Shaking Table Motion Excited with El Centro S00E 100% Motion.

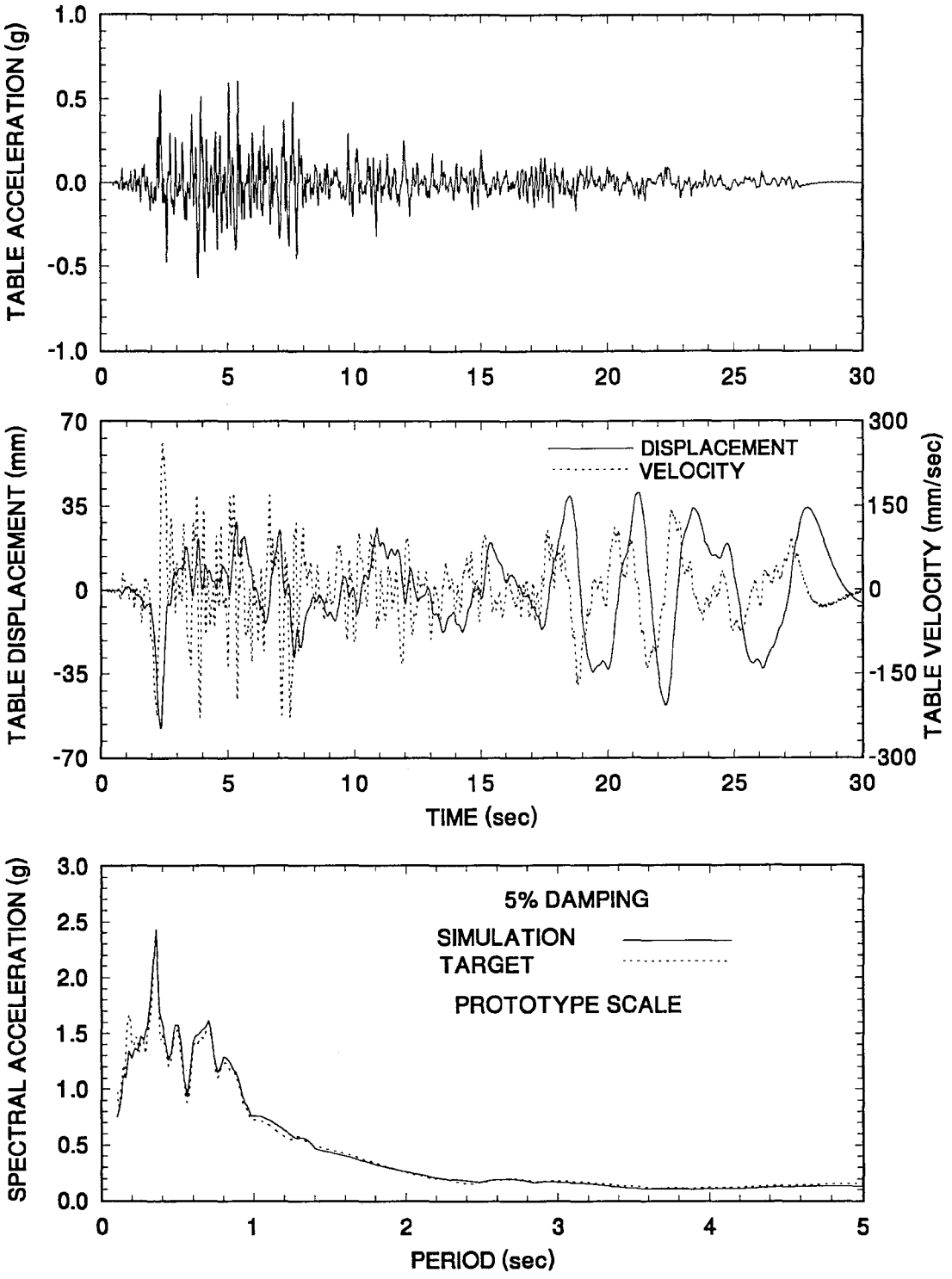

Figure 4-13 Time Histories of Displacement, Velocity and Acceleration and Acceleration Response Spectrum of Shaking Table Motion Excited with Taft N21E 400% Motion.

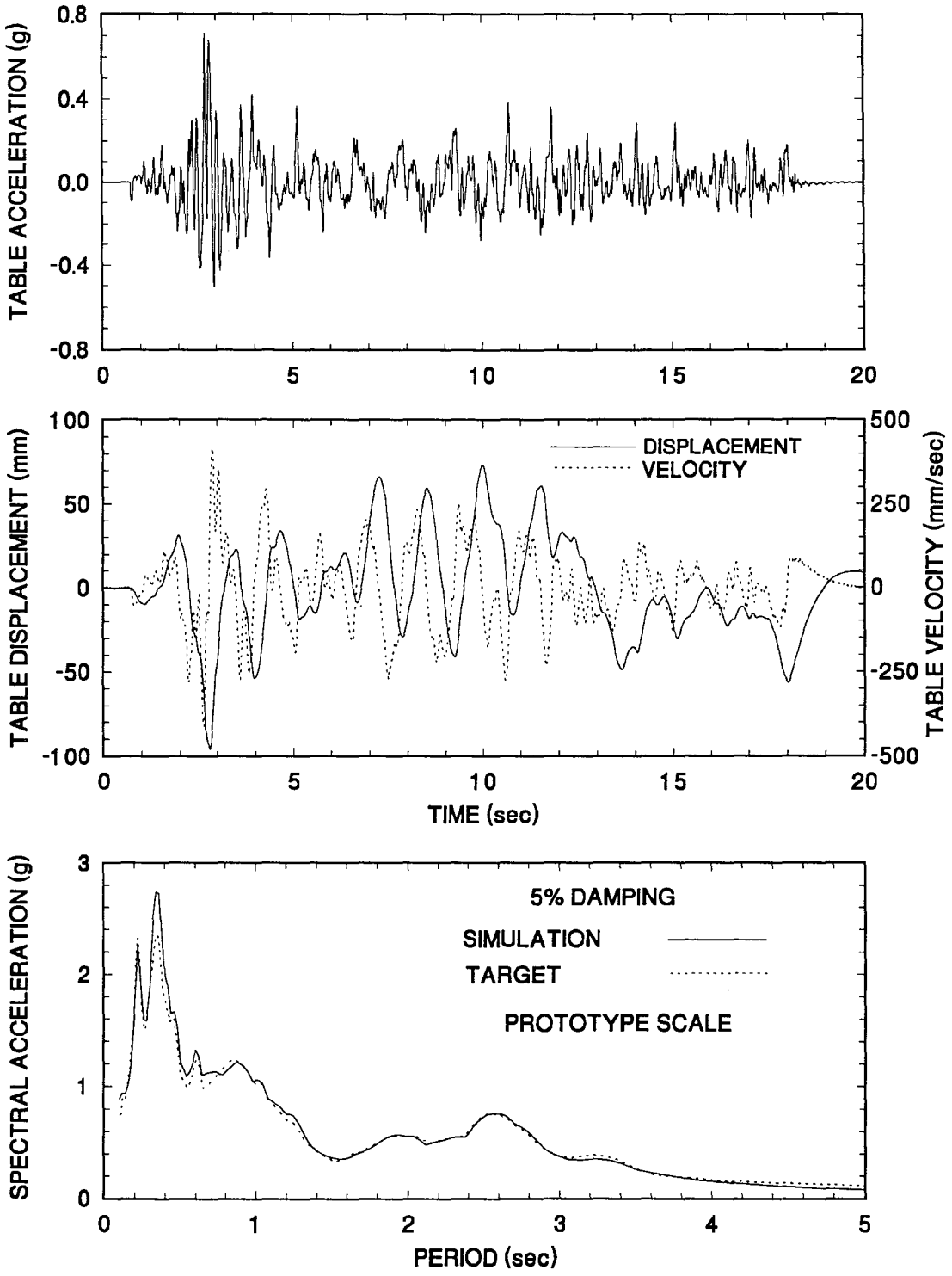

Figure 4-14 Time Histories of Displacement, Velocity and Acceleration and Acceleration Response Spectrum of Shaking Table Motion Excited with Hachinohe N-S 300% Motion.

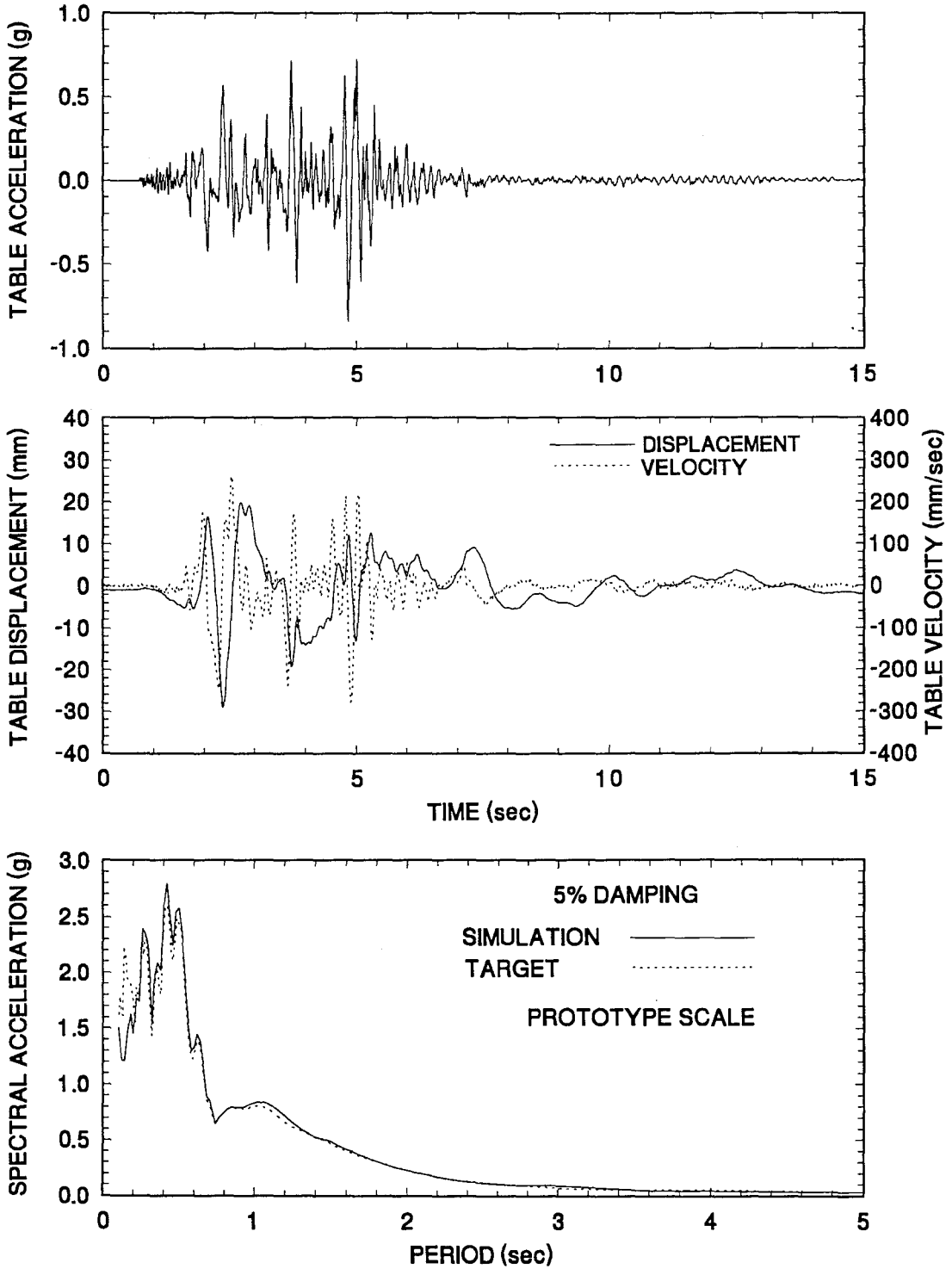

Figure 4-17 Time Histories of Displacement, Velocity and Acceleration and Acceleration Response Spectrum of Shaking Table Motion Excited with Pacoima S74W 100% Motion.

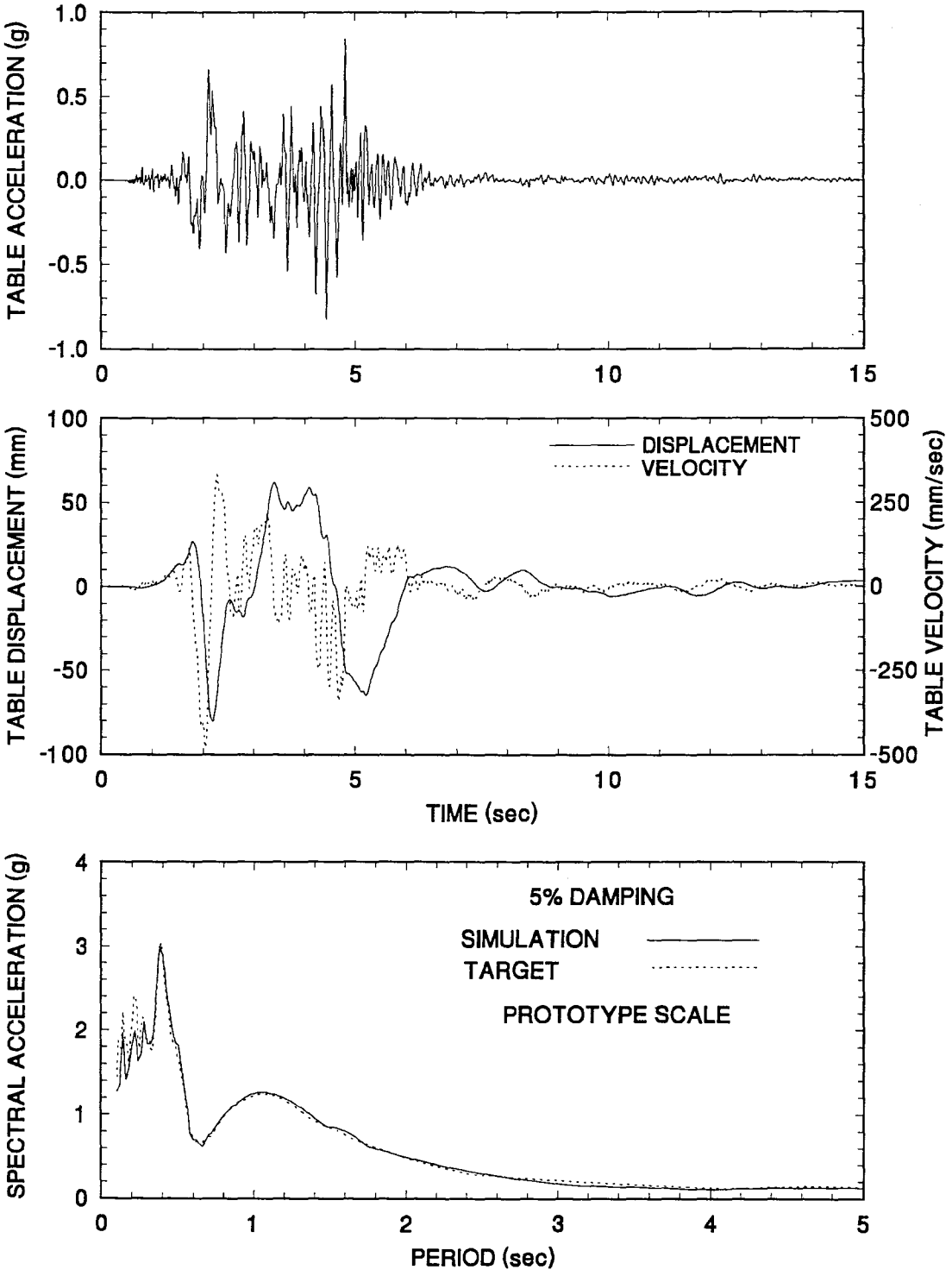

Figure 4-18 **Time Histories of Displacement, Velocity and Acceleration and Acceleration Response Spectrum of Shaking Table Motion Excited with Pacoima S16E 100% Motion.**

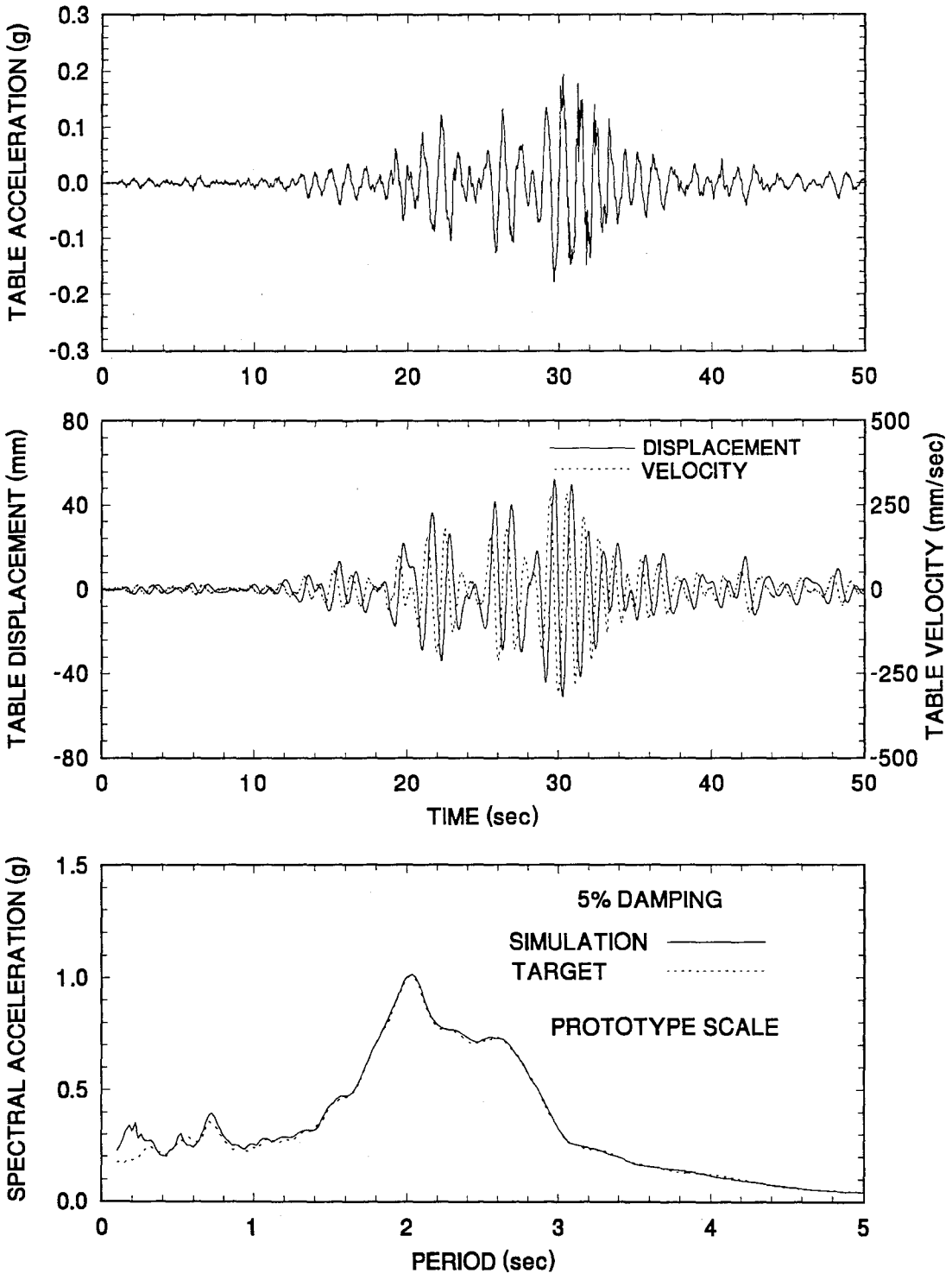

Figure 4-19 **Time Histories of Displacement, Velocity and Acceleration and Acceleration Response Spectrum of Shaking Table Motion Excited with Mexico N90W 100% Motion.**

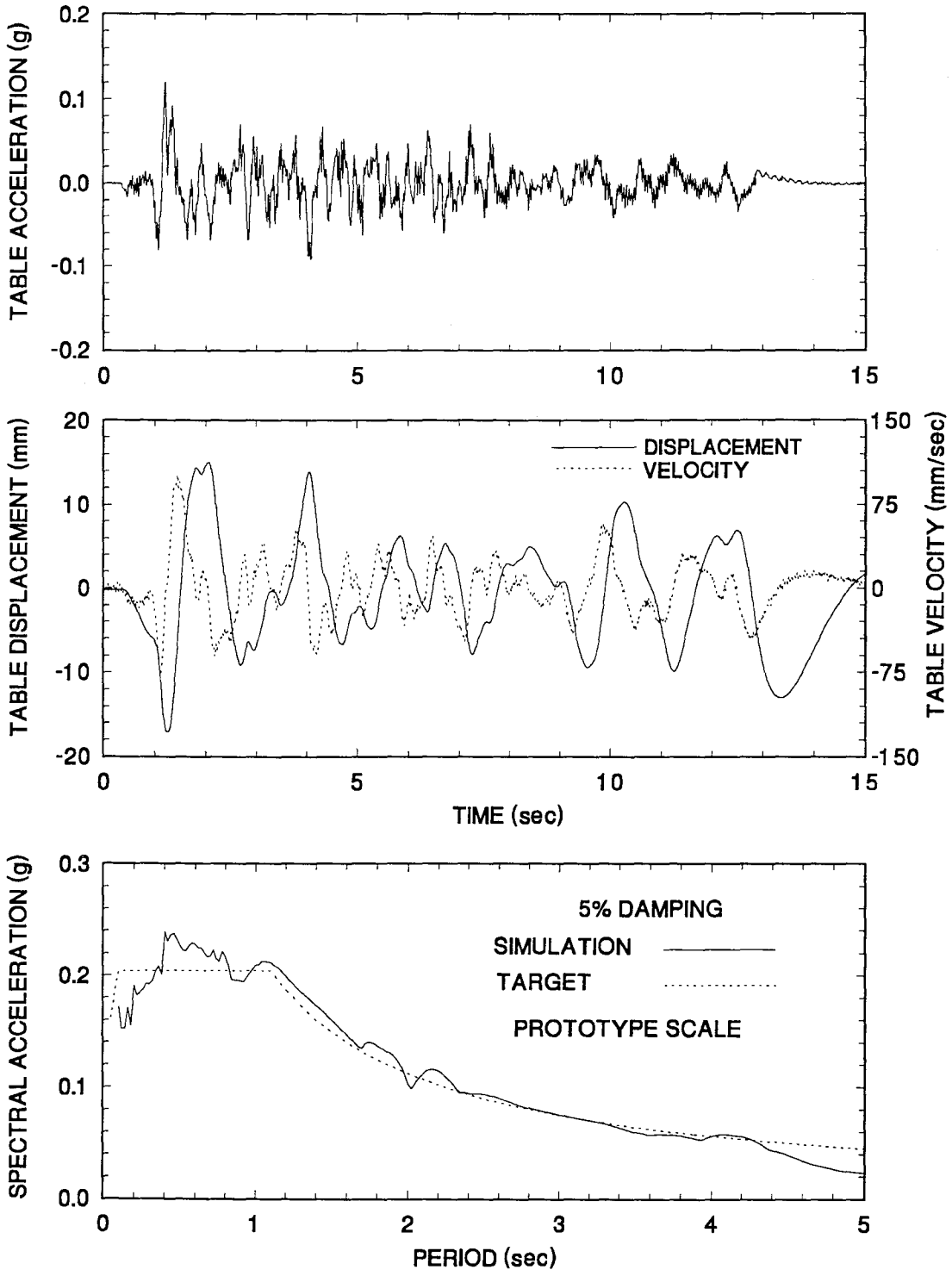

Figure 4-20 **Time Histories of Displacement, Velocity and Acceleration and Acceleration Response Spectrum of Shaking Table Motion Excited with JP. Level 1 G.C.1 100% Motion.**

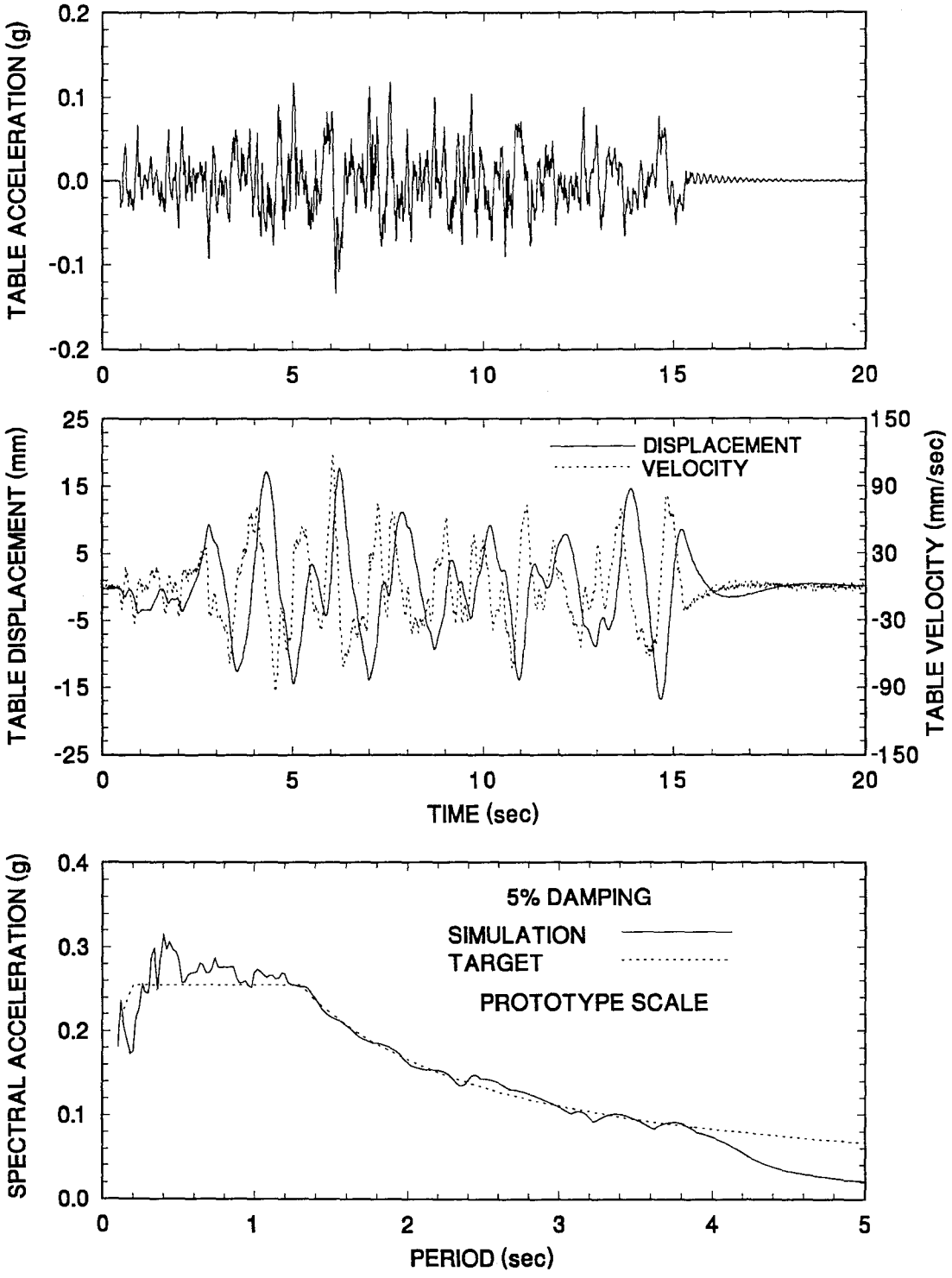

Figure 4-21 **Time Histories of Displacement, Velocity and Acceleration and Acceleration Response Spectrum of Shaking Table Motion Excited with JP. Level 1 G.C.2 100% Motion.**

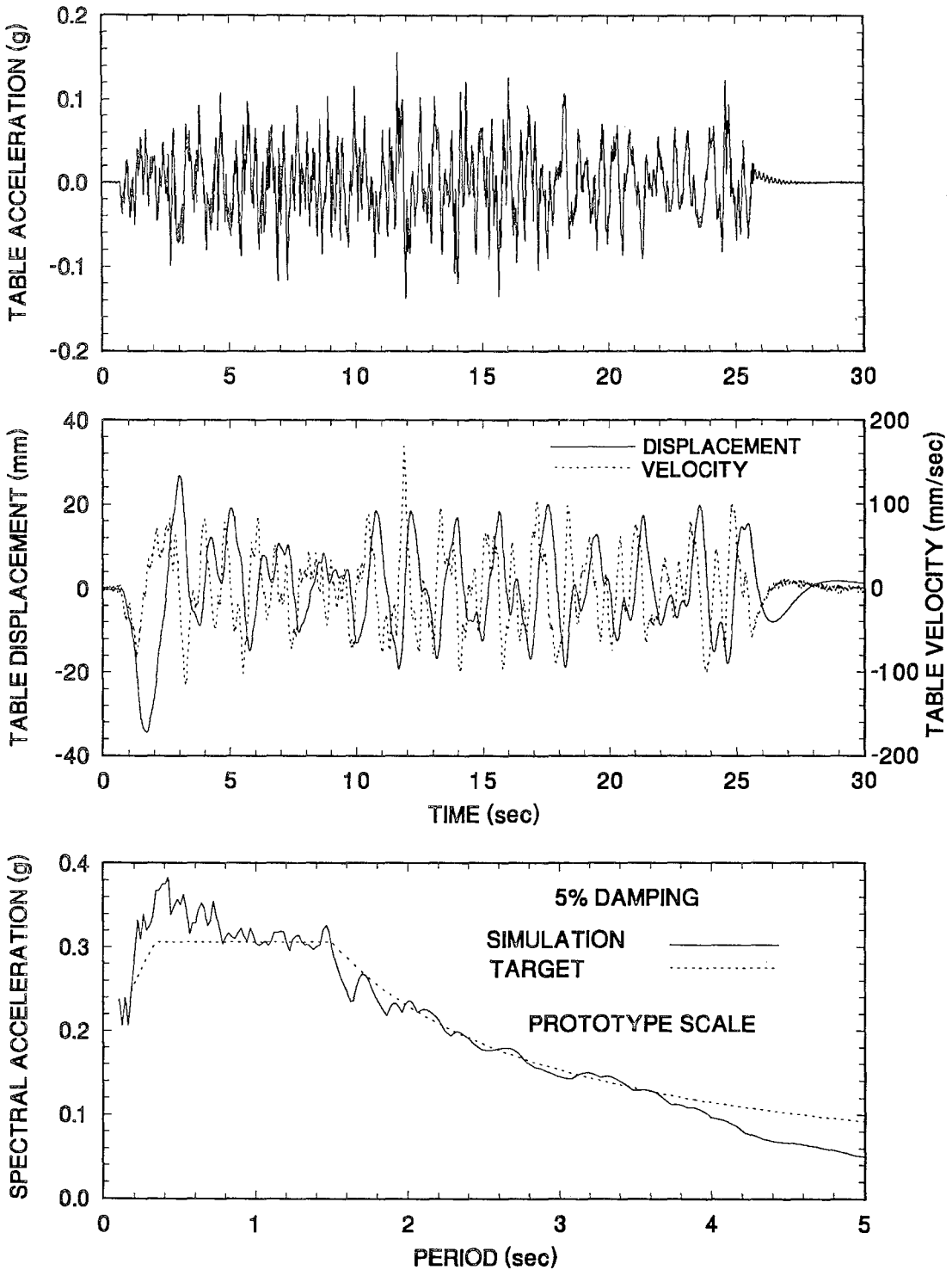

Figure 4-22 Time Histories of Displacement, Velocity and Acceleration and Acceleration Response Spectrum of Shaking Table Motion Excited with JP. Level 1 G.C.3 100% Motion.

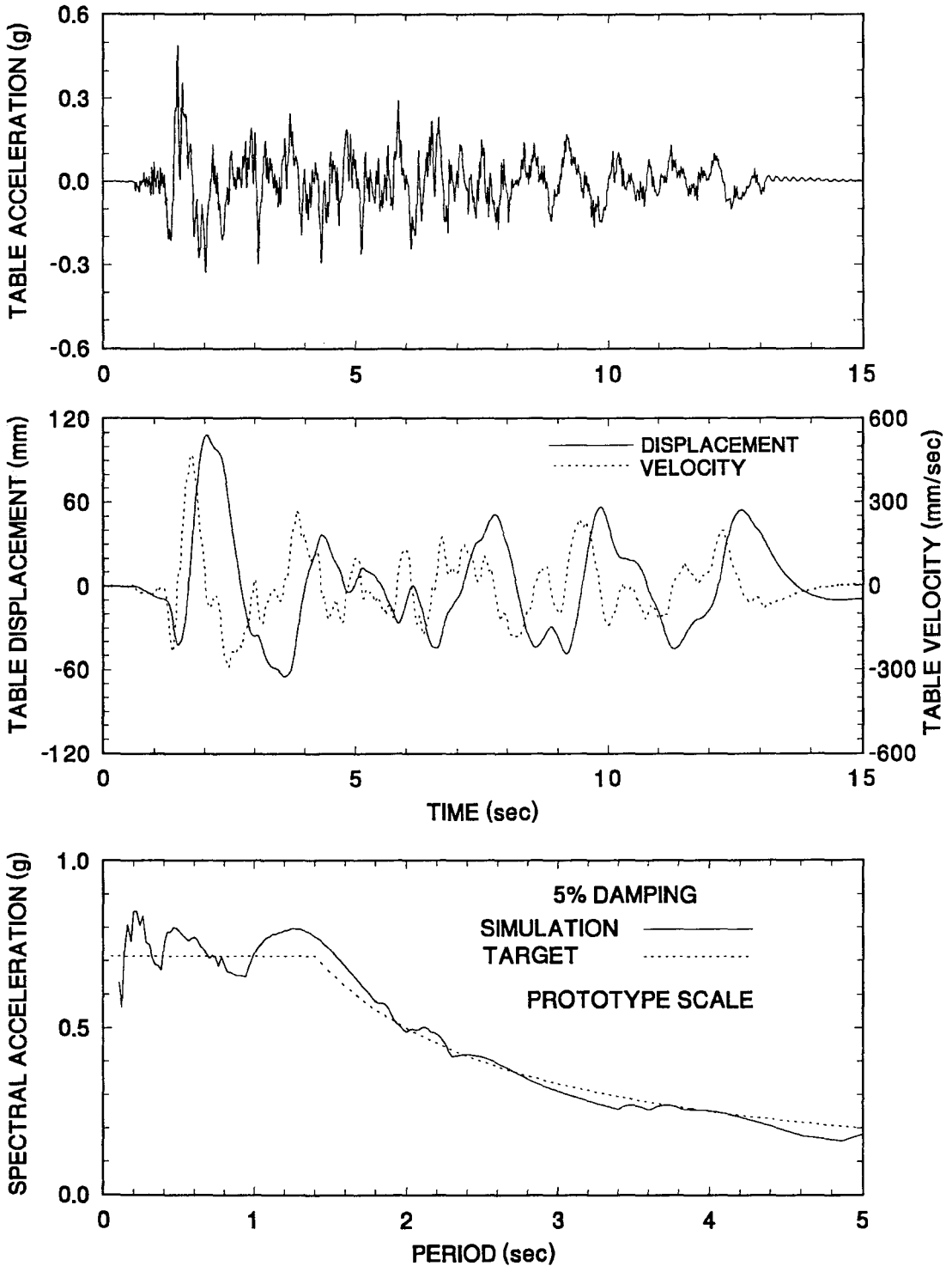

Figure 4-23 **Time Histories of Displacement, Velocity and Acceleration and Acceleration Response Spectrum of Shaking Table Motion Excited with JP. Level 2 G.C.1 100% Motion.**

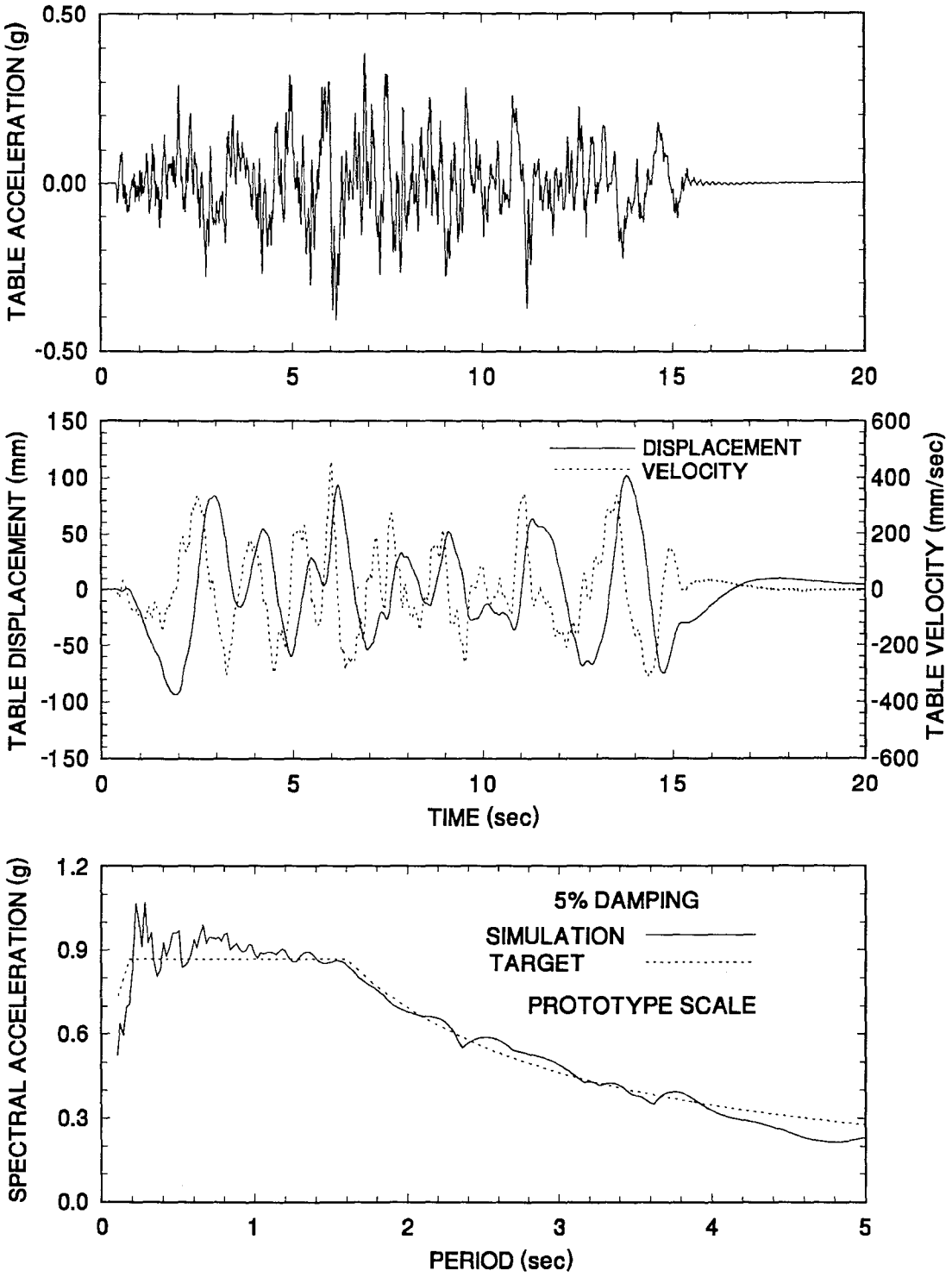

Figure 4-24 **Time Histories of Displacement, Velocity and Acceleration and Acceleration Response Spectrum of Shaking Table Motion Excited with JP. Level 2 G.C.2 100% Motion.**

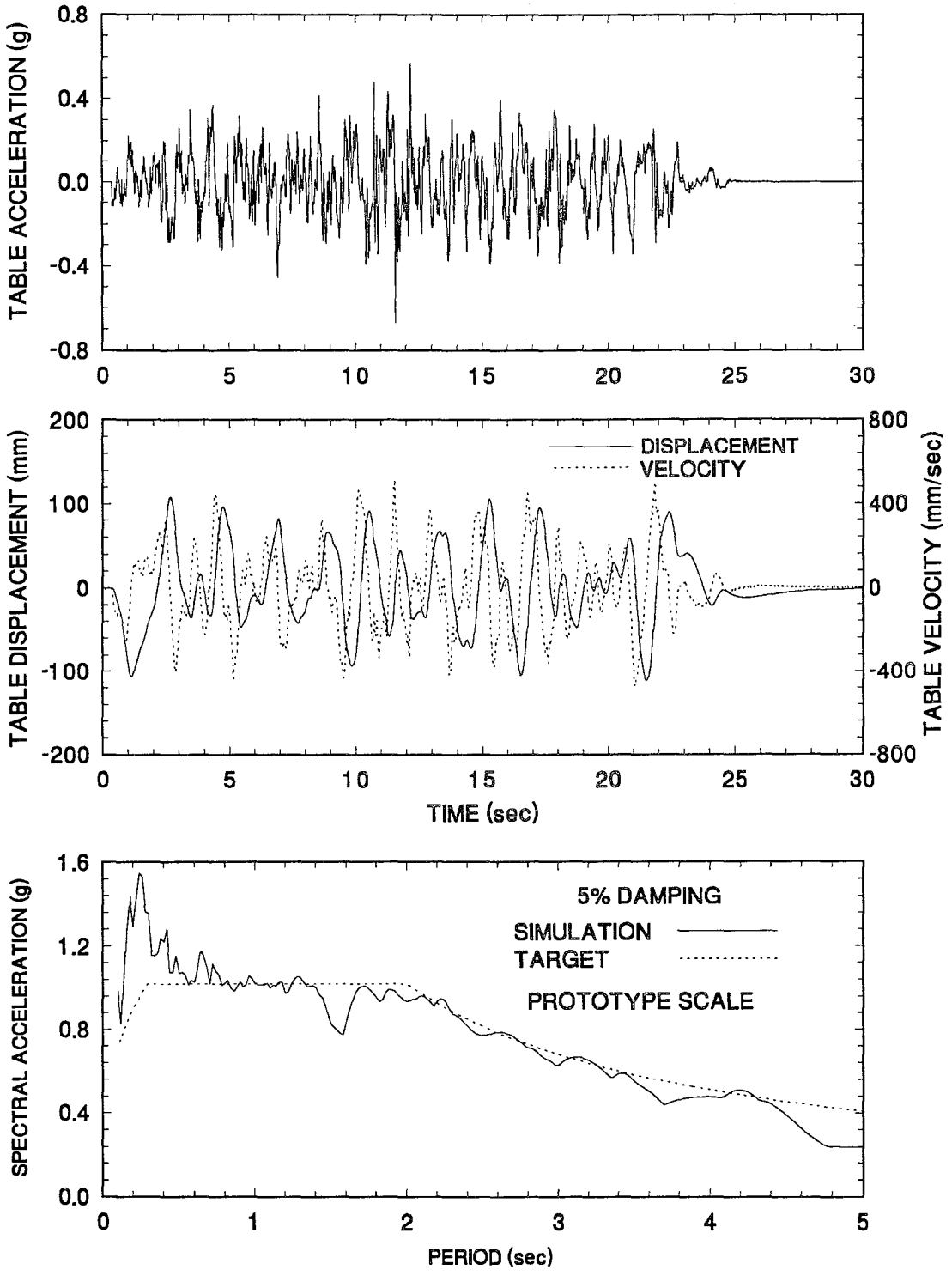

Figure 4-25 **Time Histories of Displacement, Velocity and Acceleration and Acceleration Response Spectrum of Shaking Table Motion Excited with JP. Level 2 G.C.3 100% Motion.**

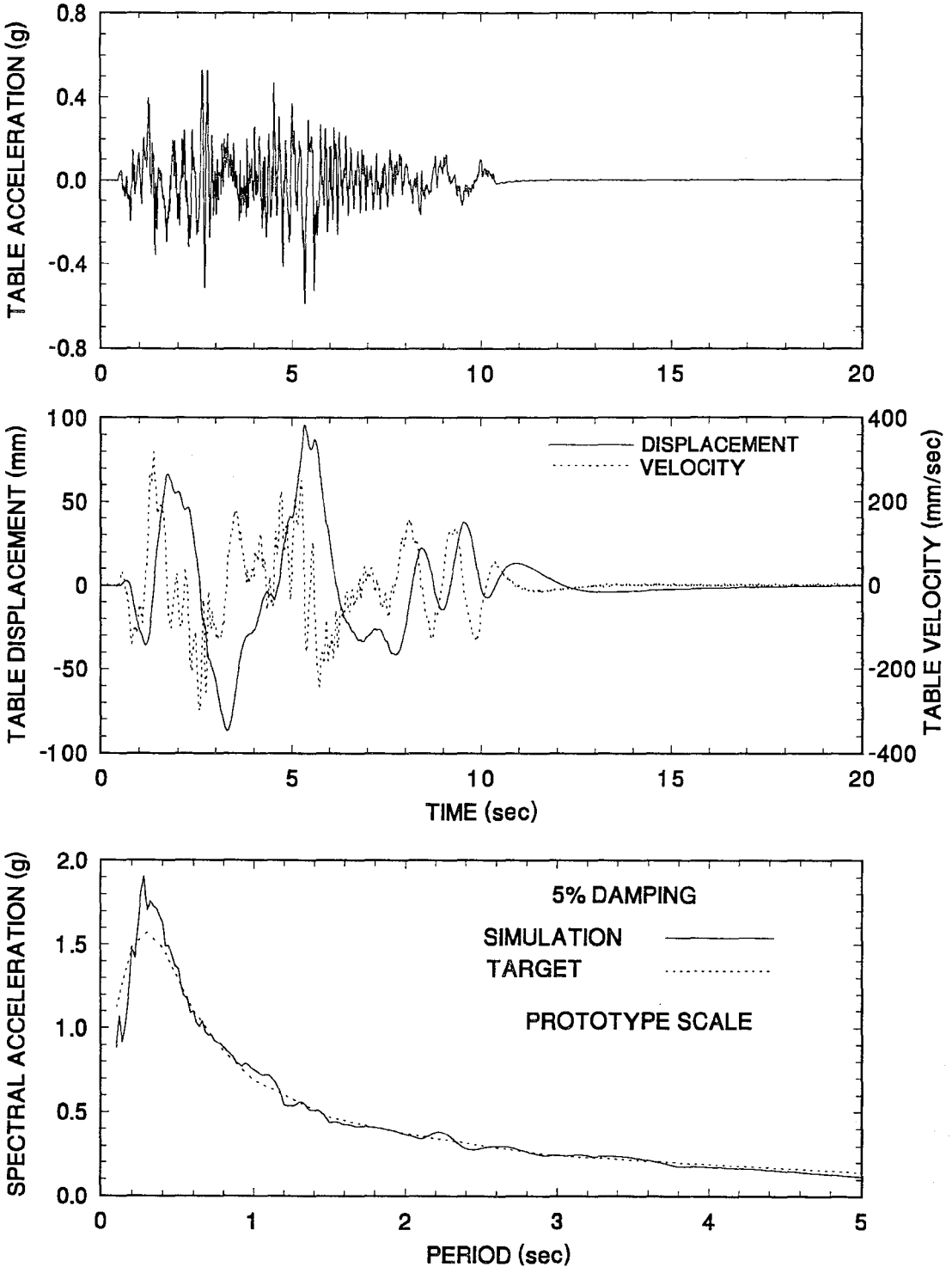

Figure 4-26 **Time Histories of Displacement, Velocity and Acceleration and Acceleration Response Spectrum of Shaking Table Motion Excited with CalTrans Rock No.3 0.6g 100% Motion.**

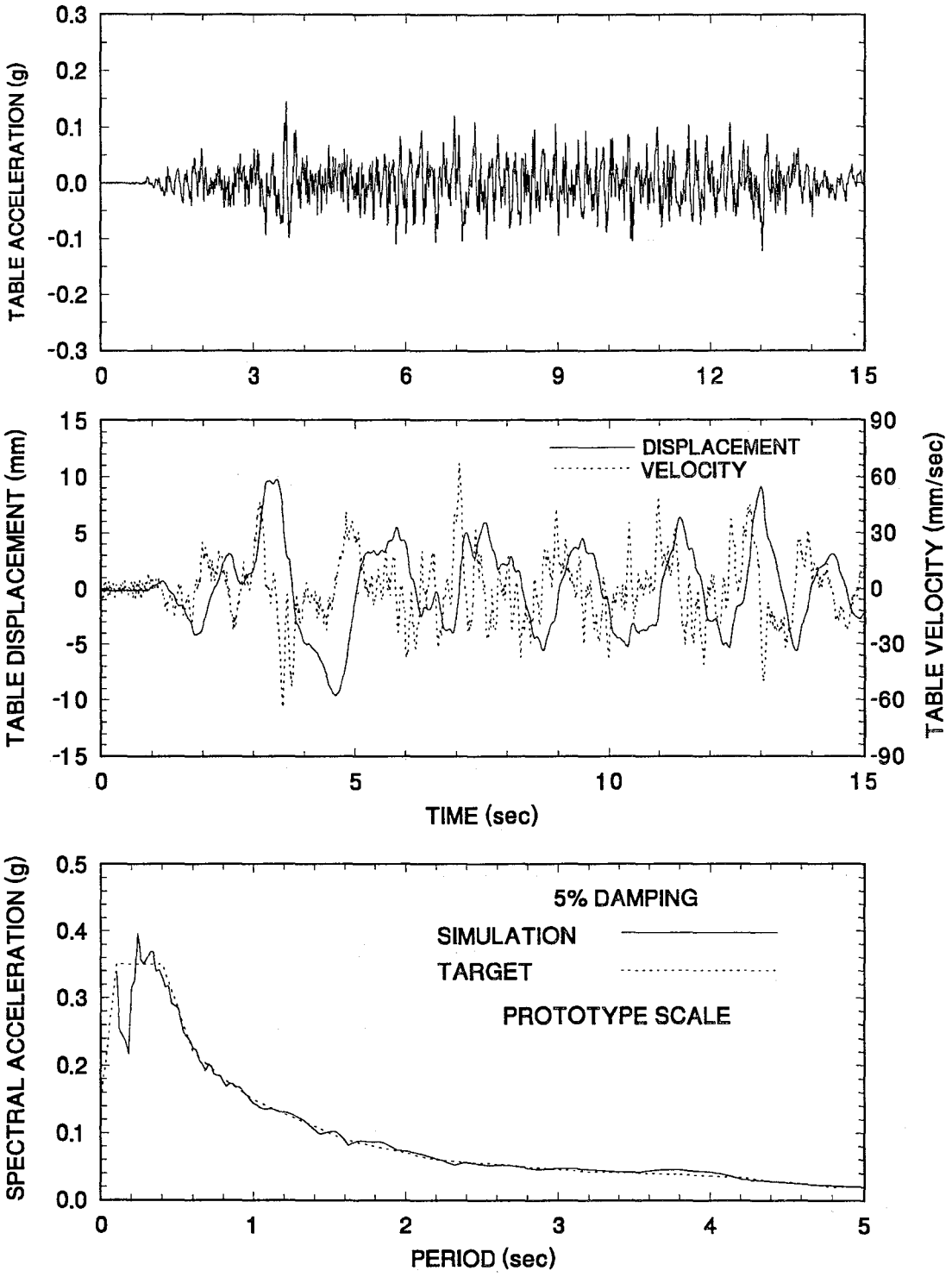

Figure 4-29 **Time Histories of Displacement, Velocity and Acceleration and Acceleration Response Spectrum of Shaking Table Motion Excited with Boston 1 100% Motion.**

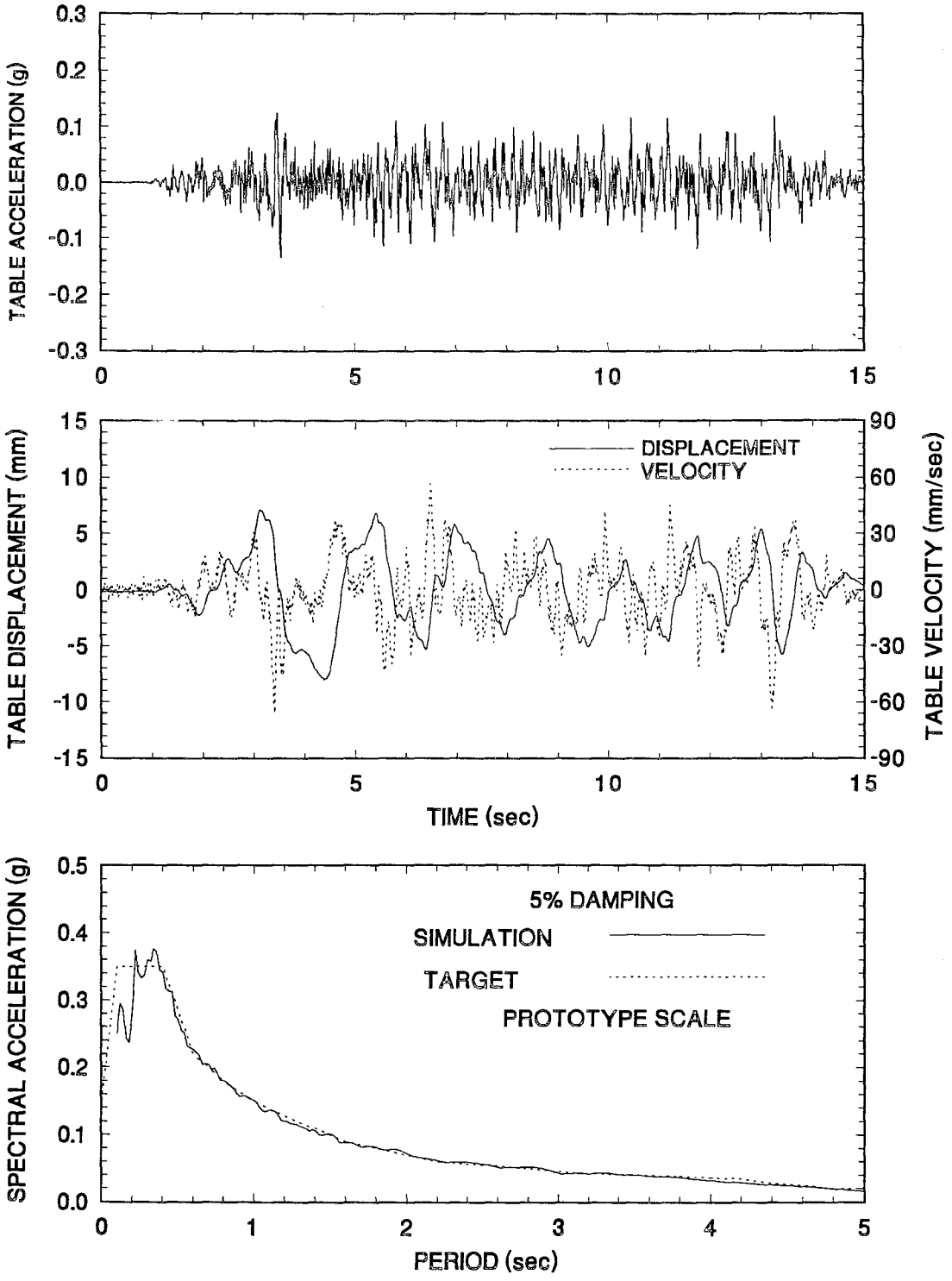

Figure 4-30 Time Histories of Displacement, Velocity and Acceleration and Acceleration Response Spectrum of Shaking Table Motion Excited with Boston 2 100% Motion.

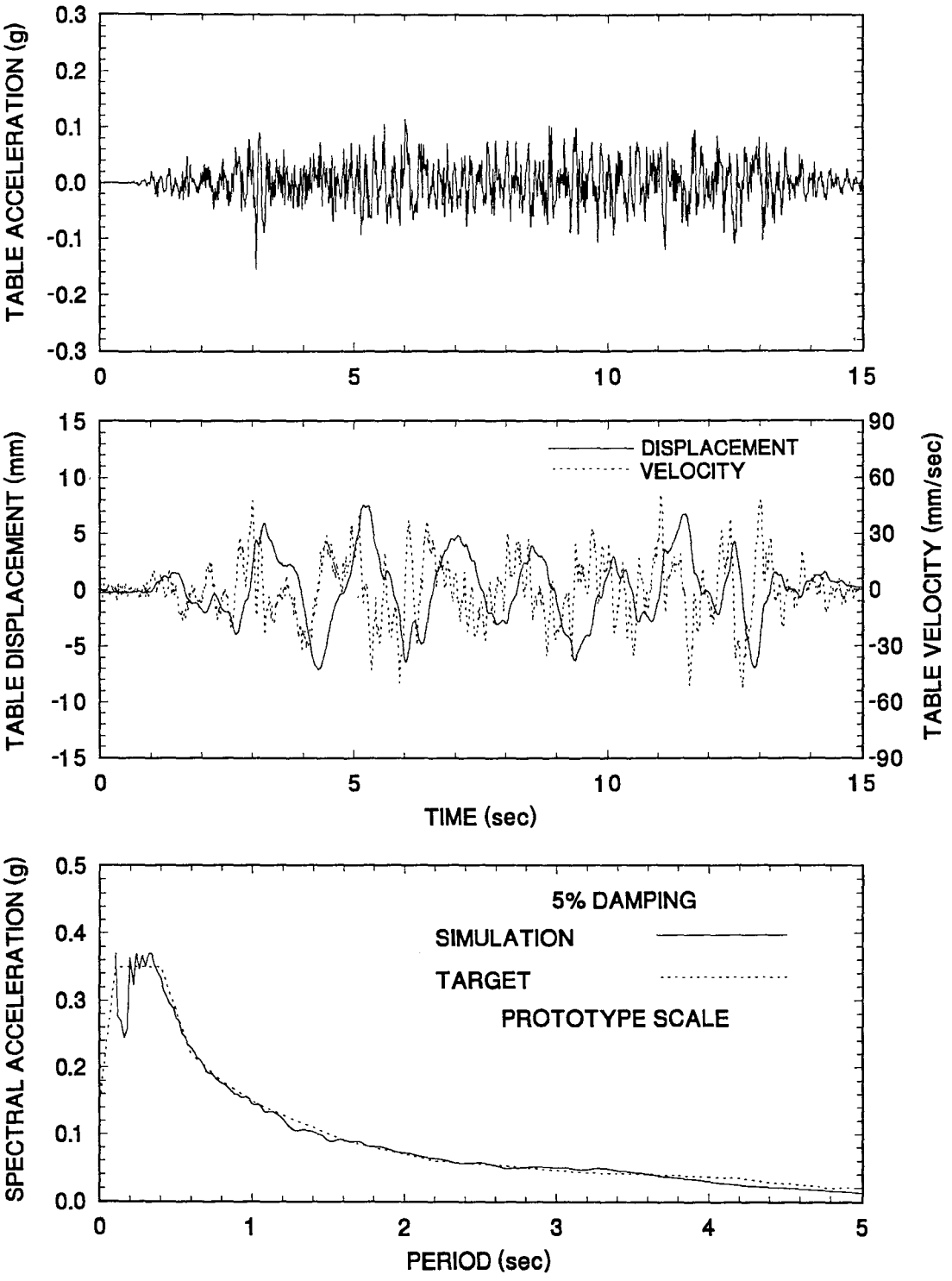

Figure 4-31 Time Histories of Displacement, Velocity and Acceleration and Acceleration Response Spectrum of Shaking Table Motion Excited with Boston 3 100% Motion.

SECTION 5

EARTHQUAKE SIMULATOR TEST RESULTS

5.1 Results for Non-isolated Bridge

Testing of the non-isolated bridge (see Figure 4-5, configuration 1 and Figure 4-6) was conducted with only horizontal excitation. The experimental results for the bridge in its non-isolated configuration are summarized in Table 5-I. For each test the peak values of the table motion in the horizontal direction are given. The displacement and acceleration were directly measured whereas the velocity was determined by numerical differentiation of the displacement record. The peak pier drift is given as a percentage of the pier height which was 1290.3mm. This is the length of the column excluding the stiffeners at the ends (see Figure 4-1). The peak shear force is given as a fraction of the axial load carried by the pier (71.5 kN each pier).

5.2 Results for Isolated Bridge

Tables 5-II and 5-III list the earthquake simulation tests and model conditions in the tests of the isolated bridge. The excitation in these tables is identified with a percentage figure which represents a scaling factor on the acceleration, velocity and displacement of the actual record. For example, the figure 200% denotes a motion scaled up by a factor of two in comparison to the actual record.

Table 5-IV and 5-V presents a summary of the experimental results of the isolated bridge. The tables include the following results:

(a) Displacement of bearings located at the south pier (see Figures 4-2 to 4-4). The transducers monitoring the south bearing displacement were continuously monitored and not initialized prior to each test (except for tests No. IRDRUN01 to IRDRUN65 and DRDRUN01 to DRDRUN14). Thus, the instruments recorded correctly the initial and permanent bearing displacements. Figure 5-1 shows an example of bearing displacement time history. The initial displacement is the permanent displacement in the previous test and the initial displacement in the current test.

Table 5-I Summary of Experimental Results of Non-Isolated Bridge

TEST No.	EXCITATION	PEAK TABLE MOTION			DECK ACCEL.	PIER SHEAR / AXIAL LOAD		PIER DRIFT RATIO (%)	
		DISP. (mm)	VEL. (mm/sec)	ACCEL. (g)	(g)	SOUTH	NORTH	SOUTH	NORTH
FRUN05	EL CENTRO S00E 25%	5.8	40.0	0.095	0.25	0.266	0.271	N/A	0.381
FRUN06	TAFT N21E 50%	7.0	32.7	0.069	0.21	0.230	0.234	N/A	0.315
FRUN07	TAFT N21E 75%	10.5	47.7	0.102	0.25	0.273	0.278	N/A	0.385
FRUN08	JP LEVEL 1 G.C.1 100%	16.6	96.0	0.109	0.21	0.231	0.222	N/A	0.346
FRUN09	JP LEVEL 1 G.C.2 100%	17.3	113.6	0.110	0.26	0.280	0.269	N/A	0.414
FRUN10	JP LEVEL 1 G.C.3 100%	33.7	158.3	0.130	0.33	0.353	0.354	N/A	0.623
FRUN11	AKITA N-S 75%	25.1	108.4	0.138	0.26	0.284	0.283	N/A	0.474
FRUN12	HACHINOHE N-S 50%	15.8	66.0	0.103	0.18	0.200	0.198	N/A	0.311
FRUN13	MIYAGIKEN OKI E-W 75%	8.0	38.0	0.080	0.22	0.242	0.235	N/A	0.384
FRUN14	MEXICO N90W 100%	51.7	303.1	0.169	0.26	0.286	0.284	N/A	0.522
FRUN15	JP LEVEL 2 G.C.1 25%	26.7	114.1	0.104	0.17	0.189	0.181	N/A	0.301
FRUN16	JP LEVEL 2 G.C.2 25%	25.0	109.8	0.098	0.21	0.232	0.225	N/A	0.365
FRUN17	JP LEVEL 2 G.C.3 25%	27.6	116.6	0.117	0.26	0.285	0.283	N/A	0.497
FRUN18	PACOIMA S74W 13%	4.0	36.4	0.103	0.2	0.221	0.214	N/A	0.346
FRUN19	PACOIMA S16E 13%	10.4	63.9	0.095	0.17	0.187	0.186	N/A	0.275
FRUN20	CALTRANS R3 0.6g 20%	23.5	124.8	0.101	0.22	0.227	0.234	N/A	0.389
FRUN21	CALTRANS S3 0.6g 20%	32.1	102.4	0.112	0.31	0.320	0.345	N/A	0.565
FRUN22	CALTRANS A2 0.6g 20%	47.2	128.3	0.104	0.27	0.278	0.298	N/A	0.475

(b) Maximum travel of bearings located at the North pier. The transducers monitoring the North bearing displacements were initialized prior to each test so that the initial displacement appeared always as zero. Thus, only the maximum travel (MAX.-INIT. in Figure 5-1) could be accurately obtained and not the initial and permanent displacements.

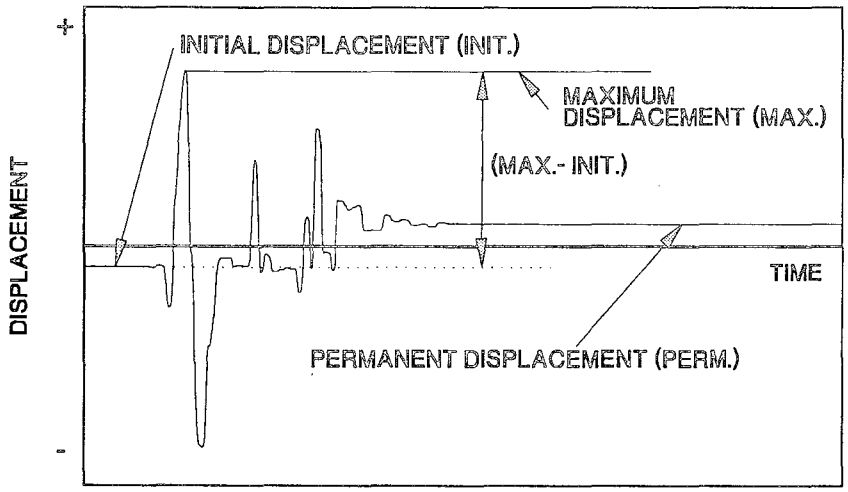

Figure 5-1 Example of Bearing Displacement History

(c) Isolation system shear force normalized by the carried weight (143 kN for total shear force and 71.5 kN for shear force at each pier). The isolation system force was not measured directly but it was rather inferred from other measurements as described below.

Case of Flexible Piers

Figure 5-2 shows a free body diagram of the bridge model. The isolation system force at the south pier location, V_S , is given by

$$V_S = F_{fs} + F_{rs} \tag{5-1}$$

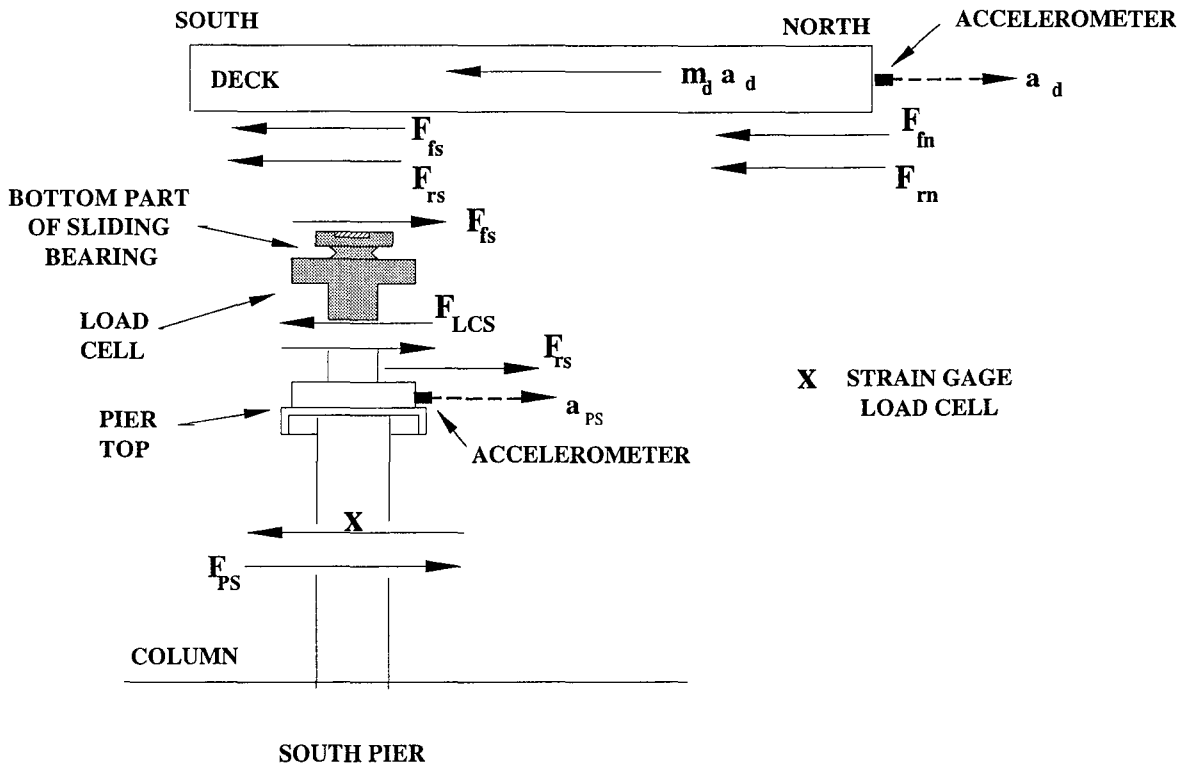

Figure 5-2 Free Body Diagram of Bridge Model used in Inference of Isolation System Shear Force and Friction Force for the Case of Flexible Piers.

where F_{fs} is the friction force in the two sliding bearings on top of the south pier and F_{rs} is the force in the rubber device (or rubber device plus two fluid dampers). A similar equation is valid for the isolation system force at the north pier location, V_N.

Direct measurements were obtained for the following quantities : column shear forces, F_{PS} and F_{PN}, shear forces at mid-height of load cells, F_{LCS} and F_{LCN}, accelerations of load cell bottoms, a_{PS} and a_{PN}, and deck acceleration (only at north), a_d. The isolation system force was derived from

$$V_S = F_{fs} + F_{rs} = F_{PS} + \frac{W_{PS}\, a_{PS}}{g} \qquad (5\text{-}2)$$

where W_{PS} is the weight of the accelerating part of the south pier above the strain gage location (8.9 kN). A similar equation gave the isolation system force at the north pier, V_N. The total isolation system force, V, was then derived from

$$V = V_S + V_N \tag{5-3}$$

Equations (5-2) and (5-3) were used to obtain time histories of forces V_S, V_N and V, from which the peak values were extracted and included in Tables 5-IV and 5-V.

It should be noted that for a rigid deck the isolation system force could be directly obtained from the deck acceleration measurement :

$$V = \frac{W_d\, a_d}{g} \tag{5-4}$$

where W_d = 143 kN. However, the deck had some flexibility which caused amplification of the recorded deck acceleration. When Equation (5-4) was used, the loops of isolation system force (as obtained from the deck acceleration) versus bearing displacement were wavy. Since the recorded loops of friction force versus displacement did not exhibit a similar wavy form, it was concluded that the recorded acceleration of the deck contained additional components caused by the deck's flexibility.

An example of the errors which may be introduced by the use of the deck acceleration is presented in Figure 5-3. The graphs compare the recorded deck acceleration to the inferred isolation system force in three tests. For an ideal case (infinitely rigid deck) the relation between the two quantities should have been a straight line. In reality it is not. The deviation from the straight line increases with increasing strength of excitation as a result of amplification of acceleration due to the deck flexibility and measurement errors due to pier top rotation.

Case of Stiff Piers

In this case the pier shear force could not be measured due to the existence of braces (see Figures 4-1, 4-5 and 4-8). Accordingly, the isolation system force was obtained from the

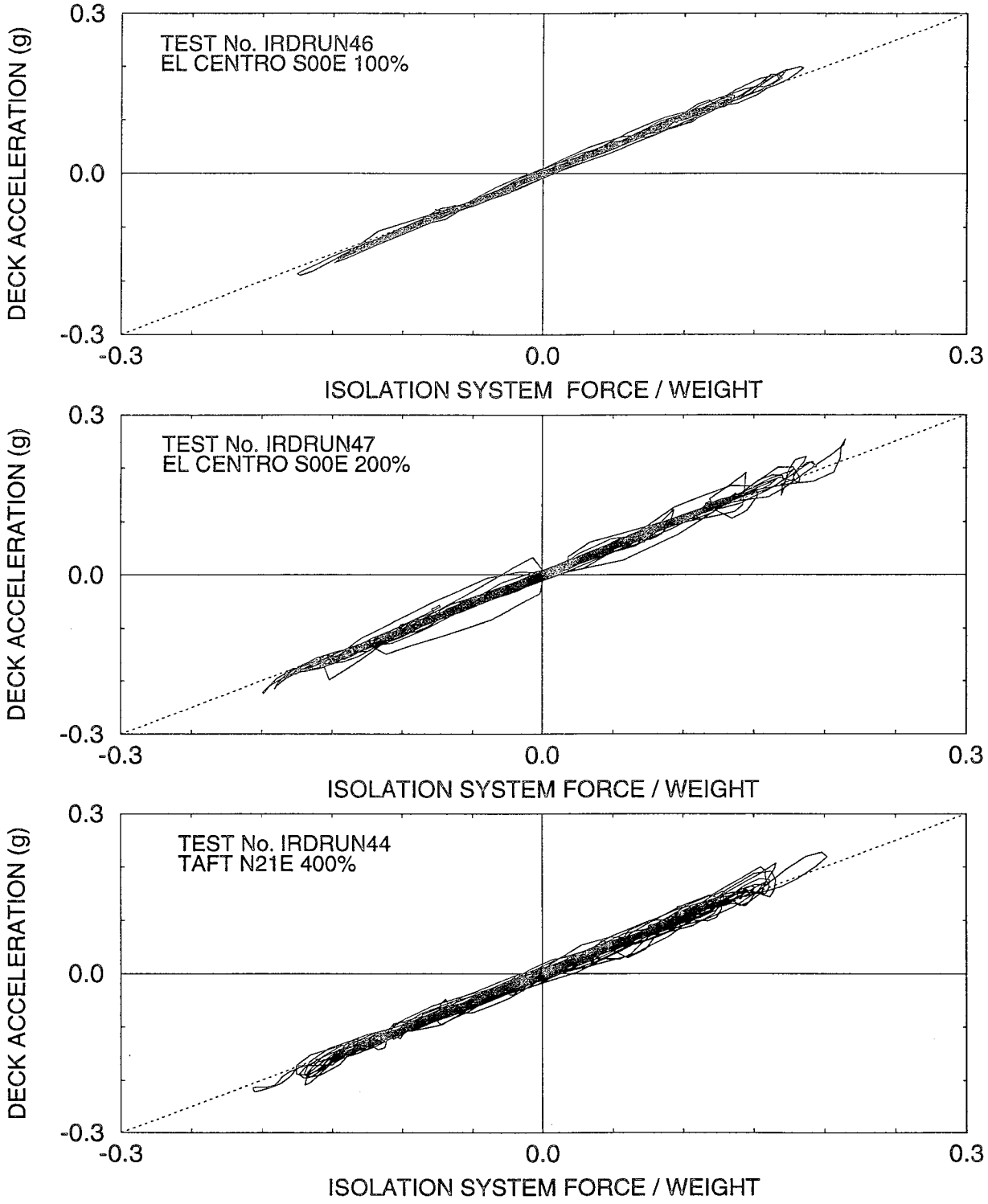

Figure 5-3 **Comparison of Deck Acceleration to Inferred Isolation System Shear Force in Tests of Model with Flexible Piers (Case of Bearing Type T1, Rubber Device No. 2).**

deck acceleration record in accordance with Equation (5-4). For the symmetric case of two stiff piers, the so calculated force was equally divided to the piers. For the case of one stiff and one flexible pier, the total isolation system force was obtained from the deck acceleration, whereas for the north pier isolation system shear force (that is the flexible pier) the procedure for flexible piers was followed (Eq. 5-2).

(d) Device force normalized by the deck weight (143 kN). This is the force in each of two rubber restoring force devices (or rubber device plus two fluid dampers). This force was not measured directly but rather determined from other measurements as follows. Based on the free body diagram of Figure 5-2, the device force, F_{rs} is

$$F_{rs} = V_S - F_{fs} \tag{5-5}$$

where V_S is the isolation system force at the south pier, as determined from Equation (5-2) , and F_{fs} is the friction force from the two sliding bearings at the south pier. This force was obtained from the two load cells which supported the sliding bearings after correction for the accelerating part of the load cell and bearing. That is, from Figure 5-2,

$$F_{fs} = F_{LCS} + \frac{W_{LC}}{g}(a_{PSE} + a_{PSW}) \tag{5-6}$$

where F_{LCS} is the sum of forces measured in the two load cells at the south pier, a_{PSE} and a_{PSW} are the accelerations of south-east and south-west load cells (measured at the top of the south piers) and W_{LC} is the weight of the part of sliding bearing and load cell between the sliding interface and the strain gage location. This part is shown shaded in Figure 5-2 and weighted 890 N.

The procedure just outlined was repeated for the north pier location to obtain the corresponding device force.

(e) Pier acceleration. The peak accelerations of the top of the South and North piers are reported.

(f) Deck horizontal acceleration.

(g) Pier shear force normalized by axial load. Each column was instrumented with strain gages to measure the shear force. The reported quantity is the sum of the shear forces in the two columns of each pier divided by the axial load on each pier (143/2=71.5 kN). The pier shear force is, in general, different than the isolation system shear force. The two forces differ by the inertia force of the accelerating part of the pier between the sliding interface and the location of the strain gages. The pier shear force in the case of stiff piers could not be measured and is not reported in the tables. It should be noted that in the case of stiff piers the columns were braced (see Figures 4-1, 4-5 and 4-8), so that the force measured by the strain gage load cells of the columns represented only part of the total pier shear force.

(h) Pier drift ratio. This is the displacement of the top of the pier relative to the shake table, divided by the length of the column (1290.3 mm).

During testing of the model bridge in its isolated condition it was observed that the overhangs of the shake table extension, which supported the piers (see Figure 4-1), underwent significant vertical motion even when only horizontal table motion was imposed. The two overhangs did not move vertically in unison. Rather, the motion of the two overhangs was anti-symmetric with the two sides moving with different amplitude and content in frequency. It was concluded that this vertical motion of the overhangs was the combined result of table-structure interaction, vertical flexibility of the overhangs and differences in the vertical stiffness of the overhangs (it was later found that on one side of the concrete table extension the reinforcement was misplaced).

The implications of this phenomenon were to increase the severity of the testing. In effect, in all tests the piers experienced out-of-phase vertical input at their bases. This caused changes in the vertical load carried by the sliding bearings, which in turn affected the friction force of the bearings. This explains the differences in the isolation system shear force, pier acceleration and pier shear force and drift between the South and North piers (see Tables 5-IV and 5-V). Furthermore, it explains the wavy nature of the recorded force versus displacement loops of the isolation system (see Appendix A).

Table 5-II List of Earthquake Simulation Tests and Model Conditions in Tests with Sliding Bearings and Rubber Restoring Force Devices

TEST No.	EXCITATION	PEAK TABLE MOTION			PIER CONDITION		BEARING MATERIAL		BEARING PRESSURE (MPa)		FRICTIONAL PROPERTIES		RUBBER RESTORING FORCE DEVICE	
		DIS. (mm)	VEL. (mm/s)	ACC. (g)	SOUTH	NORTH	SOUTH	NORTH	SOUTH	NORTH	fmax	fmin	SOUTH	NORTH
IRDRUN01	EL CENTRO S00E 100%	24.2	178.7	0.377	STIFF	STIFF	T1	T1	5.0	5.0	0.15	0.055	No.2	No.2
IRDRUN02	EL CENTRO S00E 100%	23.9	166.7	0.386	STIFF	STIFF	T1	T1	5.0	5.0	0.15	0.055	No.2	No.2
IRDRUN03	EL CENTRO S00E 150%	36.4	243.2	0.505	STIFF	STIFF	T1	T1	5.0	5.0	0.15	0.055	No.2	No.2
IRDRUN04	EL CENTRO S00E 200%	48.6	319.6	0.642	STIFF	STIFF	T1	T1	5.0	5.0	0.15	0.055	No.2	No.2
IRDRUN05	TAFT N21E 100%	14.2	71.3	0.190	STIFF	STIFF	T1	T1	5.0	5.0	0.15	0.055	No.2	No.2
IRDRUN06	TAFT N21E 200%	28.8	134.8	0.317	STIFF	STIFF	T1	T1	5.0	5.0	0.15	0.055	No.2	No.2
IRDRUN07	TAFT N21E 400%	57.7	266.4	0.590	STIFF	STIFF	T1	T1	5.0	5.0	0.15	0.055	No.2	No.2
IRDRUN08	TAFT N21E 600%	86.4	411.2	0.908	STIFF	STIFF	T1	T1	5.0	5.0	0.15	0.055	No.2	No.2
IRDRUN09	PACOIMA S74W 75%	22.1	210.5	0.574	STIFF	STIFF	T1	T1	5.0	5.0	0.15	0.055	No.2	No.2
IRDRUN10	PACOIMA S74W 100%	29.6	278.3	0.699	STIFF	STIFF	T1	T1	5.0	5.0	0.15	0.055	No.2	No.2
IRDRUN11	JP LEVEL 2 G.C.1 75%	85.5	363.7	0.403	STIFF	STIFF	T1	T1	5.0	5.0	0.15	0.055	No.2	No.2
IRDRUN12	JP LEVEL 2 G.C.1 100%	109.3	475.5	0.543	STIFF	STIFF	T1	T1	5.0	5.0	0.15	0.055	No.2	No.2
IRDRUN13	JP LEVEL 2 G.C.2 50%	51.2	225.4	0.225	STIFF	STIFF	T1	T1	5.0	5.0	0.15	0.055	No.2	No.2
IRDRUN14	JP LEVEL 2 G.C.2 75%	76.7	340.5	0.342	STIFF	STIFF	T1	T1	5.0	5.0	0.15	0.055	No.2	No.2
IRDRUN15	JP LEVEL 2 G.C.2 100%	102.1	449.3	0.415	STIFF	STIFF	T1	T1	5.0	5.0	0.15	0.055	No.2	No.2
IRDRUN16	JP LEVEL 2 G.C.3 75%	84.5	366.3	0.396	STIFF	STIFF	T1	T1	5.0	5.0	0.15	0.055	No.2	No.2
IRDRUN17	JP LEVEL 2 G.C.3 100%	112.5	498.7	0.505	STIFF	STIFF	T1	T1	5.0	5.0	0.15	0.055	No.2	No.2
IRDRUN18	JP LEVEL 2 G.C.3 100%	111.7	497.2	0.511	STIFF	STIFF	T1	T1	5.0	5.0	0.15	0.055	No.2	No.2
IRDRUN19	PACOIMA S16E 50%	40.6	239.7	0.484	STIFF	STIFF	T1	T1	5.0	5.0	0.15	0.055	No.2	No.2
IRDRUN20	PACOIMA S16E 75%	60.9	366.7	0.708	STIFF	STIFF	T1	T1	5.0	5.0	0.15	0.055	No.2	No.2
IRDRUN21	HACHINOHE N-S 100%	32.3	139.8	0.231	STIFF	STIFF	T1	T1	5.0	5.0	0.15	0.055	No.2	No.2
IRDRUN22	HACHINOHE N-S 150%	48.3	208.8	0.357	STIFF	STIFF	T1	T1	5.0	5.0	0.15	0.055	No.2	No.2
IRDRUN23	HACHINOHE N-S 200%	64.3	270.9	0.464	STIFF	STIFF	T1	T1	5.0	5.0	0.15	0.055	No.2	No.2
IRDRUN24	TAFT N21E H+V 200%	29.0	134.9	0.317	STIFF	STIFF	T1	T1	5.0	5.0	0.15	0.055	No.2	No.2
IRDRUN25	TAFT N21E H+V 400%	58.1	273.1	0.554	STIFF	STIFF	T1	T1	5.0	5.0	0.15	0.055	No.2	No.2
IRDRUN26	EL CENTRO S00E H+V 200%	48.4	323.7	0.645	STIFF	STIFF	T1	T1	5.0	5.0	0.15	0.055	No.2	No.2

Table 5-II Cont'd

TEST No.	EXCITATION	PEAK TABLE MOTION			PIER CONDITION		BEARING MATERIAL		BEARING PRESSURE (MPa)		FRICTIONAL PROPERTIES		RUBBER RESTORING FORCE DEVICE	
		DIS. (mm)	VEL. (mm/s)	ACC. (g)	SOUTH	NORTH	SOUTH	NORTH	SOUTH	NORTH	fmax	fmin	SOUTH	NORTH
IRDRUN27	JP LEVEL 1 G.C.1 100%	17.3	104.0	0.100	FLEXIBLE	FLEXIBLE	T1	T1	5.0	5.0	0.15	0.055	No.2	No.2
IRDRUN28	JP LEVEL 1 G.C.2 100%	17.9	115.1	0.117	FLEXIBLE	FLEXIBLE	T1	T1	5.0	5.0	0.15	0.055	No.2	No.2
IRDRUN29	JP LEVEL 1 G.C.3 100%	34.3	163.1	0.109	FLEXIBLE	FLEXIBLE	T1	T1	5.0	5.0	0.15	0.055	No.2	No.2
IRDRUN30	MIYAGIKENOKI E-W 100%	12.4	72.0	0.122	FLEXIBLE	FLEXIBLE	T1	T1	5.0	5.0	0.15	0.055	No.2	No.2
IRDRUN31	MIYAGIKENOKI E-W 200%	24.9	146.1	0.258	FLEXIBLE	FLEXIBLE	T1	T1	5.0	5.0	0.15	0.055	No.2	No.2
IRDRUN32	MIYAGIKENOKI E-W 300%	37.2	222.8	0.401	FLEXIBLE	FLEXIBLE	T1	T1	5.0	5.0	0.15	0.055	No.2	No.2
IRDRUN33	MIYAGIKENOKI E-W 400%	49.5	302.6	0.578	FLEXIBLE	FLEXIBLE	T1	T1	5.0	5.0	0.15	0.055	No.2	No.2
IRDRUN34	MIYAGIKENOKI E-W 500%	61.8	385.2	0.755	FLEXIBLE	FLEXIBLE	T1	T1	5.0	5.0	0.15	0.055	No.2	No.2
IRDRUN35	MIYAGIKENOKI E-W 600%	74.0	466.3	0.970	FLEXIBLE	FLEXIBLE	T1	T1	5.0	5.0	0.15	0.055	No.2	No.2
IRDRUN36	AKITA N-S 100%	34.3	146.6	0.171	FLEXIBLE	FLEXIBLE	T1	T1	5.0	5.0	0.15	0.055	No.2	No.2
IRDRUN37	AKITA N-S 200%	68.6	293.7	0.349	FLEXIBLE	FLEXIBLE	T1	T1	5.0	5.0	0.15	0.055	No.2	No.2
IRDRUN38	HACHINOHE N-S 100%	32.5	136.3	0.192	FLEXIBLE	FLEXIBLE	T1	T1	5.0	5.0	0.15	0.055	No.2	No.2
IRDRUN39	HACHINOHE N-S 200%	64.6	274.9	0.448	FLEXIBLE	FLEXIBLE	T1	T1	5.0	5.0	0.15	0.055	No.2	No.2
IRDRUN40	HACHINOHE N-S 250%	80.6	349.0	0.615	FLEXIBLE	FLEXIBLE	T1	T1	5.0	5.0	0.15	0.055	No.2	No.2
IRDRUN41	HACHINOHE N-S 300%	96.5	422.8	0.771	FLEXIBLE	FLEXIBLE	T1	T1	5.0	5.0	0.15	0.055	No.2	No.2
IRDRUN42	TAFT N21E 100%	14.4	68.1	0.135	FLEXIBLE	FLEXIBLE	T1	T1	5.0	5.0	0.15	0.055	No.2	No.2
IRDRUN43	TAFT N21E 200%	28.9	131.5	0.287	FLEXIBLE	FLEXIBLE	T1	T1	5.0	5.0	0.15	0.055	No.2	No.2
IRDRUN44	TAFT N21E 400%	57.6	266.4	0.587	FLEXIBLE	FLEXIBLE	T1	T1	5.0	5.0	0.15	0.055	No.2	No.2
IRDRUN45	TAFT N21E 500%	72.0	340.5	0.742	FLEXIBLE	FLEXIBLE	T1	T1	5.0	5.0	0.15	0.055	No.2	No.2
IRDRUN46	EL CENTRO S00E 100%	24.1	155.2	0.261	FLEXIBLE	FLEXIBLE	T1	T1	5.0	5.0	0.15	0.055	No.2	No.2
IRDRUN47	EL CENTRO S00E 200%	47.9	315.7	0.558	FLEXIBLE	FLEXIBLE	T1	T1	5.0	5.0	0.15	0.055	No.2	No.2
IRDRUN48	EL CENTRO S00E 250%	59.9	398.6	0.743	FLEXIBLE	FLEXIBLE	T1	T1	5.0	5.0	0.15	0.055	No.2	No.2
IRDRUN49	PACOIMA S74W 75%	22.2	187.7	0.686	FLEXIBLE	FLEXIBLE	T1	T1	5.0	5.0	0.15	0.055	No.2	No.2
IRDRUN50	PACOIMA S74W 100%	29.6	260.4	0.806	FLEXIBLE	FLEXIBLE	T1	T1	5.0	5.0	0.15	0.055	No.2	No.2
IRDRUN51	PACOIMA S16E 50%	41.1	247.5	0.376	FLEXIBLE	FLEXIBLE	T1	T1	5.0	5.0	0.15	0.055	No.2	No.2
IRDRUN52	PACOIMA S16E 60%	49.2	297.7	0.444	FLEXIBLE	FLEXIBLE	T1	T1	5.0	5.0	0.15	0.055	No.2	No.2

Table 5-II Cont'd

TEST No.	EXCITATION	PEAK TABLE MOTION			PIER CONDITION		BEARING MATERIAL		BEARING PRESSURE (MPa)		FRICTIONAL PROPERTIES		RUBBER RESTORING FORCE DEVICE	
		DIS. (mm)	VEL. (mm/s)	ACC. (g)	SOUTH	NORTH	SOUTH	NORTH	SOUTH	NORTH	fmax	fmin	SOUTH	NORTH
IRDRUN53	PACOIMA S16E 75%	61.5	363.0	0.590	FLEXIBLE	FLEXIBLE	T1	T1	5.0	5.0	0.15	0.055	No.2	No.2
IRDRUN54	CALTRANS R1 0.6g 100%	119.0	286.3	0.529	FLEXIBLE	FLEXIBLE	T1	T1	5.0	5.0	0.15	0.055	No.2	No.2
IRDRUN55	CALTRANS R2 0.6g 100%	75.5	266.6	0.550	FLEXIBLE	FLEXIBLE	T1	T1	5.0	5.0	0.15	0.055	No.2	No.2
IRDRUN56	CALTRANS R3 0.6g 100%	96.6	308.9	0.585	FLEXIBLE	FLEXIBLE	T1	T1	5.0	5.0	0.15	0.055	No.2	No.2
IRDRUN57	CALTRANS S2 0.6g 100%	68.4	393.7	0.641	FLEXIBLE	FLEXIBLE	T1	T1	5.0	5.0	0.15	0.055	No.2	No.2
IRDRUN58	CALTRANS S3 0.6g 100%	120.1	429.4	0.690	FLEXIBLE	FLEXIBLE	T1	T1	5.0	5.0	0.15	0.055	No.2	No.2
IRDRUN59	CALTRANS A2 0.6g 100%	126.5	552.2	0.519	FLEXIBLE	FLEXIBLE	T1	T1	5.0	5.0	0.15	0.055	No.2	No.2
IRDRUN60	JP LEVEL 2 G.C.1 100%	109.8	480.9	0.391	FLEXIBLE	FLEXIBLE	T1	T1	5.0	5.0	0.15	0.055	No.2	No.2
IRDRUN61	JP LEVEL 2 G.C.2 75%	77.1	336.8	0.282	FLEXIBLE	FLEXIBLE	T1	T1	5.0	5.0	0.15	0.055	No.2	No.2
IRDRUN62	JP LEVEL 2 G.C.3 75%	84.6	367.8	0.318	FLEXIBLE	FLEXIBLE	T1	T1	5.0	5.0	0.15	0.055	No.2	No.2
IRDRUN63	TAFT N21E H+V 400%	57.9	270.1	0.591	FLEXIBLE	FLEXIBLE	T1	T1	5.0	5.0	0.15	0.055	No.2	No.2
IRDRUN64	EL CENTRO S00E H+V 100%	24.1	155.7	0.263	FLEXIBLE	FLEXIBLE	T1	T1	5.0	5.0	0.15	0.055	No.2	No.2
IRDRUN65	EL CENTRO S00E H+V 200%	47.9	316.8	0.551	FLEXIBLE	FLEXIBLE	T1	T1	5.0	5.0	0.15	0.055	No.2	No.2
RD2RUN01	EL CENTRO S00E 100%	23.9	159.0	0.349	STIFF	STIFF	T2	T2	17.6	17.6	0.138	0.055	No.2	No.2
RD2RUN02	EL CENTRO S00E 200%	48.1	314.3	0.636	STIFF	STIFF	T2	T2	17.6	17.6	0.138	0.055	No.2	No.2
RD2RUN03	JP LEVEL 1 G.C.1 100%	17.0	101.6	0.117	STIFF	STIFF	T2	T2	17.6	17.6	0.138	0.055	No.2	No.2
RD2RUN04	JP LEVEL 1 G.C.2 100%	17.5	114.0	0.125	STIFF	STIFF	T2	T2	17.6	17.6	0.138	0.055	No.2	No.2
RD2RUN05	JP LEVEL 1 G.C.3 100%	34.3	163.4	0.139	STIFF	STIFF	T2	T2	17.6	17.6	0.138	0.055	No.2	No.2
RD2RUN06	JP LEVEL 2 G.C.1 75%	81.5	361.3	0.370	STIFF	STIFF	T2	T2	17.6	17.6	0.138	0.055	No.2	No.2
RD2RUN07	JP LEVEL 2 G.C.1 100%	108.4	470.3	0.525	STIFF	STIFF	T2	T2	17.6	17.6	0.138	0.055	No.2	No.2
RD2RUN08	JP LEVEL 2 G.C.2 75%	76.2	332.7	0.339	STIFF	STIFF	T2	T2	17.6	17.6	0.138	0.055	No.2	No.2
RD2RUN09	JP LEVEL 2 G.C.2 100%	101.4	445.6	0.403	STIFF	STIFF	T2	T2	17.6	17.6	0.138	0.055	No.2	No.2
RD2RUN10	JP LEVEL 2 G.C.3 75%	83.8	365.2	0.363	STIFF	STIFF	T2	T2	17.6	17.6	0.138	0.055	No.2	No.2
RD2RUN11	JP LEVEL 2 G.C.3 100%	111.7	485.7	0.463	STIFF	STIFF	T2	T2	17.6	17.6	0.138	0.055	No.2	No.2
RD2RUN12	TAFT N21E 100%	14.2	70.2	0.160	STIFF	STIFF	T2	T2	17.6	17.6	0.138	0.055	No.2	No.2
RD2RUN13	TAFT N21E 200%	28.6	131.3	0.284	STIFF	STIFF	T2	T2	17.6	17.6	0.138	0.055	No.2	No.2

Table 5-II Cont'd

TEST No.	EXCITATION	PEAK TABLE MOTION			PIER CONDITION		BEARING MATERIAL		BEARING PRESSURE (MPa)		FRICTIONAL PROPERTIES		RUBBER RESTORING FORCE DEVICE	
		DIS. (mm)	VEL. (mm/s)	ACC. (g)	SOUTH	NORTH	SOUTH	NORTH	SOUTH	NORTH	fmax	fmin	SOUTH	NORTH
RD2RUN14	TAFT N21E 400%	57.3	265.9	0.559	STIFF	STIFF	T2	T2	17.6	17.6	0.138	0.055	No.2	No.2
RD2RUN15	TAFT N21E 600%	85.7	406.6	0.837	STIFF	STIFF	T2	T2	17.6	17.6	0.138	0.055	No.2	No.2
RD2RUN16	PACOIMA S74W 100%	29.4	278.2	0.730	STIFF	STIFF	T2	T2	17.6	17.6	0.138	0.055	No.2	No.2
RD2RUN17	HACHINOHE N-S 100%	32.1	139.6	0.213	STIFF	STIFF	T2	T2	17.6	17.6	0.138	0.055	No.2	No.2
RD2RUN18	HACHINOHE N-S 200%	64.0	273.9	0.459	STIFF	STIFF	T2	T2	17.6	17.6	0.138	0.055	No.2	No.2
RD2RUN19	WHITE NOISE 0.1g	15.6	47.9	0.085	STIFF	STIFF	T2	T2	17.6	17.6	0.138	0.055	No.2	No.2
RD2RUN20	HACHINOHE N-S 300%	95.6	412.8	0.632	STIFF	STIFF	T2	T2	17.6	17.6	0.138	0.055	No.2	No.2
RD2RUN21	CALTRANS R3 0.6g 100%	95.8	309.1	0.665	STIFF	STIFF	T2	T2	17.6	17.6	0.138	0.055	No.2	No.2
RD2RUN22	CALTRANS S3 0.6g 100%	119.4	430.6	0.834	STIFF	STIFF	T2	T2	17.6	17.6	0.138	0.055	No.2	No.2
RD2RUN23	CALTRANS A2 0.6g 100%	125.1	547.2	0.621	STIFF	STIFF	T2	T2	17.6	17.6	0.138	0.055	No.2	No.2
RD2RUN24	MIYAGIKENOKI E-W 100%	12.3	83.2	0.133	STIFF	STIFF	T2	T2	17.6	17.6	0.138	0.055	No.2	No.2
RD2RUN25	MIYAGIKENOKI E-W 300%	37.1	236.1	0.341	STIFF	STIFF	T2	T2	17.6	17.6	0.138	0.055	No.2	No.2
RD2RUN26	MIYAGIKENOKI E-W 600%	73.8	461.8	0.881	STIFF	STIFF	T2	T2	17.6	17.6	0.138	0.055	No.2	No.2
RD2RUN27	AKITA N-S 100%	34.0	148.3	0.179	STIFF	STIFF	T2	T2	17.6	17.6	0.138	0.055	No.2	No.2
RD2RUN28	AKITA N-S 200%	68.1	297.9	0.353	STIFF	STIFF	T2	T2	17.6	17.6	0.138	0.055	No.2	No.2
RD2RUN29	PACOIMA S16E 50%	40.5	236.9	0.471	STIFF	STIFF	T2	T2	17.6	17.6	0.138	0.055	No.2	No.2
RD2RUN30	PACOIMA S16E 75%	60.6	363.2	0.660	STIFF	STIFF	T2	T2	17.6	17.6	0.138	0.055	No.2	No.2
RD2RUN31	MEXICO N90W 100%	52.5	312.5	0.183	STIFF	STIFF	T2	T2	17.6	17.6	0.138	0.055	No.2	No.2
RD2RUN32	MEXICO N90W 120%	62.9	375.1	0.219	STIFF	STIFF	T2	T2	17.6	17.6	0.138	0.055	No.2	No.2
RD2RUN33	TAFT N21E H+V 400%	57.5	267.8	0.558	STIFF	STIFF	T2	T2	17.6	17.6	0.138	0.055	No.2	No.2
RD2RUN34	EL CENTRO S00E H+V 200%	48.2	314.6	0.620	STIFF	STIFF	T2	T2	17.6	17.6	0.138	0.055	No.2	No.2
RD2RUN35	EL CENTRO S00E 100%	23.8	156.5	0.271	FLEXIBLE	FLEXIBLE	T2	T2	17.6	17.6	0.138	0.055	No.2	No.2
RD2RUN36	EL CENTRO S00E 200%	47.5	311.8	0.551	FLEXIBLE	FLEXIBLE	T2	T2	17.6	17.6	0.138	0.055	No.2	No.2
RD2RUN37	JP LEVEL 1 G.C.1 100%	17.2	103.4	0.105	FLEXIBLE	FLEXIBLE	T2	T2	17.6	17.6	0.138	0.055	No.2	No.2
RD2RUN38	JP LEVEL 1 G.C.1 150%	25.6	150.6	0.153	FLEXIBLE	FLEXIBLE	T2	T2	17.6	17.6	0.138	0.055	No.2	No.2
RD2RUN39	JP LEVEL 1 G.C.2 100%	17.7	114.5	0.100	FLEXIBLE	FLEXIBLE	T2	T2	17.6	17.6	0.138	0.055	No.2	No.2

Table 5-II Cont'd

TEST No.	EXCITATION	PEAK TABLE MOTION			PIER CONDITION		BEARING MATERIAL		BEARING PRESSURE (MPa)		FRICTIONAL PROPERTIES		RUBBER RESTORING FORCE DEVICE	
		DIS. (mm)	VEL. (mm/s)	ACC. (g)	SOUTH	NORTH	SOUTH	NORTH	SOUTH	NORTH	fmax	fmin	SOUTH	NORTH
RD2RUN40	JP LEVEL 1 G.C.2 150%	26.5	174.5	0.152	FLEXIBLE	FLEXIBLE	T2	T2	17.6	17.6	0.138	0.055	No.2	No.2
RD2RUN41	JP LEVEL 1 G.C.3 100%	34.1	163.6	0.113	FLEXIBLE	FLEXIBLE	T2	T2	17.6	17.6	0.138	0.055	No.2	No.2
RD2RUN42	JP LEVEL 1 G.C.3 150%	51.0	240.9	0.172	FLEXIBLE	FLEXIBLE	T2	T2	17.6	17.6	0.138	0.055	No.2	No.2
RD2RUN43	TAFT N21E 100%	14.3	64.8	0.134	FLEXIBLE	FLEXIBLE	T2	T2	17.6	17.6	0.138	0.055	No.2	No.2
RD2RUN44	TAFT N21E 200%	28.8	132.9	0.287	FLEXIBLE	FLEXIBLE	T2	T2	17.6	17.6	0.138	0.055	No.2	No.2
RD2RUN45	TAFT N21E 400%	57.4	265.0	0.582	FLEXIBLE	FLEXIBLE	T2	T2	17.6	17.6	0.138	0.055	No.2	No.2
RD2RUN46	TAFT N21E 500%	71.5	336.8	0.729	FLEXIBLE	FLEXIBLE	T2	T2	17.6	17.6	0.138	0.055	No.2	No.2
RD2RUN47	JP LEVEL 2 G.C.1 75%	81.6	355.8	0.276	FLEXIBLE	FLEXIBLE	T2	T2	17.6	17.6	0.138	0.055	No.2	No.2
RD2RUN48	JP LEVEL 2 G.C.2 75%	76.4	330.8	0.305	FLEXIBLE	FLEXIBLE	T2	T2	17.6	17.6	0.138	0.055	No.2	No.2
RD2RUN49	JP LEVEL 2 G.C.3 75%	84.0	366.8	0.307	FLEXIBLE	FLEXIBLE	T2	T2	17.6	17.6	0.138	0.055	No.2	No.2
RD2RUN50	PACOIMA S74W 100%	29.3	254.3	0.834	FLEXIBLE	FLEXIBLE	T2	T2	17.6	17.6	0.138	0.055	No.2	No.2
RD2RUN51	HACHINOHE N-S 100%	32.4	134.4	0.198	FLEXIBLE	FLEXIBLE	T2	T2	17.6	17.6	0.138	0.055	No.2	No.2
RD2RUN52	HACHINOHE N-S 200%	64.3	273.7	0.460	FLEXIBLE	FLEXIBLE	T2	T2	17.6	17.6	0.138	0.055	No.2	No.2
RD2RUN53	HACHINOHE N-S 300%	95.9	418.9	0.790	FLEXIBLE	FLEXIBLE	T2	T2	17.6	17.6	0.138	0.055	No.2	No.2
RD2RUN54	CALTRANS R3 0.6g 100%	95.7	301.9	0.585	FLEXIBLE	FLEXIBLE	T2	T2	17.6	17.6	0.138	0.055	No.2	No.2
RD2RUN55	CALTRANS S3 0.6g 100%	119.2	418.5	0.689	FLEXIBLE	FLEXIBLE	T2	T2	17.6	17.6	0.138	0.055	No.2	No.2
RD2RUN56	CALTRANS A2 0.6g 100%	125.4	544.3	0.509	FLEXIBLE	FLEXIBLE	T2	T2	17.6	17.6	0.138	0.055	No.2	No.2
RD2RUN57	MIYAGIKENOKI E-W 100%	12.46	75.9	0.123	FLEXIBLE	FLEXIBLE	T2	T2	17.6	17.6	0.138	0.055	No.2	No.2
RD2RUN58	MIYAGIKENOKI E-W 300%	37.1	220.7	0.385	FLEXIBLE	FLEXIBLE	T2	T2	17.6	17.6	0.138	0.055	No.2	No.2
RD2RUN59	MIYAGIKENOKI E-W 600%	73.7	458.6	0.968	FLEXIBLE	FLEXIBLE	T2	T2	17.6	17.6	0.138	0.055	No.2	No.2
RD2RUN60	AKITA N-S 100%	34.2	147.5	0.168	FLEXIBLE	FLEXIBLE	T2	T2	17.6	17.6	0.138	0.055	No.2	No.2
RD2RUN61	AKITA N-S 200%	68.4	291.2	0.361	FLEXIBLE	FLEXIBLE	T2	T2	17.6	17.6	0.138	0.055	No.2	No.2
RD2RUN62	PACOIMA S16E 50%	40.9	246.4	0.375	FLEXIBLE	FLEXIBLE	T2	T2	17.6	17.6	0.138	0.055	No.2	No.2
RD2RUN63	PACOIMA S16E 65%	53.1	316.0	0.481	FLEXIBLE	FLEXIBLE	T2	T2	17.6	17.6	0.138	0.055	No.2	No.2
RD2RUN64	MEXICO N90W 100%	52.8	312.3	0.179	FLEXIBLE	FLEXIBLE	T2	T2	17.6	17.6	0.138	0.055	No.2	No.2
RD2RUN65	MEXICO N90W 120%	63.3	374.1	0.223	FLEXIBLE	FLEXIBLE	T2	T2	17.6	17.6	0.138	0.055	No.2	No.2

Table 5-II Cont'd

TEST No.	EXCITATION	PEAK TABLE MOTION			PIER CONDITION		BEARING MATERIAL		BEARING PRESSURE (MPa)		FRICTIONAL PROPERTIES		RUBBER RESTORING FORCE DEVICE	
		DIS. (mm)	VEL. (mm/s)	ACC. (g)	SOUTH	NORTH	SOUTH	NORTH	SOUTH	NORTH	fmax	fmin	SOUTH	NORTH
RD2RUN66	TAFT N21E H+V 400%	57.8	265.0	0.591	FLEXIBLE	FLEXIBLE	T2	T2	17.6	17.6	0.138	0.055	No.2	No.2
RD2RUN67	EL CENTRO S00E H+V 200%	46.7	313.3	0.553	FLEXIBLE	FLEXIBLE	T2	T2	17.6	17.6	0.138	0.055	No.2	No.2
RHHRUN01	EL CENTRO S00E 100%	24.0	162.9	0.353	STIFF	STIFF	T2	T2	17.6	17.6	0.138	0.055	No.3	No.3
RHHRUN02	EL CENTRO S00E 200%	48.2	316.9	0.644	STIFF	STIFF	T2	T2	17.6	17.6	0.138	0.055	No.3	No.3
RHHRUN03	JP LEVEL 1 G.C.1 100%	17.1	102.7	0.117	STIFF	STIFF	T2	T2	17.6	17.6	0.138	0.055	No.3	No.3
RHHRUN04	JP LEVEL 1 G.C.2 100%	17.5	113.2	0.124	STIFF	STIFF	T2	T2	17.6	17.6	0.138	0.055	No.3	No.3
RHHRUN05	JP LEVEL 1 G.C.3 100%	34.3	165.4	0.143	STIFF	STIFF	T2	T2	17.6	17.6	0.138	0.055	No.3	No.3
RHHRUN06	JP LEVEL 2 G.C.1 100%	108.8	479.9	0.523	STIFF	STIFF	T2	T2	17.6	17.6	0.138	0.055	No.3	No.3
RHHRUN07	JP LEVEL 2 G.C.2 100%	101.7	448.9	0.400	STIFF	STIFF	T2	T2	17.6	17.6	0.138	0.055	No.3	No.3
RHHRUN08	JP LEVEL 2 G.C.3 100%	111.9	490.0	0.474	STIFF	STIFF	T2	T2	17.6	17.6	0.138	0.055	No.3	No.3
RHHRUN09	TAFT N21E 100%	14.2	70.5	0.165	STIFF	STIFF	T2	T2	17.6	17.6	0.138	0.055	No.3	No.3
RHHRUN10	TAFT N21E 400%	57.5	265.6	0.571	STIFF	STIFF	T2	T2	17.6	17.6	0.138	0.055	No.3	No.3
RHHRUN11	TAFT N21E 600%	86.0	411.3	0.862	STIFF	STIFF	T2	T2	17.6	17.6	0.138	0.055	No.3	No.3
RHHRUN12	PACOIMA S74W 100%	29.6	278.4	0.747	STIFF	STIFF	T2	T2	17.6	17.6	0.138	0.055	No.3	No.3
RHHRUN13	HACHINOHE N-S 100%	32.3	138.1	0.220	STIFF	STIFF	T2	T2	17.6	17.6	0.138	0.055	No.3	No.3
RHHRUN14	HACHINOHE N-S 300%	96.0	412.8	0.631	STIFF	STIFF	T2	T2	17.6	17.6	0.138	0.055	No.3	No.3
RHHRUN15	CALTRANS R3 0.6g 100%	96.1	307.7	0.673	STIFF	STIFF	T2	T2	17.6	17.6	0.138	0.055	No.3	No.3
RHHRUN16	CALTRANS S3 0.6g 100%	119.8	431.0	0.806	STIFF	STIFF	T2	T2	17.6	17.6	0.138	0.055	No.3	No.3
RHHRUN17	CALTRANS A2 0.6g 100%	125.5	551.1	0.610	STIFF	STIFF	T2	T2	17.6	17.6	0.138	0.055	No.3	No.3
RHHRUN18	MIYAGIKENOKI E-W 100%	12.5	81.9	0.141	STIFF	STIFF	T2	T2	17.6	17.6	0.138	0.055	No.3	No.3
RHHRUN19	MIYAGIKENOKI E-W 600%	74.1	461.4	0.904	STIFF	STIFF	T2	T2	17.6	17.6	0.138	0.055	No.3	No.3
RHHRUN20	AKITA N-S 100%	34.0	148.4	0.180	STIFF	STIFF	T2	T2	17.6	17.6	0.138	0.055	No.3	No.3
RHHRUN21	AKITA N-S 200%	68.1	295.0	0.350	STIFF	STIFF	T2	T2	17.6	17.6	0.138	0.055	No.3	No.3
RHHRUN22	PACOIMA S16E 75%	60.7	363.0	0.669	STIFF	STIFF	T2	T2	17.6	17.6	0.138	0.055	No.3	No.3
RHHRUN23	MEXICO N90W 100%	52.6	310.1	0.179	STIFF	STIFF	T2	T2	17.6	17.6	0.138	0.055	No.3	No.3
RHHRUN24	MEXICO N90W 120%	63.1	378.7	0.215	STIFF	STIFF	T2	T2	17.6	17.6	0.138	0.055	No.3	No.3

Table 5-II Cont'd

TEST No.	EXCITATION	PEAK TABLE MOTION			PIER CONDITION		BEARING MATERIAL		BEARING PRESSURE (MPa)		FRICTIONAL PROPERTIES		RUBBER RESTORING FORCE DEVICE	
		DIS. (mm)	VEL. (mm/s)	ACC. (g)	SOUTH	NORTH	SOUTH	NORTH	SOUTH	NORTH	fmax	fmin	SOUTH	NORTH
RHHRUN25	TAFT N21E H+V 400%	57.6	274.1	0.533	STIFF	STIFF	T2	T2	17.6	17.6	0.138	0.055	No.3	No.3
RHHRUN26	EL CENTRO S00E H+V 200%	48.3	314.6	0.638	STIFF	STIFF	T2	T2	17.6	17.6	0.138	0.055	No.3	No.3
RHHRUN27	PACOIMA S16E 85%	68.7	409.8	0.720	STIFF	STIFF	T2	T2	17.6	17.6	0.138	0.055	No.3	No.3
RHHRUN28	EL CENTRO S00E 100%	23.9	155.2	0.250	FLEXIBLE	FLEXIBLE	T2	T2	17.6	17.6	0.138	0.055	No.3	No.3
RHHRUN29	EL CENTRO S00E 200%	47.6	311.7	0.559	FLEXIBLE	FLEXIBLE	T2	T2	17.6	17.6	0.138	0.055	No.3	No.3
RHHRUN30	JP LEVEL 1 G.C.1 100%	17.2	104.1	0.107	FLEXIBLE	FLEXIBLE	T2	T2	17.6	17.6	0.138	0.055	No.3	No.3
RHHRUN31	JP LEVEL 1 G.C.1 150%	25.7	154.1	0.151	FLEXIBLE	FLEXIBLE	T2	T2	17.6	17.6	0.138	0.055	No.3	No.3
RHHRUN32	JP LEVEL 1 G.C.2 100%	17.7	118.3	0.106	FLEXIBLE	FLEXIBLE	T2	T2	17.6	17.6	0.138	0.055	No.3	No.3
RHHRUN33	JP LEVEL 1 G.C.2 150%	26.5	174.2	0.156	FLEXIBLE	FLEXIBLE	T2	T2	17.6	17.6	0.138	0.055	No.3	No.3
RHHRUN34	JP LEVEL 1 G.C.3 100%	34.2	163.1	0.113	FLEXIBLE	FLEXIBLE	T2	T2	17.6	17.6	0.138	0.055	No.3	No.3
RHHRUN35	JP LEVEL 1 G.C.3 150%	51.2	244.5	0.172	FLEXIBLE	FLEXIBLE	T2	T2	17.6	17.6	0.138	0.055	No.3	No.3
RHHRUN36	JP LEVEL 2 G.C.1 75%	81.9	360.0	0.270	FLEXIBLE	FLEXIBLE	T2	T2	17.6	17.6	0.138	0.055	No.3	No.3
RHHRUN37	JP LEVEL 2 G.C.1 85%	92.7	405.2	0.319	FLEXIBLE	FLEXIBLE	T2	T2	17.6	17.6	0.138	0.055	No.3	No.3
RHHRUN38	JP LEVEL 2 G.C.1 100%	108.9	482.6	0.381	FLEXIBLE	FLEXIBLE	T2	T2	17.6	17.6	0.138	0.055	No.3	No.3
RHHRUN39	JP LEVEL 2 G.C.2 75%	76.5	334.0	0.295	FLEXIBLE	FLEXIBLE	T2	T2	17.6	17.6	0.138	0.055	No.3	No.3
RHHRUN40	JP LEVEL 2 G.C.2 85%	86.6	380.2	0.351	FLEXIBLE	FLEXIBLE	T2	T2	17.6	17.6	0.138	0.055	No.3	No.3
RHHRUN41	JP LEVEL 2 G.C.3 75%	84.2	366.5	0.314	FLEXIBLE	FLEXIBLE	T2	T2	17.6	17.6	0.138	0.055	No.3	No.3
RHHRUN42	JP LEVEL 2 G.C.3 85%	95.4	419.1	0.343	FLEXIBLE	FLEXIBLE	T2	T2	17.6	17.6	0.138	0.055	No.3	No.3
RHHRUN43	TAFT N21E 100%	14.4	65.8	0.138	FLEXIBLE	FLEXIBLE	T2	T2	17.6	17.6	0.138	0.055	No.3	No.3
RHHRUN44	TAFT N21E 400%	57.6	265.0	0.630	FLEXIBLE	FLEXIBLE	T2	T2	17.6	17.6	0.138	0.055	No.3	No.3
RHHRUN45	TAFT N21E 500%	71.7	338.5	0.750	FLEXIBLE	FLEXIBLE	T2	T2	17.6	17.6	0.138	0.055	No.3	No.3
RHHRUN46	PACOIMA S74W 100%	29.4	256.2	0.840	FLEXIBLE	FLEXIBLE	T2	T2	17.6	17.6	0.138	0.055	No.3	No.3
RHHRUN47	HACHINOHE N-S 100%	32.5	136.8	0.196	FLEXIBLE	FLEXIBLE	T2	T2	17.6	17.6	0.138	0.055	No.3	No.3
RHHRUN48	HACHINOHE N-S 200%	64.4	276.9	0.452	FLEXIBLE	FLEXIBLE	T2	T2	17.6	17.6	0.138	0.055	No.3	No.3
RHHRUN49	HACHINOHE N-S 250%	80.3	349.9	0.626	FLEXIBLE	FLEXIBLE	T2	T2	17.6	17.6	0.138	0.055	No.3	No.3
RHHRUN50	HACHINOHE N-S 300%	96.2	421.2	0.790	FLEXIBLE	FLEXIBLE	T2	T2	17.6	17.6	0.138	0.055	No.3	No.3

Table 5-II Cont'd

TEST No.	EXCITATION	PEAK TABLE MOTION			PIER CONDITION		BEARING MATERIAL		BEARING PRESSURE (MPa)		FRICTIONAL PROPERTIES		RUBBER RESTORING FORCE DEVICE	
		DIS. (mm)	VEL. (mm/s)	ACC. (g)	SOUTH	NORTH	SOUTH	NORTH	SOUTH	NORTH	fmax	fmin	SOUTH	NORTH
RHHRUN51	CALTRANS R3 0.6g 100%	95.9	305.4	0.594	FLEXIBLE	FLEXIBLE	T2	T2	17.6	17.6	0.138	0.055	No.3	No.3
RHHRUN52	CALTRANS S3 0.6g 100%	119.3	424.3	0.701	FLEXIBLE	FLEXIBLE	T2	T2	17.6	17.6	0.138	0.055	No.3	No.3
RHHRUN53	CALTRANS A2 0.6g 100%	125.7	547.0	0.554	FLEXIBLE	FLEXIBLE	T2	T2	17.6	17.6	0.138	0.055	No.3	No.3
RHHRUN54	MIYAGIKENOKI E-W 100%	12.5	74.6	0.123	FLEXIBLE	FLEXIBLE	T2	T2	17.6	17.6	0.138	0.055	No.3	No.3
RHHRUN55	MIYAGIKENOKI E-W 300%	37.2	222.7	0.396	FLEXIBLE	FLEXIBLE	T2	T2	17.6	17.6	0.138	0.055	No.3	No.3
RHHRUN56	MIYAGIKENOKI E-W 600%	73.7	465.2	0.989	FLEXIBLE	FLEXIBLE	T2	T2	17.6	17.6	0.138	0.055	No.3	No.3
RHHRUN57	AKITA N-S 100%	34.2	147.5	0.169	FLEXIBLE	FLEXIBLE	T2	T2	17.6	17.6	0.138	0.055	No.3	No.3
RHHRUN58	AKITA N-S 200%	68.3	289.4	0.340	FLEXIBLE	FLEXIBLE	T2	T2	17.6	17.6	0.138	0.055	No.3	No.3
RHHRUN59	PACOIMA S16E 50%	40.9	246.5	0.414	FLEXIBLE	FLEXIBLE	T2	T2	17.6	17.6	0.138	0.055	No.3	No.3
RHHRUN60	PACOIMA S16E 65%	53.1	317.2	0.531	FLEXIBLE	FLEXIBLE	T2	T2	17.6	17.6	0.138	0.055	No.3	No.3
RHHRUN61	PACOIMA S16E 75%	61.2	363.2	0.574	FLEXIBLE	FLEXIBLE	T2	T2	17.6	17.6	0.138	0.055	No.3	No.3
RHHRUN62	MEXICO N90W 100%	52.7	310.9	0.180	FLEXIBLE	FLEXIBLE	T2	T2	17.6	17.6	0.138	0.055	No.3	No.3
RHHRUN63	MEXICO N90W 120%	63.2	375.2	0.214	FLEXIBLE	FLEXIBLE	T2	T2	17.6	17.6	0.138	0.055	No.3	No.3
RHHRUN64	TAFT N21E H+V 400%	57.6	263.7	0.610	FLEXIBLE	FLEXIBLE	T2	T2	17.6	17.6	0.138	0.055	No.3	No.3
RHHRUN65	EL CENTRO S00E H+V 200%	47.6	313.8	0.551	FLEXIBLE	FLEXIBLE	T2	T2	17.6	17.6	0.138	0.055	No.3	No.3
RSSRUN01	EL CENTRO S00E 100%	24.0	163.1	0.203	STIFF	STIFF	T2	T2	17.6	17.6	0.138	0.055	No.1	No.1
RSSRUN02	EL CENTRO S00E 200%	48.2	315.9	0.357	STIFF	STIFF	T2	T2	17.6	17.6	0.138	0.055	No.1	No.1
RSSRUN03	JP LEVEL 1 G.C.1 100%	17.0	104.3	0.068	STIFF	STIFF	T2	T2	17.6	17.6	0.138	0.055	No.1	No.1
RSSRUN04	JP LEVEL 1 G.C.2 100%	17.5	111.6	0.073	STIFF	STIFF	T2	T2	17.6	17.6	0.138	0.055	No.1	No.1
RSSRUN05	JP LEVEL 1 G.C.3 100%	34.3	164.0	0.082	STIFF	STIFF	T2	T2	17.6	17.6	0.138	0.055	No.1	No.1
RSSRUN06	JP LEVEL 2 G.C.1 100%	108.6	469.9	0.306	STIFF	STIFF	T2	T2	17.6	17.6	0.138	0.055	No.1	No.1
RSSRUN07	JP LEVEL 2 G.C.2 75%	76.3	334.9	0.201	STIFF	STIFF	T2	T2	17.6	17.6	0.138	0.055	No.1	No.1
RSSRUN08	JP LEVEL 2 G.C.2 100%	101.6	450.2	0.233	STIFF	STIFF	T2	T2	17.6	17.6	0.138	0.055	No.1	No.1
RSSRUN09	JP LEVEL 2 G.C.3 100%	111.7	495.0	0.276	STIFF	STIFF	T2	T2	17.6	17.6	0.138	0.055	No.1	No.1
RSSRUN10	CALTRANS R3 0.6g 100%	96.0	314.1	0.372	STIFF	STIFF	T2	T2	17.6	17.6	0.138	0.055	No.1	No.1
RSSRUN11	CALTRANS S3 0.6g 100%	119.6	433.4	0.446	STIFF	STIFF	T2	T2	17.6	17.6	0.138	0.055	No.1	No.1

Table 5-II Cont'd

TEST No.	EXCITATION	PEAK TABLE MOTION			PIER CONDITION		BEARING MATERIAL		BEARING PRESSURE (MPa)		FRICTIONAL PROPERTIES		RUBBER RESTORING FORCE DEVICE	
		DIS. (mm)	VEL. (mm/s)	ACC. (g)	SOUTH	NORTH	SOUTH	NORTH	SOUTH	NORTH	fmax	fmin	SOUTH	NORTH
RSSRUN12	CALTRANS A2 0.6g 100%	125.5	552.7	0.289	STIFF	STIFF	T2	T2	17.6	17.6	0.138	0.055	No.1	No.1
RSSRUN13	CALTRANS A2 0.6g 100%	125.5	555.8	0.293	STIFF	STIFF	T2	T2	17.6	17.6	0.138	0.055	No.1	No.1
RSSRUN14	HACHINOHE N-S 100%	32.2	137.6	0.125	STIFF	STIFF	T2	T2	17.6	17.6	0.138	0.055	No.1	No.1
RSSRUN15	HACHINOHE N-S 200%	64.2	273.3	0.272	STIFF	STIFF	T2	T2	17.6	17.6	0.138	0.055	No.1	No.1
RSSRUN16	HACHINOHE N-S 300%	95.8	418.2	0.352	STIFF	STIFF	T2	T2	17.6	17.6	0.138	0.055	No.1	No.1
RSSRUN17	MEXICO N90W 100%	52.6	312.5	0.103	STIFF	STIFF	T2	T2	17.6	17.6	0.138	0.055	No.1	No.1
RSSRUN18	MEXICO N90W 120%	63.1	371.0	0.121	STIFF	STIFF	T2	T2	17.6	17.6	0.138	0.055	No.1	No.1
RSSRUN19	PACOIMA S16E 50%	40.7	241.2	0.241	STIFF	STIFF	T2	T2	17.6	17.6	0.138	0.055	No.1	No.1
RSSRUN20	PACOIMA S16E 75%	60.7	368.9	0.380	STIFF	STIFF	T2	T2	17.6	17.6	0.138	0.055	No.1	No.1
RSSRUN21	AKITA N-S 100%	34.0	146.6	0.103	STIFF	STIFF	T2	T2	17.6	17.6	0.138	0.055	No.1	No.1
RSSRUN22	AKITA N-S 200%	68.0	292.9	0.219	STIFF	STIFF	T2	T2	17.6	17.6	0.138	0.055	No.1	No.1
RSSRUN23	TAFT N21E H+V 100%	14.2	70.2	0.099	STIFF	STIFF	T2	T2	17.6	17.6	0.138	0.055	No.1	No.1
RSSRUN24	TAFT N21E H+V 400%	57.5	263.7	0.309	STIFF	STIFF	T2	T2	17.6	17.6	0.138	0.055	No.1	No.1
RSSRUN25	TAFT N21E H+V 600%	86.0	405.1	0.460	STIFF	STIFF	T2	T2	17.6	17.6	0.138	0.055	No.1	No.1
RSSRUN26	EL CENTRO S00E H+V 200%	48.2	317.0	0.368	STIFF	STIFF	T2	T2	17.6	17.6	0.138	0.055	No.1	No.1
RSSRUN27	TAFT N21E H+V 400%	57.6	268.4	0.298	STIFF	STIFF	T2	T2	17.6	17.6	0.138	0.055	No.1	No.1
RSSRUN28	EL CENTRO S00E 100%	24.0	154.2	0.147	FLEXIBLE	FLEXIBLE	T2	T2	17.6	17.6	0.138	0.055	No.1	No.1
RSSRUN29	EL CENTRO S00E 200%	47.7	313.6	0.309	FLEXIBLE	FLEXIBLE	T2	T2	17.6	17.6	0.138	0.055	No.1	No.1
RSSRUN30	JP LEVEL 1 G.C.1 100%	17.1	104.6	0.060	FLEXIBLE	FLEXIBLE	T2	T2	17.6	17.6	0.138	0.055	No.1	No.1
RSSRUN31	JP LEVEL 1 G.C.1 150%	25.8	150.3	0.084	FLEXIBLE	FLEXIBLE	T2	T2	17.6	17.6	0.138	0.055	No.1	No.1
RSSRUN32	JP LEVEL 1 G.C.2 100%	17.8	114.2	0.058	FLEXIBLE	FLEXIBLE	T2	T2	17.6	17.6	0.138	0.055	No.1	No.1
RSSRUN33	JP LEVEL 1 G.C.2 150%	26.5	173.8	0.093	FLEXIBLE	FLEXIBLE	T2	T2	17.6	17.6	0.138	0.055	No.1	No.1
RSSRUN34	JP LEVEL 1 G.C.3 100%	34.1	163.6	0.065	FLEXIBLE	FLEXIBLE	T2	T2	17.6	17.6	0.138	0.055	No.1	No.1
RSSRUN35	JP LEVEL 1 G.C.3 150%	51.2	242.4	0.104	FLEXIBLE	FLEXIBLE	T2	T2	17.6	17.6	0.138	0.055	No.1	No.1
RSSRUN36	JP LEVEL 2 G.C.1 75%	81.7	351.8	0.153	FLEXIBLE	FLEXIBLE	T2	T2	17.6	17.6	0.138	0.055	No.1	No.1
RSSRUN37	JP LEVEL 2 G.C.2 75%	76.5	331.0	0.204	FLEXIBLE	FLEXIBLE	T2	T2	17.6	17.6	0.138	0.055	No.1	No.1

Table 5-II Cont'd

TEST No.	EXCITATION	PEAK TABLE MOTION			PIER CONDITION		BEARING MATERIAL		BEARING PRESSURE (MPa)		FRICTIONAL PROPERTIES		RUBBER RESTORING FORCE DEVICE	
		DIS. (mm)	VEL. (mm/s)	ACC. (g)	SOUTH	NORTH	SOUTH	NORTH	SOUTH	NORTH	fmax	fmin	SOUTH	NORTH
RSSRUN38	JP LEVEL 2 G.C.3 75%	84.1	366.6	0.182	FLEXIBLE	FLEXIBLE	T2	T2	17.6	17.6	0.138	0.055	No.1	No.1
RSSRUN39	TAFT N21E 100%	14.4	64.9	0.070	FLEXIBLE	FLEXIBLE	T2	T2	17.6	17.6	0.138	0.055	No.1	No.1
RSSRUN40	TAFT N21E 400%	57.5	265.0	0.342	FLEXIBLE	FLEXIBLE	T2	T2	17.6	17.6	0.138	0.055	No.1	No.1
RSSRUN41	TAFT N21E 500%	71.7	339.9	0.408	FLEXIBLE	FLEXIBLE	T2	T2	17.6	17.6	0.138	0.055	No.1	No.1
RSSRUN42	PACOIMA S74W 100%	29.2	257.6	0.455	FLEXIBLE	FLEXIBLE	T2	T2	17.6	17.6	0.138	0.055	No.1	No.1
RSSRUN43	HACHINOHE N-S 200%	64.4	278.1	0.260	FLEXIBLE	FLEXIBLE	T2	T2	17.6	17.6	0.138	0.055	No.1	No.1
RSSRUN44	HACHINOHE N-S 300%	96.2	417.8	0.426	FLEXIBLE	FLEXIBLE	T2	T2	17.6	17.6	0.138	0.055	No.1	No.1
RSSRUN45	HACHINOHE N-S 100%	32.6	135.0	0.112	FLEXIBLE	FLEXIBLE	T2	T2	17.6	17.6	0.138	0.055	No.1	No.1
RSSRUN46	CALTRANS R3 0.6g 100%	95.9	301.6	0.324	FLEXIBLE	FLEXIBLE	T2	T2	17.6	17.6	0.138	0.055	No.1	No.1
RSSRUN47	CALTRANS S3 0.6g 100%	119.3	424.4	0.391	FLEXIBLE	FLEXIBLE	T2	T2	17.6	17.6	0.138	0.055	No.1	No.1
RSSRUN48	CALTRANS A2 0.6g 100%	125.6	541.9	0.269	FLEXIBLE	FLEXIBLE	T2	T2	17.6	17.6	0.138	0.055	No.1	No.1
RSSRUN49	MIYAGIKENOKI E-W 100%	12.5	74.5	0.067	FLEXIBLE	FLEXIBLE	T2	T2	17.6	17.6	0.138	0.055	No.1	No.1
RSSRUN50	MIYAGIKENOKI E-W 300%	37.1	221.9	0.218	FLEXIBLE	FLEXIBLE	T2	T2	17.6	17.6	0.138	0.055	No.1	No.1
RSSRUN51	MIYAGIKENOKI E-W 600%	73.6	463.9	0.467	FLEXIBLE	FLEXIBLE	T2	T2	17.6	17.6	0.138	0.055	No.1	No.1
RSSRUN52	AKITA N-S 100%	34.2	146.0	0.101	FLEXIBLE	FLEXIBLE	T2	T2	17.6	17.6	0.138	0.055	No.1	No.1
RSSRUN53	AKITA N-S 200%	68.3	294.3	0.216	FLEXIBLE	FLEXIBLE	T2	T2	17.6	17.6	0.138	0.055	No.1	No.1
RSSRUN54	PACOIMA S16E 50%	41.1	240.8	0.213	FLEXIBLE	FLEXIBLE	T2	T2	17.6	17.6	0.138	0.055	No.1	No.1
RSSRUN55	PACOIMA S16E 65%	53.2	311.8	0.294	FLEXIBLE	FLEXIBLE	T2	T2	17.6	17.6	0.138	0.055	No.1	No.1
RSSRUN56	MEXICO N90W 100%	52.9	310.0	0.118	FLEXIBLE	FLEXIBLE	T2	T2	17.6	17.6	0.138	0.055	No.1	No.1
RSSRUN57	MEXICO N90W 120%	63.2	369.6	0.158	FLEXIBLE	FLEXIBLE	T2	T2	17.6	17.6	0.138	0.055	No.1	No.1
RSSRUN58	TAFT N21E H+V 400%	57.8	267.8	0.367	FLEXIBLE	FLEXIBLE	T2	T2	17.6	17.6	0.138	0.055	No.1	No.1
RSSRUN59	EL CENTRO S00E H+V 200%	47.7	315.3	0.324	FLEXIBLE	FLEXIBLE	T2	T2	17.6	17.6	0.138	0.055	No.1	No.1
RMLRUN01	EL CENTRO S00E 100%	24.1	157.7	0.332	STIFF	FLEXIBLE	T2	C1	17.6	111.0	*	**	No.3	No.2
RMLRUN02	EL CENTRO S00E 200%	47.9	315.9	0.545	STIFF	FLEXIBLE	T2	C1	17.6	111.0	*	**	No.3	No.2
RMLRUN03	TAFT N21E 100%	14.4	65.5	0.123	STIFF	FLEXIBLE	T2	C1	17.6	111.0	*	**	No.3	No.2
RMLRUN04	TAFT N21E 400%	57.5	269.7	0.595	STIFF	FLEXIBLE	T2	C1	17.6	111.0	*	**	No.3	No.2

* T2 : 0.138, C1 : 0.068 ** T2 : 0.055, C1 : 0.040

Table 5-II Cont'd

TEST No.	EXCITATION	PEAK TABLE MOTION			PIER CONDITION		BEARING MATERIAL		BEARING PRESSURE (MPa)		FRICTIONAL PROPERTIES		RUBBER RESTORING FORCE DEVICE	
		DIS. (mm)	VEL. (mm/s)	ACC. (g)	SOUTH	NORTH	SOUTH	NORTH	SOUTH	NORTH	fmax	fmin	SOUTH	NORTH
RMLRUN05	JP LEVEL 1 G.C.1 100%	17.2	102.9	0.126	STIFF	FLEXIBLE	T2	C1	17.6	111.0	*	**	No.3	No.2
RMLRUN06	JP LEVEL 1 G.C.2 100%	17.6	113.2	0.117	STIFF	FLEXIBLE	T2	C1	17.6	111.0	*	**	No.3	No.2
RMLRUN07	JP LEVEL 1 G.C.3 100%	34.3	164.8	0.123	STIFF	FLEXIBLE	T2	C1	17.6	111.0	*	**	No.3	No.2
RMLRUN08	JP LEVEL 2 G.C.1 75%	81.7	354.8	0.328	STIFF	FLEXIBLE	T2	C1	17.6	111.0	*	**	No.3	No.2
RMLRUN09	JP LEVEL 2 G.C.2 75%	76.6	332.1	0.284	STIFF	FLEXIBLE	T2	C1	17.6	111.0	*	**	No.3	No.2
RMLRUN10	JP LEVEL 2 G.C.3 75%	84.1	373.6	0.329	STIFF	FLEXIBLE	T2	C1	17.6	111.0	*	**	No.3	No.2
RMLRUN11	JP LEVEL 2 G.C.3 100%	112.3	489.3	0.424	STIFF	FLEXIBLE	T2	C1	17.6	111.0	*	**	No.3	No.2
RMLRUN12	PACOIMA S74W 100%	29.5	287.2	0.784	STIFF	FLEXIBLE	T2	C1	17.6	111.0	*	**	No.3	No.2
RMLRUN13	HACHINOHE N-S 100%	32.4	138.9	0.215	STIFF	FLEXIBLE	T2	C1	17.6	111.0	*	**	No.3	No.2
RMLRUN14	HACHINOHE N-S 200%	64.2	278.3	0.438	STIFF	FLEXIBLE	T2	C1	17.6	111.0	*	**	No.3	No.2
RMLRUN15	HACHINOHE N-S 300%	96.0	426.5	0.703	STIFF	FLEXIBLE	T2	C1	17.6	111.0	*	**	No.3	No.2
RMLRUN16	MIYAGIKENOKI E-W 300%	37.1	227.8	0.406	STIFF	FLEXIBLE	T2	C1	17.6	111.0	*	**	No.3	No.2
RMLRUN17	MIYAGIKENOKI E-W 600%	74.2	470.9	1.029	STIFF	FLEXIBLE	T2	C1	17.6	111.0	*	**	No.3	No.2
RMLRUN18	CALTRANS R3 0.6g 100%	96.1	311.0	0.601	STIFF	FLEXIBLE	T2	C1	17.6	111.0	*	**	No.3	No.2
RMLRUN19	EL CENTRO S00E 100%	23.8	156.9	0.271	FLEXIBLE	FLEXIBLE	T2	C1	17.6	111.0	*	**	No.3	No.2
RMLRUN20	EL CENTRO S00E 200%	47.8	316.8	0.580	FLEXIBLE	FLEXIBLE	T2	C1	17.6	111.0	*	**	No.3	No.2
RMLRUN21	TAFT N21E 100%	14.5	66.5	0.141	FLEXIBLE	FLEXIBLE	T2	C1	17.6	111.0	*	**	No.3	No.2
RMLRUN22	TAFT N21E 400%	57.4	266.5	0.600	FLEXIBLE	FLEXIBLE	T2	C1	17.6	111.0	*	**	No.3	No.2
RMLRUN23	PACOIMA S74W 100%	28.7	271.7	0.807	FLEXIBLE	FLEXIBLE	T2	C1	17.6	111.0	*	**	No.3	No.2
RMLRUN24	HACHINOHE N-S 100%	32.4	139.0	0.205	FLEXIBLE	FLEXIBLE	T2	C1	17.6	111.0	*	**	No.3	No.2
RMLRUN25	HACHINOHE N-S 200%	64.2	276.0	0.468	FLEXIBLE	FLEXIBLE	T2	C1	17.6	111.0	*	**	No.3	No.2
RMLRUN26	HACHINOHE N-S 300%	96.1	418.9	0.740	FLEXIBLE	FLEXIBLE	T2	C1	17.6	111.0	*	**	No.3	No.2
RMLRUN27	MIYAGIKENOKI E-W 300%	37.1	225.5	0.430	FLEXIBLE	FLEXIBLE	T2	C1	17.6	111.0	*	**	No.3	No.2
RMLRUN28	MIYAGIKENOKI E-W 600%	73.8	462.3	1.026	FLEXIBLE	FLEXIBLE	T2	C1	17.6	111.0	*	**	No.3	No.2
RMLRUN29	CALTRANS R3 0.6g 100%	96.1	308.8	0.581	FLEXIBLE	FLEXIBLE	T2	C1	17.6	111.0	*	**	No.3	No.2
RMLRUN30	JP LEVEL 1 G.C.1 100%	17.3	102.7	0.105	FLEXIBLE	FLEXIBLE	T2	C1	17.6	111.0	*	**	No.3	No.2

* T2 : 0.138, C1 : 0.068 ** T2 : 0.055, C1 : 0.04

Table 5-II Cont'd

TEST No.	EXCITATION	PEAK TABLE MOTION			PIER CONDITION		BEARING MATERIAL		BEARING PRESSURE (MPa)		FRICTIONAL PROPERTIES		RUBBER RESTORING FORCE DEVICE	
		DIS. (mm)	VEL. (mm/s)	ACC. (g)	SOUTH	NORTH	SOUTH	NORTH	SOUTH	NORTH	fmax	fmin	SOUTH	NORTH
RMLRUN31	JP LEVEL 1 G.C.2 100%	17.7	114.7	0.111	FLEXIBLE	FLEXIBLE	T2	C1	17.6	111.0	*	**	No.3	No.2
RMLRUN32	JP LEVEL 1 G.C.3 100%	34.3	162.8	0.114	FLEXIBLE	FLEXIBLE	T2	C1	17.6	111.0	*	**	No.3	No.2
RMLRUN33	JP LEVEL 2 G.C.1 75%	81.8	356.3	0.271	FLEXIBLE	FLEXIBLE	T2	C1	17.6	111.0	*	**	No.3	No.2
RMLRUN34	JP LEVEL 2 G.C.2 75%	76.5	335.5	0.301	FLEXIBLE	FLEXIBLE	T2	C1	17.6	111.0	*	**	No.3	No.2
RMLRUN35	JP LEVEL 2 G.C.3 75%	84.1	365.0	0.310	FLEXIBLE	FLEXIBLE	T2	C1	17.6	111.0	*	**	No.3	No.2
RMLRUN36	PACOIMA S16E 50%	40.9	245.2	0.432	FLEXIBLE	FLEXIBLE	T2	C1	17.6	111.0	*	**	No.3	No.2
RLLRUN01	EL CENTRO S00E 50%	12.0	86.0	0.172	STIFF	STIFF	C1	C1	111.0	111.0	0.068	0.040	No.3	No.3
RLLRUN02	EL CENTRO S00E H+V 50%	12.0	88.0	0.178	STIFF	STIFF	C1	C1	111.0	111.0	0.068	0.040	No.3	No.3
RLLRUN03	EL CENTRO S00E 100%	24.0	165.2	0.319	STIFF	STIFF	C1	C1	111.0	111.0	0.068	0.040	No.3	No.3
RLLRUN04	EL CENTRO S00E 150%	35.9	243.2	0.442	STIFF	STIFF	C1	C1	111.0	111.0	0.068	0.040	No.3	No.3
RLLRUN05	TAFT N21E 100%	14.4	65.0	0.147	STIFF	STIFF	C1	C1	111.0	111.0	0.068	0.040	No.3	No.3
RLLRUN06	TAFT N21E H+V 100%	14.4	67.6	0.146	STIFF	STIFF	C1	C1	111.0	111.0	0.068	0.040	No.3	No.3
RLLRUN07	TAFT N21E 200%	28.9	130.2	0.292	STIFF	STIFF	C1	C1	111.0	111.0	0.068	0.040	No.3	No.3
RLLRUN08	TAFT N21E 300%	43.3	198.1	0.445	STIFF	STIFF	C1	C1	111.0	111.0	0.068	0.040	No.3	No.3
RLLRUN09	HACHINOHE N-S 100%	32.3	134.3	0.262	STIFF	STIFF	C1	C1	111.0	111.0	0.068	0.040	No.3	No.3
RLLRUN10	HACHINOHE N-S 200%	64.3	268.4	0.477	STIFF	STIFF	C1	C1	111.0	111.0	0.068	0.040	No.3	No.3
RLLRUN11	MIYAGIKENOKI E-W 130%	16.1	102.9	0.182	STIFF	STIFF	C1	C1	111.0	111.0	0.068	0.040	No.3	No.3
RLLRUN12	MIYAGIKENOKI E-W 200%	24.8	162.4	0.301	STIFF	STIFF	C1	C1	111.0	111.0	0.068	0.040	No.3	No.3
RLLRUN13	MIYAGIKENOKI E-W 300%	37.3	237.9	0.519	STIFF	STIFF	C1	C1	111.0	111.0	0.068	0.040	No.3	No.3
RLLRUN14	BOSTON1 100%	9.8	66.2	0.138	STIFF	STIFF	C1	C1	111.0	111.0	0.068	0.040	No.3	No.3
RLLRUN15	BOSTON2 100%	8.0	65.8	0.131	STIFF	STIFF	C1	C1	111.0	111.0	0.068	0.040	No.3	No.3
RLLRUN16	BOSTON3 100%	7.5	51.5	0.151	STIFF	STIFF	C1	C1	111.0	111.0	0.068	0.040	No.3	No.3
RLLRUN21	JP LEVEL 1 G.C.1 100%	17.1	99.8	0.122	STIFF	STIFF	C1	C1	111.0	111.0	0.068	0.040	No.3	No.3
RLLRUN22	JP LEVEL 1 G.C.2 100%	17.6	116.6	0.129	STIFF	STIFF	C1	C1	111.0	111.0	0.068	0.040	No.3	No.3
RLLRUN23	JP LEVEL 1 G.C.3 100%	34.3	168.5	0.146	STIFF	STIFF	C1	C1	111.0	111.0	0.068	0.040	No.3	No.3
RLLRUN24	EL CENTRO S00E 50%	11.9	81.0	0.137	FLEXIBLE	FLEXIBLE	C1	C1	111.0	111.0	0.068	0.040	No.3	No.3

* T2 : 0.138, C1 : 0.068 ** T2 : 0.055, C1 : 0.04

Table 5-II Cont'd

TEST No.	EXCITATION	PEAK TABLE MOTION			PIER CONDITION		BEARING MATERIAL		BEARING PRESSURE (MPa)		FRICTIONAL PROPERTIES		RUBBER RESTORING FORCE DEVICE	
		DIS. (mm)	VEL. (mm/s)	ACC. (g)	SOUTH	NORTH	SOUTH	NORTH	SOUTH	NORTH	fmax	fmin	SOUTH	NORTH
RLLRUN25	EL CENTRO S00E H+V 50%	11.8	85.9	0.135	FLEXIBLE	FLEXIBLE	C1	C1	111.0	111.0	0.068	0.040	No.3	No.3
RLLRUN26	EL CENTRO S00E 100%	23.8	161.1	0.291	FLEXIBLE	FLEXIBLE	C1	C1	111.0	111.0	0.068	0.040	No.3	No.3
RLLRUN27	EL CENTRO S00E 150%	35.7	240.8	0.446	FLEXIBLE	FLEXIBLE	C1	C1	111.0	111.0	0.068	0.040	No.3	No.3
RLLRUN28	TAFT N21E 100%	14.5	64.8	0.149	FLEXIBLE	FLEXIBLE	C1	C1	111.0	111.0	0.068	0.040	No.3	No.3
RLLRUN29	TAFT N21E H+V 100%	14.6	65.4	0.143	FLEXIBLE	FLEXIBLE	C1	C1	111.0	111.0	0.068	0.040	No.3	No.3
RLLRUN30	TAFT N21E 200%	29.0	131.0	0.333	FLEXIBLE	FLEXIBLE	C1	C1	111.0	111.0	0.068	0.040	No.3	No.3
RLLRUN31	TAFT N21E 300%	43.3	205.1	0.487	FLEXIBLE	FLEXIBLE	C1	C1	111.0	111.0	0.068	0.040	No.3	No.3
RLLRUN32	HACHINOHE N-S 100%	32.4	141.4	0.227	FLEXIBLE	FLEXIBLE	C1	C1	111.0	111.0	0.068	0.040	No.3	No.3
RLLRUN33	HACHINOHE N-S 200%	64.4	280.7	0.493	FLEXIBLE	FLEXIBLE	C1	C1	111.0	111.0	0.068	0.040	No.3	No.3
RLLRUN34	MIYAGIKENOKI E-W 130%	16.2	100.9	0.197	FLEXIBLE	FLEXIBLE	C1	C1	111.0	111.0	0.068	0.040	No.3	No.3
RLLRUN35	MIYAGIKENOKI E-W 200%	24.7	154.6	0.315	FLEXIBLE	FLEXIBLE	C1	C1	111.0	111.0	0.068	0.040	No.3	No.3
RLLRUN36	MIYAGIKENOKI E-W 300%	37.2	234.6	0.466	FLEXIBLE	FLEXIBLE	C1	C1	111.0	111.0	0.068	0.040	No.3	No.3
RLLRUN37	BOSTON1 100%	9.8	64.8	0.115	FLEXIBLE	FLEXIBLE	C1	C1	111.0	111.0	0.068	0.040	No.3	No.3
RLLRUN38	BOSTON2 100%	8.1	61.8	0.123	FLEXIBLE	FLEXIBLE	C1	C1	111.0	111.0	0.068	0.040	No.3	No.3
RLLRUN39	BOSTON3 100%	7.6	53.6	0.135	FLEXIBLE	FLEXIBLE	C1	C1	111.0	111.0	0.068	0.040	No.3	No.3
RLLRUN43	JP LEVEL 1 G.C.1 100%	17.2	101.6	0.104	FLEXIBLE	FLEXIBLE	C1	C1	111.0	111.0	0.068	0.040	No.3	No.3
RLLRUN44	JP LEVEL 1 G.C.2 100%	17.6	118.5	0.110	FLEXIBLE	FLEXIBLE	C1	C1	111.0	111.0	0.068	0.040	No.3	No.3
RLLRUN45	JP LEVEL 1 G.C.3 100%	34.3	166.8	0.122	FLEXIBLE	FLEXIBLE	C1	C1	111.0	111.0	0.068	0.040	No.3	No.3

Table 5-III Earthquake Simulation Tests and Model Conditions in Tests with Sliding Bearings, Rubber Restoring Force Devices and Viscous Dampers(*)

TEST No.	EXCITATION	PEAK TABLE MOTION			PIER CONDITION		BEARING MATERIAL		BEARING PRESSURE (MPa)		FRICTIONAL PROPERTIES		RUBBER RESTORING FORCE DEVICE	
		DIS. (mm)	VEL. (mm/s)	ACC. (g)	SOUTH	NORTH	SOUTH	NORTH	SOUTH	NORTH	fmax	fmin	SOUTH	NORTH
DRDRUN01	EL CENTRO S00E 200%	48.3	311.3	0.561	FLEXIBLE	FLEXIBLE	T1	T1	5.0	5.0	0.15	0.055	No.2	No.2
DRDRUN02	CALTRANS A2 0.6g 100%	126.5	558.1	0.529	FLEXIBLE	FLEXIBLE	T1	T1	5.0	5.0	0.15	0.055	No.2	No.2
DRDRUN03	JP LEVEL 2 G.C.2 75%	77.1	338.0	0.276	FLEXIBLE	FLEXIBLE	T1	T1	5.0	5.0	0.15	0.055	No.2	No.2
DRDRUN04	JP LEVEL 2 G.C.1 75%	82.4	361.6	0.287	FLEXIBLE	FLEXIBLE	T1	T1	5.0	5.0	0.15	0.055	No.2	No.2
DRDRUN05	JP LEVEL 2 G.C.1 100%	109.6	482.5	0.416	FLEXIBLE	FLEXIBLE	T1	T1	5.0	5.0	0.15	0.055	No.2	No.2
DRDRUN06	JP LEVEL 2 G.C.3 75%	84.5	369.9	0.307	FLEXIBLE	FLEXIBLE	T1	T1	5.0	5.0	0.15	0.055	No.2	No.2
DRDRUN07	JP LEVEL 2 G.C.3 100%	112.6	498.9	0.429	FLEXIBLE	FLEXIBLE	T1	T1	5.0	5.0	0.15	0.055	No.2	No.2
DRDRUN08	JP LEVEL 2 G.C.2 100%	102.4	447.7	0.371	FLEXIBLE	FLEXIBLE	T1	T1	5.0	5.0	0.15	0.055	No.2	No.2
DRDRUN09	PACOIMA S16E 75%	61.5	365.1	0.583	FLEXIBLE	FLEXIBLE	T1	T1	5.0	5.0	0.15	0.055	No.2	No.2
DRDRUN10	PACOIMA S16E 100%	81.8	482.3	0.783	FLEXIBLE	FLEXIBLE	T1	T1	5.0	5.0	0.15	0.055	No.2	No.2
DRDRUN13	MEXICO N90W 100%	53.2	310.6	0.179	FLEXIBLE	FLEXIBLE	T1	T1	5.0	5.0	0.15	0.055	No.2	No.2
DRDRUN14	MEXICO N90W 120%	63.8	377.8	0.213	FLEXIBLE	FLEXIBLE	T1	T1	5.0	5.0	0.15	0.055	No.2	No.2
DRDRUN15	155 CYCLES, 1 Hz SINE WAVE	54.8	348.5	0.231	STIFF	STIFF	T1	T1	5.0	5.0	0.15	0.055	No.2	No.2

* : 4 VISCOUS DAMPERS

Table 5-IV Summary of Experimental Results of Isolated Bridge with Sliding Bearings and Rubber Restoring Force Devices

TEST No.	BEARING DISPLACEMENT (mm)				ISOLATION SYSTEM SHEAR / WEIGHT			DECK ACC. (g)	PIER ACC. (g)		PIER DRIFT (%)		PIER SHEAR / AXIAL LOAD		DEVICE DISPLACEMENT (mm)		DEVICE FORCE / DECK WEIGHT		
	SOUTH			NORTH															
	INIT.	MAX.	PERM.	MAX.-INIT.	SOUTH	NORTH	TOTAL		SOUTH	NORTH	SOUTH	NORTH	SOUTH	NORTH	SOUTH	NORTH	SOUTH	NORTH	
IRDRUN01	N/A	7.9	1.2	7.7	0.210	0.210	0.210	0.210	0.577	0.600	N/A	0.06	N/A	N/A	N/A	N/A	N/A	N/A	
IRDRUN02	N/A	7.2	-0.9	7.2	0.201	0.201	0.201	0.201	0.561	0.600	N/A	0.05	N/A	N/A	N/A	N/A	N/A	N/A	
IRDRUN03	N/A	16.0	2.4	15.6	0.235	0.235	0.235	0.235	0.711	0.720	N/A	0.07	N/A	N/A	N/A	N/A	N/A	N/A	
IRDRUN04	N/A	25.9	-0.2	25.8	0.243	0.243	0.243	0.243	0.883	0.821	N/A	0.07	N/A	N/A	N/A	N/A	N/A	N/A	
IRDRUN05	N/A	-3.4	-2.4	3.3	0.151	0.151	0.151	0.151	0.329	0.332	N/A	0.04	N/A	N/A	N/A	N/A	N/A	N/A	
IRDRUN06	N/A	5.7	0.2	5.5	0.190	0.190	0.190	0.190	0.442	0.490	N/A	0.06	N/A	N/A	N/A	N/A	N/A	N/A	
IRDRUN07	N/A	-22.1	2.4	21.9	0.236	0.236	0.236	0.236	0.853	0.863	N/A	0.07	N/A	N/A	N/A	N/A	N/A	N/A	
IRDRUN08	N/A	-54.5	-1.7	54.5	0.371	0.371	0.371	0.371	1.316	1.260	N/A	0.09	N/A	N/A	N/A	N/A	N/A	N/A	@@
IRDRUN09	N/A	-15.9	-4.0	15.6	0.224	0.224	0.224	0.224	0.850	0.942	N/A	0.07	N/A	N/A	N/A	N/A	N/A	N/A	
IRDRUN10	N/A	-26.8	-0.8	26.7	0.233	0.233	0.233	0.233	1.040	1.097	N/A	0.07	N/A	N/A	N/A	N/A	N/A	N/A	
IRDRUN11	N/A	-18.0	2.6	17.8	0.209	0.209	0.209	0.209	0.461	0.493	N/A	0.36	N/A	N/A	N/A	N/A	N/A	N/A	
IRDRUN12	N/A	-42.1	-0.2	42.2	0.263	0.263	0.263	0.263	0.653	0.719	N/A	0.06	N/A	N/A	N/A	N/A	N/A	N/A	
IRDRUN13	N/A	10.4	2.1	10.3	0.175	0.175	0.175	0.175	0.361	0.323	N/A	0.04	N/A	N/A	N/A	N/A	N/A	N/A	
IRDRUN14	N/A	24.4	0.5	24.2	0.222	0.222	0.222	0.222	0.490	0.498	N/A	0.05	N/A	N/A	N/A	N/A	N/A	N/A	
IRDRUN15	N/A	44.9	-2.6	44.4	0.273	0.273	0.273	0.273	0.551	0.595	N/A	0.07	N/A	N/A	N/A	N/A	N/A	N/A	
IRDRUN16	N/A	21.1	3.8	21.1	0.219	0.219	0.219	0.219	0.540	0.529	N/A	0.06	N/A	N/A	N/A	N/A	N/A	N/A	
IRDRUN17	N/A	-47.8	-7.2	47.8	0.275	0.275	0.275	0.275	0.777	0.795	N/A	0.07	N/A	N/A	N/A	N/A	N/A	N/A	
IRDRUN18	N/A	-41.2	-0.2	41.0	0.274	0.274	0.274	0.274	0.786	0.778	N/A	0.08	N/A	N/A	37.6	37.0	N/A	N/A	
IRDRUN19	N/A	-14.2	2.6	14.0	0.219	0.219	0.219	0.219	0.532	0.549	N/A	0.05	N/A	N/A	12.4	11.8	N/A	N/A	
IRDRUN20	N/A	-43.2	-1.5	43.2	0.290	0.290	0.290	0.290	0.856	0.890	N/A	0.07	N/A	N/A	39.1	38.3	N/A	N/A	
IRDRUN21	N/A	6.0	1.6	5.9	0.174	0.174	0.174	0.174	0.383	0.370	N/A	0.04	N/A	N/A	4.5	4.9	N/A	N/A	
IRDRUN22	N/A	-10.9	-1.9	10.8	0.206	0.206	0.206	0.206	0.519	0.502	N/A	0.05	N/A	N/A	8.6	7.6	N/A	N/A	
IRDRUN23	N/A	-19.5	-1.5	19.4	0.236	0.236	0.236	0.236	0.666	0.585	N/A	0.06	N/A	N/A	17.4	16.1	N/A	N/A	
IRDRUN24	N/A	6.9	0.7	6.8	0.187	0.187	0.187	0.187	0.510	0.513	N/A	0.06	N/A	N/A	5.5	5.3	N/A	N/A	
IRDRUN25	N/A	-23.3	3.6	23.3	0.253	0.253	0.253	0.253	0.902	0.784	N/A	0.09	N/A	N/A	20.5	19.5	N/A	N/A	
IRDRUN26	-0.5	25.9	-0.3	26.0	0.253	0.253	0.253	0.253	0.816	0.962	N/A	0.08	N/A	N/A	22.3	24.0	N/A	N/A	

NOTE : Results for Isolation System Shear Force in Case of Stiff Piers are Approximate
@ Displacement Restrainer Partially Activated. @@ Displacement Restrainer Fully Activated.

Table 5-IV Cont'd

TEST No.	BEARING DISPLACEMENT (mm)				ISOLATION SYSTEM SHEAR / WEIGHT			DECK ACC. (g)	PIER ACC. (g)		PIER DRIFT (%)		PIER SHEAR / AXIAL LOAD		DEVICE DISPLACEMENT (mm)		DEVICE FORCE / DECK WEIGHT	
	SOUTH			NORTH														
	INIT.	MAX.	PERM.	MAX.-INIT.	SOUTH	NORTH	TOTAL		SOUTH	NORTH	SOUTH	NORTH	SOUTH	NORTH	SOUTH	NORTH	SOUTH	NORTH
IRDRUN27	N/A	-5.9	-2.3	6.0	0.144	0.142	0.143	0.152	0.248	0.292	N/A	0.23	0.164	0.168	5.3	4.3	0.021	0.019
IRDRUN28	N/A	-4.2	0.9	4.6	0.146	0.138	0.142	0.154	0.299	0.305	N/A	0.22	0.163	0.155	4.1	3.4	0.015	0.017
IRDRUN29	N/A	-6.8	-1.1	7.0	0.140	0.150	0.145	0.157	0.366	0.330	N/A	0.22	0.161	0.169	5.9	4.8	0.021	0.022
IRDRUN30	N/A	1.4	1.0	1.5	0.102	0.108	0.105	0.110	0.140	0.156	N/A	0.15	0.115	0.120	1.9	1.7	0.009	0.009
IRDRUN31	N/A	-6.3	-0.2	6.7	0.152	0.153	0.146	0.159	0.421	0.410	N/A	0.24	0.172	0.177	5.5	4.7	0.018	0.023
IRDRUN32	N/A	10.0	0.1	9.6	0.164	0.178	0.168	0.207	0.736	0.685	N/A	0.29	0.213	0.224	8.4	8.2	0.031	0.031
IRDRUN33	N/A	-15.4	-0.3	15.8	0.184	0.184	0.179	0.221	0.923	0.817	N/A	0.32	0.230	0.235	13.7	12.9	0.042	0.043
IRDRUN34	N/A	21.7	-0.3	21.3	0.202	0.203	0.197	0.229	1.143	1.024	N/A	0.36	0.269	0.245	19.3	19.3	0.051	0.055
IRDRUN35	N/A	30.1	0.1	29.6	0.207	0.228	0.205	0.254	1.344	1.182	N/A	0.36	0.283	0.265	27.2	28.0	0.065	0.069
IRDRUN36	N/A	-5.7	0.0	6.0	0.146	0.144	0.144	0.159	0.403	0.375	N/A	0.24	0.173	0.168	5.7	4.4	0.019	0.020
IRDRUN37	N/A	40.2	0.8	39.2	0.200	0.239	0.219	0.235	0.922	0.877	N/A	0.33	0.228	0.269	35.2	35.3	0.072	0.074
IRDRUN38	N/A	-12.2	-2.1	12.5	0.167	0.159	0.163	0.176	0.323	0.282	N/A	0.24	0.184	0.174	11.2	11.1	0.033	0.035
IRDRUN39	N/A	-25.0	-3.1	25.5	0.210	0.197	0.204	0.215	0.603	0.567	N/A	0.31	0.222	0.231	23.6	24.3	0.051	0.056
IRDRUN40	N/A	-28.5	-1.7	28.8	0.226	0.203	0.214	0.225	0.848	0.803	N/A	0.34	0.240	0.257	27.3	28.9	0.053	0.061
IRDRUN41	N/A	-36.1	-2.2	36.8	0.248	0.221	0.234	0.255	1.132	0.998	N/A	0.36	0.262	0.273	34.6	33.0	0.070	0.075
IRDRUN42	N/A	7.1	5.0	6.9	0.156	0.143	0.149	0.159	0.300	0.304	N/A	0.25	0.175	0.165	6.5	5.4	0.022	0.022
IRDRUN43	N/A	10.0	2.4	9.6	0.161	0.180	0.170	0.189	0.539	0.523	N/A	0.27	0.200	0.205	7.8	9.0	0.023	0.028
IRDRUN44	N/A	-32.7	-1.6	33.3	0.218	0.221	0.207	0.228	1.084	0.998	N/A	0.35	0.257	0.267	30.3	29.8	0.059	0.066
IRDRUN45	N/A	-47.9	-1.1	47.9	0.303	0.278	0.291	0.307	1.466	1.268	N/A	0.39	0.300	0.289	43.3	42.5	0.146	0.163
IRDRUN46	N/A	12.2	2.2	11.8	0.179	0.192	0.184	0.200	0.604	0.605	N/A	0.28	0.214	0.215	13.1	12.2	0.035	0.037
IRDRUN47	N/A	25.8	1.4	25.2	0.207	0.233	0.214	0.252	1.503	1.725	N/A	0.34	0.265	0.265	26.5	25.7	0.054	0.058
IRDRUN48	N/A	35.3	0.2	34.3	0.223	0.264	0.231	0.273	1.632	2.225	N/A	0.38	0.295	0.302	36.1	34.6	0.075	0.078
IRDRUN49	N/A	-24.5	-1.2	24.7	0.206	0.201	0.201	0.218	0.810	0.871	N/A	0.33	0.243	0.258	25.6	25.2	0.053	0.057
IRDRUN50	N/A	-36.5	3.7	36.6	0.245	0.237	0.241	0.262	1.263	1.338	N/A	0.39	0.287	0.306	37.9	37.3	0.073	0.087
IRDRUN51	N/A	-31.3	-5.8	31.4	0.213	0.202	0.208	0.225	0.663	0.636	N/A	0.30	0.231	0.225	32.5	32.3	0.065	0.070
IRDRUN52	N/A	-38.9	-0.8	39.4	0.252	0.238	0.245	0.270	0.905	0.798	N/A	0.36	0.277	0.261	40.4	39.3	0.106	0.122

Table 5-IV Cont'd

TEST No.	BEARING DISPLACEMENT (mm)				ISOLATION SYSTEM SHEAR / WEIGHT			DECK ACC. (g)	PIER ACC. (g)		PIER DRIFT (%)		PIER SHEAR / AXIAL LOAD		DEVICE DISPLACEMENT (mm)		DEVICE FORCE DECK WEIGHT		
	SOUTH			NORTH															
	INIT.	MAX.	PERM.	MAX.-INIT.	SOUTH	NORTH	TOTAL		SOUTH	NORTH	SOUTH	NORTH	SOUTH	NORTH	SOUTH	NORTH	SOUTH	NORTH	
IRDRUN53	N/A	-46.1	-1.8	46.3	0.445	0.423	0.435	0.457	1.240	1.160	N/A	0.57	0.472	0.448	46.9	46.2	0.311	0.324	@@
IRDRUN54	N/A	25.1	-1.0	24.7	0.227	0.225	0.218	0.234	0.951	0.899	N/A	0.35	0.298	0.271	26.5	25.5	0.057	0.062	
IRDRUN55	N/A	23.7	5.4	22.4	0.199	0.223	0.202	0.214	0.907	0.787	N/A	0.31	0.229	0.245	24.4	23.0	0.055	0.061	
IRDRUN56	N/A	27.0	4.7	26.4	0.209	0.230	0.218	0.255	1.303	0.980	N/A	0.36	0.289	0.291	28.2	26.3	0.055	0.061	
IRDRUN57	N/A	-38.6	-5.3	38.5	0.226	0.242	0.226	0.264	1.436	1.195	N/A	0.35	0.253	0.278	39.5	39.2	0.076	0.084	
IRDRUN58	N/A	38.5	1.0	36.8	0.241	0.286	0.251	0.278	1.407	1.705	N/A	0.43	0.321	0.331	39.3	37.4	0.096	0.093	
IRDRUN59	N/A	-44.5	-8.7	44.5	0.296	0.292	0.294	0.311	1.546	1.425	N/A	0.43	0.331	0.304	45.7	45.5	0.152	0.180	@
IRDRUN60	N/A	58.5	8.8	57.5	0.453	0.480	0.466	0.480	1.071	0.834	N/A	0.55	0.464	0.509	57.2	57.1	0.373	0.356	@@
IRDRUN61	N/A	34.5	-2.4	33.6	0.208	0.243	0.223	0.240	0.690	0.660	N/A	0.33	0.240	0.273	35.3	34.7	0.063	0.068	
IRDRUN62	N/A	32.2	-0.9	31.5	0.213	0.231	0.211	0.229	0.763	0.655	N/A	0.32	0.242	0.263	33.1	31.6	0.062	0.068	
IRDRUN63	N/A	-28.2	1.7	28.5	0.228	0.233	0.227	0.259	1.196	1.102	N/A	0.36	0.267	0.271	29.7	29.4	0.054	0.059	
IRDRUN64	N/A	12.1	2.4	11.7	0.180	0.199	0.187	0.210	0.696	0.651	N/A	0.30	0.205	0.214	13.0	12.3	0.032	0.035	
IRDRUN65	N/A	26.4	1.0	24.7	0.214	0.236	0.225	0.272	1.717	1.670	N/A	0.36	0.256	0.275	26.3	25.5	0.053	0.060	
RD2RUN01	0.6	7.1	1.8	6.5	0.211	0.211	0.211	0.211	0.465	0.431	N/A	0.04	N/A	N/A	6.50	6.48	N/A	N/A	
RD2RUN02	1.8	28.6	3.1	26.7	0.249	0.249	0.249	0.249	0.840	0.362	N/A	0.06	N/A	N/A	26.82	26.59	N/A	N/A	
RD2RUN03	3.1	3.2	2.5	1.1	0.128	0.128	0.128	0.128	0.134	0.060	N/A	0.03	N/A	N/A	1.21	1.12	N/A	N/A	
RD2RUN04	2.5	3.1	1.4	2.1	0.146	0.146	0.146	0.146	0.174	0.077	N/A	0.03	N/A	N/A	2.24	2.12	N/A	N/A	
RD2RUN05	1.4	-2.3	1.0	3.6	0.166	0.166	0.166	0.166	0.218	0.096	N/A	0.03	N/A	N/A	3.75	3.40	N/A	N/A	
RD2RUN06	1.0	-13.8	0.6	14.8	0.215	0.215	0.215	0.215	0.484	0.212	N/A	0.04	N/A	N/A	14.88	14.72	N/A	N/A	
RD2RUN07	0.6	-36.9	0.1	37.3	0.257	0.257	0.257	0.257	0.674	0.310	N/A	0.05	N/A	N/A	37.49	37.16	N/A	N/A	
RD2RUN08	0.1	22.1	1.3	21.9	0.226	0.226	0.226	0.226	0.418	0.225	N/A	0.04	N/A	N/A	22.02	21.86	N/A	N/A	
RD2RUN09	1.3	45.0	-1.3	43.4	0.307	0.307	0.307	0.307	0.528	0.265	N/A	0.05	N/A	N/A	43.43	43.13	N/A	N/A	
RD2RUN10	-1.3	-20.9	1.1	19.4	0.223	0.223	0.223	0.223	0.438	0.217	N/A	0.05	N/A	N/A	19.69	19.60	N/A	N/A	
RD2RUN11	1.1	-46.8	-2.1	47.5	0.367	0.367	0.367	0.367	0.566	0.298	N/A	0.05	N/A	N/A	47.19	46.66	N/A	N/A	@
RD2RUN12	-2.1	-2.8	-0.7	2.2	0.158	0.158	0.158	0.158	0.254	0.116	N/A	0.04	N/A	N/A	2.21	2.08	N/A	N/A	
RD2RUN13	-0.7	-4.3	0.0	4.5	0.201	0.201	0.201	0.201	0.442	0.207	N/A	0.05	N/A	N/A	4.70	4.58	N/A	N/A	

Table 5-IV Cont'd

TEST No.	BEARING DISPLACEMENT (mm)				ISOLATION SYSTEM SHEAR / WEIGHT			DECK ACC. (g)	PIER ACC. (g)		PIER DRIFT (%)		PIER SHEAR / AXIAL LOAD		DEVICE DISPLACEMENT (mm)		DEVICE FORCE / DECK WEIGHT		
	SOUTH			NORTH															
	INIT.	MAX.	PERM.	MAX.-INIT.	SOUTH	NORTH	TOTAL		SOUTH	NORTH	SOUTH	NORTH	SOUTH	NORTH	SOUTH	NORTH	SOUTH	NORTH	
RD2RUN14	0.0	-19.5	1.7	19.3	0.233	0.233	0.233	0.233	0.790	0.372	N/A	0.05	N/A	N/A	19.62	19.45	N/A	N/A	
RD2RUN15	1.7	-47.6	1.1	49.3	0.411	0.411	0.411	0.411	1.138	0.522	N/A	0.06	N/A	N/A	48.79	48.84	N/A	N/A	@@
RD2RUN16	1.1	-25.2	-0.8	25.9	0.238	0.238	0.238	0.238	0.921	0.503	N/A	0.06	N/A	N/A	26.29	25.93	N/A	N/A	
RD2RUN17	-0.6	-3.6	-0.1	3.6	0.180	0.180	0.180	0.180	0.308	0.147	N/A	0.05	N/A	N/A	3.72	3.64	N/A	N/A	
RD2RUN18	-0.1	-22.2	-3.5	21.7	0.231	0.231	0.231	0.231	0.649	0.247	N/A	0.06	N/A	N/A	22.09	21.94	N/A	N/A	
RD2RUN19	-5.4	-5.4	-2.0	3.4	0.106	0.106	0.106	0.106	0.101	0.046	N/A	0.03	N/A	N/A	4.45	4.73	N/A	N/A	
RD2RUN20	0.2	-44.2	-6.2	44.0	0.347	0.347	0.347	0.347	0.870	0.339	N/A	0.07	N/A	N/A	44.40	44.12	N/A	N/A	@
RD2RUN21	0.1	21.5	1.8	21.1	0.230	0.230	0.230	0.230	0.775	0.377	N/A	0.05	N/A	N/A	21.5	21.5	N/A	N/A	
RD2RUN22	1.9	33.5	0.4	31.5	0.246	0.246	0.246	0.246	0.981	0.495	N/A	0.06	N/A	N/A	31.6	31.4	N/A	N/A	
RD2RUN23	0.4	38.9	-4.2	38.0	0.235	0.235	0.235	0.235	0.826	0.337	N/A	0.06	N/A	N/A	38.4	38.2	N/A	N/A	
RD2RUN24	1.6	1.9	0.6	2.3	0.157	0.157	0.157	0.157	0.218	0.111	N/A	0.04	N/A	N/A	2.4	2.1	N/A	N/A	
RD2RUN25	0.6	-10.6	0.8	11.1	0.206	0.206	0.206	0.206	0.535	0.214	N/A	0.05	N/A	N/A	11.2	10.9	N/A	N/A	
RD2RUN26	0.8	28.1	-1.0	28.5	0.232	0.232	0.232	0.232	1.241	0.566	N/A	0.06	N/A	N/A	28.8	28.0	N/A	N/A	
RD2RUN27	-0.9	-2.6	-0.3	2.6	0.162	0.162	0.162	0.162	0.233	0.108	N/A	0.04	N/A	N/A	2.7	2.6	N/A	N/A	
RD2RUN28	-0.3	20.1	-0.3	20.2	0.213	0.213	0.213	0.213	0.480	0.226	N/A	0.04	N/A	N/A	20.4	20.1	N/A	N/A	
RD2RUN29	-0.6	-15.7	-1.1	15.0	0.214	0.214	0.214	0.214	0.472	0.216	N/A	0.04	N/A	N/A	15.2	14.7	N/A	N/A	
RD2RUN30	-1.1	-43.5	-2.4	42.5	0.317	0.317	0.317	0.317	0.807	0.369	N/A	0.05	N/A	N/A	42.4	42.2	N/A	N/A	
RD2RUN31	-2.1	6.0	-1.3	8.0	0.159	0.159	0.159	0.159	0.197	0.087	N/A	0.03	N/A	N/A	8.1	8.3	N/A	N/A	
RD2RUN32	-1.3	-18.1	-2.7	16.5	0.194	0.194	0.194	0.194	0.231	0.105	N/A	0.03	N/A	N/A	16.9	16.8	N/A	N/A	
RD2RUN33	-2.7	-22.0	1.7	21.8	0.244	0.244	0.244	0.244	0.849	0.365	N/A	0.06	N/A	N/A	21.9	21.6	N/A	N/A	
RD2RUN34	1.7	29.1	2.3	27.2	0.243	0.243	0.243	0.243	0.800	0.438	N/A	0.07	N/A	N/A	27.5	27.3	N/A	N/A	
RD2RUN35	1.4	12.7	1.5	10.5	0.167	0.193	0.178	0.194	0.679	0.554	N/A	0.34	0.218	0.238	11.8	11.4	0.034	0.036	
RD2RUN36	1.5	27.6	2.8	25.4	0.198	0.205	0.200	0.238	1.320	1.388	N/A	0.41	0.276	0.296	26.5	25.8	0.056	0.058	
RD2RUN37	2.8	3.1	0.5	5.2	0.142	0.146	0.143	0.154	0.234	0.209	N/A	0.24	0.160	0.162	5.9	5.6	0.017	0.018	
RD2RUN38	0.5	-11.1	0.0	11.6	0.163	0.166	0.164	0.179	0.382	0.336	N/A	0.29	0.196	0.198	12.3	12.3	0.033	0.035	
RD2RUN39	0.0	-4.7	-0.1	5.0	0.153	0.157	0.155	0.169	0.289	0.268	N/A	0.27	0.180	0.183	5.4	5.3	0.018	0.020	

Table 5-IV Cont'd

TEST No.	BEARING DISPLACEMENT (mm)				ISOLATION SYSTEM SHEAR / WEIGHT			DECK ACC. (g)	PIER ACC. (g)		PIER DRIFT (%)		PIER SHEAR / AXIAL LOAD		DEVICE DISPLACEMENT (mm)		DEVICE FORCE / DECK WEIGHT		
	SOUTH			NORTH															
	INIT.	MAX.	PERM.	MAX.-INIT.	SOUTH	NORTH	TOTAL		SOUTH	NORTH	SOUTH	NORTH	SOUTH	NORTH	SOUTH	NORTH	SOUTH	NORTH	
RD2RUN40	-0.1	9.7	-0.5	9.3	0.166	0.171	0.167	0.184	0.433	0.401	N/A	0.31	0.207	0.210	10.3	9.9	0.029	0.032	
RD2RUN41	-0.5	6.2	-1.5	6.2	0.150	0.167	0.157	0.171	0.366	0.299	N/A	0.28	0.174	0.191	7.2	6.9	0.021	0.022	
RD2RUN42	-1.5	11.9	-1.8	13.0	0.157	0.181	0.169	0.186	0.513	0.420	N/A	0.31	0.193	0.216	13.9	13.7	0.036	0.038	
RD2RUN43	-1.8	-3.8	0.0	3.6	0.154	0.163	0.156	0.163	0.295	0.130	N/A	0.27	0.176	0.176	4.6	4.5	0.015	0.013	
RD2RUN44	0.0	10.0	-0.2	9.8	0.164	0.198	0.171	0.190	0.624	0.250	N/A	0.32	0.209	0.227	10.6	10.5	0.032	0.034	
RD2RUN45	-0.2	-31.0	-1.4	30.9	0.196	0.226	0.195	0.212	1.148	0.505	N/A	0.37	0.244	0.265	31.7	31.5	0.061	0.069	
RD2RUN46	-1.3	-45.3	-2.3	44.4	0.358	0.368	0.362	0.373	1.487	0.622	N/A	0.50	0.382	0.377	45.1	45.0	0.234	0.261	@+
RD2RUN47	-2.2	-36.2	-1.6	34.0	0.206	0.208	0.206	0.226	0.679	0.646	N/A	0.35	0.238	0.241	34.9	35.1	0.071	0.079	
RD2RUN48	-1.6	40.2	0.6	40.9	0.216	0.240	0.227	0.239	0.765	0.712	N/A	0.35	0.242	0.256	42.4	41.8	0.109	0.112	
RD2RUN49	0.6	36.1	-4.4	35.0	0.198	0.224	0.210	0.228	0.848	0.748	N/A	0.34	0.225	0.258	36.2	36.0	0.073	0.079	
RD2RUN50	0.5	-36.4	3.2	37.1	0.221	0.223	0.221	0.243	1.321	1.306	N/A	0.42	0.289	0.301	37.7	37.3	0.087	0.087	
RD2RUN51	2.83	-10.7	0.6	13.4	0.165	0.166	0.165	0.176	0.353	0.356	N/A	0.28	0.182	0.186	14.1	13.9	0.037	0.039	
RD2RUN52	0.6	-25.1	-0.9	25.8	0.191	0.198	0.192	0.205	0.640	0.591	N/A	0.36	0.225	0.250	26.5	26.1	0.051	0.058	
RD2RUN53	-0.9	-38.6	-5.1	38.0	0.216	0.213	0.213	0.241	1.138	1.037	N/A	0.42	0.266	0.291	38.6	38.1	0.089	0.100	
RD2RUN54	0.5	32.4	11.5	30.9	0.190	0.221	0.202	0.231	1.350	1.128	N/A	0.41	0.280	0.304	32.6	31.9	0.061	0.069	
RD2RUN55	2.7	40.9	0.4	36.5	0.223	0.244	0.233	0.244	1.409	1.538	N/A	0.44	0.294	0.317	38.6	37.1	0.113	0.100	
RD2RUN56	0.4	45.0	-4.3	44.6	0.305	0.320	0.304	0.320	1.344	1.401	N/A	0.42	0.314	0.327	45.4	45.1	0.182	0.196	@
RD2RUN57	1.1	1.4	0.5	1.8	0.124	0.125	0.124	0.131	0.143	0.086	N/A	0.20	0.135	0.134	2.1	2.0	0.009	0.006	
RD2RUN58	0.5	12.8	0.3	11.8	0.175	0.187	0.181	0.209	0.850	0.768	N/A	0.35	0.227	0.246	12.8	12.5	0.039	0.041	
RD2RUN59	0.3	34.6	0.1	33.8	0.199	0.224	0.209	0.239	1.219	1.263	N/A	0.38	0.249	0.269	34.8	34.1	0.070	0.080	
RD2RUN60	0.1	-6.1	0.3	6.2	0.154	0.159	0.157	0.172	0.384	0.376	N/A	0.29	0.183	0.187	6.8	6.7	0.022	0.023	
RD2RUN61	0.3	41.0	0.8	39.9	0.232	0.259	0.245	0.261	0.957	0.972	N/A	0.36	0.232	0.270	41.4	40.7	0.116	0.118	
RD2RUN62	0.7	-30.8	-7.4	31.4	0.195	0.205	0.200	0.223	0.729	0.718	N/A	0.33	0.221	0.232	32.3	32.1	0.058	0.067	
RD2RUN63	-1.9	-44.1	-6.6	42.3	0.315	0.323	0.319	0.341	1.001	1.007	N/A	0.46	0.335	0.332	43.2	43.1	0.187	0.210	
RD2RUN64	0.0	-17.2	-4.5	17.0	0.163	0.166	0.164	0.178	0.327	0.334	N/A	0.27	0.181	0.186	17.8	17.2	0.040	0.043	@
RD2RUN65	-1.3	-44.2	-1.9	44.1	0.289	0.294	0.292	0.305	0.559	0.631	N/A	0.41	0.307	0.312	45.4	44.8	0.177	0.195	@

+ Displacement Restrainer Partially Activated at South Pier Only.

Table 5-IV Cont'd

TEST No.	BEARING DISPLACEMENT (mm)				ISOLATION SYSTEM SHEAR / WEIGHT			DECK ACC. (g)	PIER ACC. (g)		PIER DRIFT (%)		PIER SHEAR / AXIAL LOAD		DEVICE DISPLACEMENT (mm)		DEVICE FORCE / DECK WEIGHT		
	SOUTH			NORTH															
	INIT.	MAX.	PERM.	MAX.-INIT.	SOUTH	NORTH	TOTAL		SOUTH	NORTH	SOUTH	NORTH	SOUTH	NORTH	SOUTH	NORTH	SOUTH	NORTH	
RD2RUN66	-1.9	-32.4	-1.4	30.7	0.197	0.202	0.197	0.222	1.187	1.161	N/A	0.37	0.248	0.267	31.4	31.3	0.060	0.067	
RD2RUN67	-1.4	26.0	2.6	26.8	0.207	0.209	0.208	0.250	1.475	1.467	N/A	0.39	0.271	0.287	28.0	27.4	0.060	0.060	
RHHRUN01	3.0	10.0	4.6	7.0	0.214	0.214	0.214	0.214	0.505	0.498	N/A	0.05	N/A	N/A	7.1	6.8	N/A	N/A	
RHHRUN02	4.6	29.2	5.5	24.3	0.276	0.276	0.276	0.276	0.854	0.778	N/A	0.06	N/A	N/A	24.5	24.1	N/A	N/A	
RHHRUN03	5.5	5.6	5.1	1.3	0.127	0.127	0.127	0.127	0.141	0.1390	N/A	0.03	N/A	N/A	1.3	1.3	N/A	N/A	
RHHRUN04	5.1	5.6	4.0	2.1	0.144	0.144	0.144	0.144	0.184	0.182	N/A	0.03	N/A	N/A	2.2	2.2	N/A	N/A	
RHHRUN05	4.3	5.3	4.0	3.5	0.160	0.160	0.160	0.160	0.231	0.210	N/A	0.04	N/A	N/A	3.5	3.6	N/A	N/A	
RHHRUN06	4.1	-28.9	3.0	32.8	0.281	0.281	0.281	0.281	0.715	0.664	N/A	0.05	N/A	N/A	32.8	32.5	N/A	N/A	
RHHRUN07	3.0	46.4	0.9	43.0	0.357	0.357	0.357	0.357	0.534	0.559	N/A	0.06	N/A	N/A	42.9	42.2	N/A	N/A	@
RHHRUN08	0.9	46.8	0.0	45.6	0.353	0.353	0.353	0.353	0.620	0.635	N/A	0.06	N/A	N/A	45.5	44.8	N/A	N/A	@
RHHRUN09	0.0	2.8	2.0	2.8	0.152	0.152	0.152	0.152	0.266	0.258	N/A	0.03	N/A	N/A	2.9	3.0	N/A	N/A	
RHHRUN10	2.0	22.0	4.6	19.9	0.252	0.252	0.252	0.252	0.766	0.770	N/A	0.06	N/A	N/A	19.9	19.9	N/A	N/A	
RHHRUN11	4.6	-41.2	3.4	45.9	0.433	0.433	0.433	0.433	1.177	1.132	N/A	0.07	N/A	N/A	45.0	44.5	N/A	N/A	@@
RHHRUN12	3.4	-21.4	2.5	24.6	0.243	0.243	0.243	0.243	0.969	1.039	N/A	0.05	N/A	N/A	24.8	24.6	N/A	N/A	
RHHRUN13	2.7	6.3	2.4	3.9	0.174	0.174	0.174	0.174	0.286	0.335	N/A	0.04	N/A	N/A	3.8	3.9	N/A	N/A	
RHHRUN14	2.4	-41.8	-2.4	43.9	0.459	0.459	0.459	0.459	0.885	0.762	N/A	0.06	N/A	N/A	43.6	42.8	N/A	N/A	@@
RHHRUN15	3.9	23.9	3.4	20.1	0.252	0.252	0.252	0.252	0.822	0.782	N/A	0.06	N/A	N/A	19.9	20.1	N/A	N/A	
RHHRUN16	3.5	35.8	2.9	32.2	0.282	0.282	0.282	0.282	0.969	1.069	N/A	0.05	N/A	N/A	32.2	32.1	N/A	N/A	
RHHRUN17	2.9	38.6	0.4	35.2	0.259	0.259	0.259	0.259	0.855	0.778	N/A	0.05	N/A	N/A	35.6	35.1	N/A	N/A	
RHHRUN18	0.4	2.4	1.9	1.9	0.149	0.149	0.149	0.149	0.235	0.241	N/A	0.03	N/A	N/A	2.1	2.2	N/A	N/A	
RHHRUN19	2.0	31.4	1.8	29.0	0.245	0.245	0.245	0.245	1.283	1.211	N/A	0.06	N/A	N/A	29.5	29.0	N/A	N/A	
RHHRUN20	1.8	4.5	2.5	2.7	0.160	0.160	0.160	0.160	0.241	0.252	N/A	0.04	N/A	N/A	2.7	2.8	N/A	N/A	
RHHRUN21	2.5	21.8	2.5	19.1	0.231	0.231	0.231	0.231	0.470	0.501	N/A	0.04	N/A	N/A	19.2	19.2	N/A	N/A	
RHHRUN22	2.2	-34.4	1.2	36.7	0.321	0.321	0.321	0.321	0.767	0.754	N/A	0.05	N/A	N/A	36.5	35.9	N/A	N/A	
RHHRUN23	1.4	8.2	1.8	6.6	0.170	0.170	0.170	0.170	0.185	0.180	N/A	0.03	N/A	N/A	6.8	6.7	N/A	N/A	
RHHRUN24	1.8	15.0	0.8	14.5	0.212	0.212	0.212	0.212	0.225	0.223	N/A	0.03	N/A	N/A	14.5	14.3	N/A	N/A	

Table 5-IV Cont'd

TEST No.	BEARING DISPLACEMENT (mm)				ISOLATION SYSTEM SHEAR / WEIGHT			DECK ACC. (g)	PIER ACC. (g)		PIER DRIFT (%)		PIER SHEAR / AXIAL LOAD		DEVICE DISPLACEMENT (mm)		DEVICE FORCE / DECK WEIGHT		
	SOUTH			NORTH															
	INIT.	MAX.	PERM.	MAX.-INIT.	SOUTH	NORTH	TOTAL		SOUTH	NORTH	SOUTH	NORTH	SOUTH	NORTH	SOUTH	NORTH	SOUTH	NORTH	
RHHRUN25	0.8	22.0	4.2	21.0	0.268	0.268	0.268	0.268	0.878	0.826	N/A	0.06	N/A	N/A	21.0	20.4	N/A	N/A	
RHHRUN26	4.2	28.1	4.5	23.9	0.274	0.274	0.274	0.274	0.793	0.917	N/A	0.07	N/A	N/A	23.7	22.9	N/A	N/A	
RHHRUN27	4.5	-44.6	0.5	49.0	0.531	0.531	0.531	0.531	0.921	0.881	N/A	0.07	N/A	N/A	47.2	46.8	N/A	N/A	@@
RHHRUN28	0.9	12.3	2.8	10.5	0.187	0.212	0.196	0.212	0.729	0.638	N/A	0.33	0.214	0.240	12.1	11.7	0.058	0.059	
RHHRUN29	2.8	26.8	3.2	25.5	0.233	0.243	0.237	0.272	1.393	1.635	N/A	0.41	0.280	0.297	26.2	26.6	0.091	0.094	
RHHRUN30	3.2	4.5	2.3	4.4	0.150	0.156	0.153	0.166	0.218	0.221	N/A	0.25	0.164	0.171	5.1	5.6	0.024	0.030	
RHHRUN31	2.3	-7.9	2.3	10.3	0.177	0.183	0.180	0.194	0.366	0.359	N/A	0.30	0.197	0.204	10.9	10.9	0.050	0.056	
RHHRUN32	2.3	3.7	1.7	4.8	0.162	0.169	0.165	0.178	0.285	0.294	N/A	0.28	0.182	0.190	5.4	5.2	0.031	0.037	
RHHRUN33	1.7	10.5	1.5	8.5	0.179	0.186	0.183	0.200	0.462	0.490	N/A	0.31	0.206	0.215	9.4	9.0	0.048	0.053	
RHHRUN34	1.6	7.2	1.1	5.4	0.160	0.176	0.168	0.182	0.396	0.350	N/A	0.28	0.178	0.195	6.3	6.2	0.033	0.034	
RHHRUN35	1.1	13.7	0.8	12.3	0.175	0.196	0.185	0.205	0.540	0.478	N/A	0.31	0.199	0.221	13.3	13.1	0.056	0.061	
RHHRUN36	0.8	-28.8	0.9	29.6	0.235	0.235	0.235	0.255	0.707	0.671	N/A	0.36	0.258	0.258	30.4	30.8	0.102	0.107	
RHHRUN37	0.9	36.7	1.3	36.1	0.279	0.277	0.278	0.298	0.827	0.791	N/A	0.40	0.302	0.300	36.8	37.1	0.156	0.167	
RHHRUN38	1.3	50.8	4.2	47.1	0.479	0.532	0.505	0.515	1.024	0.909	N/A	0.69	0.516	0.583	47.6	46.7	0.394	0.412	@@
RHHRUN39	4.2	41.6	3.6	36.3	0.249	0.282	0.264	0.281	0.784	0.720	N/A	0.39	0.261	0.298	38.2	37.6	0.133	0.148	
RHHRUN40	3.6	46.7	4.4	41.9	0.327	0.377	0.351	0.368	0.824	0.761	N/A	0.51	0.360	0.409	43.8	42.8	0.232	0.253	@
RHHRUN41	4.4	35.3	0.2	30.3	0.221	0.246	0.233	0.252	0.823	0.754	N/A	0.36	0.243	0.279	31.6	31.8	0.097	0.104	
RHHRUN42	0.2	42.0	-0.1	40.8	0.254	0.289	0.270	0.289	0.911	0.835	N/A	0.38	0.264	0.304	42.5	41.8	0.148	0.160	
RHHRUN43	-0.1	5.3	3.5	4.9	0.158	0.160	0.159	0.169	0.286	0.274	N/A	0.27	0.174	0.178	5.9	5.6	0.024	0.025	
RHHRUN44	3.5	-22.6	3.0	26.2	0.225	0.225	0.225	0.240	1.192	1.061	N/A	0.38	0.255	0.280	27.0	27.5	0.087	0.090	
RHHRUN45	3.0	-36.6	1.6	40.2	0.339	0.321	0.330	0.345	1.489	1.283	N/A	0.44	0.362	0.339	39.8	41.1	0.215	0.221	@
RHHRUN46	1.6	-34.1	5.4	36.1	0.291	0.279	0.285	0.302	1.322	1.396	N/A	0.43	0.308	0.304	36.7	37.1	0.156	0.154	
RHHRUN47	4.6	7.6	4.0	12.3	0.186	0.185	0.186	0.198	0361.	0.371	N/A	0.29	0.205	0.204	12.9	13.4	0.053	0.058	
RHHRUN48	4.0	-23.6	3.0	27.7	0.233	0.2323	0.232	0.247	0.609	0.627	N/A	0.36	0.249	0.260	28.4	28.8	0.094	0.099	
RHHRUN49	3.0	-29.3	1.5	32.7	0.253	0.245	0.249	0.265	0.884	0.844	N/A	0.40	0.250	0.277	33.2	33.4	0.122	0.120	
RHHRUN50	1.5	-34.5	0.2	36.9	0.294	0.287	0.289	0.320	1.146	1.087	N/A	0.42	0.269	0.295	36.8	37.6	0.172	0.175	

Table 5-IV Cont'd

TEST No.	BEARING DISPLACEMENT (mm)				ISOLATION SYSTEM SHEAR / WEIGHT			DECK ACC. (g)	PIER ACC. (g)		PIER DRIFT (%)		PIER SHEAR / AXIAL LOAD		DEVICE DISPLACEMENT (mm)		DEVICE FORCE / DECK WEIGHT		
	SOUTH			NORTH															
	INIT.	MAX.	PERM.	MAX.-INIT.	SOUTH	NORTH	TOTAL		SOUTH	NORTH	SOUTH	NORTH	SOUTH	NORTH	SOUTH	NORTH	SOUTH	NORTH	
RHHRUN51	0.2	30.6	8.5	29.3	0.224	0.243	0.231	0.262	1.317	1.177	N/A	0.41	0.279	0.310	31.1	30.5	0.099	0.102	
RHHRUN52	5.4	41.8	3.7	34.8	0.269	0.289	0.276	0.287	1.398	1.646	N/A	0.45	0.311	0.330	37.0	35.9	0.160	0.144	
RHHRUN53	3.7	41.7	1.5	41.3	0.340	0.323	0.332	0.350	1.381	1.512	N/A	0.44	0.362	0.337	41.4	41.9	0.220	0.221	@
RHHRUN54	1.5	2.3	2.2	0.9	0.122	0.126	0.123	0.133	0.134	0.130	N/A	0.21	0.134	0.140	1.3	1.8	0.009	0.010	
RHHRUN55	2.2	15.4	3.4	12.8	0.195	0.207	0.200	0.228	0.856	0.803	N/A	0.35	0.228	0.247	13.8	13.8	0.061	0.062	
RHHRUN56	3.4	33.5	3.2	29.6	0.233	0.243	0.235	0.272	1.298	1.315	N/A	0.39	0.270	0.276	30.7	30.3	0.095	0.101	
RHHRUN57	3.1	8.0	3.5	5.4	0.164	0.167	0.165	0.180	0.423	0.408	N/A	0.28	0.181	0.190	5.9	6.0	0.032	0.034	
RHHRUN58	3.5	38.6	4.0	34.3	0.247	0.267	0.257	0.272	0.956	1.033	N/A	0.38	0.253	0.290	35.8	35.4	0.129	0.130	
RHHRUN59	3.8	-24.4	-1.1	28.5	0.228	0.232	0.230	0.252	0.687	0.691	N/A	0.37	0.257	0.262	29.2	29.3	0.092	0.095	
RHHRUN60	3.5	-37.4	-1.0	42.0	0.363	0.351	0.357	0.381	1.005	1.005	N/A	0.50	0.397	0.375	41.9	43.1	0.249	0.255	@
RHHRUN61	-1.0	-41.6	-1.1	41.4	0.479	0.487	0.483	0.504	1.304	1.215	N/A	0.70	0.527	0.528	41.3	41.9	0.352	0.386	@@
RHHRUN62	-1.1	10.8	-0.8	11.4	0.173	0.175	0.174	0.188	0.306	0.310	N/A	0.28	0.192	0.194	12.4	12.1	0.050	0.055	
RHHRUN63	-0.8	30.3	0.5	30.6	0.230	0.227	0.228	0.246	0.468	0.497	N/A	0.34	0.251	0.244	31.8	31.5	0.092	0.100	
RHHRUN64	2.2	-24.4	1.5	26.5	0.223	0.222	0.221	0.261	1.204	1.246	N/A	0.38	0.256	0.276	27.4	27.4	0.093	0.099	
RHHRUN65	1.5	26.8	3.9	24.6	0.234	0.240	0.236	0.281	1.612	1.582	N/A	0.40	0.282	0.297	25.7	25.3	0.088	0.089	
RSSRUN01	3.9	11.5	6.1	7.5	0.194	0.194	0.194	0.194	0.511	0.494	N/A	0.05	N/A	N/A	7.6	7.6	N/A	N/A	
RSSRUN02	7.3	43.0	8.3	35.3	0.220	0.220	0.220	0.220	0.847	0.802	N/A	0.06	N/A	N/A	35.8	35.7	N/A	N/A	
RSSRUN03	8.3	8.3	7.7	1.1	0.125	0.125	0.125	0.125	0.141	0.139	N/A	0.03	N/A	N/A	1.3	1.1	N/A	N/A	
RSSRUN04	7.7	8.2	5.8	2.7	0.140	0.140	0.140	0.140	0.187	0.187	N/A	0.03	N/A	N/A	2.8	2.8	N/A	N/A	
RSSRUN05	5.8	6.1	5.0	4.6	0.159	0.159	0.159	0.159	0.230	0.223	N/A	0.03	N/A	N/A	4.7	4.6	N/A	N/A	
RSSRUN06	3.8	-45.7	5.6	49.4	0.264	0.264	0.264	0.264	0.673	0.693	N/A	0.05	N/A	N/A	49.6	49.1	N/A	N/A	@
RSSRUN07	5.6	29.8	4.7	24.1	0.194	0.194	0.194	0.194	0.463	0.471	N/A	0.04	N/A	N/A	24.3	24.1	N/A	N/A	
RSSRUN08	4.7	48.4	4.3	43.4	0.206	0.206	0.206	0.206	0.600	0.628	N/A	0.05	N/A	N/A	43.8	43.6	N/A	N/A	
RSSRUN09	4.3	56.0	-1.9	51.9	0.273	0.273	0.273	0.273	0.601	0.608	N/A	0.05	N/A	N/A	52.2	51.9	N/A	N/A	@
RSSRUN10	-1.8	31.0	13.2	32.5	0.209	0.209	0.209	0.209	0.818	0.791	N/A	0.06	N/A	N/A	33.0	33.0	N/A	N/A	
RSSRUN11	13.2	40.8	7.6	27.4	0.206	0.206	0.206	0.206	0.974	1.069	N/A	0.06	N/A	N/A	27.6	27.5	N/A	N/A	

Table 5-IV Cont'd

TEST No.	BEARING DISPLACEMENT (mm)				ISOLATION SYSTEM SHEAR / WEIGHT			DECK ACC. (g)	PIER ACC. (g)		PIER DRIFT (%)		PIER SHEAR / AXIAL LOAD		DEVICE DISPLACEMENT (mm)		DEVICE FORCE / DECK WEIGHT		
	SOUTH			NORTH															
	INIT.	MAX.	PERM.	MAX.-INIT.	SOUTH	NORTH	TOTAL		SOUTH	NORTH	SOUTH	NORTH	SOUTH	NORTH	SOUTH	NORTH	SOUTH	NORTH	
RSSRUN12	7.6	50.9	-8.8	43.1	0.218	0.218	0.218	0.218	0.660	0.626	N/A	0.05	N/A	N/A	43.4	43.1	N/A	N/A	
RSSRUN13	-8.8	48.7	-9.9	57.0	0.202	0.202	0.202	0.202	0.670	0.636	N/A	0.05	N/A	N/A	57.6	57.4	N/A	N/A	
RSSRUN14	1.3	6.8	3.5	5.4	0.161	0.161	0.161	0.161	0.303	0.304	N/A	0.04	N/A	N/A	5.6	5.6	N/A	N/A	
RSSRUN15	3.5	-18.9	-3.8	22.1	0.195	0.195	0.195	0.195	0.662	0.542	N/A	0.05	N/A	N/A	22.6	22.5	N/A	N/A	
RSSRUN16	-3.8	-42.9	-10.4	39.0	0.228	0.228	0.228	0.228	0.832	0.723	N/A	0.06	N/A	N/A	39.2	39.1	N/A	N/A	
RSSRUN17	-10.4	-10.5	-1.1	17.6	0.150	0.150	0.150	0.150	0.196	0.186	N/A	0.03	N/A	N/A	17.8	17.9	N/A	N/A	
RSSRUN18	-1.1	23.6	-2.8	24.6	0.166	0.166	0.166	0.166	0.234	0.234	N/A	0.03	N/A	N/A	24.8	24.7	N/A	N/A	
RSSRUN19	-2.8	-21.0	-2.8	18.1	0.192	0.192	0.192	0.192	0.554	0.529	N/A	0.04	N/A	N/A	18.5	18.6	N/A	N/A	
RSSRUN20	-2.8	-48.7	-4.3	45.6	0.286	0.286	0.286	0.286	0.904	0.887	N/A	0.06	N/A	N/A	45.9	45.2	N/A	N/A	@
RSSRUN21	-3.8	-3.9	0.7	4.9	0.158	0.158	0.158	0.158	0.242	0.260	N/A	0.04	N/A	N/A	5.1	5.1	N/A	N/A	
RSSRUN22	0.7	27.0	1.7	26.2	0.183	0.183	0.183	0.183	0.488	0.484	N/A	0.04	N/A	N/A	26.5	26.3	N/A	N/A	
RSSRUN23	1.4	2.9	2.4	1.6	0.149	0.149	0.149	0.149	0.274	0.267	N/A	0.03	N/A	N/A	1.7	1.7	N/A	N/A	
RSSRUN24	2.4	23.8	4.8	24.0	0.194	0.194	0.194	0.194	0.835	0.810	N/A	0.06	N/A	N/A	24.2	24.0	N/A	N/A	
RSSRUN25	4.8	-54.0	4.4	58.5	0.396	0.396	0.396	0.396	1.133	1.158	N/A	0.08	N/A	N/A	58.1	57.4	N/A	N/A	@@
RSSRUN26	4.4	40.8	6.7	36.2	0.216	0.216	0.216	0.216	0.783	0.926	N/A	0.07	N/A	N/A	36.7	36.6	N/A	N/A	
RSSRUN27	6.7	24.0	5.0	27.1	0.222	0.222	0.222	0.222	0.877	0.810	N/A	0.05	N/A	N/A	27.4	27.5	N/A	N/A	
RSSRUN28	4.9	19.0	4.3	13.1	0.156	0.178	0.160	0.174	0.576	0.538	N/A	0.32	0.205	0.232	14.7	14.0	0.026	0.022	
RSSRUN29	4.3	35.6	9.6	31.1	0.171	0.174	0.172	0.206	1.207	1.329	N/A	0.38	0.268	0.285	31.9	32.4	0.037	0.033	
RSSRUN30	9.3	9.4	4.8	6.7	0.131	0.137	0.131	0.142	0.238	0.237	N/A	0.23	0.152	0.154	7.4	7.3	0.016	0.013	
RSSRUN31	4.8	-9.3	2.1	14.0	0.144	0.149	0.147	0.159	0.409	0.393	N/A	0.28	0.183	0.186	14.7	14.7	0.022	0.020	
RSSRUN32	2.1	4.2	2.6	5.4	0.140	0.145	0.142	0.153	0.301	0.313	N/A	0.26	0.168	0.174	6.0	5.9	0.014	0.011	
RSSRUN33	2.5	-10.8	1.7	13.2	0.148	0.153	0.150	0.165	0.456	0.463	N/A	0.29	0.192	0.197	14.0	14.2	0.022	0.020	
RSSRUN34	1.7	10.5	2.0	8.6	0.136	0.151	0.143	0.156	0.337	0.313	N/A	0.26	0.166	0.181	9.4	9.5	0.017	0.015	
RSSRUN35	2.0	17.6	0.8	15.4	0.143	0.162	0.152	0.169	0.458	0.447	N/A	0.29	0.183	0.202	16.2	16.2	0.023	0.021	
RSSRUN36	0.8	-40.8	2.6	41.8	0.188	0.186	0.187	0.200	0.674	0.653	N/A	0.33	0.220	0.224	42.6	42.5	0.058	0.065	
RSSRUN37	2.6	-40.0	8.2	42.7	0.184	0.181	0.183	0.193	0.758	0.727	N/A	0.33	0.221	0.226	43.4	43.4	0.053	0.059	

Table 5-IV Cont'd

TEST No.	BEARING DISPLACEMENT (mm)				ISOLATION SYSTEM SHEAR / WEIGHT			DECK ACC. (g)	PIER ACC. (g)		PIER DRIFT (%)		PIER SHEAR / AXIAL LOAD		DEVICE DISPLACEMENT (mm)		DEVICE FORCE / DECK WEIGHT		
	SOUTH			NORTH															
	INIT.	MAX.	PERM.	MAX.-INIT.	SOUTH	NORTH	TOTAL		SOUTH	NORTH	SOUTH	NORTH	SOUTH	NORTH	SOUTH	NORTH	SOUTH	NORTH	
RSSRUN38	7.3	43.3	-0.9	38.0	0.163	0.181	0.171	0.187	0.854	0.791	N/A	0.33	0.222	0.247	39.0	39.1	0.038	0.035	
RSSRUN39	-0.9	3.9	1.3	4.6	0.142	0.147	0.141	0.149	0.295	0.287	N/A	0.25	0.166	0.171	5.3	5.1	0.014	0.012	
RSSRUN40	1.3	-36.7	-2.0	38.1	0.168	0.172	0.167	0.189	1.215	1.132	N/A	0.37	0.241	0.257	38.9	38.9	0.042	0.039	
RSSRUN41	-2.0	-50.8	-3.9	48.5	0.350	0.366	0.358	0.376	1.394	1.294	N/A	0.49	0.362	0.379	50.0	50.0	0.226	0.262	@@
RSSRUN42	-3.9	28.7	7.7	32.0	0.169	0.177	0.172	0.190	1.327	1.258	N/A	0.40	0.267	0.288	33.1	32.7	0.043	0.039	
RSSRUN43	0.7	-20.5	-2.9	21.2	0.158	0.172	0.162	0.179	0.705	0.676	N/A	0.34	0.218	0.240	21.9	21.9	0.028	0.026	
RSSRUN44	-2.9	-41.0	-13.9	38.2	0.197	0.195	0.195	0.201	1.124	1.079	N/A	0.40	0.262	0.285	38.9	39.1	0.052	0.063	
RSSRUN45	-1.8	-13.9	-1.9	12.1	0.146	0.150	0.148	0.161	0.342	0.353	N/A	0.27	0.178	0.184	12.8	12.8	0.018	0.015	
RSSRUN46	-1.9	38.1	28.0	39.8	0.163	0.179	0.168	0.197	1.320	1.235	N/A	0.41	0.272	0.304	40.7	41.0	0.039	0.036	
RSSRUN47	11.3	47.2	6.5	36.3	0.176	0.203	0.187	0.206	1.354	1.492	N/A	0.40	0.274	0.299	36.6	37.2	0.049	0.055	
RSSRUN48	6.5	56.6	-16.8	51.9	0.278	0.315	0.296	0.302	1.131	1.258	N/A	0.38	0.250	0.285	53.2	53.2	0.168	0.177	@
RSSRUN49	7.7	8.0	6.0	2.7	0.116	0.118	0.117	0.126	0.155	0.145	N/A	0.20	0.129	0.132	3.2	3.2	0.010	0.009	
RSSRUN50	6.0	15.3	4.8	11.3	0.152	0.164	0.157	0.186	0.846	0.730	N/A	0.34	0.224	0.238	11.9	12.0	0.023	0.020	
RSSRUN51	4.8	-33.9	4.8	38.2	0.174	0.176	0.174	0.192	1.141	1.127	N/A	0.37	0.245	0.262	38.8	38.6	0.043	0.038	
RSSRUN52	4.6	11.5	4.2	9.1	0.140	0.149	0.143	0.157	0.373	0.387	N/A	0.28	0.178	0.184	9.7	9.7	0.018	0.016	
RSSRUN53	4.2	51.1	5.9	46.4	0.202	0.225	0.213	0.226	0.809	0.829	N/A	0.32	0.207	0.232	47.7	47.6	0.083	0.082	@
RSSRUN54	5.8	-27.6	-14.6	33.4	0.163	0.167	0.165	0.184	0.756	0.766	N/A	0.34	0.220	0.230	34.1	34.4	0.035	0.033	
RSSRUN55	6.4	-40.4	-16.5	46.8	0.198	0.197	0.197	0.211	0.946	0.963	N/A	0.36	0.230	0.245	47.7	47.8	0.063	0.067	
RSSRUN56	5.2	-22.3	-8.1	27.4	0.147	0.150	0.148	0.160	0.378	0.388	N/A	0.26	0.166	0.173	28.2	28.4	0.030	0.030	
RSSRUN57	4.5	56.8	-0.4	52.2	0.268	0.298	0.282	0.291	0.612	0.672	N/A	0.41	0.282	0.314	53.3	53.1	0.168	0.170	@
RSSRUN58	-0.3	-37.0	-1.0	37.0	0.174	0.181	0.176	0.205	1.125	1.128	N/A	0.38	0.249	0.275	37.6	37.8	0.040	0.040	
RSSRUN59	-1.0	32.28	9.7	33.1	0.178	0.177	0.176	0.239	1.350	1.279	N/A	0.39	0.269	0.285	34.0	34.0	0.041	0.036	
RMLRUN01	-0.6	12.5	2.6	11.3	N/A	0.100	0.163	0.163	0.489	0.903	N/A	0.22	N/A	0.160	13.1	11.7	N/A	0.038	
RMLRUN02	2.6	37.8	2.4	32.3	N/A	0.143	0.207	0.207	0.918	1.512	N/A	0.27	N/A	0.203	35.0	33.1	N/A	0.069	
RMLRUN03	2.4	4.1	1.0	1.8	N/A	0.067	0.117	0.117	0.216	0.152	N/A	0.13	N/A	0.083	3.3	2.2	N/A	0.007	
RMLRUN04	1.0	-32.3	0.8	30.8	N/A	0.129	0.215	0.215	0.903	1.053	N/A	0.26	N/A	0.192	33.2	31.4	N/A	0.063	

Table 5-IV Cont'd

TEST No.	BEARING DISPLACEMENT (mm)				ISOLATION SYSTEM SHEAR / WEIGHT			DECK ACC. (g)	PIER ACC. (g)		PIER DRIFT (%)		PIER SHEAR / AXIAL LOAD		DEVICE DISPLACEMENT (mm)		DEVICE FORCE / DECK WEIGHT		
	SOUTH			NORTH															
	INIT.	MAX.	PERM.	MAX.-INIT.	SOUTH	NORTH	TOTAL		SOUTH	NORTH	SOUTH	NORTH	SOUTH	NORTH	SOUTH	NORTH	SOUTH	NORTH	
RMLRUN05	0.8	-2.4	-0.2	1.3	N/A	0.077	0.116	0.116	0.191	0.128	N/A	0.13	N/A	0.091	3.3	1.8	N/A	0.005	
RMLRUN06	-0.2	3.6	-0.5	2.2	N/A	0.077	0.119	0.119	0.220	0.140	N/A	0.13	N/A	0.092	3.8	2.5	N/A	0.008	
RMLRUN07	-0.5	3.4	0.0	2.4	N/A	0.083	0.126	0.126	0.256	0.172	N/A	0.14	N/A	0.097	3.9	2.9	N/A	0.009	
RMLRUN08	0.0	-32.5	1.4	29.5	N/A	0.139	0.206	0.206	0.468	0.656	N/A	0.27	N/A	0.188	32.4	30.3	N/A	0.060	
RMLRUN09	1.4	40.8	-1.1	36.4	N/A	0.147	0.236	0.236	0.471	0.595	N/A	0.22	N/A	0.167	39.2	37.1	N/A	0.083	
RMLRUN10	-1.1	37.0	-2.5	35.5	N/A	0.152	0.226	0.226	0.467	0.658	N/A	0.25	N/A	0.174	37.9	36.4	N/A	0.075	
RMLRUN11	-2.5	61.6	-7.8	53.3	N/A	0.486	0.631	0.631	0.665	1.039	N/A	0.66	N/A	0.528	57.2	52.8	N/A	0.426	@@
RMLRUN12	-6.2	-42.9	-2.9	33.3	N/A	0.156	0.243	0.243	1.072	1.245	N/A	0.30	N/A	0.206	36.6	33.8	N/A	0.083	
RMLRUN13	-2.8	-13.0	-5.4	8.5	N/A	0.092	0.149	0.149	0.344	0.293	N/A	0.17	N/A	0.122	10.2	8.9	N/A	0.027	
RMLRUN14	-5.3	-31.9	-6.5	24.2	N/A	0.125	0.200	0.200	0.556	0.799	N/A	0.25	N/A	0.183	26.6	24.6	N/A	0.050	
RMLRUN15	-6.5	-49.5	-10.0	39.1	N/A	0.226	0.326	0.326	0.693	1.133	N/A	0.29	N/A	0.206	42.6	39.8	N/A	0.176	
RMLRUN16	-9.7	-17.5	-3.1	12.3	N/A	0.102	0.164	0.164	0.623	0.752	N/A	0.20	N/A	0.148	14.2	12.5	N/A	0.035	
RMLRUN17	-3.0	33.4	-3.0	34.5	N/A	0.147	0.215	0.215	1.173	1.556	N/A	0.32	N/A	0.228	35.9	34.5	N/A	0.071	
RMLRUN18	-3.1	24.0	-1.4	24.7	N/A	0.135	0.197	0.197	0.971	1.242	N/A	0.28	N/A	0.215	27.1	25.0	N/A	0.058	
RMLRUN19	-1.0	-11.6	-1.4	13.2	0.197	0.119	0.153	0.166	0.565	0.857	0.33	0.23	0.221	0.167	11.4	13.4	0.059	0.039	
RMLRUN20	-1.4	31.6	-0.8	35.3	0.254	0.145	0.198	0.208	1.314	1.458	0.41	0.25	0.283	0.184	33.5	35.9	0.138	0.074	
RMLRUN21	-0.8	-3.8	-2.2	4.4	0.156	0.089	0.119	0.127	0.228	0.310	0.26	0.16	0.170	0.110	3.6	5.1	0.018	0.017	
RMLRUN22	-2.1	-41.0	-3.8	40.9	0.289	0.222	0.255	0.260	1.429	0.984	0.38	0.29	0.298	0.221	39.8	41.2	0.153	0.155	@
RMLRUN23	1.4	-40.8	2.3	43.4	0.279	0.204	0.238	0.247	1.360	1.270	0.45	0.30	0.327	0.225	37.9	39.2	0.141	0.138	
RMLRUN24	1.8	-12.9	-2.9	16.1	0.181	0.114	0.148	0.156	0.330	0.383	0.26	0.20	0.187	0.143	15.2	16.8	0.063	0.045	
RMLRUN25	-2.9	-27.1	-5.8	26.4	0.226	0.121	0.175	0.188	0.793	0.727	0.32	0.24	0.240	0.171	25.0	26.8	0.085	0.056	
RMLRUN26	-5.8	-43.8	-8.7	39.7	0.326	0.234	0.281	0.304	1.269	1.122	0.37	0.31	0.308	0.255	38.9	40.3	0.184	0.187	@
RMLRUN27	-1.9	-13.4	-2.5	13.6	0.192	0.108	0.145	0.170	0.797	0.669	0.34	0.22	0.222	0.156	12.0	14.2	0.053	0.041	
RMLRUN28	-2.5	-34.3	-1.8	38.2	0.271	0.157	0.215	0.219	1.298	1.471	0.39	0.31	0.279	0.214	35.8	38.1	0.156	0.083	
RMLRUN29	-2.06	28.7	1.2	32.7	0.226	0.142	0.183	0.200	1.282	1.255	0.42	0.27	0.290	0.202	31.3	32.8	0.109	0.064	
RMLRUN30	1.2	-5.3	-2.2	6.9	0.152	0.105	0.117	0.127	0.220	0.288	0.25	0.19	0.164	0.132	7.0	7.4	0.027	0.022	

Table 5-IV Cont'd

TEST No.	BEARING DISPLACEMENT (mm)				ISOLATION SYSTEM SHEAR / WEIGHT			DECK ACC. (g)	PIER ACC. (g)		PIER DRIFT (%)		PIER SHEAR / AXIAL LOAD		DEVICE DISPLACEMENT (mm)		DEVICE FORCE / DECK WEIGHT	
	SOUTH			NORTH														
	INIT.	MAX.	PERM.	MAX.-INIT.	SOUTH	NORTH	TOTAL		SOUTH	NORTH	SOUTH	NORTH	SOUTH	NORTH	SOUTH	NORTH	SOUTH	NORTH
RMLRUN31	-2.2	-6.4	-2.9	6.5	0.161	0.093	0.125	0.135	0.263	0.368	0.26	0.18	0.174	0.121	4.9	6.7	0.028	0.024
RMLRUN32	-2.8	-6.0	-4.0	8.5	0.156	0.099	0.126	0.138	0.304	0.334	0.27	0.18	0.174	0.127	7.7	8.9	0.039	0.027
RMLRUN33	-4.0	-39.8	-2.2	40.0	0.277	0.191	0.235	0.246	0.700	0.669	0.37	0.28	0.294	0.199	38.2	40.6	0.171	0.125
RMLRUN34	-2.2	38.6	-2.2	44.6	0.368	0.216	0.292	0.309	0.765	0.565	0.48	0.27	0.396	0.212	41.0	45.4	0.268	0.142
RMLRUN35	-2.2	-43.5	-4.2	43.3	0.335	0.238	0.268	0.280	0.751	0.708	0.41	0.33	0.329	0.258	42.1	44.1	0.236	0.181
RMLRUN36	-4.2	-38.3	-7.9	37.0	0.259	0.174	0.217	0.229	0.770	0.825	0.38	0.25	0.276	0.182	35.0	37.5	0.117	0.106
RLLRUN01	-1.6	-4.6	-0.9	3.3	0.110	0.110	0.110	0.110	0.222	0.248	0.03	0.03	N/A	N/A	3.1	3.1	N/A	N/A
RLLRUN02	-0.9	-4.5	-0.9	3.7	0.112	0.112	0.112	0.112	0.223	0.249	0.04	0.03	N/A	N/A	3.7	3.8	N/A	N/A
RLLRUN03	-0.9	11.4	-0.7	12.1	0.154	0.154	0.154	0.154	0.479	0.412	0.04	0.03	N/A	N/A	12.2	12.0	N/A	N/A
RLLRUN04	-0.7	22.1	-0.8	22.8	0.185	0.185	0.185	0.185	0.603	0.599	0.04	0.03	N/A	N/A	22.7	22.4	N/A	N/A
RLLRUN05	-0.8	-3.7	-1.4	2.9	0.107	0.107	0.107	0.107	0.233	0.241	0.03	0.02	N/A	N/A	3.0	2.8	N/A	N/A
RLLRUN06	-1.3	-3.9	-1.4	2.5	0.105	0.105	0.105	0.105	0.252	0.249	0.03	0.03	N/A	N/A	2.6	2.5	N/A	N/A
RLLRUN07	-1.4	-10.7	-1.3	9.4	0.132	0.132	0.132	0.132	0.429	0.443	0.04	0.03	N/A	N/A	9.4	9.2	N/A	N/A
RLLRUN08	-1.3	-23.6	-1.4	22.3	0.176	0.176	0.176	0.176	0.600	0.603	0.05	0.03	N/A	N/A	22.1	22.3	N/A	N/A
RLLRUN09	-1.4	-13.3	-3.2	11.7	0.138	0.138	0.138	0.138	0.349	0.321	0.04	0.03	N/A	N/A	12.0	11.7	N/A	N/A
RLLRUN10	-3.2	-35.8	-5.9	32.5	0.233	0.233	0.233	0.233	0.627	0.617	0.05	0.03	N/A	N/A	32.5	32.2	N/A	N/A
RLLRUN11	-5.8	-7.0	-2.3	6.1	0.116	0.116	0.116	0.116	0.242	0.242	0.03	0.03	N/A	N/A	6.1	6.0	N/A	N/A
RLLRUN12	-2.3	-9.4	-2.0	7.2	0.130	0.130	0.130	0.130	0.417	0.401	0.04	0.04	N/A	N/A	7.2	7.0	N/A	N/A
RLLRUN13	-2.0	-16.9	-2.1	14.7	0.155	0.155	0.155	0.155	0.675	0.665	0.05	0.03	N/A	N/A	14.8	15.0	N/A	N/A
RLLRUN14	-2.1	-3.6	-1.9	1.5	0.093	0.093	0.093	0.093	0.193	0.234	0.03	0.03	N/A	N/A	1.6	1.7	N/A	N/A
RLLRUN15	-1.8	-3.4	-2.1	1.6	0.092	0.092	0.092	0.092	0.199	0.214	0.03	0.03	N/A	N/A	1.7	1.6	N/A	N/A
RLLRUN16	-2.1	-3.4	-0.9	2.3	0.097	0.097	0.097	0.097	0.189	0.185	0.04	0.02	N/A	N/A	2.3	2.4	N/A	N/A
RLLRUN21	-1.0	-4.1	-1.7	3.0	0.093	0.093	0.093	0.093	0.150	0.162	0.03	0.02	N/A	N/A	3.1	3.0	N/A	N/A
RLLRUN22	-1.6	-3.7	-1.7	3.8	0.103	0.103	0.103	0.103	0.181	0.195	0.05	0.02	N/A	N/A	3.8	3.7	N/A	N/A
RLLRUN23	-1.7	-6.5	-2.8	4.7	0.113	0.113	0.113	0.113	0.196	0.222	0.04	0.03	N/A	N/A	4.8	4.6	N/A	N/A
RLLRUN24	-2.6	-6.4	-1.6	4.9	0.101	0.114	0.108	0.115	0.419	0.394	0.18	0.19	0.112	0.131	5.7	5.3	N/A	N/A

Table 5-IV Cont'd

TEST No.	BEARING DISPLACEMENT (mm)				ISOLATION SYSTEM SHEAR / WEIGHT			DECK ACC. (g)	PIER ACC. (g)		PIER DRIFT (%)		PIER SHEAR / AXIAL LOAD		DEVICE DISPLACEMENT (mm)		DEVICE FORCE / DECK WEIGHT	
	SOUTH			NORTH														
	INIT.	MAX.	PERM.	MAX.-INIT.	SOUTH	NORTH	TOTAL		SOUTH	NORTH	SOUTH	NORTH	SOUTH	NORTH	SOUTH	NORTH	SOUTH	NORTH
RLLRUN25	-1.6	-6.5	-1.5	4.6	0.103	0.114	0.108	0.114	0.404	0.409	0.17	0.19	0.118	0.134	5.1	4.9	N/A	N/A
RLLRUN26	-1.5	-13.3	-0.8	11.6	0.130	0.143	0.136	0.155	0.801	0.845	0.21	0.23	0.144	0.172	12.1	11.9	N/A	N/A
RLLRUN27	-0.8	-26.4	-0.8	25.4	0.154	0.166	0.156	0.172	1.052	1.285	0.23	0.26	0.166	0.195	26.0	26.1	N/A	N/A
RLLRUN28	-0.8	-4.4	-1.2	3.6	0.092	0.107	0.099	0.109	0.273	0.274	0.15	0.17	0.102	0.123	3.8	3.8	N/A	N/A
RLLRUN29	-1.2	-4.4	-1.3	4.0	0.098	0.107	0.102	0.115	0.278	0.317	0.14	0.17	0.106	0.126	4.2	4.3	N/A	N/A
RLLRUN30	-1.3	-12.5	-1.7	10.9	0.123	0.133	0.128	0.138	0.624	0.620	0.19	0.22	0.137	0.151	11.5	11.2	N/A	N/A
RLLRUN31	-1.7	-30.4	-2.5	28.4	0.169	0.178	0.173	0.182	0.749	0.806	0.28	0.29	0.200	0.210	29.2	29.1	N/A	N/A
RLLRUN32	-2.5	-14.9	-1.7	12.2	0.131	0.138	0.135	0.143	0.276	0.315	0.17	0.20	0.129	0.143	12.8	12.7	N/A	N/A
RLLRUN33	-1.7	-30.2	-4.1	28.2	0.168	0.176	0.172	0.183	0.756	0.746	0.22	0.23	0.165	0.178	29.0	28.9	N/A	N/A
RLLRUN34	-4.1	-6.2	-1.7	4.7	0.089	0.104	0.096	0.104	0.288	0.248	0.16	0.18	0.103	0.119	5.2	5.3	N/A	N/A
RLLRUN35	-1.7	-9.1	-1.6	7.9	0.108	0.116	0.111	0.133	0.473	0.470	0.20	0.19	0.128	0.135	8.6	8.4	N/A	N/A
RLLRUN36	-1.6	-19.2	-1.6	17.4	0.140	0.149	0.145	0.152	0.851	0.762	0.26	0.27	0.179	0.186	18.0	17.8	N/A	N/A
RLLRUN37	-1.6	-3.4	-1.7	2.2	0.085	0.092	0.087	0.093	0.209	0.183	0.15	0.16	0.097	0.106	2.7	2.7	N/A	N/A
RLLRUN38	-1.7	-3.8	-1.4	2.5	0.087	0.097	0.091	0.095	0.182	0.169	0.14	0.16	0.098	0.107	3.0	3.0	N/A	N/A
RLLRUN39	-1.4	-3.5	-1.9	2.2	0.090	0.101	0.096	0.100	0.173	0.165	0.15	0.16	0.100	0.112	2.7	2.6	N/A	N/A
RLLRUN43	-1.3	-9.2	-1.2	7.7	0.107	0.117	0.112	0.120	0.290	0.238	0.17	0.18	0.119	0.131	8.3	7.8	N/A	N/A
RLLRUN44	-1.2	7.4	-1.7	8.2	0.113	0.124	0.118	0.127	0.296	0.303	0.19	0.20	0.123	0.139	8.8	8.7	N/A	N/A
RLLRUN45	-1.7	-8.7	-1.1	9.8	0.114	0.124	0.119	0.129	0.324	0.308	0.19	0.18	0.123	0.140	10.3	10.3	N/A	N/A

Table 5-V Summary of Experimental Resuslts of Isolated Bridge with Sliding Bearings, Rubber Restoring Force Devices and Viscous Dampers

TEST No.	BEARING DISPLACEMENT (mm)				ISOLATION SYSTEM SHEAR / WEIGHT			DECK ACC. (g)	PIER ACC. (g)		PIER DRIFT (%)		PIER SHEAR / AXIAL LOAD		DEVICE DIS-PLACEMENT (mm)		*DEVICE FORCE / DECK WEIGHT	
	SOUTH			NORTH														
	INIT.	MAX.	PERM.	MAX.-INIT.	SOUTH	NORTH	TOTAL		SOUTH	NORTH	SOUTH	NORTH	SOUTH	NORTH	SOUTH	NORTH	SOUTH	NORTH
DRDRUN01	N/A	23.6	0.5	23.1	0.286	0.338	0.309	0.336	1.045	0.981	N/A	0.44	0.309	0.356	24.3	23.7	0.146	0.158
DRDRUN02	N/A	-32.7	-7.6	33.2	0.318	0.292	0.304	0.325	1.092	1.078	N/A	0.42	0.337	0.313	34.0	34.3	0.154	0.144
DRDRUN03	N/A	28.8	3.2	27.9	0.253	0.296	0.271	0.291	0.659	0.666	N/A	0.39	0.281	0.323	29.9	28.3	0.118	0.128
DRDRUN04	N/A	-22.4	4.0	22.8	0.251	0.240	0.242	0.258	0.606	0.570	N/A	0.36	0.278	0.262	23.5	23.8	0.083	0.090
DRDRUN05	N/A	-39.7	1.4	40.1	0.305	0.292	0.293	0.310	0.785	0.697	N/A	0.42	0.332	0.323	40.9	41.0	0.140	0.144
DRDRUN06	N/A	-21.7	-3.4	21.9	0.260	0.290	0.274	0.294	0.734	0.748	N/A	0.40	0.297	0.325	22.8	22.7	0.106	0.111
DRDRUN07	N/A	47.3	-2.5	36.5	0.284	0.323	0.299	0.329	0.882	0.831	N/A	0.44	0.319	0.360	37.7	36.9	0.138	0.152
DRDRUN08	N/A	38.7	0.5	38.0	0.292	0.343	0.316	0.334	0.855	0.765	N/A	0.45	0.323	0.375	39.5	38.9	0.146	0.167
DRDRUN09	N/A	-34.9	-2.0	35.5	0.339	0.317	0.328	0.347	0.953	0.754	N/A	0.47	0.368	0.349	36.3	36.2	0.161	0.161
DRDRUN10	N/A	-44.2	-0.7	44.6	0.468	0.445	0.457	0.467	1.318	1.162	N/A	0.56	0.461	0.445	44.8	44.5	0.293	0.319
DRDRUN13	N/A	8.5	-1.3	8.4	0.187	0.183	0.185	0.197	0.309	0.291	N/A	0.29	0.203	0.203	9.2	8.7	0.034	0.038
DRDRUN14	N/A	15.7	0.1	15.0	0.221	0.218	0.216	0.232	0.385	0.401	N/A	0.32	0.246	0.245	16.3	15.9	0.054	0.059
DRDRUN15	N/A	32.0	5.7	31.5	0.205	0.193	0.192	0.227	0.254	0.283	N/A	0.05	N/A	N/A	32.0	31.2	N/A	N/A

* : FORCE FROM RUBBER DEVICE AND TWO VISCOUS DAMPERS

SECTION 6

INTERPRETATION OF EXPERIMENTAL RESULTS

6.1 Behavior of Low Friction Isolation System

In one of the tested configurations (see Table 3-III), sliding bearings of low friction (f_{max}= 0.068) were combined with high stiffness rubber devices. The effective period of vibration of the isolation system was 1.33 sec (or 2.66 secs in prototype scale).

Figure 6-1 presents a comparison of the recorded response of the isolated bridge to that of the non-isolated bridge (both for the case of flexible piers). Some of the results for the non-isolated bridge have been obtained by extrapolation of recorded results at lower amplitude motions. The extrapolation is presumed to be valid for pier shear forces up to 0.5 times the carried axial load. This has been the theoretical elastic limit of the piers. The results vividly demonstrate the significant benefits offered by seismic isolation.

In a different comparison, Figure 6-2 compares the recorded pier shear force versus pier drift loops of the isolated and non-isolated bridges in the case of the low amplitude Japanese Level 1 motions. In these weak motions, with peak ground acceleration of about 0.1g, it might have been expected that the isolation system is ineffective. To the contrary, the isolated bridge substructure response exhibits a marked insensitivity to the frequency content of the input (Ground Condition 1 through 3) and significantly lower shear forces and column drifts than the non-isolated bridge. Of interest is to note the significant energy dissipated by the columns of the non-isolated bridge. The source of this energy dissipation was not yielding of the columns, but rather it was cracking of the concrete shake table extension which supported the columns (see Figure 4-1).

Figure 6-3 depicts the response of the isolated bridge as a function of increasing intensity of certain earthquake motions, which represent weak to moderately strong excitations. It may be observed that the bearing displacement is always less than the table displacement. Furthermore, the pier shear force appears to be only marginally affected by the intensity of the input.

Figure 6-4 compares the response of the isolated bridge with stiff and with flexible piers in selected earthquakes. We observe that the bearing displacements in the bridge with flexible piers

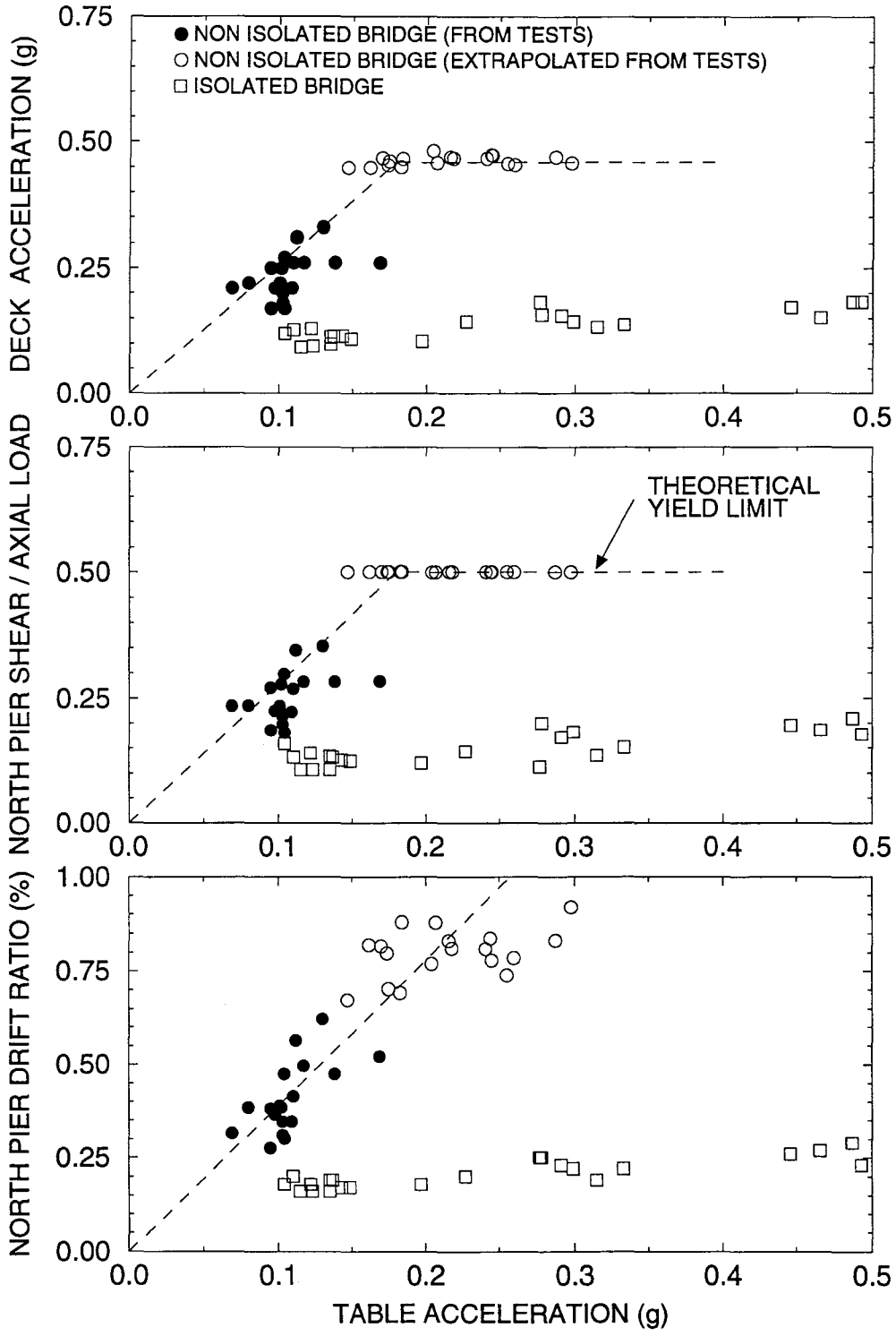

Figure 6-1 **Comparison of Response of Non-Isolated and Isolated Bridges. Case of System with Low Friction Bearings (C1), High Stiffness Rubber Devices (No. 3) and Flexible Piers.**

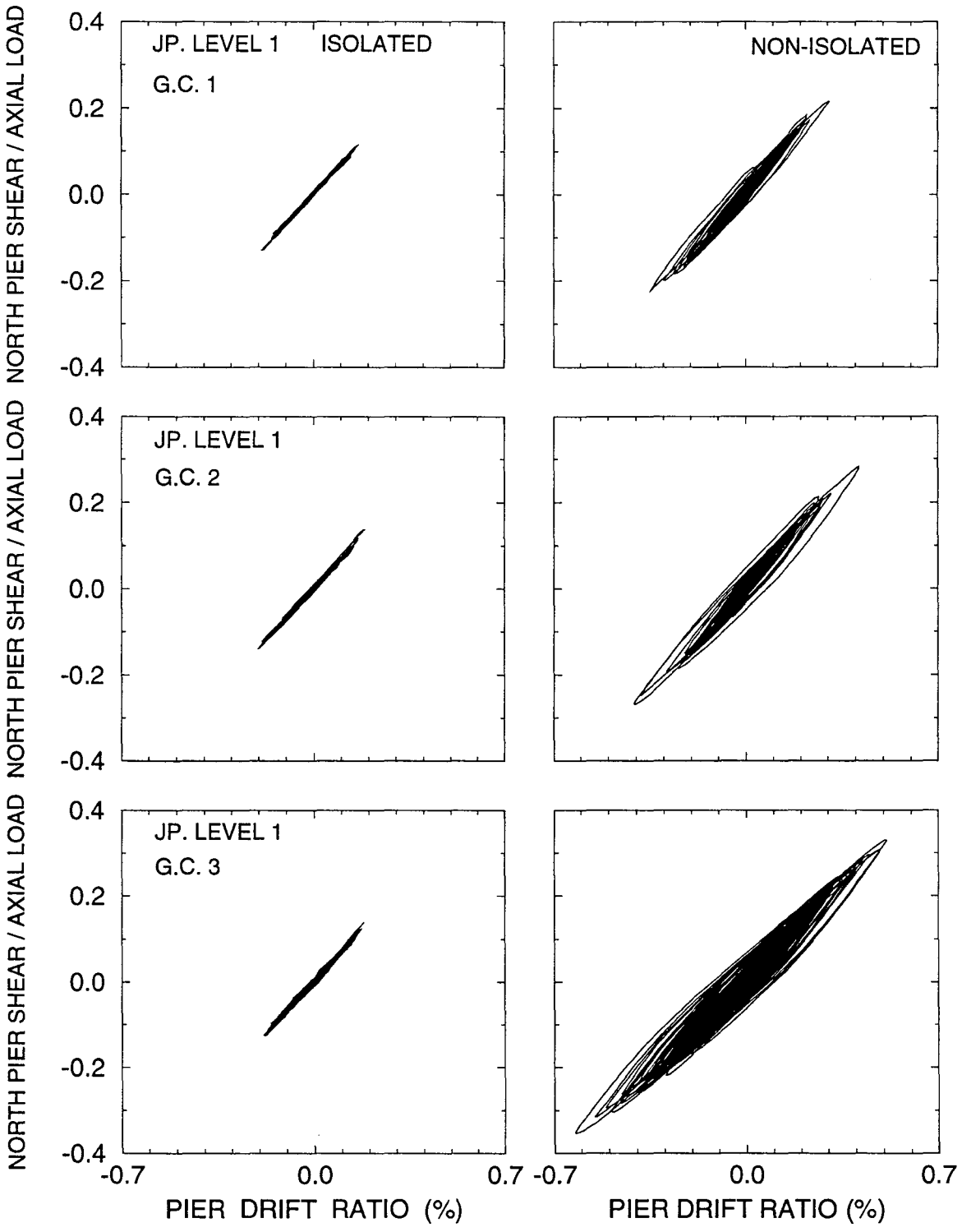

Figure 6-2 **Comparison of Pier Response of Non-Isolated and Isolated Bridge with Low Friction (C1) Bearings and High Stiffness (No. 3) Rubber Devices Recorded for the Japanese Level 1 Motions.**

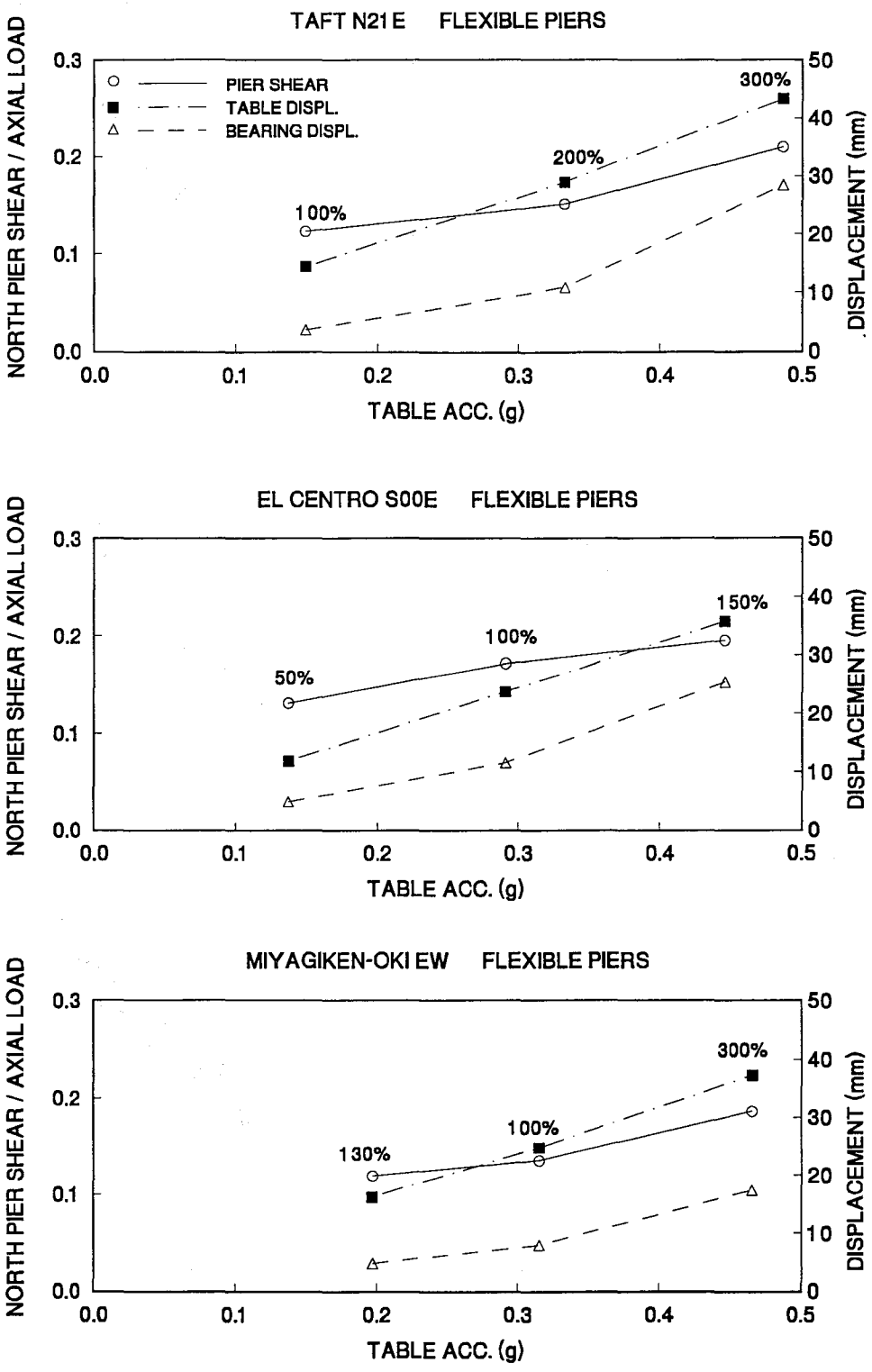

Figure 6-3 **Response of Isolated Bridge with Low Friction (C1) Bearings, High Stiffness (No. 3) Rubber Devices and Flexible Piers to Input with Increasing Intensity.**

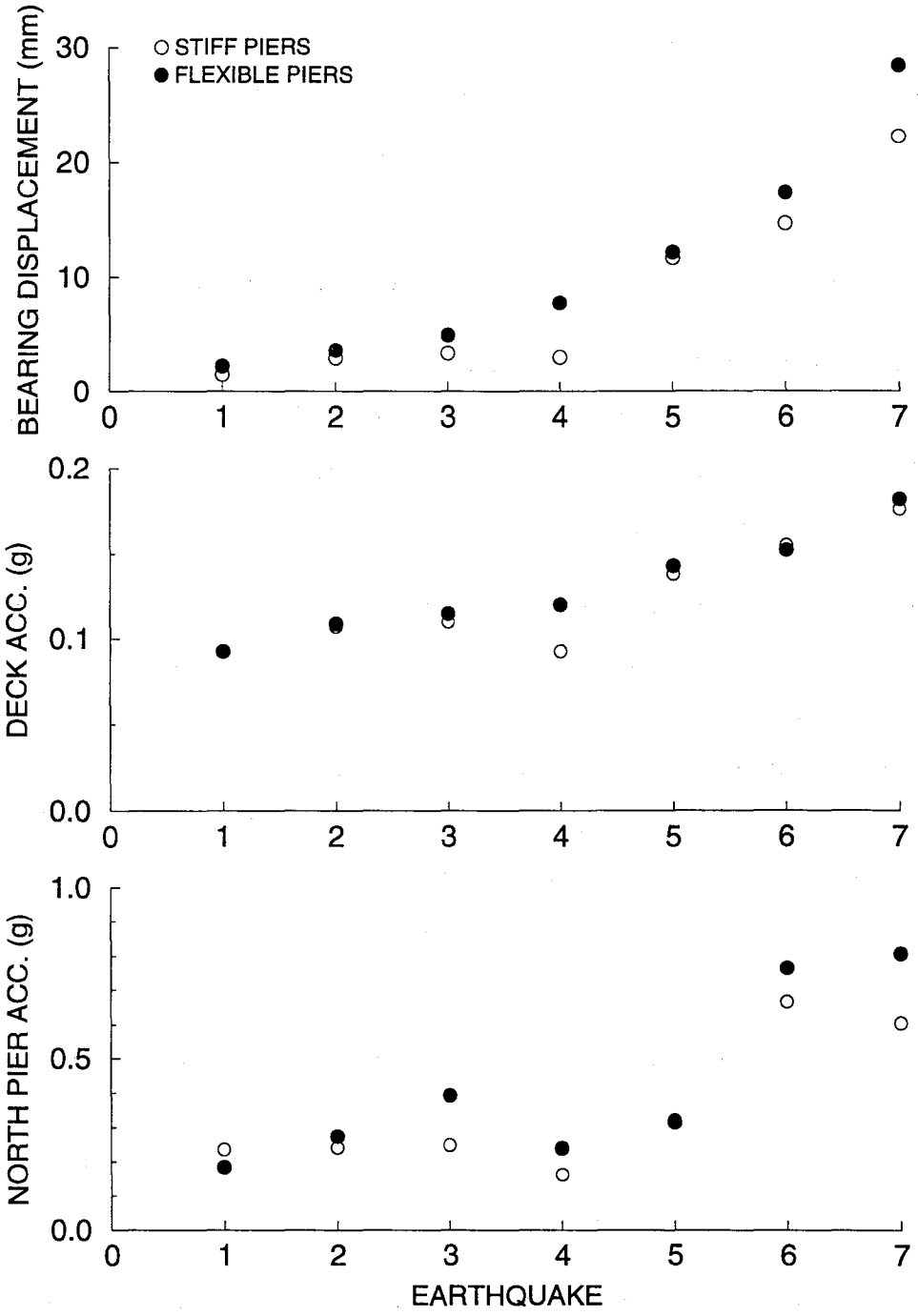

1 BOSTON 1 100% ; 2 TAFT N21E 100% ; 3 EL CENTRO S00E 50% ;
4 JP. LEVEL1 G.C.1 100% ; 5 HACHINOHE N-S 100% ;
6 MIYAGIKEN-OKI EW 300% ; 7 TAFT N21E 300%

Figure 6-4 **Comparison of Response of Isolated Bridge with Stiff and Flexible Piers. Case of Low Friction (C1) Bearings and High Stiffness (No. 3) Rubber Devices.**

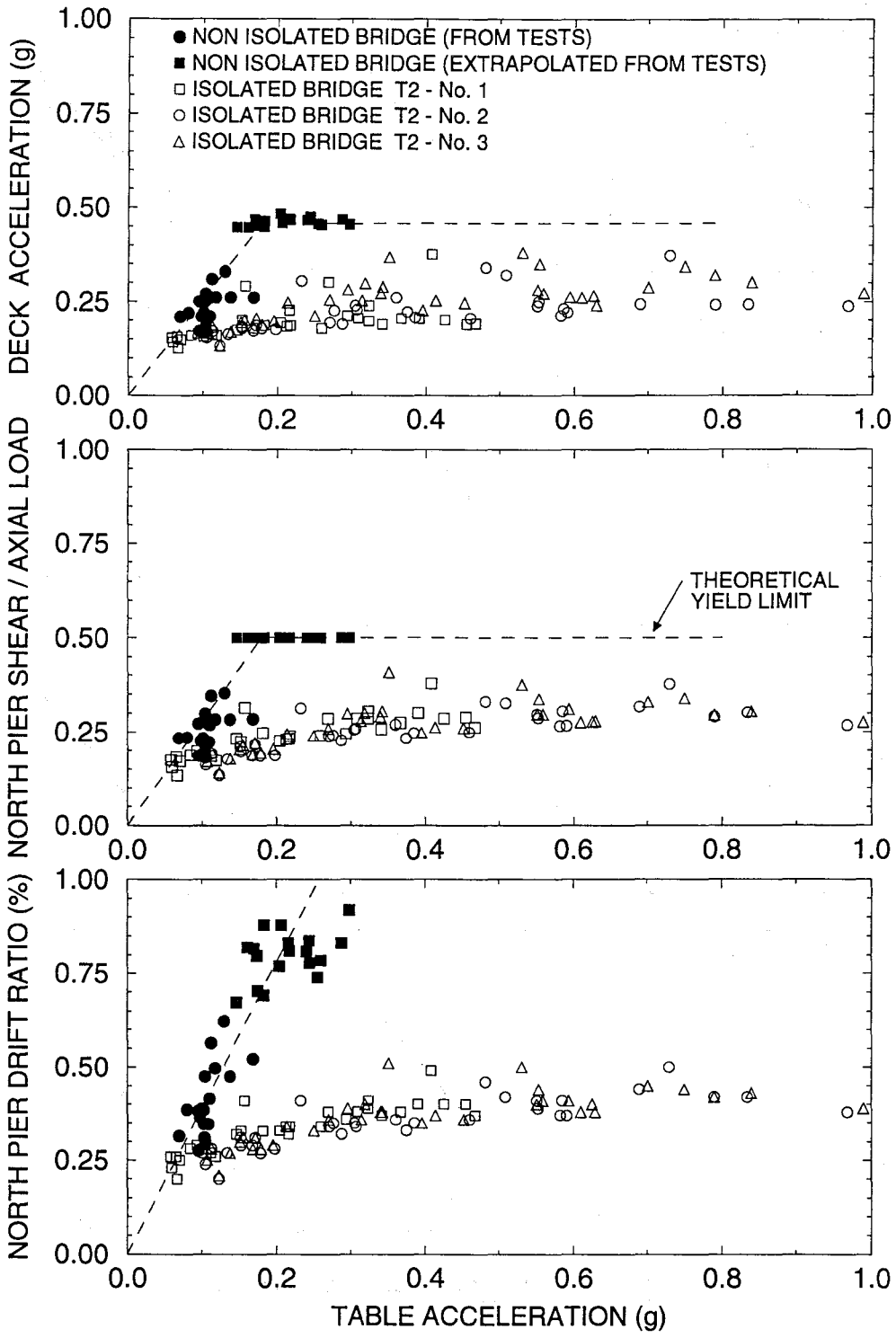

Figure 6-6 **Comparison of Response of Non-Isolated and Isolated Bridges. Case of System with Medium Friction Bearing (T2), Rubber Devices No. 1,2 and 3, and Flexible Bridge Piers.**

should be noted that the input had peak acceleration between 0.05 and nearly 1g, with significantly varying content in frequency.

The tested bridge remained elastic (theoretical yield limit equal to 0.5W) while bearing displacements were maintained at less than about 40 mm (or 160 mm in prototype scale). The results of two tests (i.e. tests No. RHHRUN38 and RHHRUN61) were not included in Figure 6-6. In these tests with system T2-No. 3 (highest stiffness, period of 1.33 secs in model scale) and excitation being the Japanese Level 2 Ground Condition 1 and Pacoima S16E signals, the displacement restraint of the rubber devices was fully activated. This resulted in effective control of the bearing displacement to below 50 mm, at the expense of higher pier shear forces. These forces reached the limit 0.5 W. The effects of activating the displacement restraint and ways of reduction of these effects are discussed later in this report.

The effects of increasing intensity of seismic excitation on the response of the isolated bridge are illustrated in Figures 6-7 to 6-9, which depict the response of the isolated bridge with flexible piers. Similarly, Figures 6-10 to 6-11 depict the response of the isolated bridge with stiff piers as a function of increasing intensity of earthquake input. The intensity of the excitation is represented by the peak table velocity, which is regarded as a better single measure of intensity of input than the peak table acceleration. This is because the response of isolated structures is primarily influenced by the amplitude and frequency content of the velocity domain of the response spectrum of the input.

It may be observed that the acceleration and force responses of the isolated bridge are only marginally affected by the intensity of the input, except for the cases in which the displacement restrainer was activated. Rather, we observe a noticeable effect of input intensity on the bearing displacement. However, the bearing displacement is always less than the table displacement (typically less than or about equal to half the table displacement, see Figures 6-8 and 6-11).

Of interest is to note in Figures 6-7 to 6-11 that the response of the three isolation systems is nearly the same for the same seismic input conditions and despite their significantly different stiffness characteristics. This phenomenon occurred because all three systems had weak restoring force, that is peak restoring force which was always less than the peak friction force. For

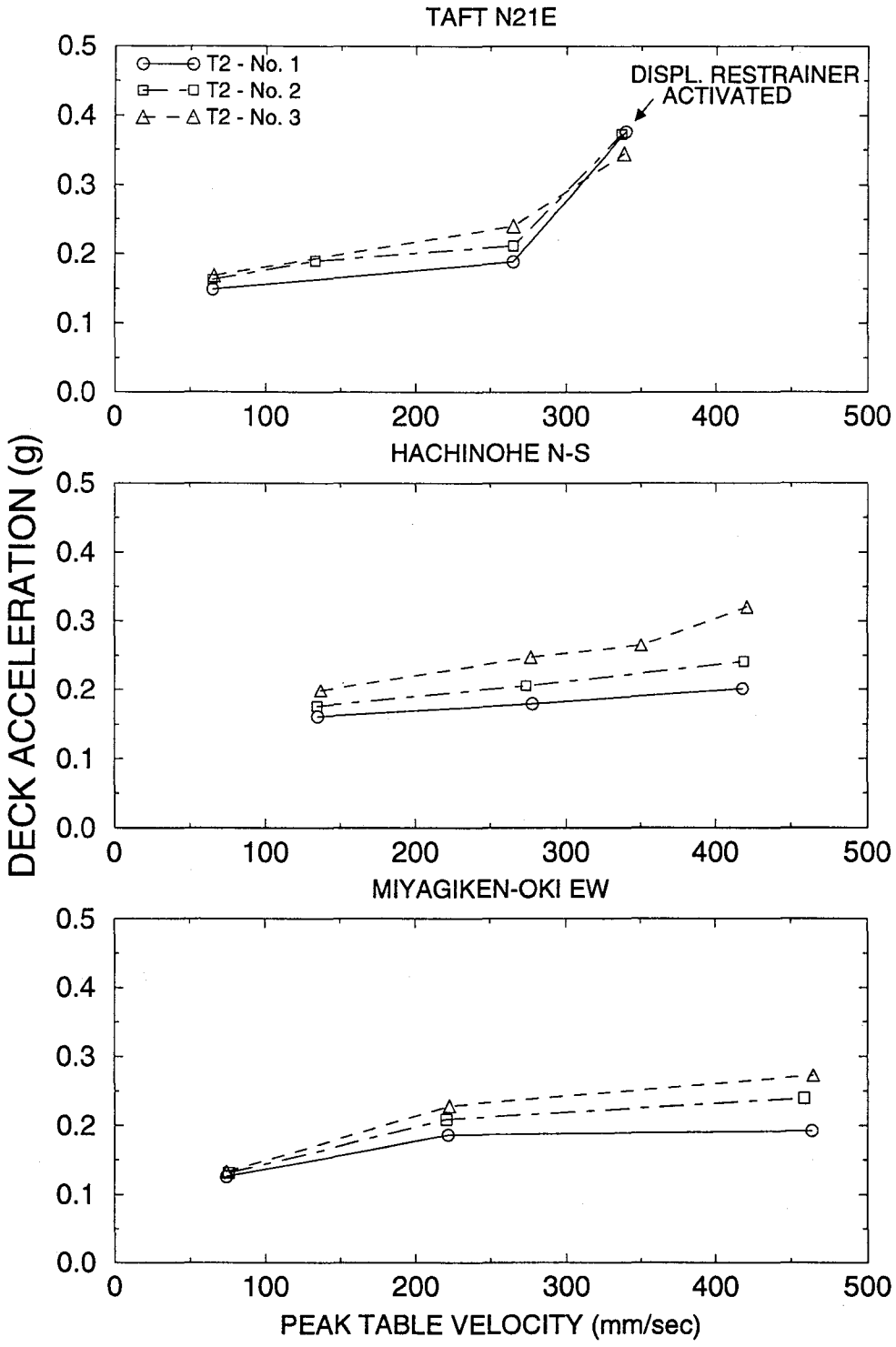

Figure 6-7 **Deck Acceleration of Isolated Bridge with Medium Friction Bearings and Flexible Piers under Increasing Intensity of Input (Represented by Peak Table Velocity).**

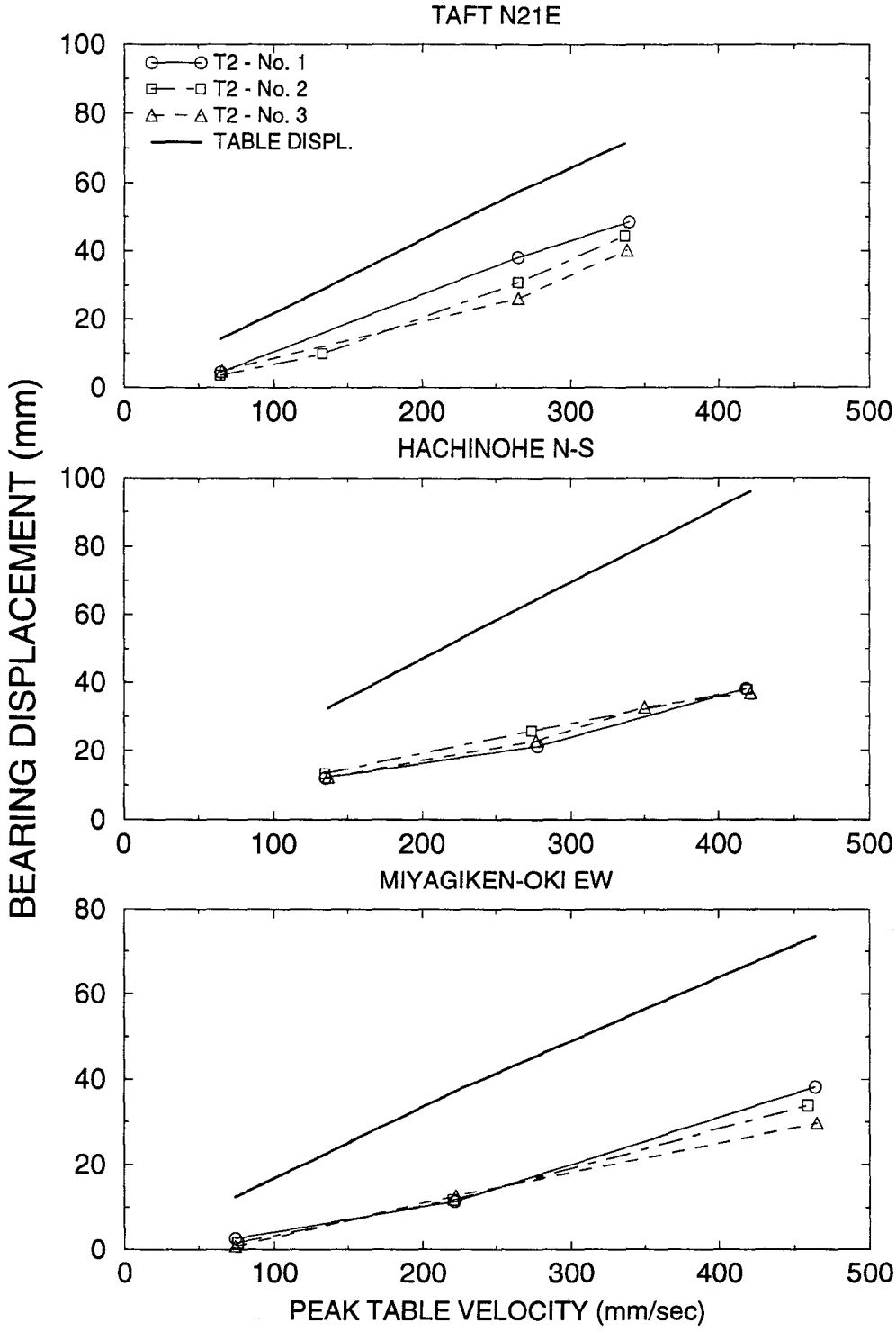

Figure 6-8 **Bearing Displacement of Isolated Bridge with Medium Friction Bearings and Flexible Piers under Increasing Intensity of Input (Represented by Peak Table Velocity).**

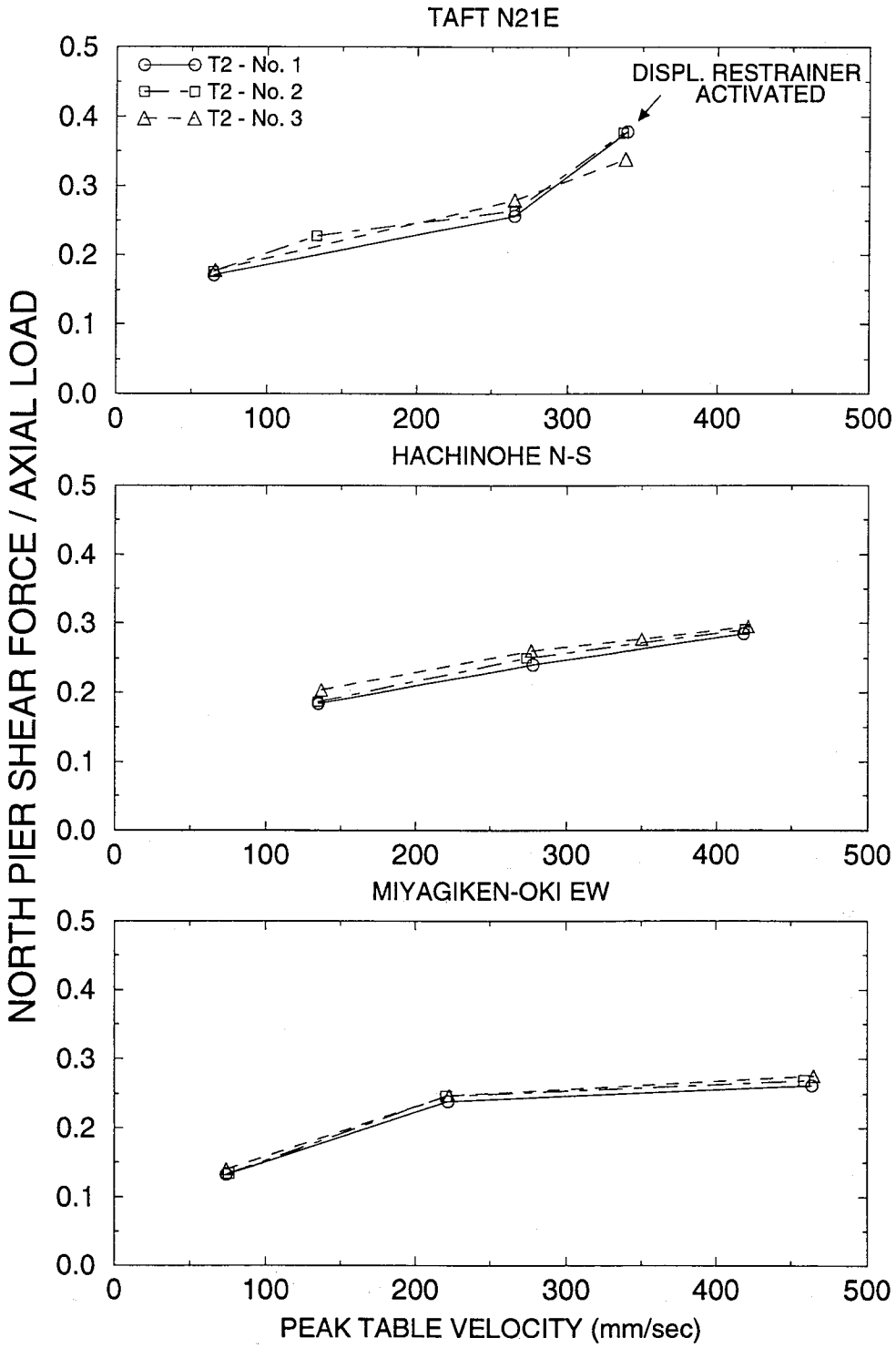

Figure 6-9 **Pier Shear Force of Isolated Bridge with Medium Friction Bearings and Flexible Piers under Increasing Intensity of Input (Represented by Peak Table Velocity).**

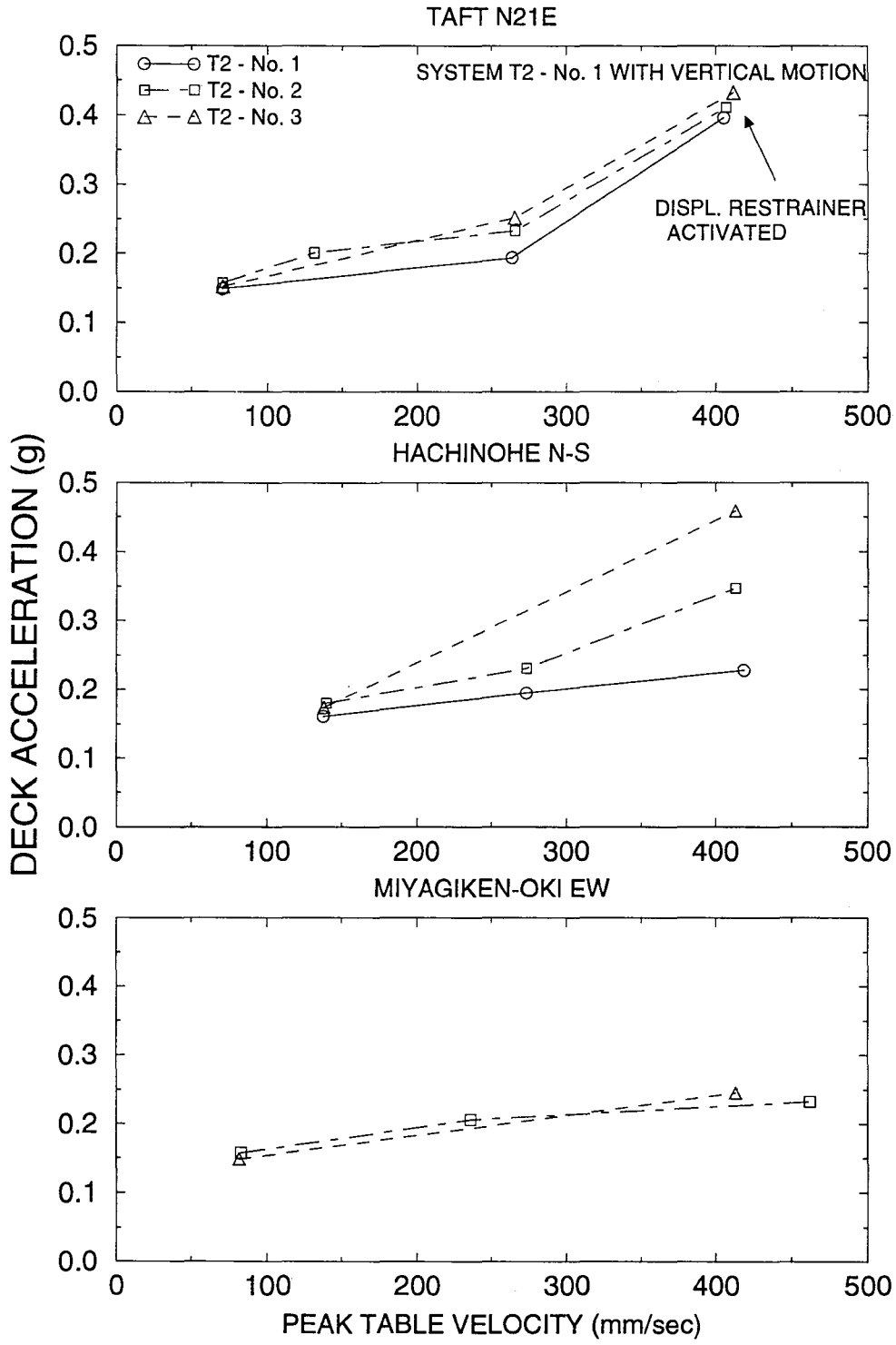

Figure 6-10 **Deck Acceleration of Isolated Bridge with Medium Friction Bearings and Stiff Piers under Increasing Intensity of Input (Represented by Peak Table Velocity).**

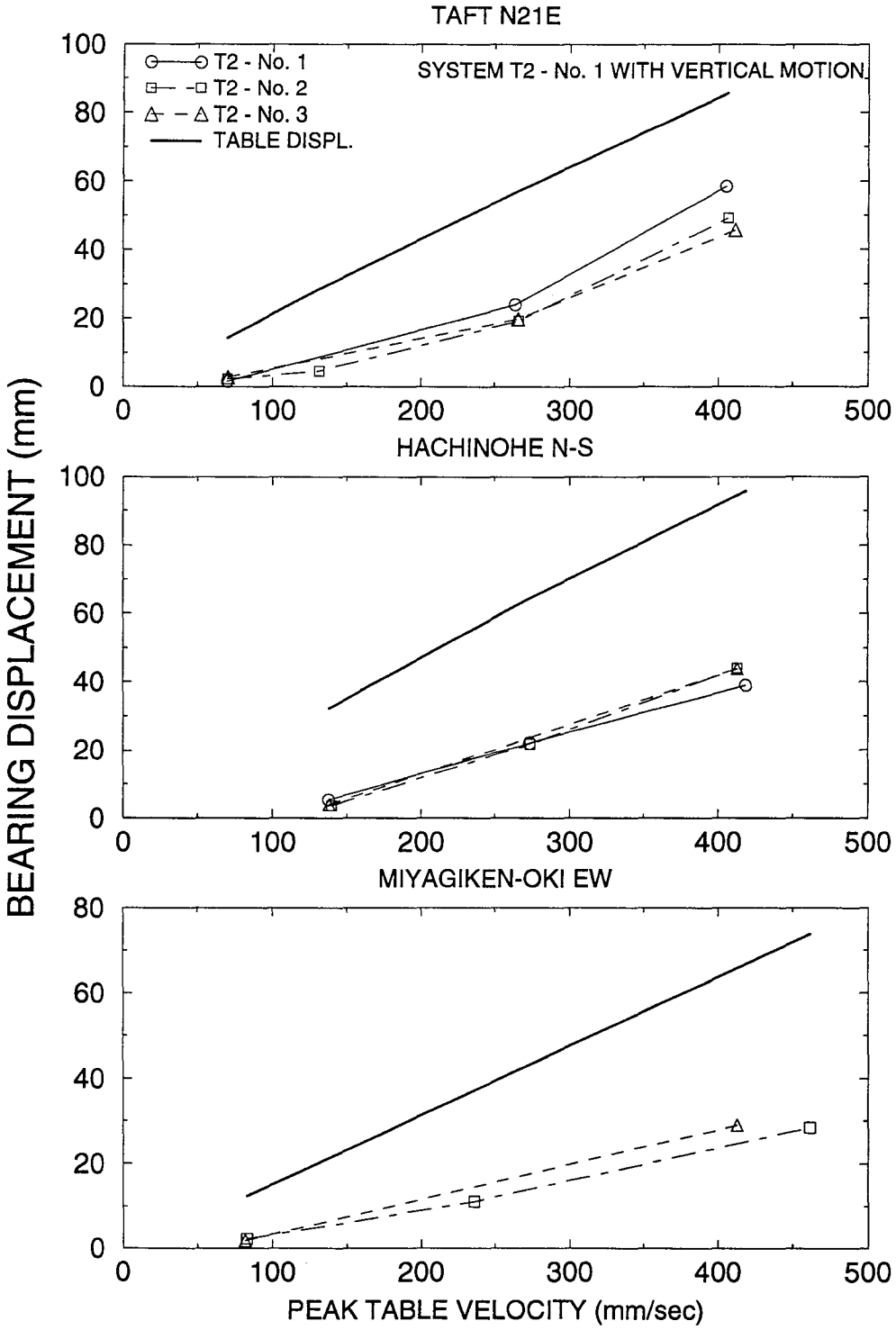

Figure 6-11 **Bearing Displacement of Isolated Bridge with Medium Friction Bearings and Stiff Piers under Increasing Intensity of Input (Represented by Peak Table Velocity).**

comparison, all three systems had a peak friction force at each pier equal to 9.9 kN and peak restoring force at 40 mm displacement equal to 1.9, 4.5 and 6.5 kN in systems with rubber devices No. 1 to 3, respectively. Under these conditions the rubber devices acted primarily as devices for controlling the bearing displacement rather than as devices for shifting the frequency of the isolated structure to low values (Constantinou 1990b).

6.4 Behavior of High Friction Isolation System

The high friction isolation system (bearing type T1, f_{max}= 0.15) was tested in combination with medium stiffness (No. 2) rubber restoring force devices. The behavior of this system is nearly the same as that of system T2-No. 2 (see Section 6.3). The two systems have a small difference in the friction coefficient, f_{max} (0.15 in system T1 versus 0.138 in system T2).

A comparison of the response of these two systems is presented in Figures 6-12 to 6-14. The response of the two systems is nearly the same, except for the case of the strongest Taft motion in which the medium friction (T2) system has more deck acceleration and pier shear force than the high friction (T1) system. This appears to be inconsistent with the bearing displacement response of the two systems which is nearly the same (see Figure 6-13). The explanation for this "anomaly" is actually simple. The bearing displacement shown in Figure 6-13 (also in Figures 6-8 and 6-11) is the bearing travel (maximum minus initial displacement, as depicted in Figure 5-1). This quantity alone does not indicate the degree to which the displacement restrainer was activated. For example consider two cases with identical bearing travel of 46 mm. The first has initial displacement equal to -4 mm and peak displacement equal to -50 mm. The second has initial displacement equal to +4 mm and peak displacement of -42 mm. Apparently, the displacement restrainer will be fully activated in the first case and this will result in significantly more deck acceleration and pier shear force than the second case. This is exactly what happened in the strongest Taft motion tests of systems T1-No. 2 and T2-No. 2.

6.5 Behavior of System with Combined Low and Medium Friction Sliding Bearings

Tests were conducted with a system having medium friction (type T2) bearings and high stiffness (No. 3) rubber devices installed at the south pier and low friction (type C1) bearings and medium

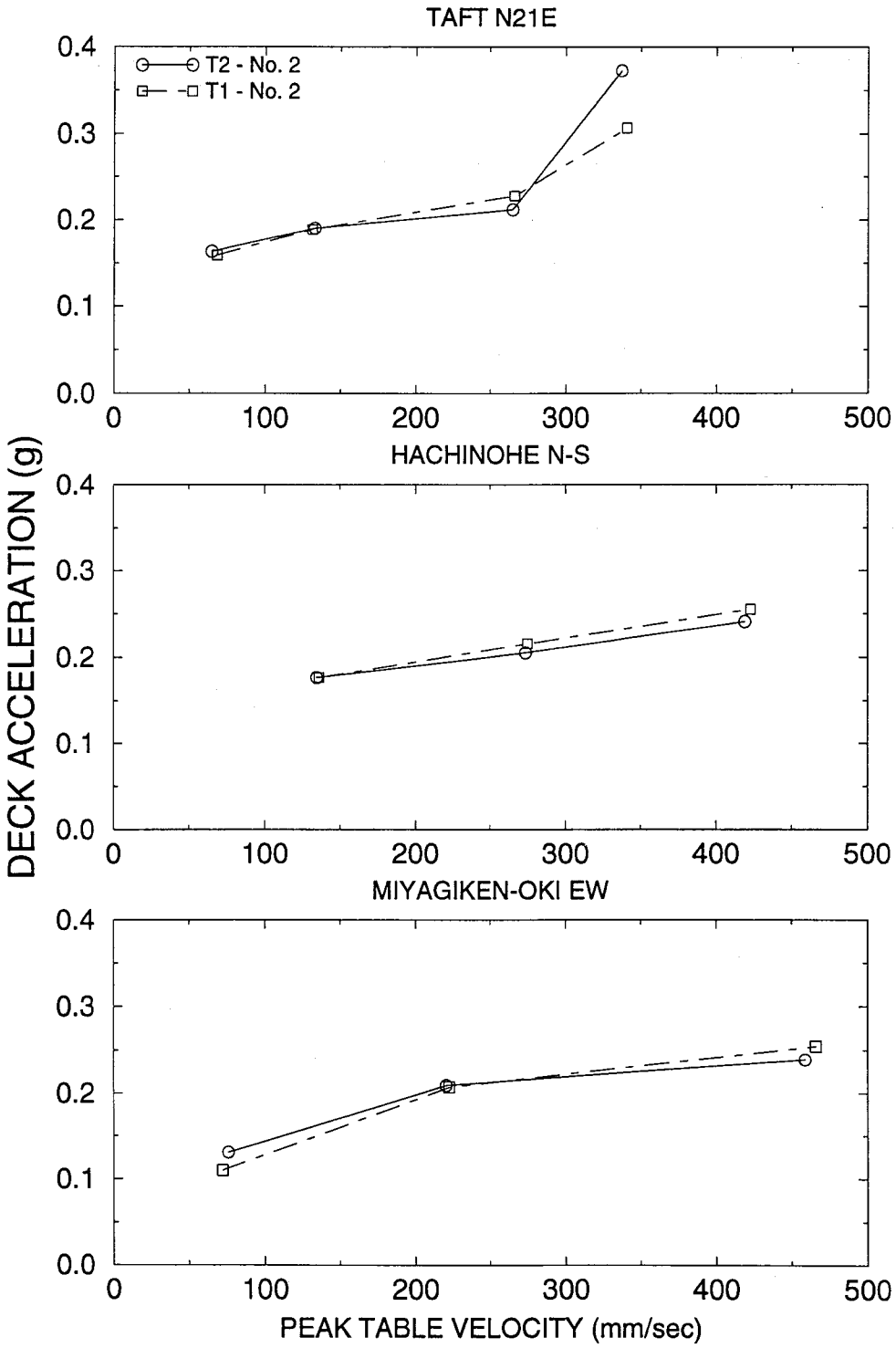

Figure 6-12 Comparison of Deck Acceleration Response of Isolated Bridges with Medium Friction (T2-No. 2) and High Friction (T1-No. 2) Bearings and Flexible Piers.

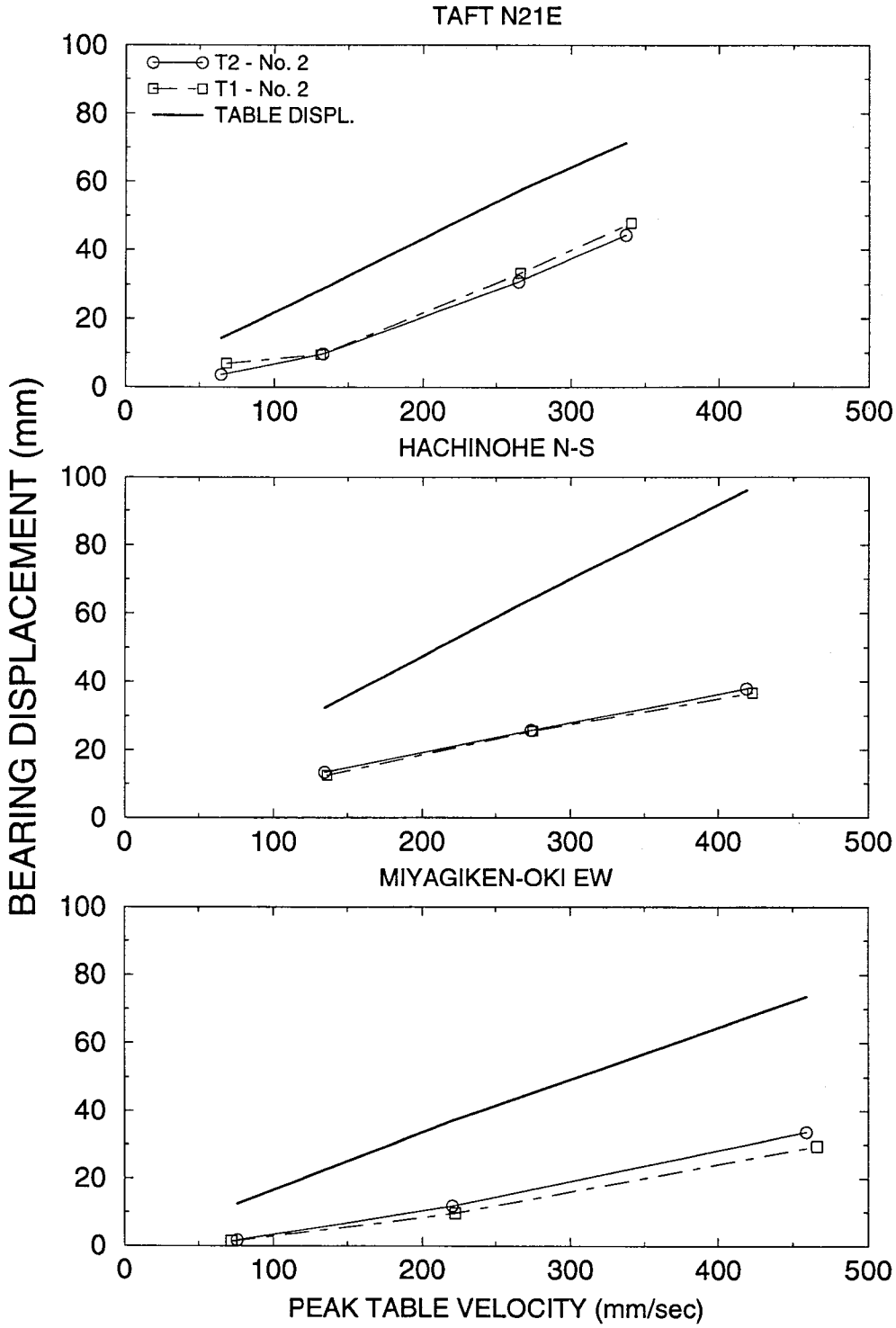

Figure 6-13 Comparison of Bearing Displacement Response of Isolated Bridges with Medium Friction (T2-No. 2) and High Friction (T1-No. 2) Bearings and Flexible Piers.

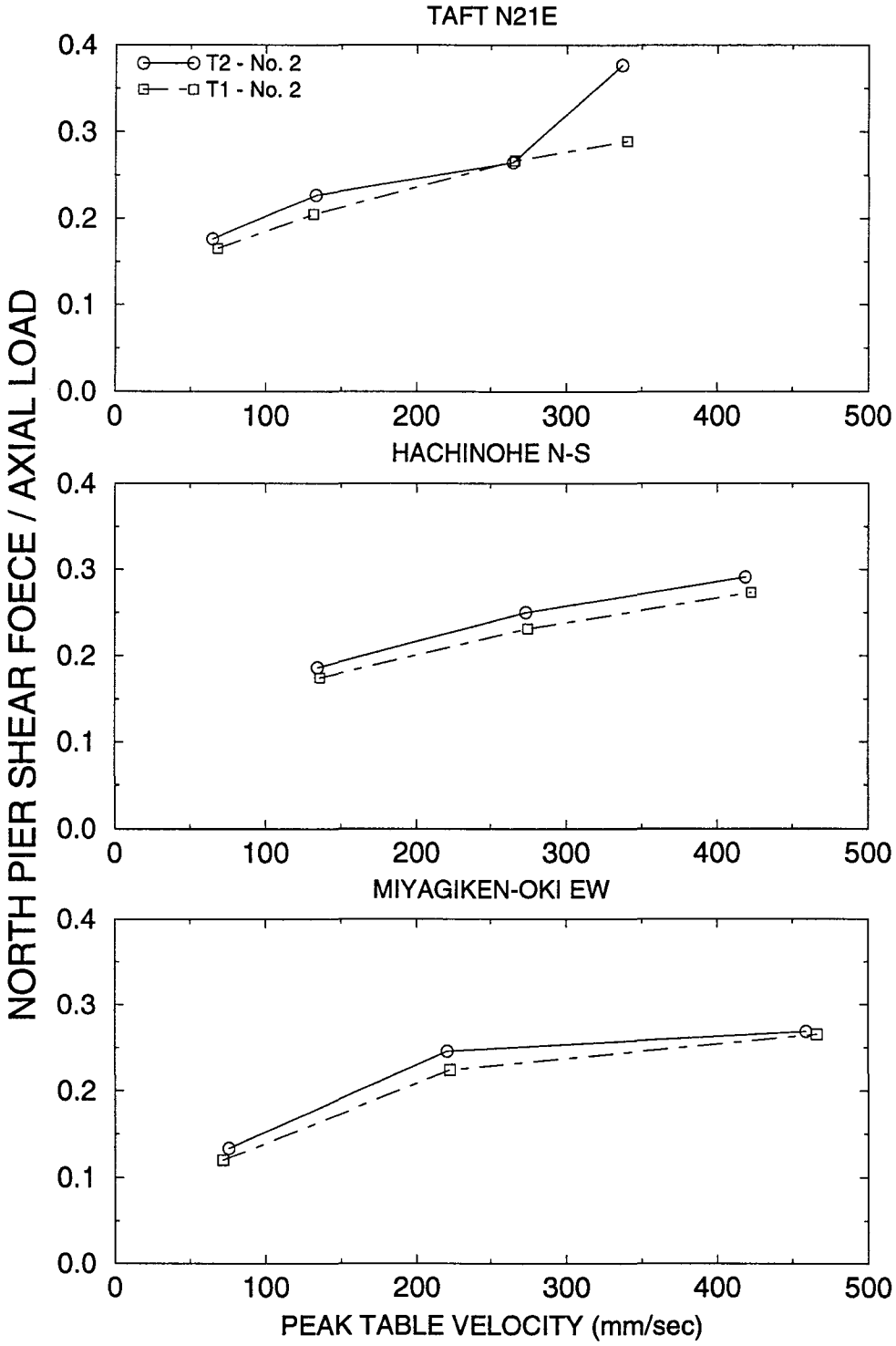

Figure 6-14 Comparison of Pier Shear Force Response of Isolated Bridges with Medium Friction (T2-No. 2) and High Friction (T1-No. 2) Bearings and Flexible Piers.

stiffness (No. 2) rubber devices installed at the north pier. The system had a weighted friction coefficient at large velocities equal to about 0.10 and effective period of 1.45 seconds. Thus in terms of global behavior, the system falls in-between systems C1-No. 3 and T2-No. 2. However, the use of high friction and high stiffness elements at the south pier results in direction of the seismic forces to that pier and mitigation of the seismic forces at the other pier.

A vivid illustration of this desirable behavior is provided in Figure 6-15, which presents the response of the isolated bridge with both flexible piers in test No. RMLRUN34 with Japanese Level 2, Ground Condition 2 input. The rubber device restoring force, the isolation system force and the pier shear force at the north pier are nearly one half of the corresponding forces at the south pier (note that weight in Figure 6-15 is the weight carried by each pier which is equal to 71.5 kN).

6.6 Effect of Activating the Displacement Restrainer

The engagement of the displacement restrainer of the rubber restoring force devices resulted in restriction of the isolation system displacement to within about 50 mm (or 200 mm in prototype scale), at the expense of higher deck accelerations and substructure forces. Nevertheless, the piers of the isolated bridge remained elastic or nearly so, whereas those of the non-isolated bridge would have suffered significant yielding under similar seismic input conditions (from extrapolation of the results of Table 5-I).

For example, Figure 6-16 compares the north pier responses of the isolated bridge with medium friction bearings (system T2-No. 2) and the non-isolated bridge under the simulated CalTrans A2 input. The isolated bridge (test No. RD2RUN56) is subjected to an input nearly five times stronger than that of the non-isolated bridge (test No. FRUN22). Yet, the responses of the two bridges are nearly identical, despite the fact that the displacement restrainer of the isolated bridge has been partially activated.

The experimental results demonstrated that, for the tested bridge, it is possible to restrict the isolation system displacement to within 200 mm in prototype scale and maintain elastic behavior (or nearly so) of the piers provided that the piers are designed for a lateral force between 0.3 and

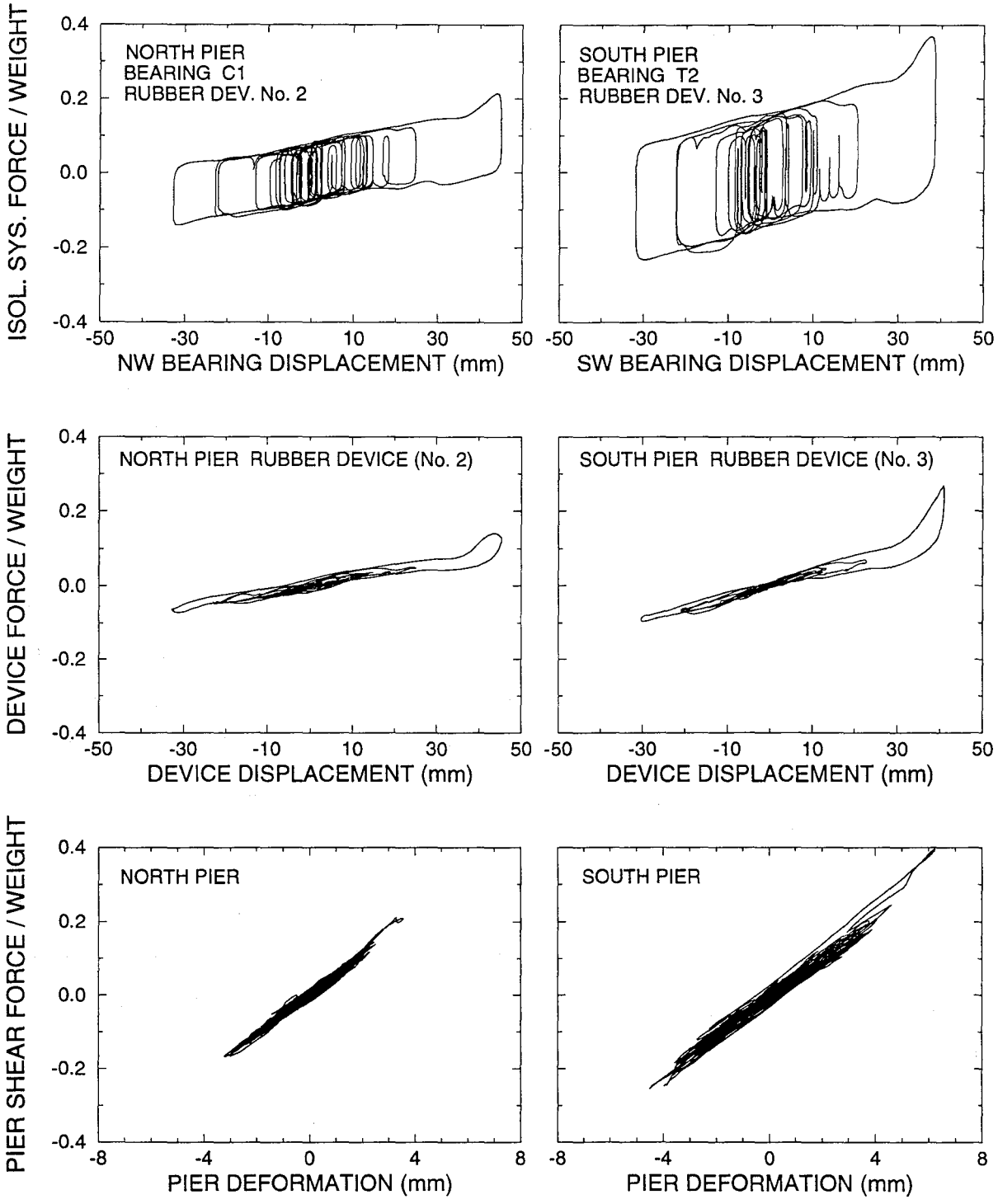

Figure 6-15 Example of Direction of Seismic Forces to Selected Elements. Case of Test No. RMLRUN34, JP Level 2, G.C. 2 75% Input, both Flexible Piers.

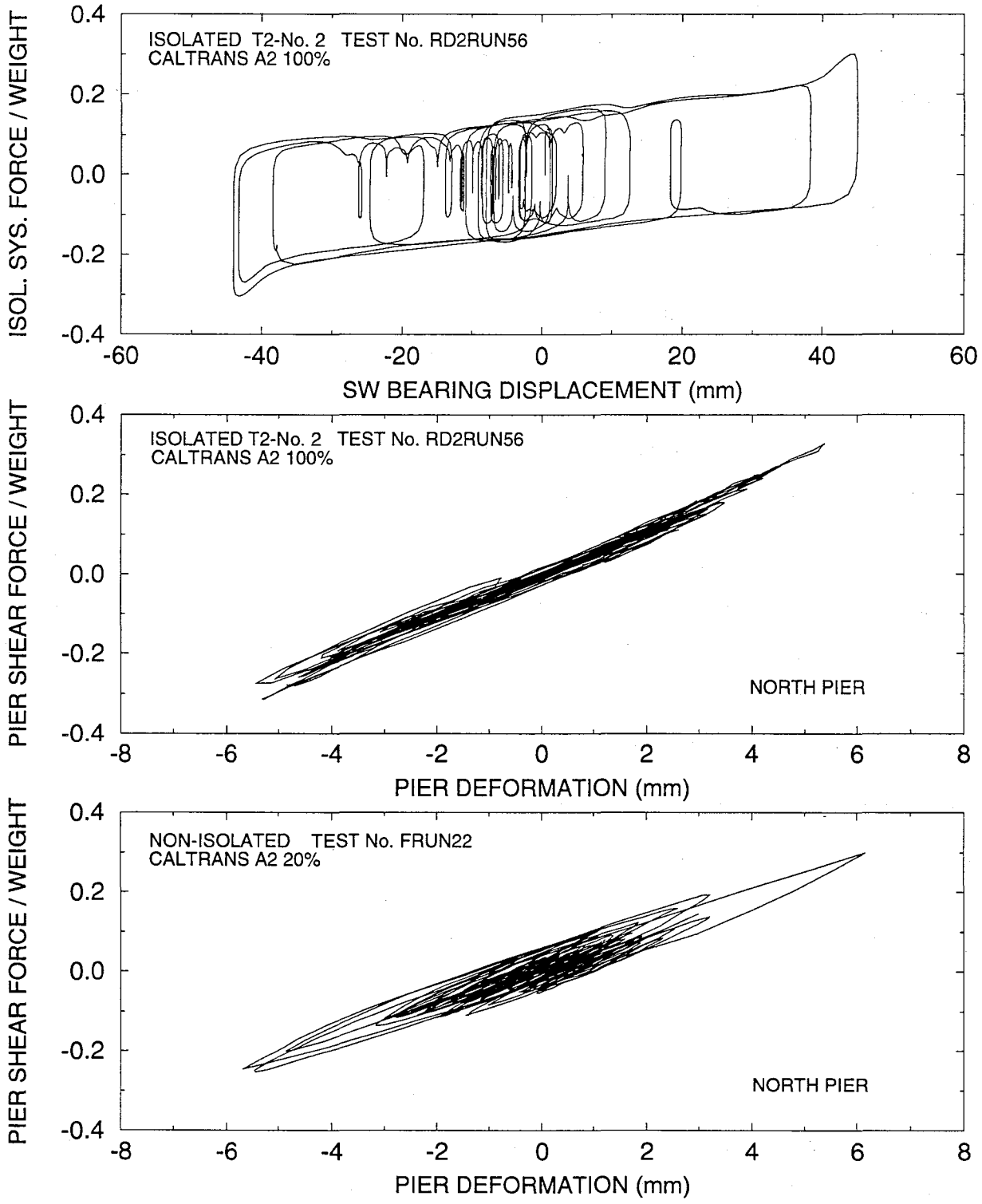

Figure 6-16 Comparison of Non-Isolated and Isolated Bridge Response. Note that Displacement Restrainer of Isolated Bridge is Activated. Responses are Nearly the Same for Input Being Five Times Stronger in the Isolated Case.

0.5 times the carried weight. On this we note that piers of isolated bridges in Japan are designed for seismic coefficient of at least 0.3 to avoid very flexible structures (CERC 1992). This minimum value of 0.3 includes the effect of inelastic pier behavior, that is reduction by factor $1/\sqrt{2\mu - 1}$, where μ is the pier allowable ductility factor.

6.7 Significance of Fluid Viscous Damping in Maintaining Low Bearing Displacements and Pier Forces

Fluid dampers were used in the isolation system configuration T1-No. 2 (high friction bearings, medium stiffness rubber devices) for the purpose of enhancing energy dissipation so that the displacement restrainer was not activated. Of particular interest was the Japanese Level 2 input, for which all systems without fluid dampers resulted in activation of the displacement restrainer when the flexible pier configuration was tested.

The addition of fluid dampers enhanced energy dissipation to the point that the displacement restrainer was not activated in all conducted tests (see Table 5-V). As an example, Figure 6-17 compares the response of system T1-No. 2 without and with fluid dampers in the Japanese Level 2, Ground Condition 1 input. Prevention in this case of activation of the displacement restrainer resulted in substantial reduction of the isolation system force and pier shear force.

Of particular interest is to note in Table 5-V the marked insensitivity of the system with fluid dampers to the frequency content of the input in the sequence of Japanese Level 2 motions. The peak response of the isolated bridge is nearly the same in these three motions which have significantly different content in frequency and number of cycles of motion.

The results shown in Figure 6-18 (also Table 5-V) demonstrate that the combined sliding-rubber device-fluid damper system may be designed to provide effective bridge isolation for the Japanese Level 2 input with bearing displacement at or below 160 mm in prototype scale and pier seismic coefficient between 0.325 and 0.375 under elastic conditions. In this respect, we note that piers of isolated bridges in Japan are typically designed for a seismic coefficient of at least 0.3. It is, thus, possible to design bridge isolation systems which, for elastic substructure behavior and for all seismic conditions in Japan, maintain the bearing displacements below 200 mm and the pier shear forces at the minimum allowed design level.

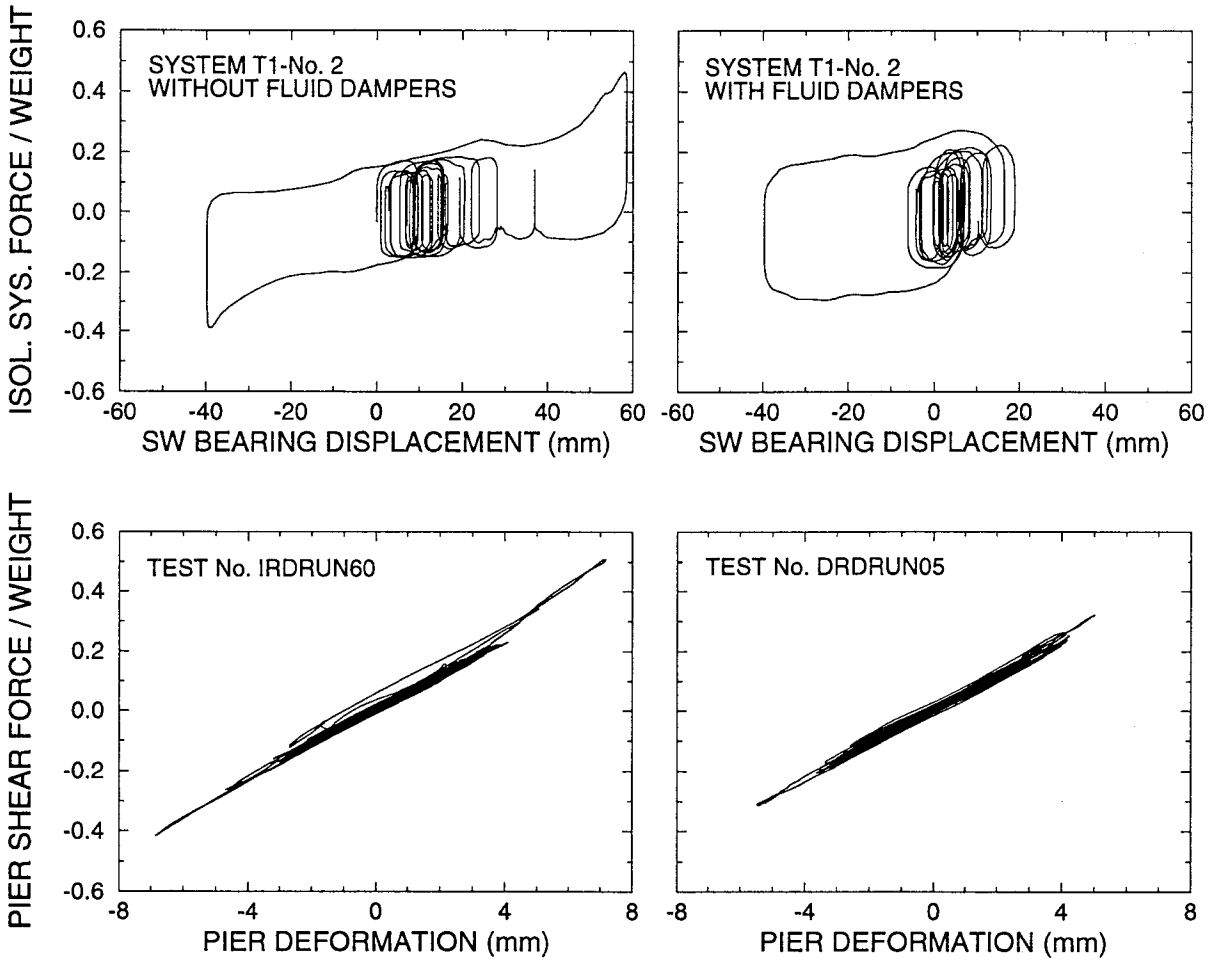

Figure 6-17 Comparison of Response of System T1-No. 2 with Flexible Piers, Without and With Fluid Dampers in the Japanese Level 2, Ground Condition 1 Input.

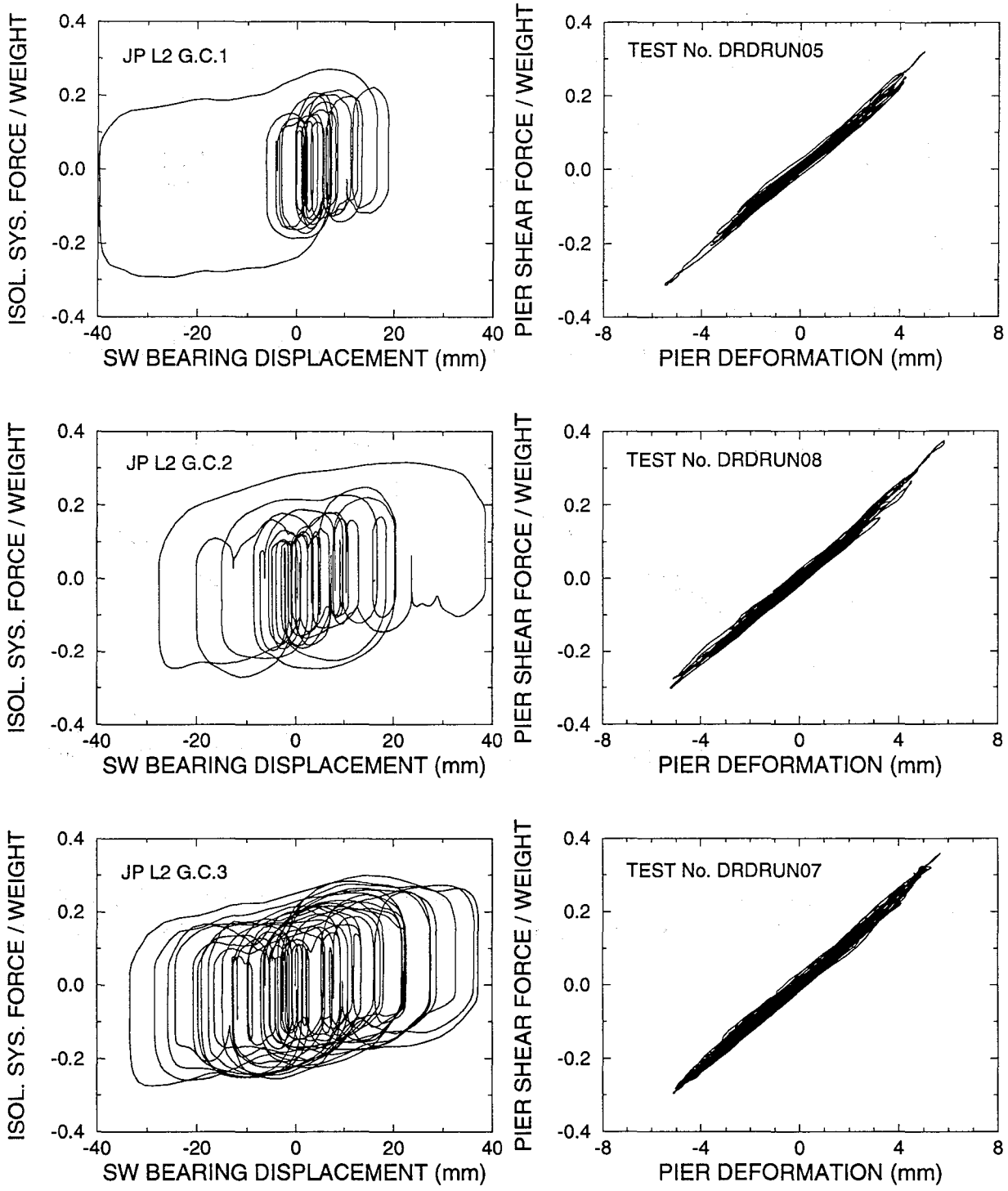

Figure 6-18 **Comparison of Response of System T1-No. 2 with Fluid Dampers to the Three Japanese Level 2 Motions. Note that Peak Bearing Displacement, Peak Isolation System Force and Peak Pier Shear Force and Deformation are Nearly Identical.**

6.8 Effect of Vertical Ground Motion

Tests were conducted with only horizontal and with combined horizontal-vertical input. Even when only horizontal input was applied, the overhangs of the shake table (see Figure 4-1) underwent significant vertical motion. As seen in Figure 6-19, the vertical acceleration at the north and south piers in the case of only horizontal input were typically out-of-phase with peak values about equal to 1/3 the peak horizontal table acceleration. In the case of combined horizontal-vertical input, the pier vertical accelerations were either out-of-phase or in-phase with peak values between 1/2 and 2/3 of the peak horizontal table acceleration.

Despite the severity of vertical input in the combined horizontal-vertical input, the response of the isolated bridge was only marginally affected. For example, Figures 6-20 and 6-21 compare the responses of the system with high friction bearings and medium stiffness rubber devices (T1-No. 2) to the Taft 400% and El Centro 200% motions, respectively. Other than the wavy form of the loops in the case of combined horizontal-vertical input, the vertical motion had no effect on the peak response of the tested system.

6.9 Permanent Displacements

The permanent displacements were recorded in all tests and are listed in Tables 5-IV and 5-V. The initial displacement (that is, the permanent at the start of each experiment) was monitored in all tests, except those tests with the high friction bearings (tests No. IRDRUN01 to IRDRUN65 and DRDRUN01 to DRDRUN14). The bridge was never recentered prior to conducting a test. However, it was observed that permanent displacements tended to reduce during idle times of the shake table in-between tests. This was caused by very small amplitude, high frequency motions of the shake table during the idle times.

A theoretical upper bound on the permanent displacement may be obtained from equilibrium of the isolated bridge under static conditions (that is, by equating the restoring force to the minimum friction force) :

$$u_p \leq \frac{f_{\min} g T^2}{4\pi^2} \qquad (6\text{-}1)$$

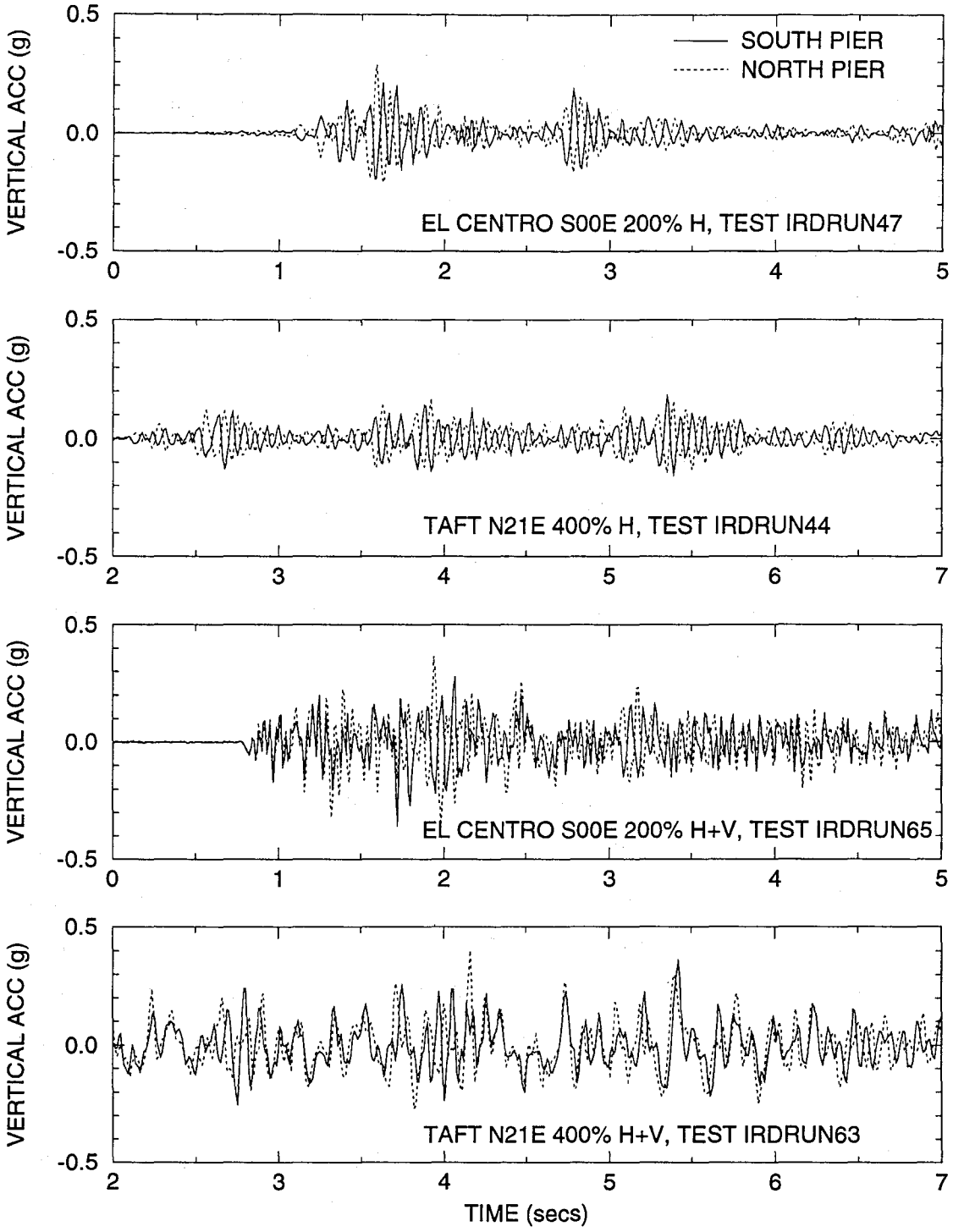

Figure 6-19 Recorded Vertical Acceleration at the Base of Piers in Tests with only Horizontal and with Combined Horizontal-Vertical Excitation.

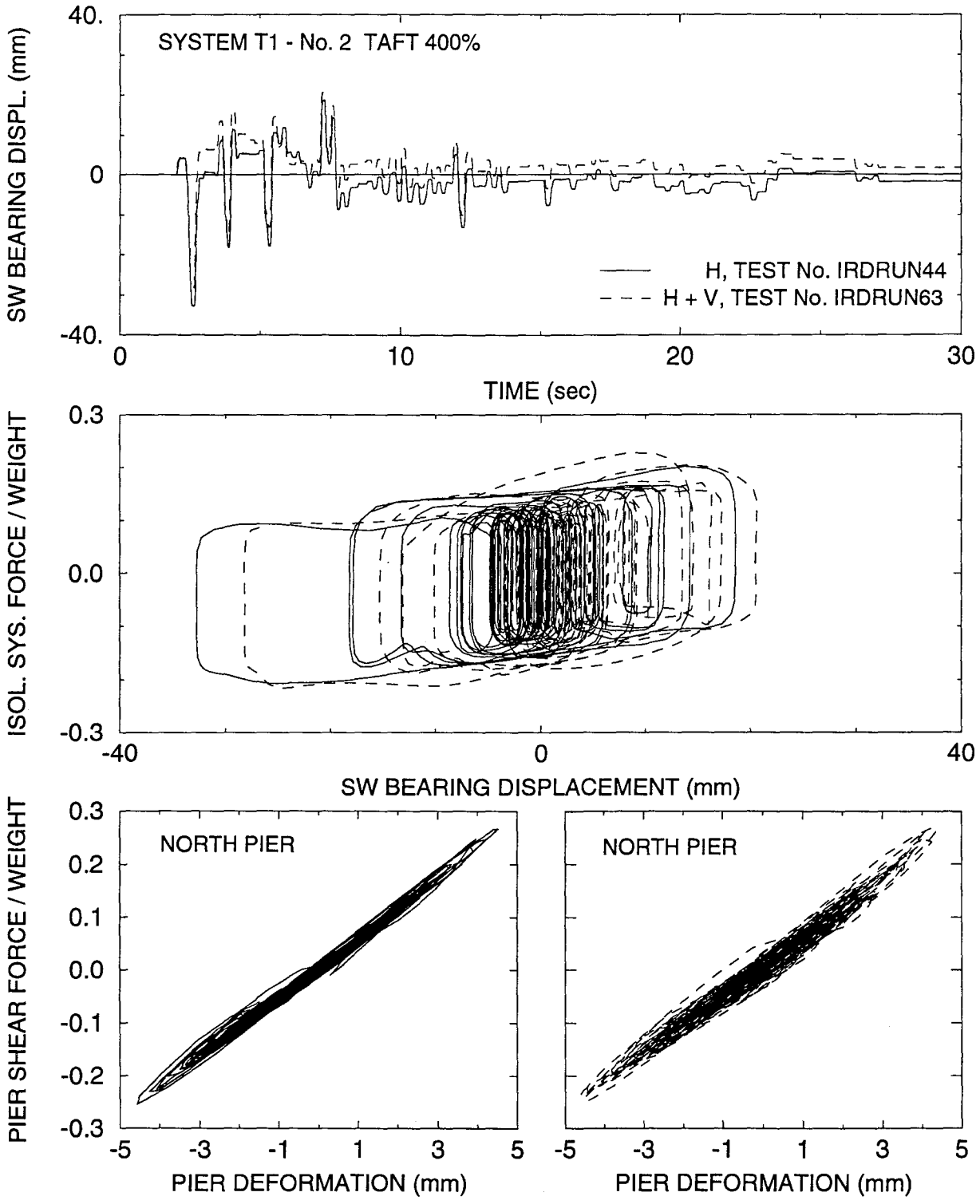

Figure 6-20 Effect of Vertical Ground Motion on Response of System T1-No. 2 (High Friction, Medium Stiffness) Subjected to Taft 400% Input.

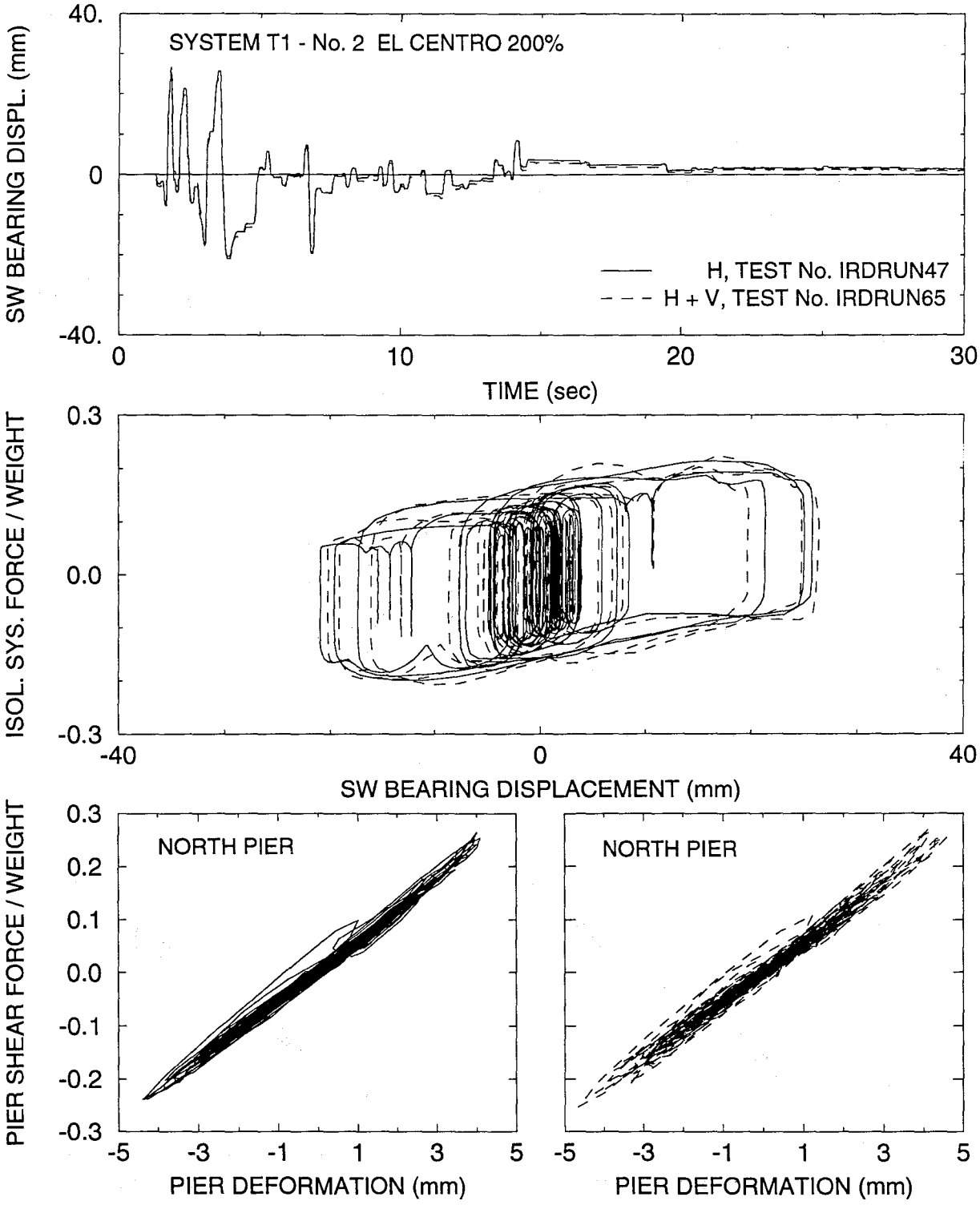

Figure 6-21 Effect of Vertical Ground Motion on Response of System T1-No. 2 (High Friction, Medium Stiffness) Subjected to El Centro 200% Input.

where f_{min}= coefficient of friction at zero sliding velocity, T = period of vibration (see Table 3-III) and u_p = permanent displacement.

Table 6-I lists the tested isolation systems, the theoretical upper bound on the permanent displacement and the maximum recorded permanent displacement. It may be observed that the permanent displacement in the case of simulated earthquake motions (such as the Japanese Level 2 and CalTrans motions) is typically larger than that recorded in tests with actual earthquake motions. Furthermore, the recorded permanent displacement is significantly less than the theoretical upper limit.

Table 6-I Recorded Permanent Displacements

ISOLATION SYSTEM*	FRICTION COEFFICIENT f_{min}	PERIOD T (sec)	THEORETICAL UPPER LIMIT OF PERMANENT DISPL. (mm)	RECORDED PERMANENT DISPL. (mm)	
				ACTUAL EARTHQUAKES	SIMULATED EARTHQUAKES
T1-No. 2	0.055	1.60	35.0	5.8	8.8
T2-No. 1	0.055	2.47	83.4	16.5	28.0
T2-No. 2	0.055	1.60	35.0	7.4	11.5
T2-No. 3	0.055	1.30	24.0	5.5	8.5
T2-No.2/FLUID DAMPERS	0.055	1.60	35.0	2.0	7.6
T2,C1-No. 2,3	0.0475	1.45	24.8	7.9	10.0
C1-No. 3	0.040	1.33	17.6	5.9	2.8**

* WITH REFERENCE TO TABLES 3-I TO 3-III

** ONLY FOR JP LEVEL 1. JP LEVEL 2 AND CALTRANS MOTIONS WERE NOT USED.

The permanent displacements were not cumulative, even in the case of least rubber restoring force device stiffness (No. 1). Rather, the isolated bridge had the tendency to recenter itself on initial movement. An example of this behavior is presented in Figure 6-22. Tests No. RSSRUN12 and RSSRUN13 were conducted on the low stiffness system T2-No. 1 with input being the simulated CalTrans A2 0.6g motion. The two tests were identical except for the initial displacement, which was +7.6 mm in the first test and -8.8 mm in the second. If the permanent displacements were cumulative, the permanent displacement in the second test should have been about -25 mm. To the contrary, the isolated bridge in the second test recentered itself on initial movement and subsequently followed a nearly identical motion path as it did in the first test.

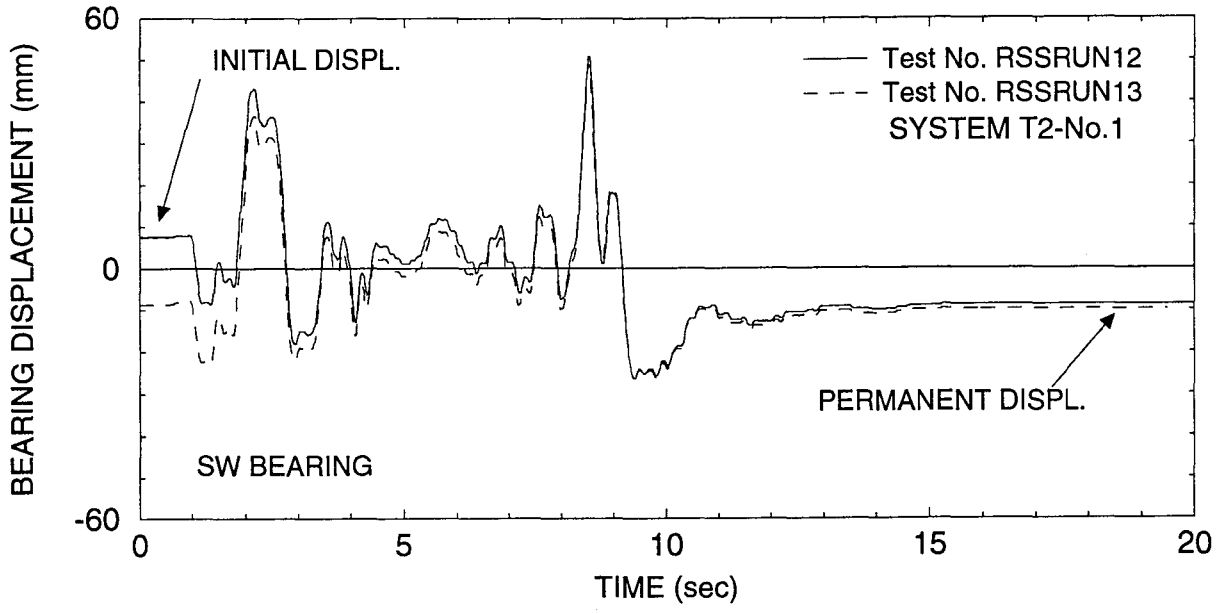

Figure 6-22 Comparison of Bearing Displacement Histories in Identical Tests with Different Initial Displacements. System T2-No. 1 with Stiff Piers Subjected to CalTrans A2 0.6g Motion. Observe that Permanent Displacement is not Affected by the Difference in Initial Displacements.

It should be noted that a minimum restoring force is required for a specific level of friction force to prevent the accumulation of permanent displacement. Lack of sufficient restoring force will inevitably lead to large and cumulative permanent displacements. The 1991 AASHTO, Section 12.2 requires that the isolation system is configured to produce a minimum force which exceeds a specified limit related to the seismic dead load (deck weight). For the tested isolation system, the AASHTO requirement is equivalent to

$$Kd_i \geq 0.05W \tag{6-2}$$

where K = total stiffness of rubber restoring force devices, d_i = design displacement (40 mm) and W = deck weight. Table 6-II lists the restoring force and AASHTO limits of the tested systems. All systems, except system T2-No. 1 (least stiffness system), satisfy the AASHTO requirements.

The AASHTO minimum restoring force requirements provide a basis for the applicability of the static analysis procedure of the provisions. Isolation systems which do not meet the aforementioned minimum requirements are allowed but require to be configured for accommodating a significantly larger displacement. The AASHTO recognizes that systems with

very weak or no restoring force will have cumulative permanent displacements. Indeed, the tested system which did not meet the AASHTO requirements had significantly more permanent displacement than the other systems. However, the system did not have cumulative permanent displacements.

The AASHTO limits on the restoring force do not recognize the significance of the characteristic strength or friction force. That is, the ability of an isolation system to recenter itself and the validity of the AASHTO static analysis procedure are dependent on the relation between the characteristic strength, Q , or friction force, F_f , and the restoring force, F_r , at the design displacement. For example, Table 6-II presents the ratio F_f / F_r of the tested systems. Apparently, there is a correlation between this ratio and the recorded peak permanent displacement. It appears that for F_f / F_r larger than about 5.0, large permanent displacements occur. Interestingly, this limit is consistent with earlier experimental observations (Constantinou 1990b).

Table 6-II Restoring Force Characteristics of Tested Systems

ISOLATION SYSTEM	RESTORING FORCE AT d_i = 40 mm (kN)	MIN. VALUE OF RESTORING FORCE PER 1991 AASHTO (kN)	1991 AASHTO REQUIREMENT	RATIO F_f / F_r AT d_i=40 mm	PEAK PERMANENT DISPL. (mm)
T1-No. 2	8.98	7.15	SATISFIED	2.39	8.8
T2-No. 1	3.75	7.15	NOT SATISFIED	5.26	28.0
T2-No.2	8.98	7.15	SATISFIED	2.2	11.5
T2-No. 3	12.98	7.15	SATISFIED	1.52	8.5
T2, C1-No. 2, No. 3	10.98	7.15	SATISFIED	1.34	10.0
C1-No. 3	12.98	7.15	SATISFIED	0.75	2.8

We propose that an isolation system be characterized as having sufficient restoring force when

$$\frac{F_f}{F_r} \leq 3 \qquad (6\text{-}3)$$

where F_f is the peak frictional force or characteristic strength of the isolation system and F_r is the restoring force of the isolation system at the design displacement.

The requirement imposed by the proposed Equation (6-3) and the related requirement of Section 12.2 of the 1991 AASHTO are not incompatible. For example, in sliding isolation systems with friction coefficient f_{max} and stiffness of restoring force devices K, the two requirements can be written as :

The 1991 AASHTO

$$d_i \geq \frac{T^2 g}{80\pi^2} \tag{6-4}$$

The proposed Equation (6-3)

$$d_i \geq \frac{f_{\max} T^2 g}{12\pi^2} \tag{6-5}$$

where d_i is the design displacement and T is the period of the isolation system ($T = 2\pi\sqrt{W/gK}$ where W = deck weight). It should be noted that T is not the effective period as defined in the 1991 AASHTO.

Evidently, the two requirements are identical for $f_{max} = 0.15$. However, the proposed requirement is more conservative than the 1991 AASHTO for $f_{max} > 0.15$, whereas the AASHTO requirement is more conservative than the proposed requirement when $f_{max} < 0.15$. This is illustrated in Figure 6-23, where the required minimum value of the design displacement is plotted against the period T.

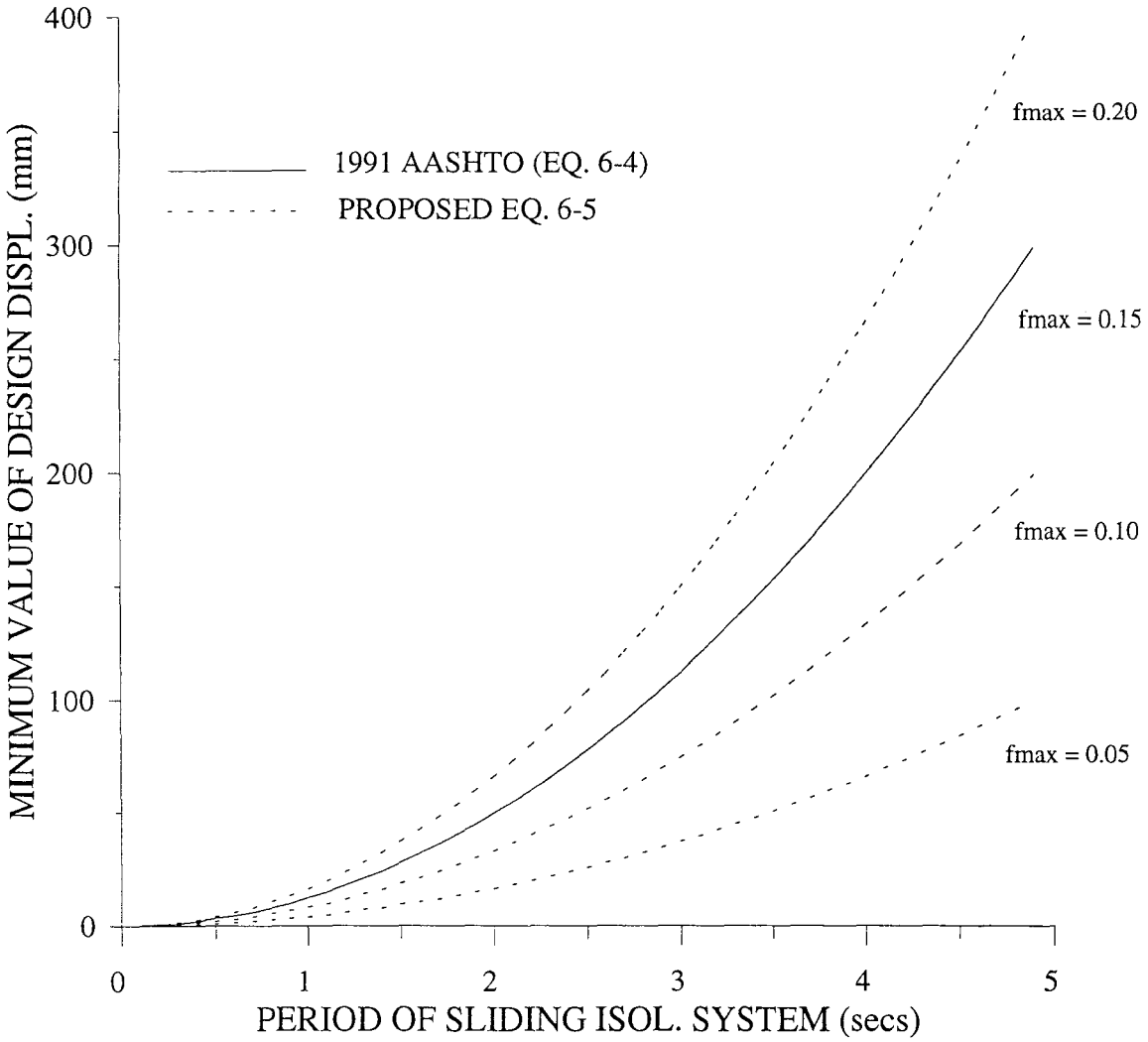

Figure 6-23 Minimum Value of Design Displacement as Function of Period of Sliding Isolation Systems. A System with Design Displacement Larger than the Minimum Value has Sufficient Restoring Force.

SECTION 7

ANALYTICAL PREDICTION OF RESPONSE

7.1 Introduction

Analytical techniques for predicting the dynamic response of sliding isolation systems are available (Mokha 1988, 1990b and 1991; Constantinou 1990a, 1990b, 1991a 1991b and 1993). These analytical techniques are employed herein in the prediction of the response of the tested bridge model. The analytical model accounts for the pier flexibility, pier top rotation, vertical motion effects on the properties of the sliding bearings, and nonlinear hysteretic characteristics of the restoring force devices.

7.2 Analytical Model

Figure 7-1 shows the analytical model in the case of the bridge with flexible piers. The degrees of freedom are selected to be the deck displacement with respect to the table, U_d , the pier displacements with respect to the table, U_{p1} and U_{p2} , and the pier rotations, ϕ_{p1} and ϕ_{p2} .

Each pier is modeled by a beam element of length L_i, moment of inertia I_i and modulus of elasticity E_i (i=1 or 2). The beam element is fixed to the table and connected at its top to a rigid block of height h , mass m_{pi} and mass moment of inertia about the center of mass (C.M.) I_{pi}. The center of mass is located at distance h_i from the bottom of the block. This block represents the pier top.

Free body diagrams of the deck and pier tops of the bridge model are shown in Figure 7-2. It should be noted that it was assumed that there is no transfer of moment between the deck and the supporting pier top. In reality, there is transfer of moment due to the rotational stiffness of the supporting disc of the sliding bearings. The equations of motion are derived by consideration of dynamic equilibrium of the deck and piers in the horizontal direction and of the piers in the rotational direction :

$$m_d(\ddot{U}_d + \ddot{U}_g) + F_{b1} + F_{b2} = 0 \tag{7-1}$$

$$m_{p1}(\ddot{U}_{p1} + \ddot{U}_g - h_1\ddot{\phi}_{p1}) + F_{p1} - F_{b1} = 0 \tag{7-2}$$

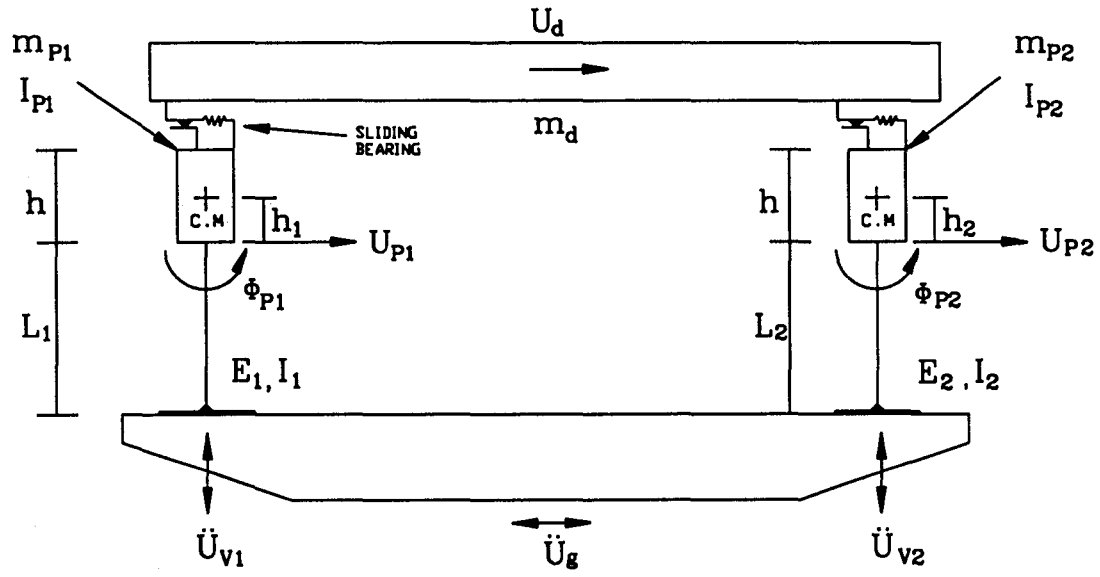

Figure 7-1 Longitudinal Direction Model of Isolated Bridge.

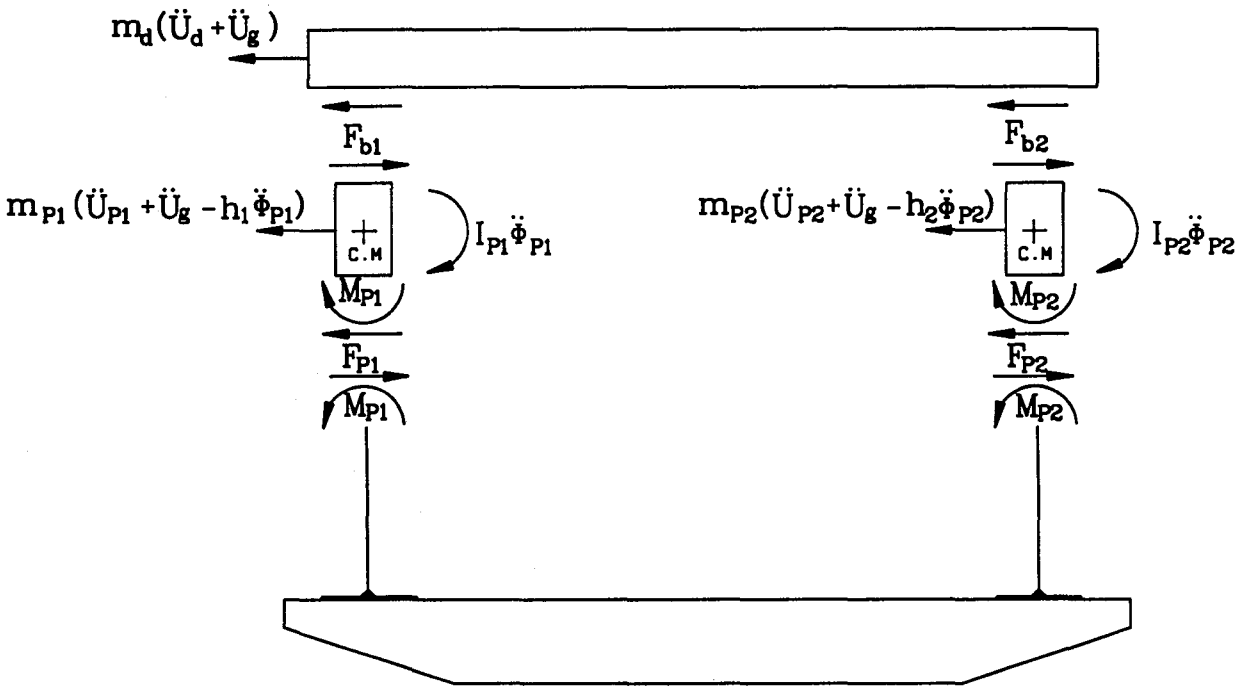

Figure 7-2 Free Body Diagram of Bridge Model.

$$m_{p2}(\ddot{U}_{p2}+\ddot{U}_g-h_2\ddot{\phi}_{p2})+F_{p2}-F_{b2}=0 \tag{7-3}$$

$$I_{p1}\ddot{\phi}_{p1}+M_{p1}+F_{p1}h_1+F_{b1}(h-h_1)=0 \tag{7-4}$$

$$I_{p2}\ddot{\phi}_{p2}+M_{p2}+F_{p2}h_2+F_{b2}(h-h_2)=0 \tag{7-5}$$

where $\ddot{U}_g$ is the horizontal table (ground) acceleration, F_{b1} and F_{b2} are the lateral forces in the isolation system (sliding bearings, restoring force devices and fluid dampers), and F_{pi} and M_{pi} are the lateral force and bending moment at the connection of the pier top to the end of the column:

$$\begin{Bmatrix} F_{pi} \\ M_{pi} \end{Bmatrix} = E_i I_i \begin{bmatrix} \frac{12}{L_i^3} & \frac{6}{L_i^2} \\ \frac{6}{L_i^2} & \frac{4}{L_i} \end{bmatrix} \begin{Bmatrix} U_{pi} \\ \phi_{pi} \end{Bmatrix} + \begin{bmatrix} C_{pi}^1 & 0 \\ 0 & C_{pi}^2 \end{bmatrix} \begin{Bmatrix} \dot{U}_{pi} \\ \dot{\phi}_{pi} \end{Bmatrix} \tag{7-6}$$

The first part of Equation (7-6) describes the elastic forces, whereas the second part is used to account for linear viscous energy dissipation in the piers.

Forces F_{bi} (i=1,2) include the component from friction in the sliding bearings and the component from the restoring force devices and the forces from the fluid dampers, when used. These forces are described as follows:

$$F_{bi}=\mu_i(\dot{U}_{bi})W_i^*Z_i+F_{ri}+nC_{0i}\dot{U}_{bi} \tag{7-7}$$

where μ_i = coefficient of sliding friction at pier i, W^*_i = normal load on two sliding interfaces at pier i, F_{ri} = restoring force from the rubber device at pier i, n= number of fluid dampers at pier i (either 0 or 2) and C_{0i} = damping constant of one fluid damper. Furthermore, U_{bi} is the bearing displacement at pier i:

$$U_{bi}=U_d-U_{pi}+h\phi_{pi} \tag{7-8}$$

The coefficient of sliding friction follows the relation (Constantinou 1990a, see also Section 3)

$$\mu_i=f_{\max i}-(f_{\max i}-f_{\min i})\exp(-a_i|\dot{U}_{bi}|) \tag{7-9}$$

with parameters f_{maxi}, f_{mini} and a_i (i=1,2) listed in Table 3-I. The normal load, W^*_i, is given by

$$W_i^*=W_i\left(1+\frac{\ddot{U}_{vi}}{g}\right) \tag{7-10}$$

where W_i = weight carried by pier i and $\ddot{U}_{vi}$ is the table (ground) vertical acceleration of pier i. Furthermore, variable Z_i in Equation (7-7) satisfies the following equation (Constantinou 1990a):

$$Y_i\dot{Z}_i + \gamma|\dot{U}_{bi}|Z_i|Z_i| + \beta\dot{U}_{bi}Z_i^2 - \dot{U}_{bi} = 0 \tag{7-11}$$

In this equation, Y_i= "yield" displacement (=0.25 mm) and β and γ = parameters satisfying the condition $\beta+\gamma=1$.

Force F_{ri} is described by (Demetriades 1992):

$$F_{ri} = F_{oi}(U_{bi}) + \frac{1}{2}F_{Di}(U_{bi})Z_{ri} \tag{7-12}$$

where $F_{oi}(U_{bi})$ is the displacement-dependent skeleton curve and $F_{Di}(U_{bi})$ is the also displacement-dependent difference between the loading and unloading branches of the hysteresis loop of a rubber restoring force device. F_{oi} and F_{Di} may be expressed as odd and even polynomial functions of displacement, respectively :

$$F_{oi} = \sum_{n=1,3,5,\ldots}^{N} A_n U_{bi}^n \tag{7-13}$$

$$F_{Di} = \sum_{m=0,2,4,\ldots}^{M} B_m U_{bi}^m \tag{7-14}$$

In Equation (7-12), Z_{ri} is a new hysteretic variable which satisfies Equation (7-11) with $\beta+\gamma=1$ and Y_{ri} being a new "yield" displacement.

Table 7-I presents values of parameters in the model of the rubber device No. 2 (Equations 7-12 to 7-14). The parameters were determined by regression analysis of experimental results over the entire range of displacements (0 to 50 mm). While the number of parameters is large, the model indeed captures very well the behavior of the device over the tested range of displacements. Figure 7-3 compares experimental loops of the medium stiffness device (Type No. 2) to the predictions of the calibrated model of Equations (7-12) to (7-14).

It should be noted that when displacements are below the displacement at which stiffening occurs (about 35 mm), the device may be modeled by a linear spring with effective stiffness being the one given in Table 3-III. The hysteretic behavior of the device is not significant since its characteristic

Table 7-I Parameters in Model of Rubber Restoring Force Device No. 2 (Equations 7-12 to 7-14)

INDEX n	PARAMETER A_n (kN/(mm)^n)	INDEX m	PARAMETER B_m (kN/(mm)^m)
1	0.16785	0	0.88960
3	-0.42315×10^{-3}	2	-0.12536×10^{-2}
5	0.15806×10^{-5}	4	0.29312×10^{-5}
7	-0.36645×10^{-8}	6	-0.16564×10^{-8}
9	0.51239×10^{-11}	8	0.43320×10^{-12}
11	-0.4341×10^{-14}	≥ 10	0
13	0.22194×10^{-17}		
15	-0.64897×10^{-21}		
17	0.95316×10^{-25}		
19	-0.48472×10^{-29}		
≥ 21	0		

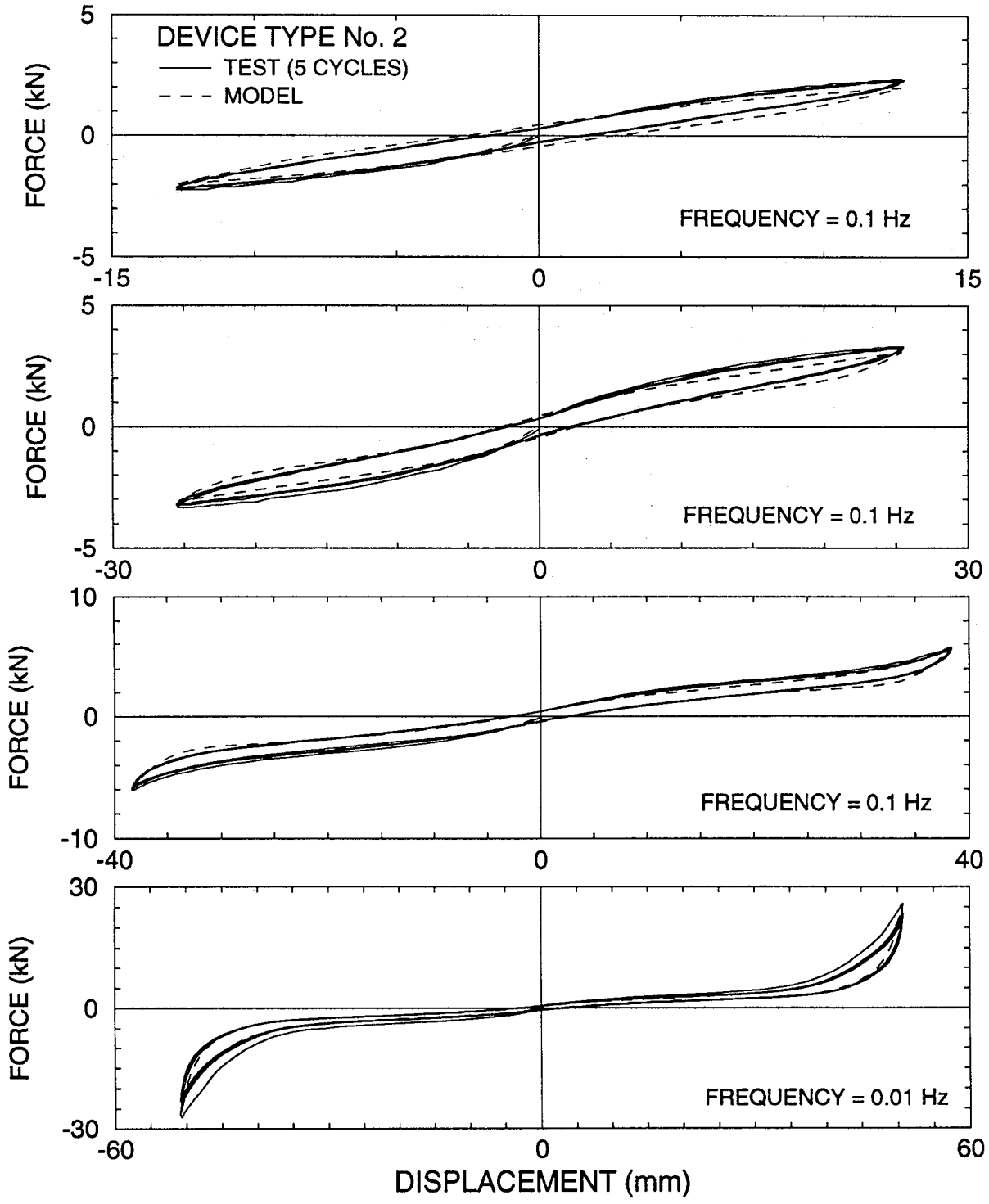

Figure 7-3 **Comparison of Experimental and Analytical Force-Displacement Loops of Rubber Device. Note that the Behavior of the Device is Nearly Frequency Independent (see also Figure 3-8).**

strength is between 0.01 and 0.02 times the deck weight, thus very small in comparison to the friction coefficient in the medium and high friction cases.

7.3 Comparison of Analytical and Experimental Results

Solution of the governing Equations (7-1) through (7-14) was obtained by first reducing the equations to a system of first order differential equations and then numerically integrating the system by using an adaptive integration scheme with truncation error control (Gear 1971). In order to obtain accurate predictions of the experimental response, the initial conditions were carefully specified. The initial conditions included the initial displacement (that is, permanent displacement from previous test) and the associated friction force. The latter required the specification of the initial value of Z_i (Equations 7-7 to 7-14). Since at start $F_{bi} = 0$, it follows that

$$Z_i = \frac{-F_{oi}(U_o)}{f_{\min i} W_i} \tag{7-15}$$

where U_o = initial displacement.

The data used in the analytical model were : deck weight $m_d g$ = 143 kN, pier weight $m_{pi} g$ = 8.9 kN, $L_1 = L_2$ = 1600 mm, $h_1 = h_2$ = 98 mm, h = 413 mm, $I_{p1} = I_{p2}$ = 38.22 kN s^2 mm, $E_1 = E_2$ = 200000 MPa, $I_1 = I_2$ = 3.022x10^{-5} m^4 (2 AISC tubes Ts 6x6x5/16). Based on these data the fundamental period of each pier, in its cantilever position, was calculated to be 0.092s. This is in close agreement with the experimentally determined value of 0.096s. The second mode of the cantilever pier had a calculated frequency of 102 Hz. This frequency could neither be detected in the tests nor have any significance in the analysis.

Damping in the piers was described by the second term in Equation (7-6). The fact that the calculated second frequency of the cantilever pier is much larger than the first frequency indicates that the second mode of the pier may be neglected. Accordingly, constant C^2_{pi} in Equation (7-6) was set equal to zero and constant C^1_{pi} was assigned a value equal to 0.0062 kNs/mm. Based on this value, the damping ratio in the fundamental mode of the cantilever pier was calculated to be 5% of critical. This is consisted with the experimental data.

Comparisons of analytical and experimental results are presented in Figures 7-4 to 7-12 in the case of tests with only horizontal excitation. The analyzed systems were the high friction-medium stiffness isolation system (T1-No. 2) and the medium friction-medium stiffness isolation system (T2-No. 2) without and with fluid viscous dampers. The analysis was based on Equations (7-1) to (7-14) but with $\ddot{U}_{vi}$ set equal to zero (vertical acceleration effects were neglected). Evidently, the analytical results are in very good agreement with the experimental results.

Figures 7-13 to 7-16 compare experimental and analytical results in the tests with combined horizontal-vertical El Centro 200% and Taft 400% inputs of the T1-No. 2 and T2-No. 2 systems. The analysis accounted for the vertical acceleration effects. The analysis captures correctly the wavy form of the bearing shear force-displacement loops and the two sets of results appear to be in good agreement.

Finally, Figures 7-17 to 7-19 compare experimental results to analytical results obtained with a simple model for the rubber restoring force devices. Rather than using Equations (7-12) to (7-14), the restoring force in each rubber device was described by

$$F_{ri} = K_{ri} U_{bi} + C_{ri} \dot{U}_{bi} \qquad (7\text{-}16)$$

where K_{ri} = 112.30 kN/m and C_{ri} = 2.86 kN-s/m for the No. 2 device. These values correspond to period of vibration of 1.60 secs and damping ratio of 0.05 in accordance with the data of Table 3-III. The predictions of this simple linear-viscous model for the rubber devices are nearly as good as those of the considerably more complicated model of Equations (7-12) to (7-14). Of course, the model of Equation (7-16) is valid when the displacement restrainer is not activated.

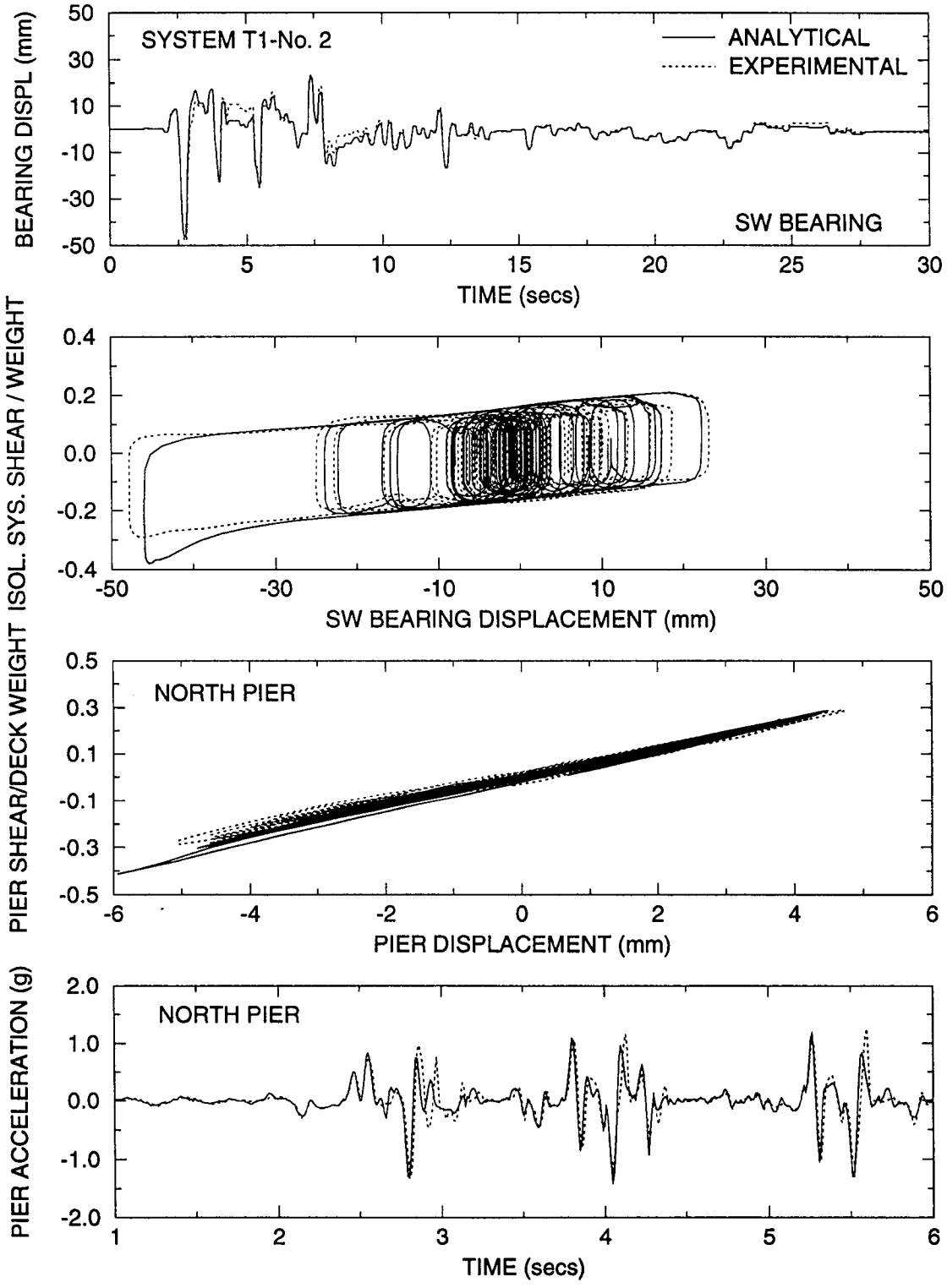

Figure 7-4 **Comparison of Experimental and Analytical Results in Test with Taft N21E 500% Input (Test No.IRDRUN45). Analysis Performed without the Effect of Vertical Pier Acceleration ($\ddot{U}_{vi}$ =0).**

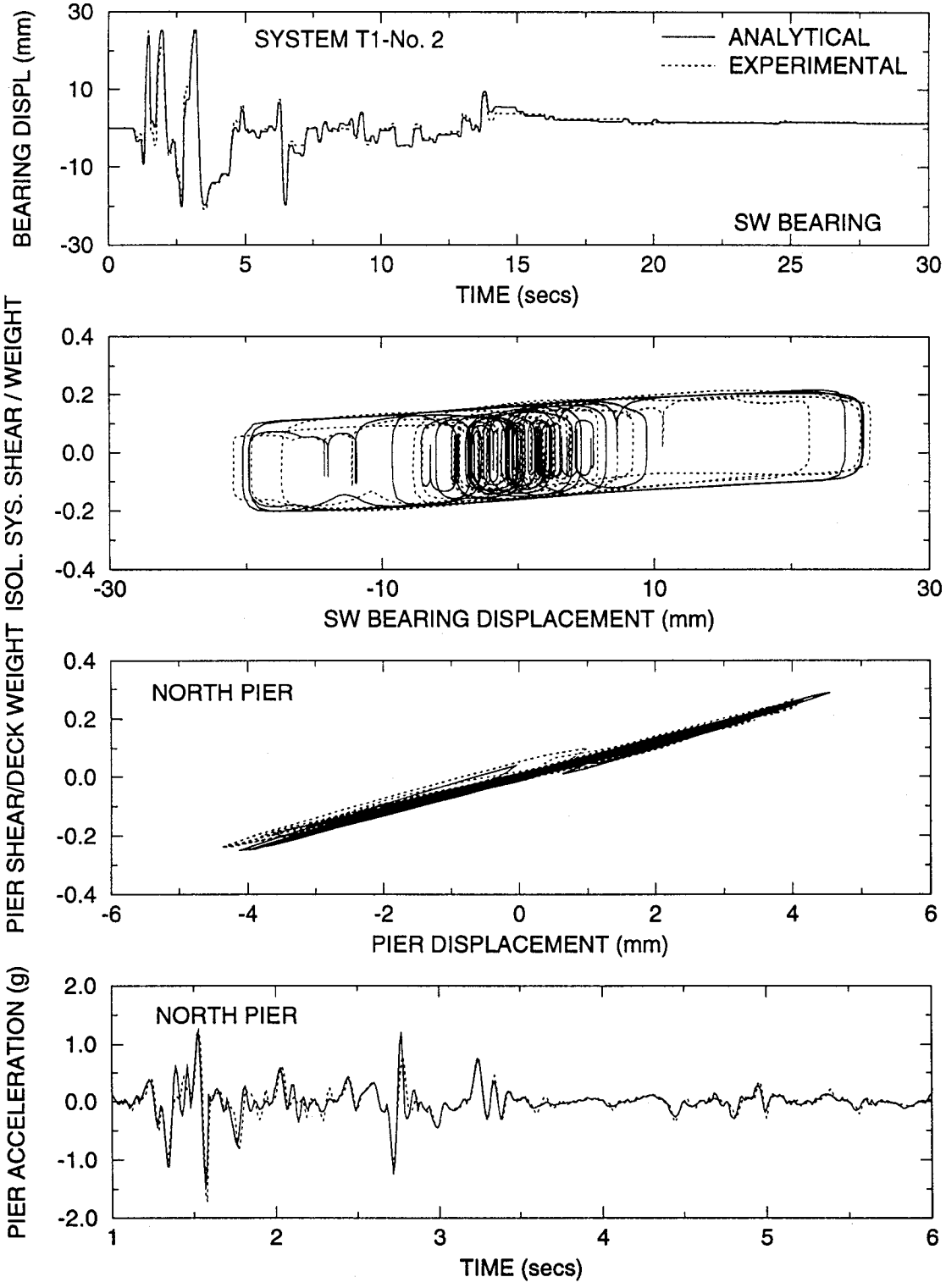

Figure 7-5 **Comparison of Experimental and Analytical Results in Test with El Centro 200% Input (Test No.IRDRUN47). Analysis Performed without the Effect of Vertical Pier Acceleration ($\ddot{U}_{vi}$ =0).**

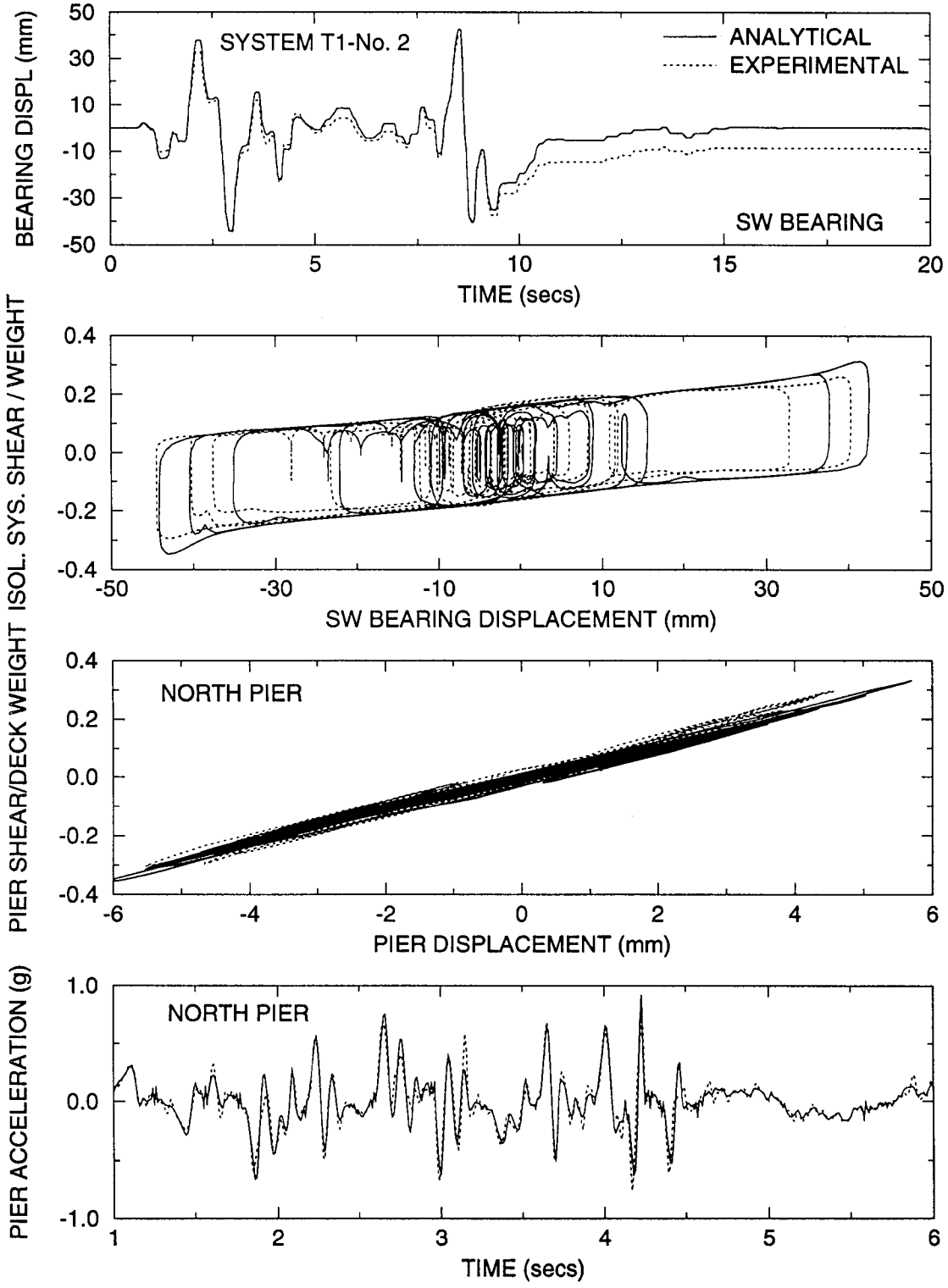

Figure 7-6 **Comparison of Experimental and Analytical Results in Test with CalTrans 0.6g A2 100% Input (Test No.IRDRUN59). Analysis Performed without the Effect of Vertical Pier Acceleration ($\ddot{U}_{vi}$ =0).**

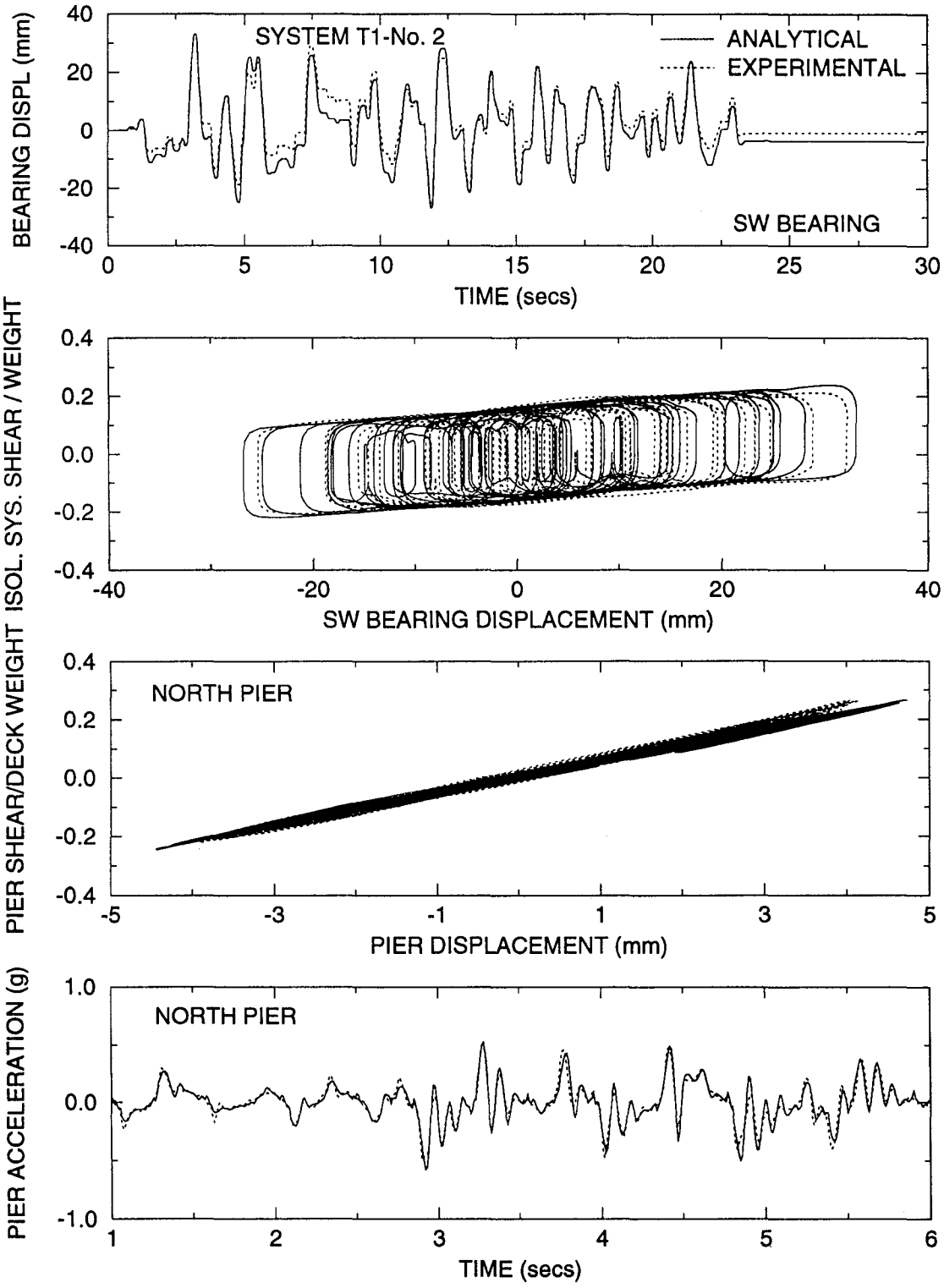

Figure 7-7 **Comparison of Experimental and Analytical Results in Test with Japanese Level 2 G.C.3 75% Input (Test No.IRDRUN62). Analysis Performed without the Effect of Vertical Pier Acceleration ($\ddot{U}_{vi}$=0).**

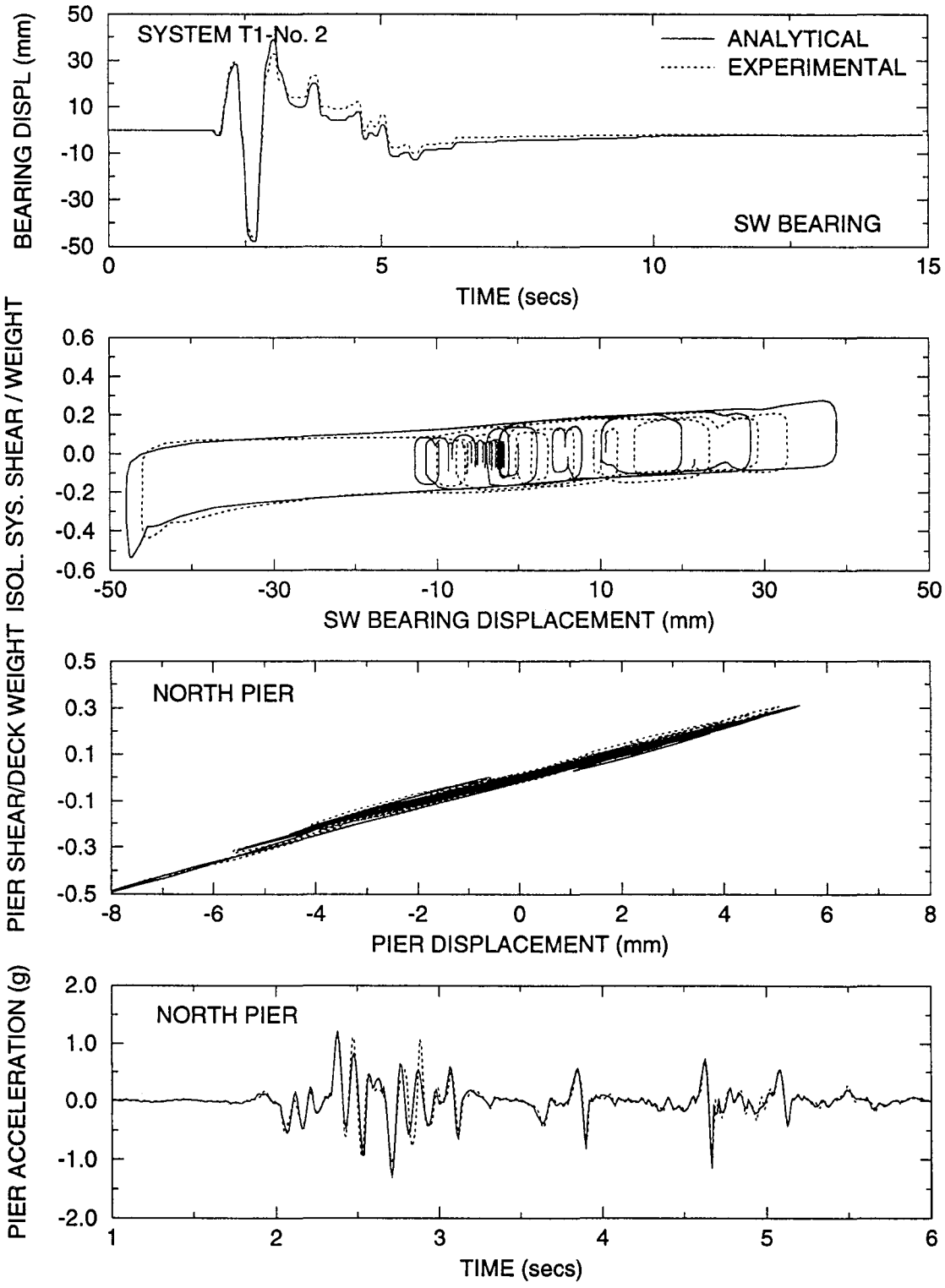

Figure 7-8 **Comparison of Experimental and Analytical Results in Test with Pacoima S16E 75% Input (Test No.IRDRUN53). Analysis Performed without the Effect of Vertical Pier Acceleration ($\ddot{U}_{vi}$ =0).**

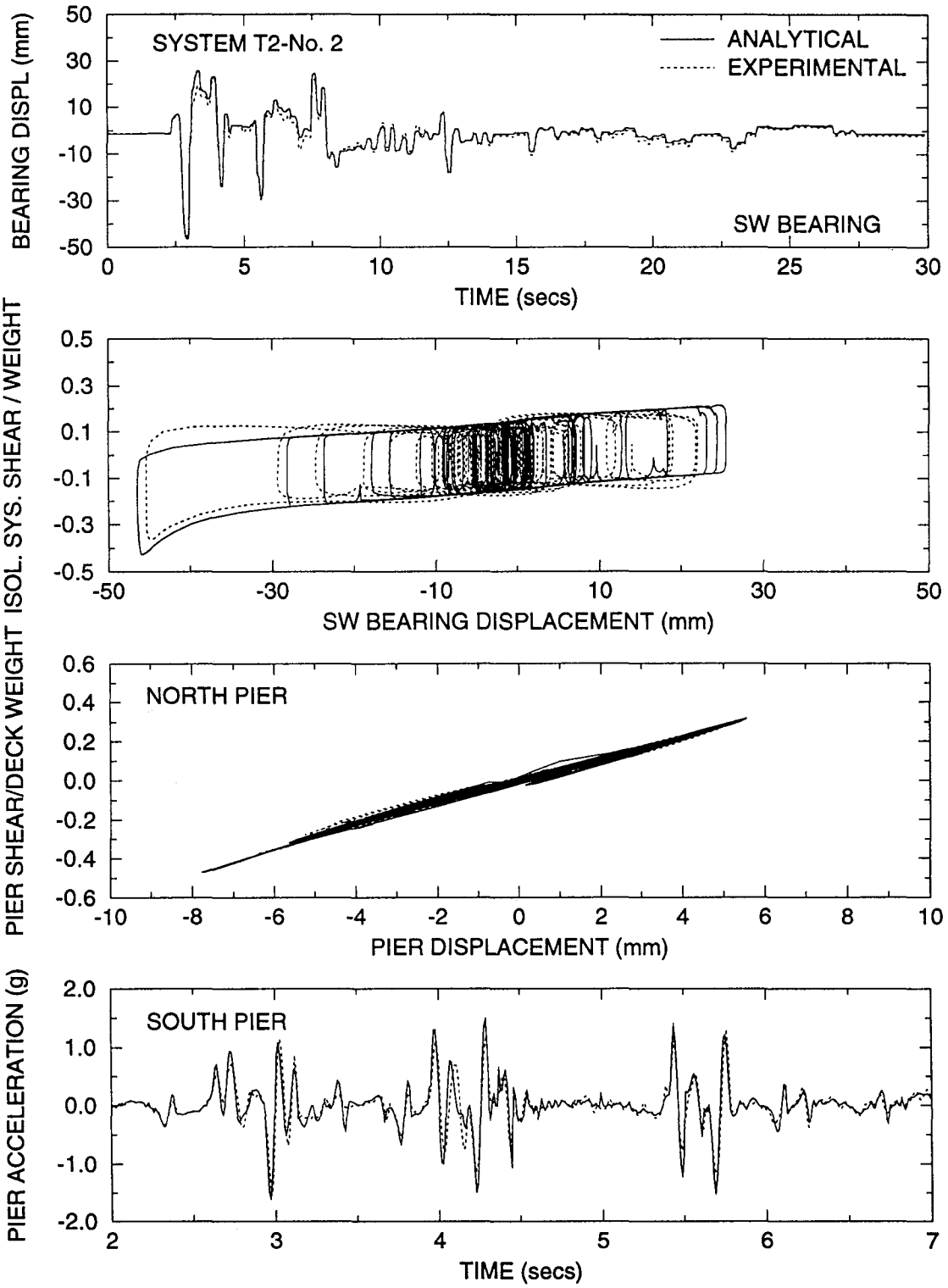

Figure 7-9 **Comparison of Experimental and Analytical Results in Test with Taft N21E 500% Input (Test No.RD2RUN46). Analysis Performed without the Effect of Vertical Pier Acceleration ($\ddot{U}_{vi}$=0). In this Test only the South Pier Displacement Restrainer was Partially Activated.**

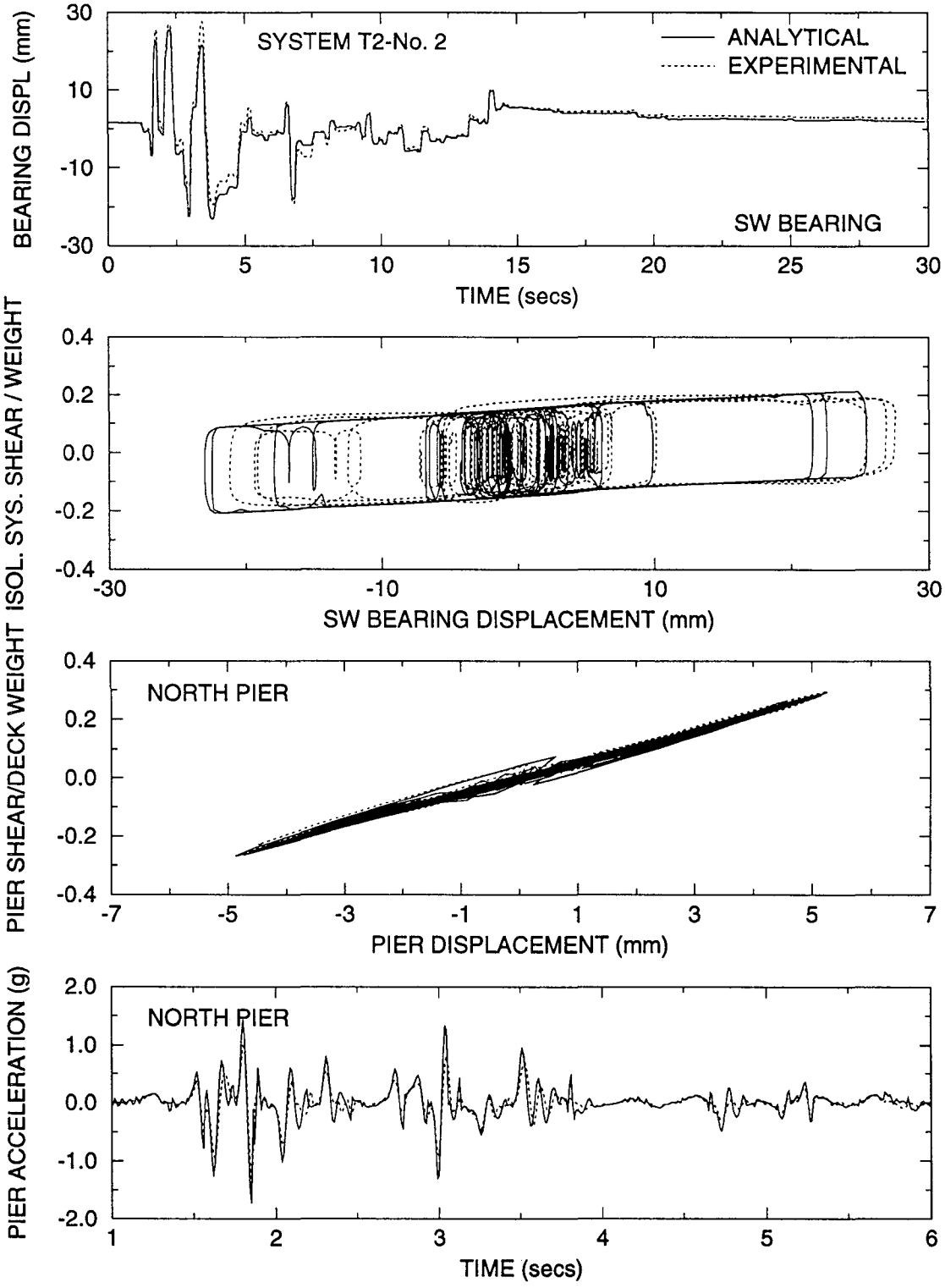

Figure 7-10 **Comparison of Experimental and Analytical Results in Test with El Centro S00E 200% Input (Test No.RD2RUN36). Analysis Performed without the Effect of Vertical Pier Acceleration ($\ddot{U}_{vi}$=0).**

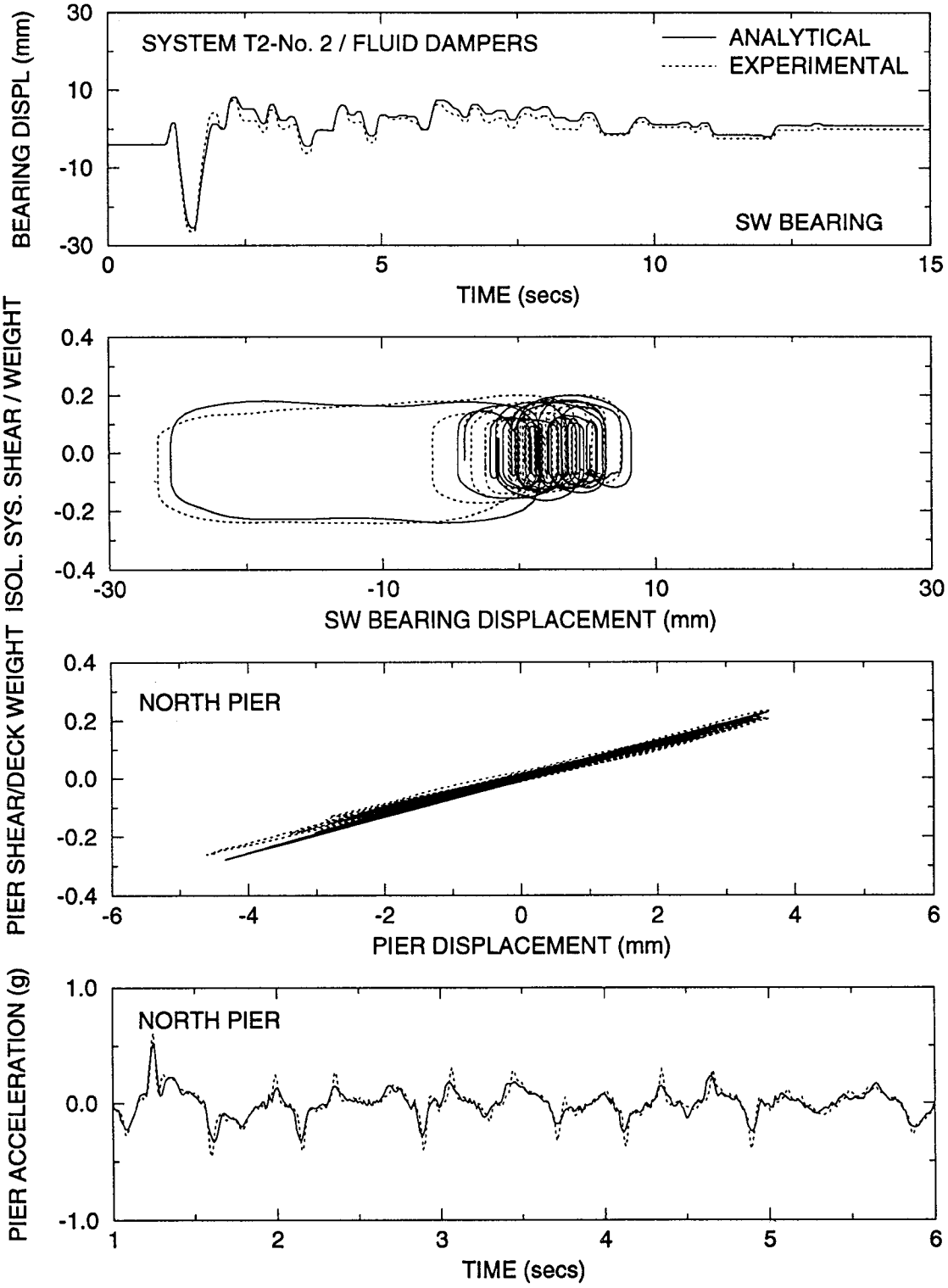

Figure 7-11 **Comparison of Experimental and Analytical Results in Test with Japanese Level 2 G.C. 1 100% Input (Test No.DRDRUN04). Analysis Performed without the Effect of Vertical Pier Acceleration ($\ddot{U}_{vi}$=0). System with Fluid Dampers.**

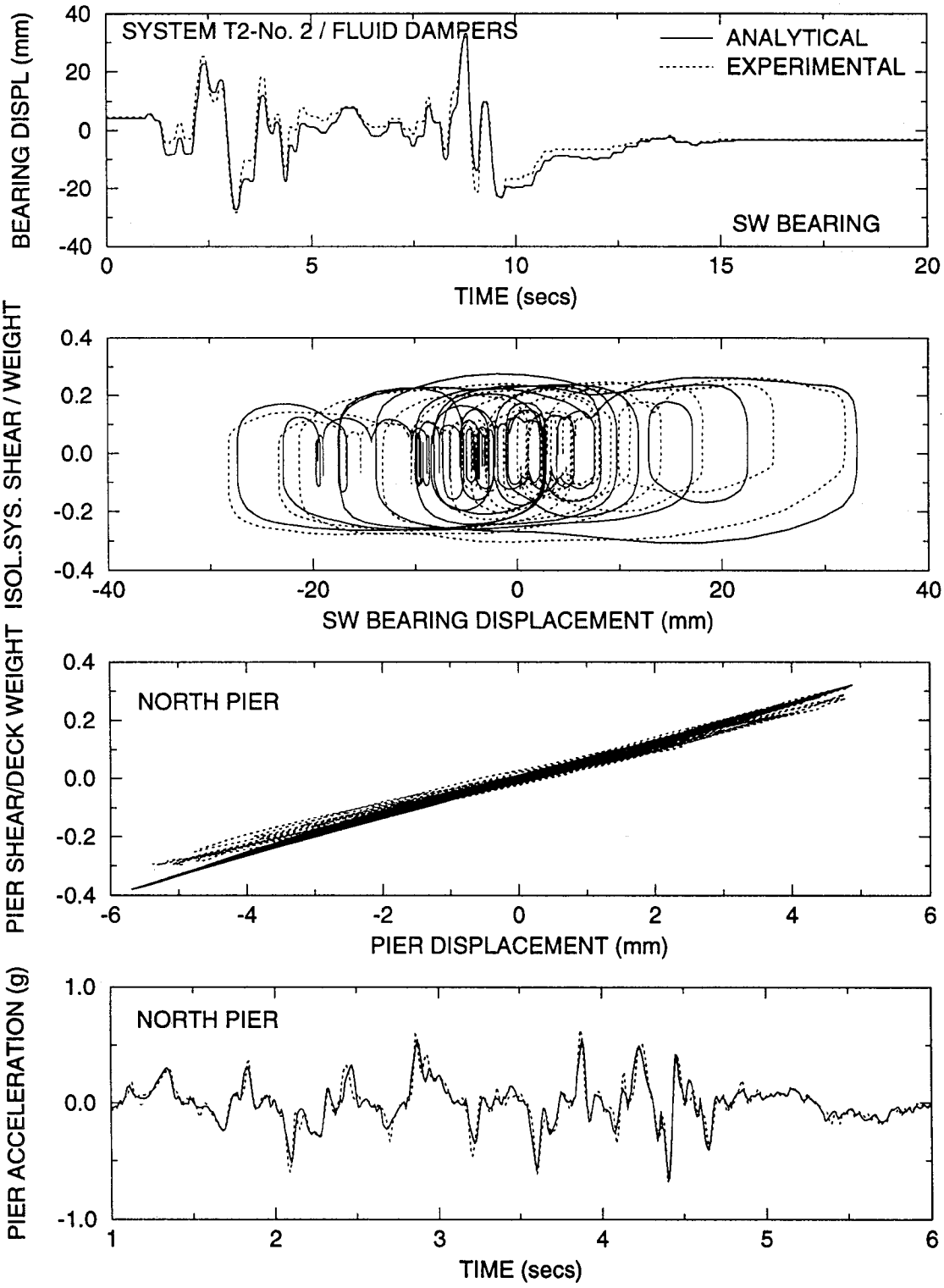

Figure 7-12 **Comparison of Experimental and Analytical Results in Test with CalTrans 0.6g A2 100% Input (Test No.DRDRUN02). Analysis Performed without the Effect of Vertical Pier Acceleration ($\ddot{U}_{vi}$ =0). System with Fluid Dampers.**

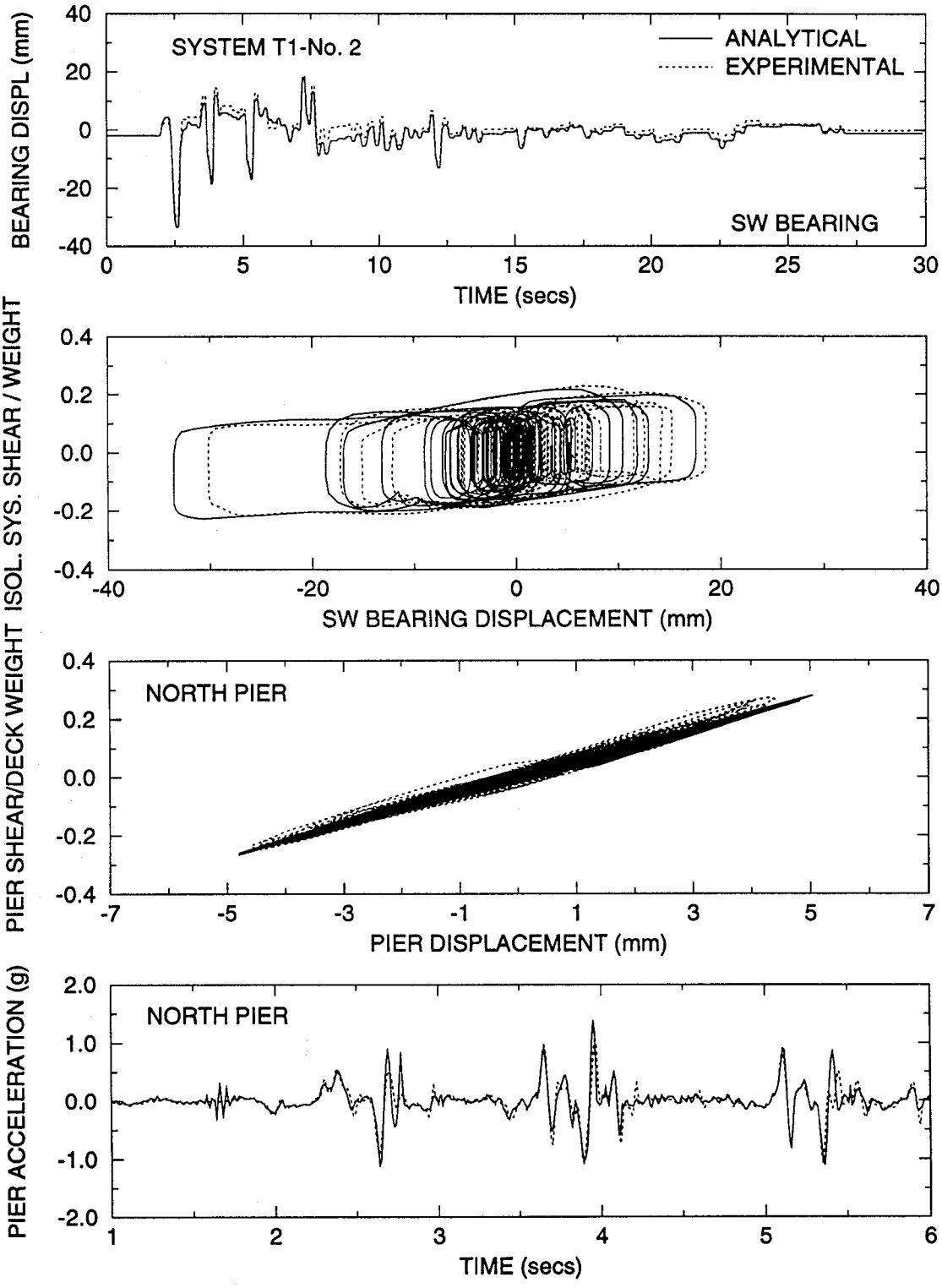

Figure 7-13 Comparison of Experimental and Analytical Results in Test with Taft N21E plus Vertical 400% Input (Test No.IRDRUN63). Analysis Performed with the Effects of Vertical Pier Acceleration.

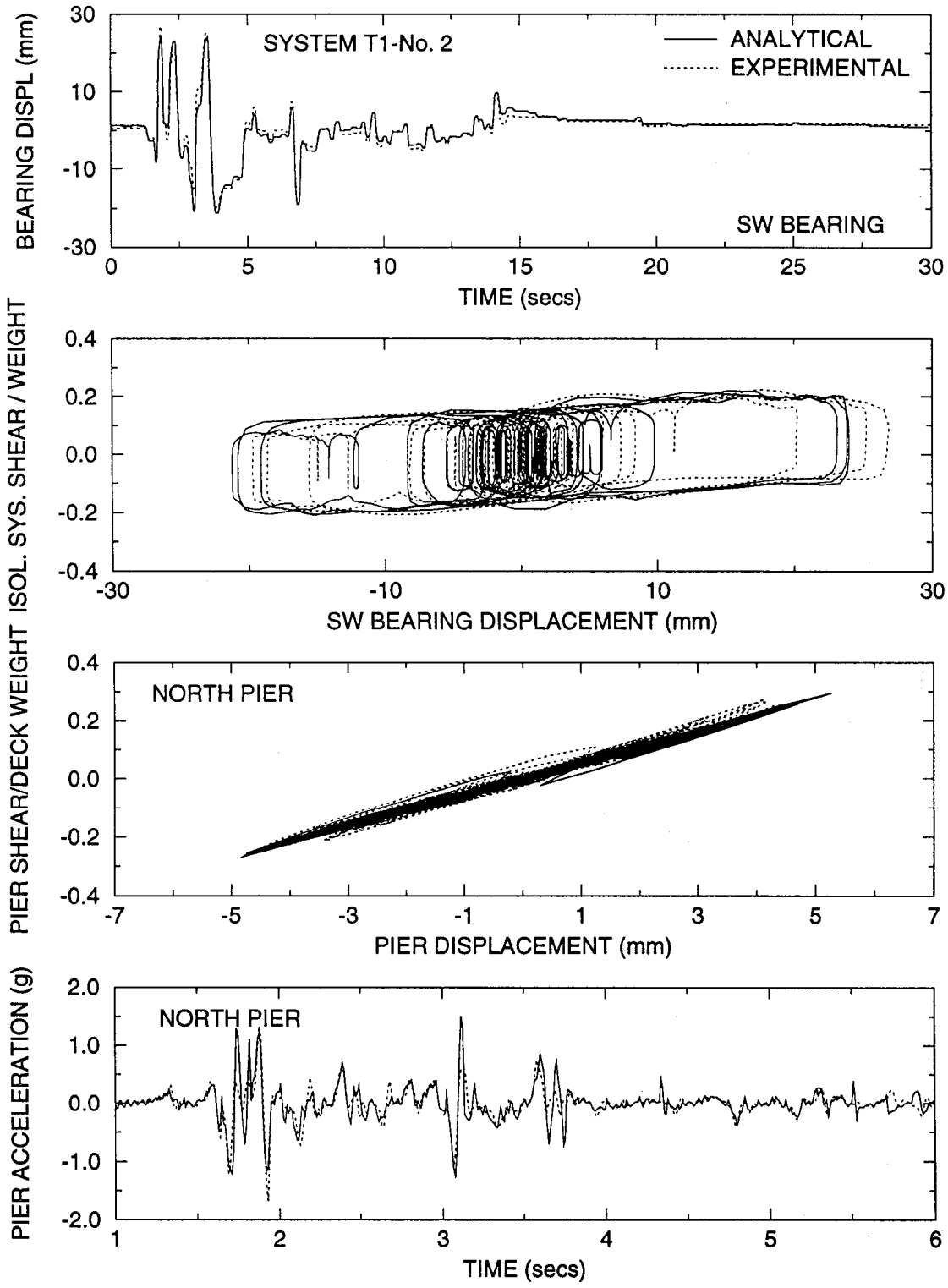

Figure 7-14 **Comparison of Experimental and Analytical Results in Test with El Centro S00E plus Vertical 200% Input (Test No.IRDRUN65). Analysis Performed with the Effects of Vertical Pier Acceleration.**

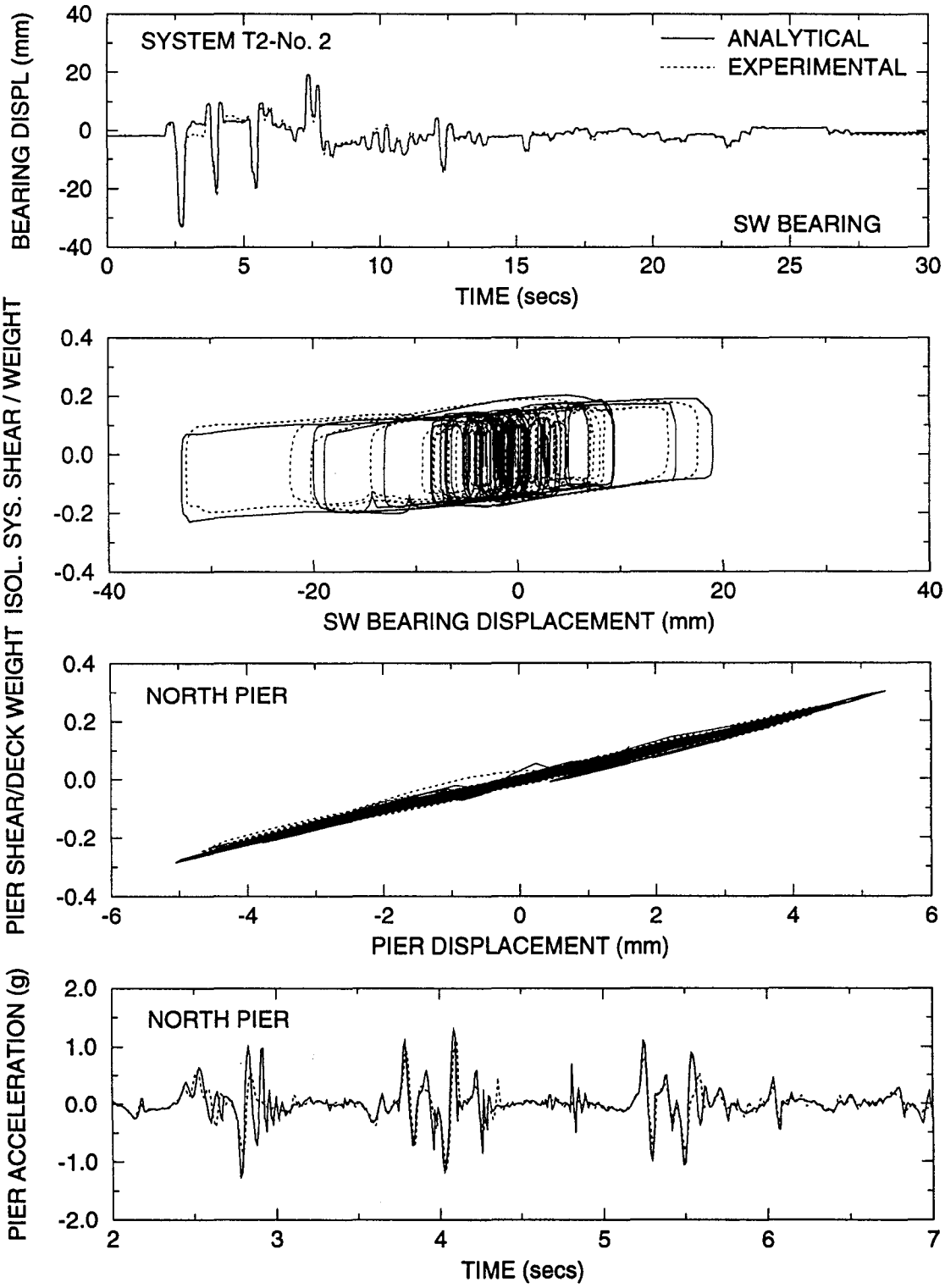

Figure 7-15 Comparison of Experimental and Analytical Results in Test with Taft N21E plus Vertical 400% Input (Test No.RD2RUN66). Analysis Performed with the Effects of Vertical Pier Acceleration.

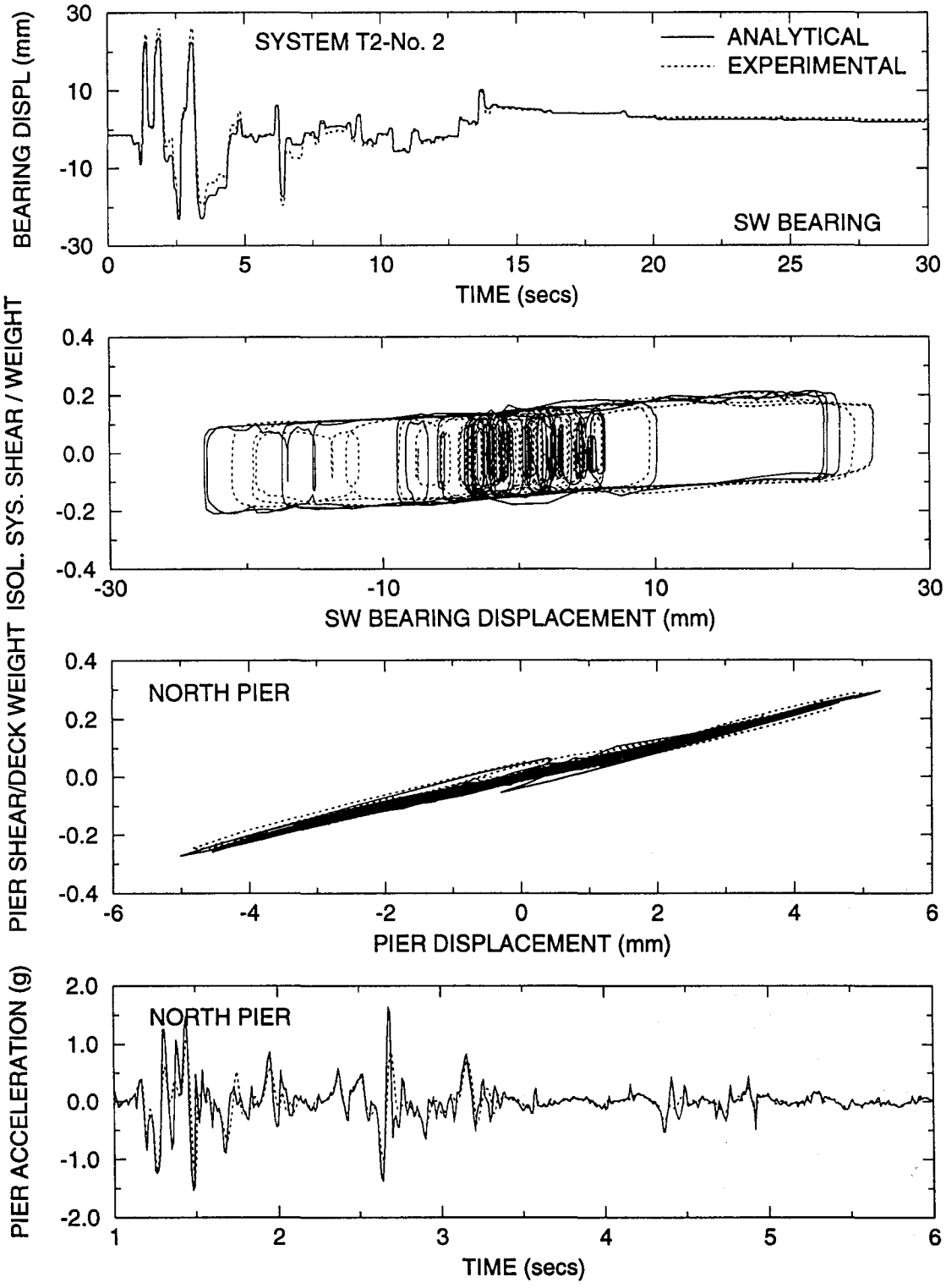

Figure 7-16 Comparison of Experimental and Analytical Results in Test with El Centro S00E plus Vertical 200% Input (Test No.RD2RUN67). Analysis Performed with the Effects of Vertical Pier Acceleration.

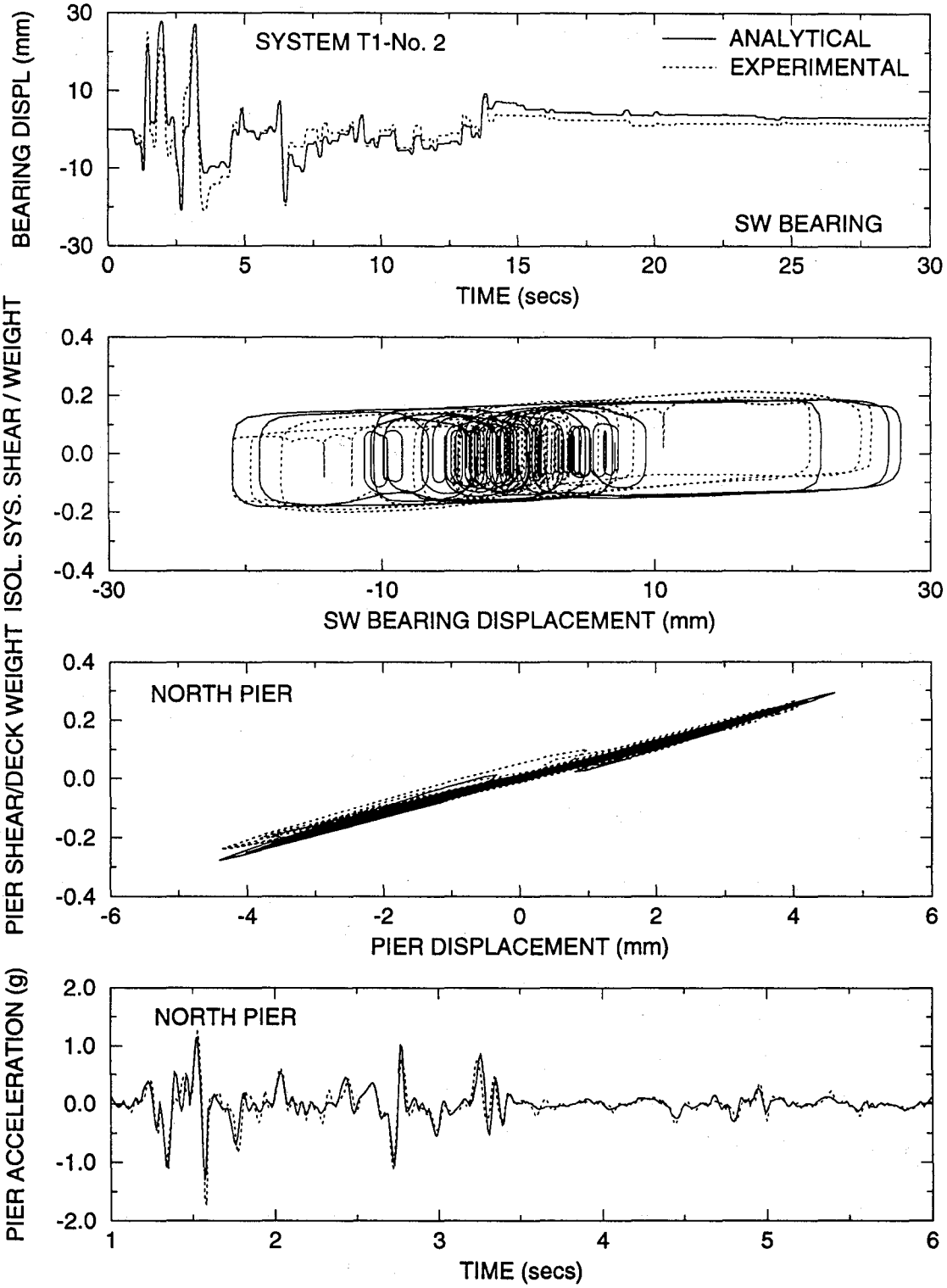

Figure 7-17 **Comparison of Experimental and Analytical Results in Test with El Centro S00E 200% Input (Test No.IRDRUN47). Analysis Performed without the Effects of Vertical Pier Acceleration and Utilizing a Simple Linear-Viscous Model for the Rubber Devices.**

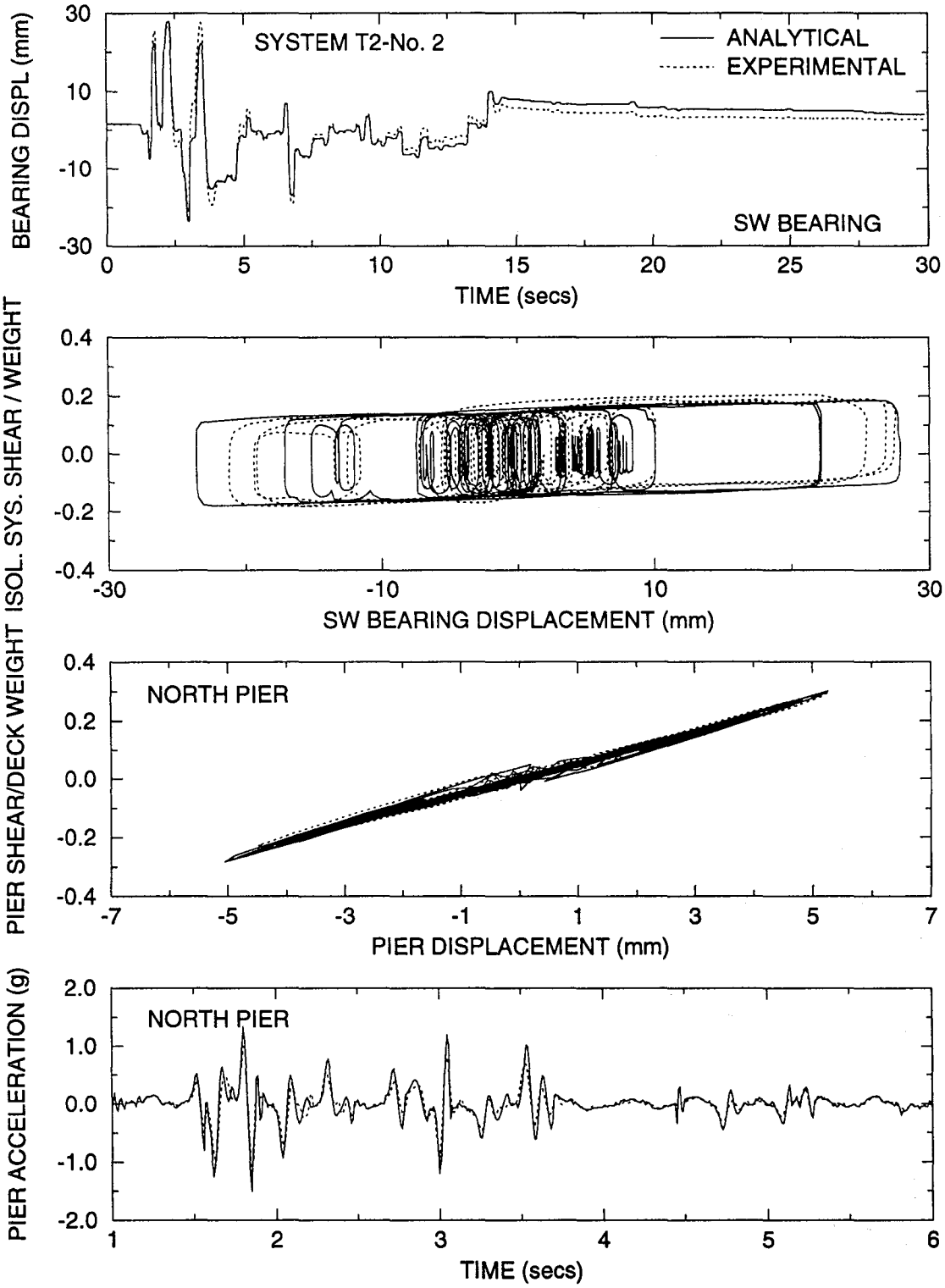

Figure 7-18 **Comparison of Experimental and Analytical Results in Test with Japanese Level 2 G.C. 3 75% Input (Test No.IRDRUN62). Analysis Performed without the Effects of Vertical Pier Acceleration and Utilizing a Simple Linear-Viscous Model for the Rubber Devices.**

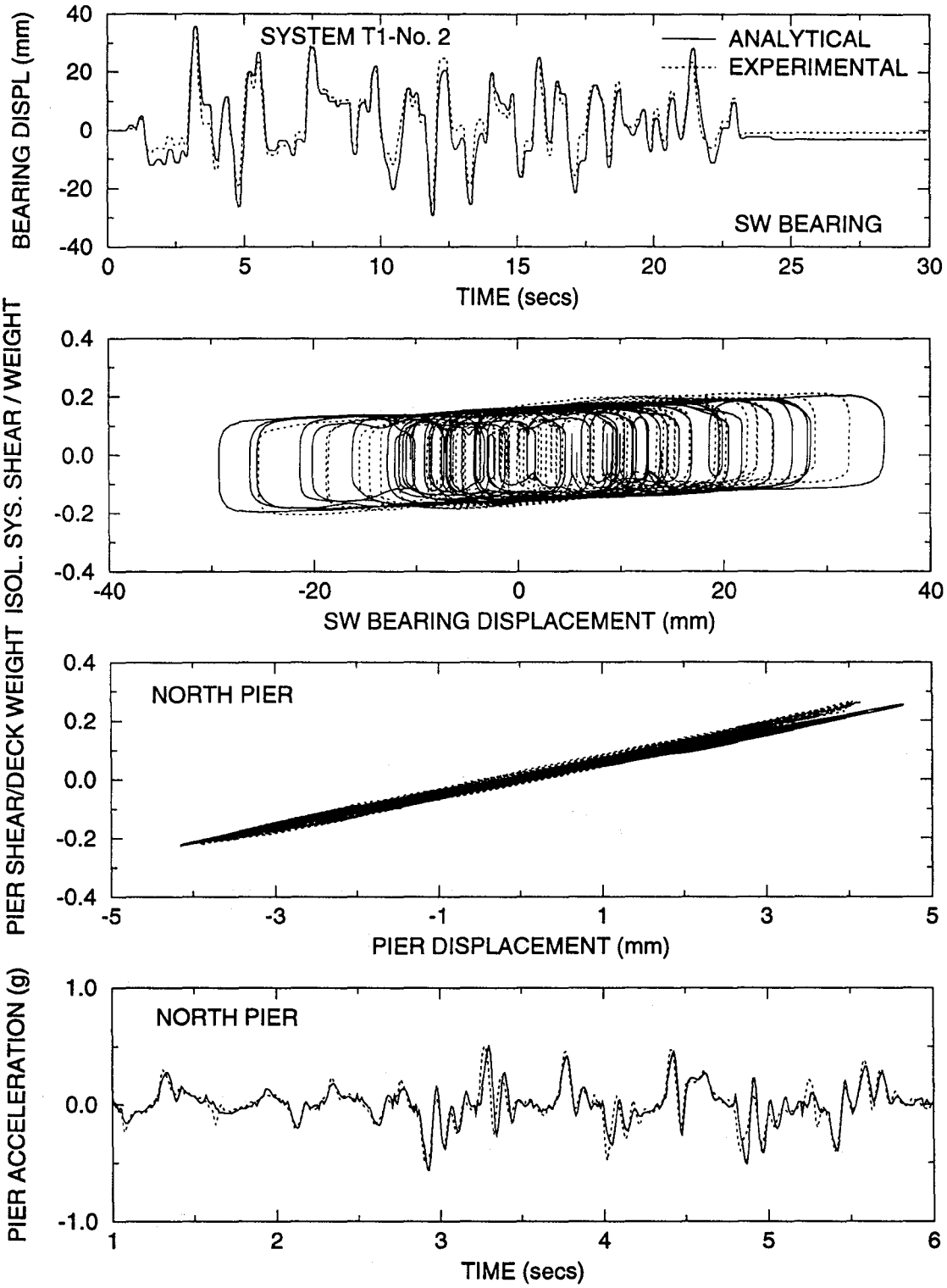

Figure 7-19 **Comparison of Experimental and Analytical Results in Test with El Centro S00E 200% Input (Test No.RD2RUN36). Analysis Performed without the Effects of Vertical Pier Acceleration and Utilizing a Simple Linear-Viscous Model for the Rubber Devices.**

SECTION 8

NONLINEAR RESPONSE SPECTRA OF SLIDING ISOLATION SYSTEMS

8.1 Introduction

The design of bridge seismic isolation systems requires that preliminary estimates of the response of the isolated bridge be made. For example, the 1991 AASHTO provides prescriptive formulae which can be used for preliminary design.

Alternatively, non-linear response spectra may be developed, which depict the response of isolated bridges for a wide range of design parameters. An advantage of the use of such spectra is that they provide a direct feel of the sensitivity of the response on the various design parameters. Constantinou, 1991a presented such non-linear response spectra of sliding isolation systems for the CalTrans motions.

Similar spectra are presented in this section for the Japanese bridge design motions. The presented spectra are for two simple models, of which one completely neglects the effects of pier flexibility and the other accounts for the pier flexibility in a way that is representative of the behavior of isolated multiple-span bridges. Furthermore, the models do not account for the effect of displacement restrainers in either the restoring force devices, the viscous dampers or the sliding bearings. Rather, it is assumed that the isolation system has sufficient displacement capacity to accommodate the demand without engaging any restraint.

The spectra represent a useful tool in the preliminary design of sliding bridge isolation systems. They are not intended to replace non-linear dynamic analysis of the isolated bridge, if such analysis is required by applicable specifications.

8.2 Simplified Deck Model

In the simplified deck model, the isolated bridge is represented by a single-degree-of-freedom system with the deck and piers assumed to be infinitely rigid. This model is representative of single-span bridges, in which the abutments may be presumed to be very stiff.

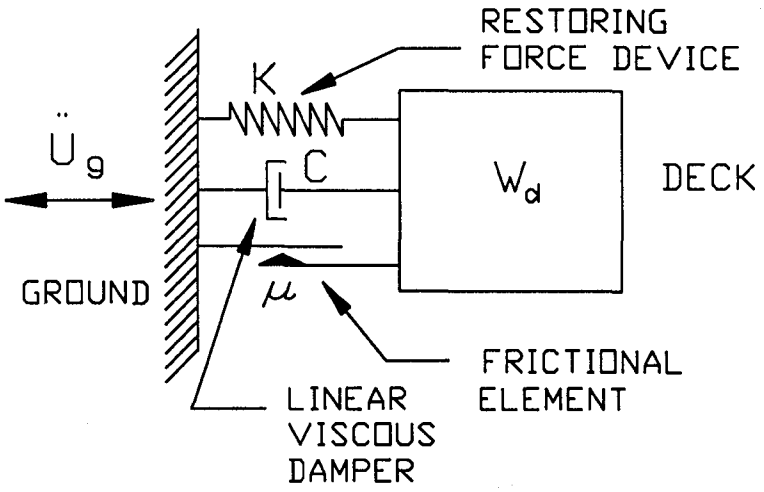

Figure 8-1 Simplified Deck Model.

The simplified deck model is illustrated in Figure 8-1. It is a frictional oscillator with viscous damping. In terms of the relative deck displacement u, the equation of motion is

$$\ddot{u}+\frac{4\pi\xi}{T}\dot{u}+\mu(\dot{u})gZ+\frac{4\pi^2}{T^2}u=-\ddot{u}_g \tag{8-1}$$

where T is the period, ξ is the viscous damping ratio, Z is a variable described by Equation (7-11) and μ is the velocity dependent coefficient of friction, described by Equation (3-1). It should be noted that T and ξ are defined by

$$T=2\pi\left(\frac{W_d}{Kg}\right)^{1/2} \tag{8-2}$$

$$\xi=\frac{CgT}{4\pi W_d} \tag{8-3}$$

The peak response of the simplified deck model to the Japanese bridge design motions has been calculated for values of period, T, in the range of 1.5 to 4.0 secs, values of damping ratio, ξ, of 0, 0.2, 0.4 and 0.5 and friction coefficient, f_{max}, values of 0.05, 0.1 and 0.15. The minimum value of friction, f_{min}, was assumed equal to $f_{max}/3$, with parameter a (see Equation 3-1) equal

to 23 sec/m. The results are presented in Appendix B. They are presented in terms of the shear force transmitted through the isolation interface and the isolation system displacement.

8.3 Pier-Deck Model

This model is representative of multiple-span isolated bridges. Depicted in Figure 8-2, the model consists of a rigid deck on the top of a flexible pier with the isolation system placed between the deck and the pier top. This model allows for the evaluation of the effects of the pier flexibility.

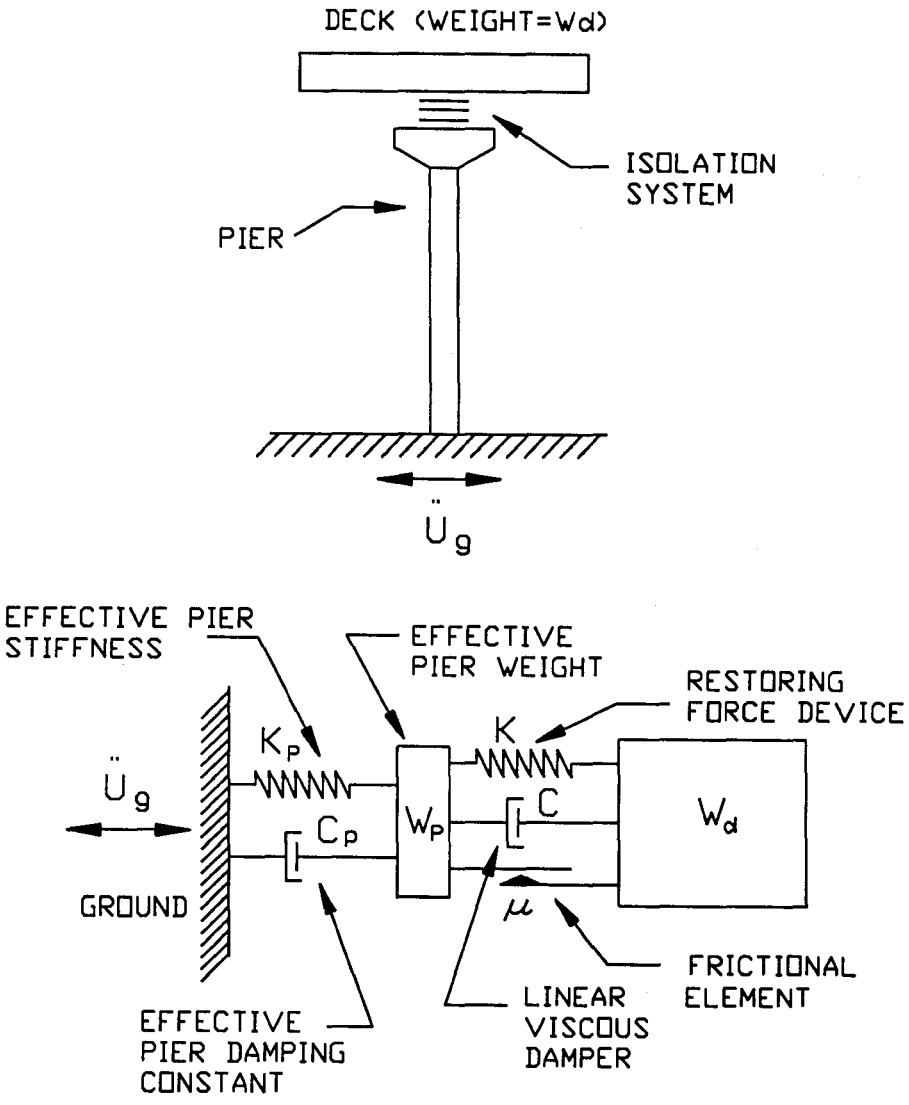

Figure 8-2 Pier-Deck Model and Mathematical Representation.

The parameters in the mathematical representation of the pier-deck model are the coefficient of friction, μ, the isolation system period, T (Equation 8-2), the isolation system damping ratio, ξ (Equation 8-3), the ratio of effective pier weight to deck weight, W_p/W_d, and the dynamic characteristics of the pier. These characteristics are expressed in terms of the effective period and damping ratio of the free standing pier :

$$T_p = 2\pi\left(\frac{W_p}{K_p g}\right)^{1/2} \tag{8-4}$$

$$\xi_p = \frac{C_p g T_p}{4\pi W_p} \tag{8-5}$$

The peak response of the pier-deck model to the Japanese Level 2 bridge motions has been calculated for the following range of parameters : ξ_p = 0.05, T_p= 0, 0.2, 0.4 and 0.8 secs, ξ = 0, 0.2, and 0.40, T = 1.5 to 4.0 secs, ratio W_p/W_d = 1/5, 1/10, 1/20 and coefficient of friction μ = f_{max}= 0.1 and 0.15. In the analyses, the velocity dependence of friction has been disregarded. This did not have any effect on the calculated peak response since the velocity of sliding was large enough to mobilize the peak value of friction, f_{max}.

The results, in terms of the peak bearing displacement with respect to the pier, the peak shear force transmitted through the isolation system and the pier shear force, are presented in Appendix C. It should be noted that the pier shear force differs from the isolation system force by the inertial force of the pier top. Furthermore, the case of $T_p = 0$ represents an infinitely stiff pier and the results are identical to those of the simplified deck model.

8.4 Discussion

The usefulness of the response spectra of sliding isolation systems is demonstrated herein with an example. Figure 8-3 shows the response of the pier-deck model for the Japanese level 2, ground condition 2 input. The values of the model parameters T_p, ξ and W_p / W_d are approximately those of one of the tested configurations (flexible piers without fluid dampers). The results in Figure 8-3 were extracted from the spectra of Appendix C and enhanced by additional data over the range of 0.05 to 0.15 for the coefficient of friction f_{max}.

Requiring that the pier shear force is less than or equal to 0.3 times the carried weight (minimum design force in Japan), the spectra call for the use of a value of T in the range of 3 to 4 secs. Apparently, a value $T = 3$ secs results in lower bearing displacement. Thus, a preliminary design may be selected to have $T = 3$ secs and $f_{max} = 0.10$ with a bearing displacement of less than 300 mm. Of particular importance is to note in Figure 8-3 the insensitivity of the response of the system with $T = 3$ secs to variations of the coefficient of friction. Even a 50% increase of friction (from 0.1 to 0.15) results in only minor increase of the pier shear force, which is still within the design limit of 0.3W. This result provides confidence in the use of the system even when unanticipated changes in the frictional properties occur over time.

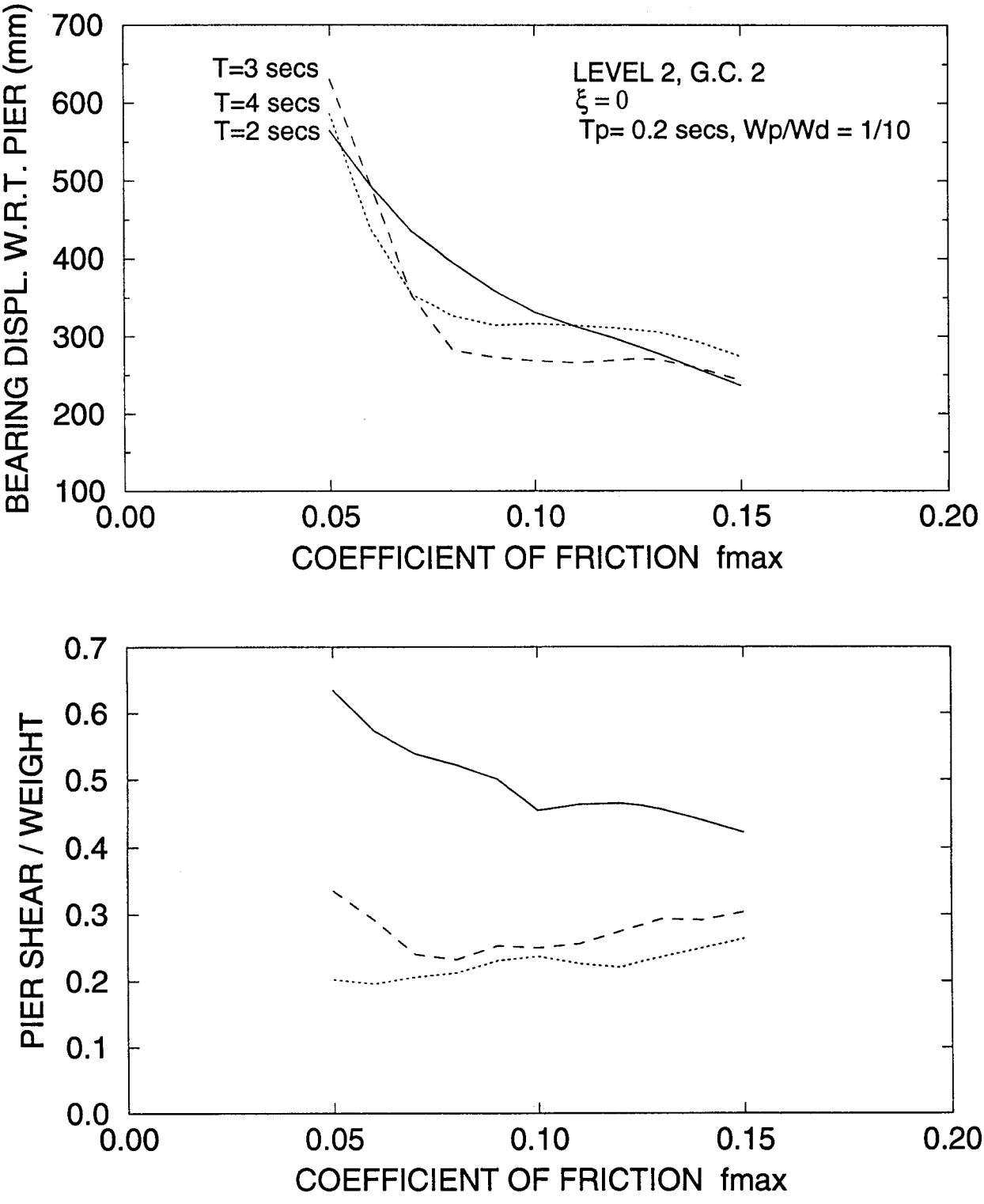

Figure 8-3 **Response Spectra of Pier-Deck Model of Isolated Bridge for Japanese Level 2, Ground Condition 2 Input.**

SECTION 9

CONCLUSIONS

An experimental study of an isolated bridge and a comparable non-isolated bridge has been conducted. A total of seven different isolation system configurations and three bridge configurations were tested. The isolation systems consisted of sliding bearings and rubber restoring force devices. The sliding bearings were configured to produce either low friction ($f_{max} \approx$ 0.07) or high friction (f_{max}= 0.14 to 0.15) under dynamic conditions. The rubber devices were configured to produce an isolation system period in prototype scale in the range of 2.66 to nearly 5.0 seconds. Furthermore, in one configuration, fluid viscous dampers were included, which enhanced viscous damping to nearly 60% of critical.

The low friction isolation systems were configured for application in areas of moderate seismic excitation, whereas the high friction systems were configured for applications in areas of strong seismic excitation, such as California and Japan. All systems, except the one with the largest period (5.0 secs), satisfied the minimum requirements of the 1991 AASHTO.

The conclusions of the study are:

(1) The low friction sliding isolation system resulted in substantial reduction of the substructure forces in comparison to the response of the non-isolated comparable bridge. For weak to moderate seismic excitations, with peak ground acceleration of 0.1 to 0.5g, the isolated bridge responded with peak bearing displacements less than 130 mm in prototype scale and pier shear forces less than about 0.2W (W=weight). Vivid illustration of the performance of this system is provided in Figure 6-2, where the response of the isolated bridge is compared to that of the non-isolated bridge in the Japanese Level 1 motions. Even in these weak excitations, the substructure response of the isolated bridge showed marked insensitivity to the content in frequency of the input and completely elastic behavior. In contrast, the non-isolated bridge underwent inelastic action.

(2) The high friction isolation systems maintained elastic behavior of the bridge substructure with bearing displacements of less than 160 mm in prototype scale under all seismic

excitations, except those of the Japanese Level 2 and Pacoima S16E motions. For these excitations, the displacement restraint of the rubber restoring force device was activated and restricted displacements to about 200 mm, at the expense of higher substructure forces.

(3) The high friction isolation systems enhanced the performance of the tested bridge even in the weak seismic excitations, for which the peak ground acceleration was less than $f_{max}g$. The substantial reduction of the substructure forces in the high friction isolation systems is illustrated in Figure 6-5. This desirable performance is attributed to the velocity dependence of friction in PTFE and PTFE-based sliding bearings.

(4) The tested high friction isolation system with fluid viscous dampers sustained the strongest seismic excitations, including the Japanese Level 2 motions, while preventing activation of the displacement restrainer of the rubber devices. Particularly for the Japanese Level 2 motions, the combined sliding bearing-rubber device-fluid damper system maintained the substructure forces between 0.325 and $0.375W$ with bearing displacements below 160 mm in prototype scale. We note that bridges in Japan are designed for a lateral force of at least $0.3W$, even when seismic isolation and pier inelastic behavior are utilized.

It is, thus, possible to design sliding seismic isolation systems which, for elastic substructure behavior and for all seismic conditions in Japan, maintain the pier forces at the minimum allowed design level, while allowing bearing displacements of less than 200 mm. Such low bearing displacements are desirable for a variety of reasons, such as the use of short expansion joints and preclusion of the use of knock-off elements. Particularly, short expansion joints are less costly, need less maintenance and produce less noise on automobile crossing than long expansion joints.

(5) The vertical ground motion had insignificant effects on peak response of all tested sliding isolation systems.

(6) Tests conducted with combinations of high and low friction sliding bearings and rubber devices of varying stiffness demonstrated that the seismic forces may be effectively

directed to selected substructure elements, which are more capable of sustaining them and transferring them to the ground. This desirable performance was achieved merely by utilizing rubber of different hardness in the restoring force devices and different type of PTFE in the sliding bearings.

(7) The tested sliding isolation systems developed permanent displacements at the conclusion of each test. These permanent displacements were, generally, not cumulative and did not affect the performance of the isolated bridge in subsequent tests. Specifically, tests were repeated under identical conditions, except for the initial displacement, (see Figure 6-22) and the results demonstrated a totally insignificant effect on the response.

However, the one system which did not meet the 1991 AASHTO minimum requirements on the restoring force (system with isolation period equal to 5.0 secs) had significantly larger permanent displacements than the other systems, which met the AASHTO requirements. The writers believe that the AASHTO requirement for minimum restoring force represents a simple and reasonable requirement for preventing the development of significant permanent displacements. However, the writers also believe that a more rational requirement needs to be developed. It is proposed that such a requirement takes the following form : **the isolation system shall be configured to produce a lateral force at the design displacement, F_r such that F_f / F_r is not grater than 3, where F_f is the friction force or characteristic strength of the isolation system.**

(8) Analytical models of the tested isolation systems were presented which were capable of describing the observed response of the isolated bridge, including the effects of vertical ground motion, pier flexibility and stiffening behavior of the rubber restoring force devices.

SECTION 10

REFERENCES

American Association of State Highway and Transportation Officials-AASHTO (1991). "Guide Specifications for Seismic Isolation Design." Washington, D.C.

Bird, R.B., Armostrong, R.C. and Hassager, O. (1987). Dynamics of Polymeric Liquids, J.Wiley and Sons, New York, NY.

Buckle, I.G. and Mayes, R.L. (1990). "Seismic Isolation History, Application, and Performance - A World View." Earthquake Spectra, 6(2), 161-201.

Civil Engineering Research Center-CERC (1992). "Temporary Manual of Design Method for Base-Isolated Highway Bridges." Japan (in Japanese).

Constantinou, M.C., Mokha, A. and Reinhorn, A.M. (1990a). "Teflon Bearings in Base Isolation II: Modeling." J. Stuct. Engrg., ASCE, 116(2), 455-474.

Constantinou, M.C., Mokha, A. and Reinhorn, A.M. (1990b). "Experimental and Analytical Study of a Combined Sliding Disc Bearing and Helical Steel Spring Isolation System." NCEER-90-0019, Nat. Ctr. for Earthquake Engrg. Res., State Univ. of New York, Buffalo, NY.

Constantinou, M.C., Kartoum, A., Reinhorn, A.M. and Bradford, P. (1991a). "Experimental and Theoretical Study of a Sliding Isolation System for Bridges." Report No. NCEER-91-0027, Nat. Ctr. for Earthquake Engrg. Res., State Univ. of New York, Buffalo, NY.

Constantinou, M.C., Mokha, A. and Reinhorn, A.M. (1991b). "Study of Sliding Bearing and Helical-Steel-Spring Isolation System." J. Struct. Engrg., ASCE, 117(4), 1257-1275.

Constantinou, M.C. (1992a). "NCEER-Taisei Research on Sliding Isolation Systems for Bridges." NCEER Bulletin, Nat. Ctr. for Earthquake Engrg. Res., State Univ. of New York, Buffalo, NY, 6(3), 1-4.

Constantinou, M.C., Fujii, S., Tsopelas, P., and Okamoto, S. (1992b). "University at Buffalo - Taisei Corporation Research Program in Bridge Seismic Isolation Systems." Proc. 3rd Workshop on Bridge Engineering Research in Progress, La Jolla, California, 235-238.

Constantinou, M.C. and Symans, M.D. (1992c). "Experimental and Analytical Investigation of Seismic Response of Structures with Supplemental Fluid Viscous Dampers." Report No. NCEER-92-0032, Nat. Ctr. for Earthquake Engrg. Res., State Univ. of New York, Buffalo, NY.

Constantinou, M.C., Tsopelas, P., Kim, Y-S., and Okamoto, S. (1993). "NCEER-TAISEI Corporation Research Program on Sliding Seismic Isolation Systems for Bridges-Experimental and Analytical Study of Friction Pendulum System (FPS)." Report No. NCEER 93-0020. Nat. Ctr. for Earthquake Engrg. Res., State Univ. of New York, Buffalo, NY.

Demetriades, G.F., Constantinou, M.C. and Reinhorn, A.M. (1992). "Study of Wire Rope Systems for Seismic Protection of Equipment in Buildings." Report No. NCEER-92-0012, Nat. Ctr. for Earthquake Engrg. Res., State Univ. of New York, Buffalo, NY.

Eisenberg J.M., Melentyev, A.M., Smirov, V.I. and Nemykin, A.N. (1992). "Applications of Seismic Isolation in the USSR." Proc. 10th WCEE, Madrid, Spain, 4:2039-2046.

Gates, J.H. (1979). "Factors Considered in the Development of the California Seismic Design Criteria for Bridges." Proc. Workshop on Earthquake Resistance of Highway Bridges, Applied Technology Council, Palo Alto, Calif., 141-162.

Gear, C.W. (1971). "The Automatic Integration of Ordinary Differential Equations." Numer. Math., Commun. of ACM, 14(3), 176-190.

International Conference of Building Officials ICBO (1991). "Uniform Building Code, Earthquake Regulations for Seismic-Isolated Structures." Whittier, Calif.

Kartoum, A., Constantinou, M.C. and Reinhorn, A.M. (1992). "Sliding Isolation System for Bridges: Analytical Study." Earthquake Spectra, 8(3), 345-372.

Kawamura, S., Kitazawa, K., Hisano, M. and Nagashima, I. (1988). "Study of a Sliding-Type Base Isolation System. System Composition and Element Properties." Proceedings of 9th World Conference on Earthquake Engineering, Tokyo-Kyoto, Vol. V, 735-740.

Kawashima, K., Hasegawa, K. and Nagashima, H. (1991). "A Perspective of Menshin Design for Highway Bridges in Japan." First US-Japan Workshop on Earthquake Protective Systems for Bridges, Buffalo, NY, September.

Kelly, J.M., Buckle, I.G., and Tsai, H-C. (1986). "Earthquake Simulator Testing of a Base-Isolated Bridge Deck." Report No. UCB/EERC-85/09, Earthquake Engrg. Res. Ctr., Univ. of California, Berkeley, Calif., Jan.

Kelly, J. (1993). "State-of-the-Art and State-of-the-Practice in Base Isolation." ATC-17-1 Seminar on Seismic Isolation, Passive Energy Dissipation and Active Control, San Francisco, CA, March.

Marioni, A. (1991). "Antiseismic Devices for Bridges in Italy." 3rd World Congress on joint Sealing and Bearing Systems for Concrete Structures. Vol. 2 of Preprints, 1263- 1280, Toronto, Canada.

Martelli, A., Parducci, A. and Forni, M. (1993). "State-of-the-Art on Development and Application of Seismic Isolation and Other Innovative Seismic Design Techniques in Italy." ATC-17-1 Seminar on Seismic Isolation, Passive Energy Dissipation and Active Control, San Francisco, CA, March.

Mayes, R.L., Jones, L.R. and Buckle, I.G., (1990). "Impediments to the Implementation of Seismic Isolation." Earthquake Spectra, 6(2), 283-296.

Medeot, R. (1991). "The Evolution of Aseismic Devices for Bridges in Italy." 3rd World Congress on Joint Sealing and Bearing Systems for Concrete Structures, Vol. 2 of Preprints, 1295-1320, Toronto, Canada.

Mokha, A., Constantinou, M.C., and Reinhorn, A.M. (1988). "Teflon Bearings in Aseismic Base Isolation. Experimental Studies and Mathematical Modeling." Report No. NCEER- 88-0038, Nat. Ctr. for Earthquake Engrg. Res., State Univ. of New York, Buffalo, NY.

Mokha, A., Constantinou, M.C. and Reinhorn, A.M. (1990a). "Teflon Bearings in Base Isolation. I: Testing." J. Struct. Engrg., ASCE, 116(2), 438-454.

Mokha, A., Constantinou, M.C. and Reinhorn, A.M. (1990b). "Experimental Study and Analytical Prediction of Earthquake Response of a Sliding Isolation System with a Spherical Surface." Report No. NCEER-90-0020, Nat. Ctr. for Earthquake Engrg. Res., State Univ. of New York, Buffalo, NY.

Mokha, A., Constantinou, M.C., Reinhorn, A.M., and Zayas, V. (1991). "Experimental Study of Friction Pendulum Isolation System." J. Struct. Engrg., ASCE, 117(4), 1201- 1217.

Palfalvi, B., Amin, A., Mokha, A., Fatehi, H. and Lee, P. (1993). "Implementation Issues in Seismic Isolation Retrofit of Government Buildings." ATC-17-1 Seminar on Seismic Isolation, Passive Energy Dissipation and Active Control, San Francisco, CA, March.

Sabnis, G.M., Harris, H.G., White, R.N. and Mirza, M.S. (1983). "Structural Modeling and Experimental Techniques." Prentice-Hall, Inc., Englewood Cliffs, N.J.

Shinozuka, M., Constantinou, M.C. and Ghanem, R. (1992) "Passive and Active Fluid Dampers in Structural Applications." Proc. of US/China/Japan Trilateral Workshop on Structural Control, (337) Shanghai, PRC.

Soong, T.T. and Constantinou, M.C. (1992). "Base Isolation and Active Control Technology Case Studies in the U.S.A." Proc. IDNDR Intl. Symp. on Earthq. Disaster Reduction Technol.-30th Anniv. of IISEE, Tsukuba, Japan, 455-469.

Zayas, V., Low, S.S and Mahin, S.A. (1987). "The FPS Earthquake Resisting System, Experimental Report." Report No. UCB/ EERC-87/01, Earthquake Engineering Research Center, University of California, Berkeley, Calif., June.